frontiers | Research Topics

Helicobacter pylori-transmission, pathogenesis, host-pathogen interaction, prevention and treatment

Edited by
Zhongming Ge, Rao Narasimha Desirazu and Paula Roszczenko-Jasinska

Published in
Frontiers in Microbiology

ISSN 1664-8714
ISBN 978-2-8325-4030-5
DOI 10.3389/978-2-8325-4030-5

About Frontiers

Frontiers is more than just an open access publisher of scholarly articles: it is a pioneering approach to the world of academia, radically improving the way scholarly research is managed. The grand vision of Frontiers is a world where all people have an equal opportunity to seek, share and generate knowledge. Frontiers provides immediate and permanent online open access to all its publications, but this alone is not enough to realize our grand goals.

Frontiers journal series

The Frontiers journal series is a multi-tier and interdisciplinary set of open-access, online journals, promising a paradigm shift from the current review, selection and dissemination processes in academic publishing. All Frontiers journals are driven by researchers for researchers; therefore, they constitute a service to the scholarly community. At the same time, the *Frontiers journal series* operates on a revolutionary invention, the tiered publishing system, initially addressing specific communities of scholars, and gradually climbing up to broader public understanding, thus serving the interests of the lay society, too.

Dedication to quality

Each Frontiers article is a landmark of the highest quality, thanks to genuinely collaborative interactions between authors and review editors, who include some of the world's best academicians. Research must be certified by peers before entering a stream of knowledge that may eventually reach the public - and shape society; therefore, Frontiers only applies the most rigorous and unbiased reviews. Frontiers revolutionizes research publishing by freely delivering the most outstanding research, evaluated with no bias from both the academic and social point of view. By applying the most advanced information technologies, Frontiers is catapulting scholarly publishing into a new generation.

What are Frontiers Research Topics?

Frontiers Research Topics are very popular trademarks of the *Frontiers journals series*: they are collections of at least ten articles, all centered on a particular subject. With their unique mix of varied contributions from Original Research to Review Articles, Frontiers Research Topics unify the most influential researchers, the latest key findings and historical advances in a hot research area.

Find out more on how to host your own Frontiers Research Topic or contribute to one as an author by contacting the Frontiers editorial office: frontiersin.org/about/contact

Helicobacter pylori-transmission, pathogenesis, host-pathogen interaction, prevention and treatment

Topic editors

Zhongming Ge — Massachusetts Institute of Technology, United States
Rao Narasimha Desirazu — Indian Institute of Science (IISc), India
Paula Roszczenko-Jasinska — University of Warsaw, Poland

Citation

Ge, Z., Desirazu, R. N., Roszczenko-Jasinska, P., eds. (2023). *Helicobacter pylori-transmission, pathogenesis, host-pathogen interaction, prevention and treatment*. Lausanne: Frontiers Media SA. doi: 10.3389/978-2-8325-4030-5

Table of contents

04 Are molecular methods helpful for the diagnosis of *Helicobacter pylori* infection and for the prediction of its antimicrobial resistance?
Belen Fernandez-Caso, Ana Miqueleiz, Verónica B. Valdez and Teresa Alarcón

10 Treatment of refractory *Helicobacter pylori* infection: A new challenge for clinicians
XinBo Xu, Cong He and Yin Zhu

18 Aspartate α-decarboxylase a new therapeutic target in the fight against *Helicobacter pylori* infection
Kareem A. Ibrahim, Mona T. Kashef, Tharwat R. Elkhamissy, Mohammed A. Ramadan and Omneya M. Helmy

34 Vitamin D_3 eradicates *Helicobacter pylori* by inducing VDR-CAMP signaling
Ye Zhang, Chunya Wang, Li Zhang, Jie Yu, Wenjie Yuan and Lei Li

44 A positive feedback loop of the TAZ/β-catenin axis promotes *Helicobacter pylori*-associated gastric carcinogenesis
Xinbo Xu, Chunxi Shu, Xidong Wu, Yaobin Ouyang, Hong Cheng, Yanan Zhou, Huan Wang, Cong He, Chuan Xie, Xingxing He, Junbo Hong, Nonghua Lu, Zhongming Ge, Yin Zhu and Nianshuang Li

59 Characteristics of different types of *Helicobacter pylori*: New evidence from non-amplified white light endoscopy
Weidong Liu, Wenjie Kong, Wenjia Hui, Chun Wang, Qi Jiang, Hong Shi and Feng Gao

68 Amoxicillin-docosahexaenoic acid encapsulated chitosan-alginate nanoparticles as a delivery system with enhanced biocidal activities against *Helicobacter pylori* and improved ulcer healing
Saeed Khoshnood, Babak Negahdari, Vahab Hassan Kaviar, Nourkhoda Sadeghifard, Mohd Azmuddin Abdullah, Mohamed El-Shazly and Mohammad Hossein Haddadi

81 Application of biomaterials in the eradication of *Helicobacter pylori*: A bibliometric analysis and overview
Chunxi Shu, Zhou Xu, Cong He, Xinbo Xu, Yanan Zhou, Baihui Cai and Yin Zhu

98 Gastric microbiota: an emerging player in gastric cancer
Shizhen Zhou, Chenxi Li, Lixiang Liu, Qinggang Yuan, Ji Miao, Hao Wang, Chao Ding and Wenxian Guan

111 Therapeutic effect of demethylated hydroxylated phillygenin derivative on *Helicobacter pylori* infection
Ru-Jia Li, Jia-yin Xu, Xue Wang, Li-juan Liao, Xian Wei, Ping Xie, Wen-yan Xu, Zhen-yi Xu, Shuo-hua Xie, Yu-ying Jiang, Liang Huang, Lu-yao Wang, Gan-rong Huang and Yan-Qiang Huang

frontiers | Frontiers in Microbiology

TYPE Perspective
PUBLISHED 09 August 2022
DOI 10.3389/fmicb.2022.962063

OPEN ACCESS

EDITED BY
Zhongming Ge,
Massachusetts Institute of Technology, United States

REVIEWED BY
Maria Teresa Mascellino,
Sapienza University of Rome, Italy
Leila Ganji,
Ministry of Health and Medical Education, Iran

*CORRESPONDENCE
Teresa Alarcón
talarcon@helicobacterspain.com

†These authors have contributed equally to this work and share first authorship

SPECIALTY SECTION
This article was submitted to Infectious Agents and Disease, a section of the journal Frontiers in Microbiology

RECEIVED 05 June 2022
ACCEPTED 18 July 2022
PUBLISHED 09 August 2022

CITATION
Fernandez-Caso B, Miqueleiz A, Valdez VB and Alarcón T (2022) Are molecular methods helpful for the diagnosis of *Helicobacter pylori* infection and for the prediction of its antimicrobial resistance? *Front. Microbiol.* 13:962063. doi: 10.3389/fmicb.2022.962063

Are molecular methods helpful for the diagnosis of *Helicobacter pylori* infection and for the prediction of its antimicrobial resistance?

Belen Fernandez-Caso[1†], Ana Miqueleiz[2†], Verónica B. Valdez[3] and Teresa Alarcón[3*]

[1]Department of Microbiology, Hospital Universitario de Cabueñes, Asturias, Spain, [2]Department of Microbiology, Hospital Universitario de Navarra, Navarra, Spain, [3]Department of Microbiology, Instituto de Investigación Sanitaria Princesa, Hospital Universitario La Princesa, Madrid, Spain

Infections produced by *Helicobacter pylori* (*H. pylori*), a spiral Gram-negative bacterium, can cause chronic gastritis, peptic ulcer, and gastric cancer. Antibiotic therapy is the most effective treatment for *H. pylori* infection at present. However, owing to the increasing antibiotic resistance of *H. pylori* strains, it has become a serious threat to human health. Therefore, the accurate diagnosis of *H. pylori* infections and its antibiotic resistance markers is of great significance. Conventional microbiological diagnosis of *H. pylori* is based on culture; however, successful isolation of *H. pylori* from gastric biopsy specimens is a challenging task affected by several factors and has limitations in terms of the time of response. To improve conventional methods, some molecular techniques, such as PCR, have been recently used in both invasive and non-invasive *H. pylori* diagnosis, enabling simultaneous detection of *H. pylori* and point mutations responsible for frequent antibiotic resistance. The advantages and disadvantages of molecular methods, mainly PCR, versus conventional culture for the *H. pylori* identification and the detection of antibiotic resistance are discussed. As expected, the combination of both diagnostic methods will lead to the most efficient identification of the *H. pylori* strains and the resistance patterns.

KEYWORDS

***Helicobacter pylori*, antibiotics, resistance, culture, PCR, GenoType® HelicoDR test**

Introduction

Helicobacter pylori (*H. pylori*) is one of the most prevalent pathogens worldwide which affects about 50% of the world population (Peleteiro et al., 2014). It colonizes the human stomach, and, although the majority of people (>80%) can remain asymptomatic throughout their life, it is largely related to gastrointestinal diseases. In the absence of

treatment, its manifestations can range from pathologies, such as chronic gastritis, peptic ulcers, atrophic gastritis to intestinal metaplasia, gastric cancer, and mucosa-associated lymphoid tissue (Sirous et al., 2011).

The bases of *H. pylori* treatment are antibiotics. The most commonly used are macrolides (clarithromycin or azithromycin), imidazole (metronidazole or tinidazole), amoxicillin, tetracycline, and levofloxacin. Multiple regimens such as triple therapy, sequential therapy, quadruple therapy, and levofloxacin-based triple therapy (Malfertheiner et al., 2017) have been evaluated. Nevertheless, the successful eradication treatment regimen has not yet been achieved due to the increasing rates of resistance to antibiotics included in current regimens. Subsequently, a substantial fall in *H. pylori* treatment efficacy has been observed globally making the eradication of *H. pylori*, a major public health problem (Thung et al., 2016).

Enhanced efforts are required for improving diagnostic tools for *H. pylori,* as well as for a clearer understanding of the development and spread of drug-resistant bacteria. Likewise, the study of antibiotic susceptibility is key to implement the most appropriate treatments and to define treatment guidelines since the choice of antibiotics must be tailored according to local resistance (Malfertheiner et al., 2017).

Clinical tests for *H. pylori* identification that are also useful for the detection of antibiotic susceptibility include culture, as conventional method, and molecular techniques, usually involving gastric biopsy. Although bacteriological culture is considered the reference method for diagnosing infection, *H. pylori* is regarded as a demanding bacterium as it requires supplemented means for its growth, microaerophilic atmosphere, and prolonged incubation which leads to time-consuming limitations when performing sensitivity studies (e.g., Wang et al., 2015). Due to the technical difficulties of *H. pylori* culture, it is shown that easier and faster techniques are required to detect *H. pylori* and to determine its resistance. In this regard, molecular methods have shown remarkable results (Alba et al., 2017).

This article summarizes our current viewpoint of molecular methods, focusing on polymerase chain reaction (PCR) and its applications, both in the diagnosis of *H. pylori* infection and the prediction of its resistance to antibiotics.

TABLE 1 Genotypic determination of clarithromycin and levofloxacin resistance mutations by PCR.

Antibiotic			n (%)
Clarithromycin	No mutation		123 (40.2)
	Detected mutation	A2146G	12 (3.9)
		A2146C	2 (0.7)
		A2147G	165 (53.9)
		Double mutation	4 (1.3)
	Total		306 (100)
Levofloxacin	No mutation		261 (91.6)
	Detected mutation	N87K	9 (3.1)
		D91N	5 (1.7)
		D91G	6 (2.1)
		D91Y	4 (1.4)
	Total		285* (100)

*In 21 samples the PCR result for levofloxacin resistance was indeterminate.

Polymerase chain reaction for *Helicobacter pylori* detection

In recent years, many molecular methods have been developed as alternatives for the identification of *H. pylori*. Most of them are based on PCR or real-time PCR (RT-PCR) directly from gastric biopsies. Other molecular methods that have been tested include nested-PCR, droplet digital PCR, fluorescent *in situ* hybridization, and next-generation sequencing, such as 16S rRNA amplicon sequencing, transcriptomics, and metagenomics (Gong and El-Omar, 2021).

There are several molecular assays commercially available for the identification of *H. pylori*. The extraction of genetic material (DNA) directly from the sample allows for the detection of *H. pylori* through the amplification of specific genes, mainly conserved regions of the *H. pylori* genome. The most used genes are the ureA, ureC, glmM, and Hsp60 or the 16SrRNA or 23S rRNA regions (e.g., Clayton et al., 1991; Wang et al., 2015; Sulo and Šipková, 2021).

The advantage of molecular biology techniques over other methods remains in the increase of sensitivity and the fact that they may allow quantification of the bacteria (Shukla et al., 2011; Belda et al., 2012). However, false-negatives and false-positives arise from the primers employed, due to polymorphism or the use of non-specific primers, respectively (Sulo and Šipková, 2021).

It has been suggested that nested-PCR can achieve sufficient specificity and is much more sensitive than regular PCR as it involves two rounds of amplification, enabling it to amplify the target sequence in a lower concentration (Šeligová et al., 2020; Sulo and Šipková, 2021).

In addition, the combination of several target genes for detection, such as ureA, ureC, glmM, Hsp60, 16S rRNA, 23S rRNA, and vacA, may help to improve the diagnostic performance by reducing the number of false positive results (e.g., Wang et al., 2015; Wongphutorn et al., 2018).

On the other hand, as an alternative to the use of gastric biopsies specimens, different studies that perform PCR on gastric juice (Hsieh et al., 2019) or on non-invasive samples, such as saliva (Sayed et al., 2011) and stool (Beckman et al., 2017; Leonardi et al., 2020), have been published obtaining promising results. So far, there are different sensitivities and specificities depending on the DNA extraction method and the PCR assay

TABLE 2 Presence or absence of PCR mutations for clarithromycin and levofloxacin versus sensitivity or resistance results by *E*-test (gold standard).

		Susceptible by *E*-test	Resistant by *E*-test	Total	Sensitivity	Specificity
Clarithromycin PCR	Mutation	21 (15.4%)	115 (84.5%)	136	99.1%	80.0%
	No mutation	84 (98.8%)	1 (1.1%)	85		
Levofloxacin PCR	Mutation	0 (0%)	16 (100%)	16	100%	100%
	No mutation	198 (100%)	0 (0%)	198		

used. Other limitations found are requirements of facilities and experts, smaller abundance of the bacteria, presence of an inhibitory substance, and interference from the dead bacteria or DNA degradation.

Polymerase chain reaction for detection of resistance

Molecular techniques also allow the detection of antibiotic resistance. *H. pylori* strains have developed different mechanisms of antibiotic resistance, such as point mutations or other genetic changes. Molecular mechanisms underlying this resistance have been intensively studied, especially in the cases of clarithromycin and levofloxacin, the most commonly used antibiotics for *H. pylori* eradication, given that the vast majority of resistance to these two antibiotics is due to known localized mutations.

Hence, by targeting the genes responsible for antibiotic resistance, it is feasible to obtain genotypic susceptibility information for the common antibiotics used, without performing an antibiogram. Furthermore, the detection of genes and mutations involved in antibiotic resistance using molecular techniques has been already acknowledged as a useful tool to be performed directly on the gastric biopsy specimen by Maastricht V/Florence Consensus Report (Malfertheiner et al., 2017).

Polymerase chain reaction is the most widely used molecular determination approach (Hortelano et al., 2021). Several commercial kits (Cambau et al., 2009; Nishizawa and Suzuki, 2014; Redondo et al., 2018) are available to detect different mutations that confer resistance to clarithromycin combined or not with levofloxacin. PCR has also been applied to detect resistance to tetracycline and rifampicin by in-house protocols which are largely described in the literature (Chisholm and Owen, 2009; Contreras et al., 2019).

When referring to clarithromycin, most methods identify the main mutations which are found in the 23S rRNA gene, targeting point mutations at nucleotide positions A2146 and A2147 (Redondo et al., 2018). These two mutations were previously named 2,142 and 2,143 (Wang and Taylor, 1998). For its part, resistance to fluoroquinolones is due, in a very significant percentage, to mutations in genes gyrA and gyrB DNA gyrase, positions 86, 87, 88, and 91 (Rimbara et al., 2012). Also, PCR techniques have been applied to detect tetracycline resistance (Contreras et al., 2019) due to mutations in the 16S rRNA gene (positions 926–928) and rifampicin in the rpoB gene (positions 525–545 and 547) (Chisholm and Owen, 2009). In the case of metronidazole, its resistance mechanisms are quite complex (Nishizawa and Suzuki, 2014) and not as well defined, so for the moment, there are no commercial kits for its detection.

Polymerase chain reaction *vs.* culture

Keeping the above observation in mind, we have compared *H. pylori* identification performance efficacy among culture and molecular *H. pylori* identification GenoType® HelicoDR kit (HAIN Life Science, Hardwiesenstraße, Germany). In terms of antibiotic resistance, phenotypic susceptibility was studied in all culture-positive and was compared to GenoType® HelicoDR kit which allows simultaneous detection of *H. pylori* and its resistances to clarithromycin and levofloxacin and is applicable to gastric biopsy specimens. The Genotype® HelicoDR test allows the detection of point mutations responsible for the resistance to clarithromycin and levofloxacin: three-point mutations in the V domain of the 23S rRNA gene (positions 2,146 and 2,147) for clarithromycin and 4 mutations in the A subunit of DNA gyrase (1 at codon 87 and 3 at codon 91) for quinolones.

Patients and methods

The specimens used for this study were gastric biopsy samples taken from 616 patients aged between 2 and 82 years old who had undergone endoscopy due to gastroduodenal diseases. One sample per patient was analyzed. Data including age and sex were collected. The study was performed from January 2016 to October 2017 and samples were collected from a variety of Spanish hospitals. Gastric biopsy specimens of the patients were referred to the Clinical Microbiology laboratory of Hospital Universitario La Princesa in Madrid. Freshly taken biopsy specimens were either placed into Portagerm Pylori (BioMérieux) solution and sent within 24 h under room temperature or into sterile glass tubes and kept at 4°C. Once at the laboratory, if the process could not be continued within

3 h, the samples were stored at −80°C deep freezer until further processing.

Biopsy specimens' culture was performed in a biological safety cabin and then preserved at −80°C deep freezer for further molecular processing. The specimens were discharged with the aid of a sterile swab into two commercial culture media: blood agar (Columbia agar + 5% sheep blood, BioMérieux) and Helicobacter selective agar media (Pylori agar, BioMérieux). The samples were incubated for 15 days at 37°C in a micro-aerobic atmosphere (5% O_2, 10% CO_2, and 85% N_2). *H. pylori* colonies are small, translucent to yellowish colonies, which can be identified based on a Gram-negative helical-shaped in Gram-staining procedure followed by positive oxidase, catalase, and urease tests, along with the confirmation by MALDI-TOF mass spectrometry (Bruker).

The antibiotic sensitivity study was performed using the gradient strip diffusion method in blood agar plates. *H. pylori* isolates collected were examined for their susceptibility to antimicrobial agents by gradient diffusion strip method (*E*-test, BioMérieux) on blood agar incubated at 37°C in a micro-aerobic atmosphere (5% O_2, 10% CO_2, and 85% N_2). Six antimicrobial agents were tested: clarithromycin, metronidazole, amoxicillin, levofloxacin, tetracycline, and rifampicin, on which MIC values were read after 3 and 5 days and interpreted according to the clinical breakpoints of EUCAST guidelines.

For the molecular method, DNA extraction included a previous stage meant for the digestion of proteins. Solid biopsies were mixed with Proteinase K, lysis buffer, and distilled water followed by incubation in agitation for at least 3 h at 37°C. The DNA isolation was carried out by automated DNA extraction using the NucliSens® easyMAG™ (BioMérieux), following the manufacturer's description for the tissues. All the eluted DNA were stored at −80°C.

The biopsy material itself, as well as the culture material extracted from it, can be used as the starting material. Briefly, multiplex amplification of DNA regions of interest was performed. Typical PCR reaction mixtures contained 5 μl of reaction buffer, 2.5 μl of $MgCl_2$, 35 μl of 5′-biotinylated primers and nucleotide mixture, 0.4 μl of Taq polymerase, 2.5 μl of PCR grade water, and 5 μl of extracted DNA. The PCR run comprised 30 cycles. The denaturation cycle was 1 cycle at 94°C for 5 min. Then, 30 cycles which were composed of a first step at 94°C for 30 s, a second step at 55°C for 30 s, and a third step at 72°C for 30 s. The PCR ended with 7 min at 72°C. The test was developed and interpreted according to the manufacturers' instructions.

The PCR was followed by hybridization with DNA strips, coated with different specific oligonucleotides (probes). Hybridization was performed using the TwinCubator (Hain Life Science) system at a temperature of 45°C. The denaturation solution was mixed with 20 μl of the amplified sample and was hybridized using a standard hybridization protocol. Each strip contains a total of 18 hybridization probes. The first band contains the conjugate control designed to indicate effective binding to the substrate. The second band includes a universal control, and it is used to check that the amplification has taken place correctly. The third band contains a sequence from a region of the 23S rRNA that is common to all *H. pylori* strains. The next ten and five bands are for quinolone and clarithromycin sensitivity studies, respectively. The probes were designed to hybridize with both the sequences of the wild-type (WT) and the mutated alleles (MUT).

Interpretation was performed after strips were attached to the evaluation sheet after hybridization, with the template aligned side by side with the conjugate control band of the respective strip. Control bands that should appear positive to validate the test. A positive band was determined by comparing each band stain with the amplification control band. A stronger stain than the amplification band was interpreted as positive for the presence of the allele. WT specimens were determined by the presence of WT bands only. *H. pylori* strain mutations included clarithromycin resistant, fluoroquinolone resistant, and resistant to both antibiotics. Mutants were determined by the presence of the MUT band.

Results

Therefore, a total of 616 specimens were examined for *H. pylori* presence using the two methods. Results indicate that 234 (37.9%) were found positive for the presence of the *H. pylori* bacterium by both methods and 308 (50%) were negative. In terms of discrepancies observed, 2 (0.32%) specimens were only detected by culture. On the contrary, 72 (11.6%) specimens were found positive only by means of PCR. If we consider culture as gold standard, the comparison revealed a sensitivity of 99.1% and a specificity of 81% in favor of the molecular kit. It should be borne in mind that the positives by PCR and negative by the culture were not false positives, as the PCR was able to detect more positives than the culture.

Regarding the *E*-test susceptibility testing, it was not possible to determine antibiotic sensitivity in the 236 isolates for all antibiotics; only 223 isolates could be studied for clarithromycin and levofloxacin. For clarithromycin, 107 (47.9%) isolates had a sensitive phenotype; while for levofloxacin, 206 (92.3%) isolates had a sensitive phenotype. Despite the isolation of H. pylori in culture from 236 strains, the antibiogram was not viable in all of them. Only the sensitivity of 223 strains could be studied phenotypically while in 13 strains, the antibiogram was not viable.

Resistance to clarithromycin was 52% for fenotypic while 59% for genotypic method and to levofloxacin was 76% for fenotypic while 84% for genotypic method (No statistically significant differences).

On the other hand, the results of the genotypic study of antibiotic sensitivity to clarithromycin and levofloxacin performed with GenoType® HelicoDR are shown in **Table 1**.

When comparing the results obtained in all samples in which both phenotypic antibiotic sensitivity and genotypic PCR were available, a difference between the two antibiotics was observed (Table 2).

Based on these results, a sensitivity of 99.1% and a specificity of 80% were calculated for the detection of clarithromycin resistance by the genotypic PCR method. For levofloxacin, no discrepancy was observed between the two methods, so the sensitivity and specificity for the detection of levofloxacin resistance by PCR were 100%.

Discussion

Efficient diagnosis is required for successful clinical management to relieve symptoms and to eradicate bacteria. As with any diagnostic method, culture and molecular techniques have advantages, but also disadvantages.

Molecular techniques for the diagnosis of *H. pylori* have a very high sensitivity (over 95%), detecting more positive specimens than culture, and specificity (close to 100%). PCR techniques do not depend on the lability of the bacteria, as culture does. In addition, some molecular methods can be applied directly on the sample, gastric biopsy or non-invasive samples. Moreover, in relation to working time, amplification of genome specific regions in *H. pylori* using appropriate primers allows faster identification than culture, as *H. pylori* takes 10–14 days for cultures to be negative.

The advantages of genotypic methods over phenotypic methods include providing insight into underlying resistance mechanisms in a fairly short time (<4 h).

Meanwhile, among the disadvantages, are the higher price in comparison to conventional methods and the need for appropriate equipment and experience personnel. That is the main reason why approaches involving DNA amplification have not been widely accepted in general practice.

It is worth mentioning, as an alternative to the use of gastric biopsies, the appearance of PCRs for the diagnosis of *H. pylori* directly from non-invasive samples. This could be a great advance as it avoids the need for endoscopy and biopsy, thus preventing all the discomfort and risks that they entail for the patient, as well as the associated healthcare costs.

Besides, molecular techniques have limitations when it comes to detecting antibiotic resistance. The main disadvantage of PCR in detecting resistance as opposed to *H. pylori* culture is that the most commercial systems only detect specific resistance mutations to clarithromycin and quinolones, whereas culture allows the study of sensitivity to all antibiotics and the detection of resistant isolates by other mutations or resistance mechanisms. They only detect specific mutations, so there is a possibility of not detecting resistant isolates due to mutations other than those amplified by PCR or resistant isolates due to other resistance mechanisms unrelated to these.

In conclusion, both methods are still necessary for the study of sensitivity, and neither should be displaced. These procedures could represent an essential component of the efforts needed to prevent the further development of infections caused by *H. pylori* and the spread of the increasing resistance to antibiotics.

Data availability statement

The original contributions presented in this study are included in the article/supplementary material, further inquiries can be directed to the corresponding author.

Ethics statement

Ethical review and approval was not required for the study on human participants in accordance with the local legislation and institutional requirements. Written informed consent for participation was not required for this study in accordance with the national legislation and the institutional requirements.

Author contributions

TA conceived the presented idea and was in charge of overall direction and planning. VV carried out the experiments. AM contributed to the interpretation of the results. AM and BF-C wrote the main manuscript text. TA, AM, BF-C, and VV contributed to the final manuscript. All authors contributed to the article and approved the submitted version.

Conflict of interest

TA has received sporadically funding for congress assistance from Hain Life Science.

The remaining authors declare that the research was conducted in the absence of any commercial or financial relationships that could be construed as a potential conflict of interest.

Publisher's note

All claims expressed in this article are solely those of the authors and do not necessarily represent those of their affiliated organizations, or those of the publisher, the editors and the reviewers. Any product that may be evaluated in this article, or claim that may be made by its manufacturer, is not guaranteed or endorsed by the publisher.

References

Alba, C., Blanco, A., and Alarcón, T. (2017). Antibiotic resistance in *Helicobacter pylori*. *Curr. Opin. Infect. Dis.* 30, 489–497.

Beckman, E., Saracino, I., Fiorini, G., Clark, C., Slepnev, V., Patel, D., et al. (2017). A novel stool PCR test for *Helicobacter pylori* may predict clarithromycin resistance and eradication of infection at a high rate. *J. Clin. Microbiol.* 55, 2400–2405. doi: 10.1128/JCM.00506-17

Belda, S., Saez, J., Santibáñez, M., Rodríguez, J. C., Galiana, A., Sola-Vera, J., et al. (2012). Quantification of *Helicobacter pylori* in gastric mucosa by real-time polymerase chain reaction: comparison with traditional diagnostic methods. *Diagn. Microbiol. Infect. Dis.* 74, 248–252. doi: 10.1016/j.diagmicrobio.2012.07.007

Cambau, E., Allerheiligen, V., Coulon, C., Corbel, C., Lascols, C., Deforges, L., et al. (2009). Evaluation of a new test, genotype HelicoDR, for molecular detection of antibiotic resistance in *Helicobacter pylori*. *J. Clin. Microbiol.* 47, 3600–3607. doi: 10.1128/JCM.00744-09

Chisholm, S. A., and Owen, R. J. (2009). Frequency and molecular characteristics of ciprofloxacin- and rifampicin-resistant *Helicobacter pylori* from gastric infections in the UK. *J. Med. Microbiol.* 58, 1322–1328. doi: 10.1099/jmm.0.011270-0

Clayton, C., Kleanthous, K., and Tabaqchali, S. (1991). Detection and identification of *Helicobacter pylori* by the polymerase chain reaction. *J. Clin. Pathol.* 44, 515–516.

Contreras, M., Benejat, L., Mujica, H., Peña, J., García-Amado, M. A., Michelangeli, F., et al. (2019). Real-time PCR detection of a 16S rRNA single mutation of *Helicobacter pylori* isolates associated with reduced susceptibility and resistance to tetracycline in the gastroesophageal mucosa of individual hosts. *J. Med. Microbiol.* 68, 1287–1291. doi: 10.1099/jmm.0.001051

Gong, L., and El-Omar, E. M. (2021). Application of molecular techniques in *Helicobacter pylori* detection: limitations and improvements. *Helicobacter* 26:12841. doi: 10.1111/hel.12841

Hortelano, I., Moreno, M. Y., García-Hernández, J., and Ferrús, M. A. (2021). Optimization of pre- treatments with Propidium monoazide and PEMAXTM before real-time quantitative PCR for detection and quantification of viable Helicobacter pylori cells. *J. Microbiol. Methods* 185:106223. doi: 10.1016/j.mimet.2021.106223

Hsieh, M., Liu, C. J., Hsu, W. H., Li, C. J., Tsai, P. Y., Hu, H. M., et al. (2019). Gastric juice-based PCR assay: an alternative testing method to aid in the management of previously treated *Helicobacter pylori* infection. *Helicobacter* 24:12568. doi: 10.1111/hel.12568

Leonardi, M., La Marca, G., Pajola, B., Perandin, F., Ligozzi, M., and Pomari, E. (2020). Assessment of real-time PCR for *Helicobacter pylori* DNA detection in stool with co-infection of intestinal parasites: a comparative study of DNA extraction methods. *BMC Microbiol.* 20:131. doi: 10.1186/s12866-020-01824-5

Malfertheiner, P., Megraud, F., O'Morain, C. A., Gisbert, J. P., Kuipers, E. J., Axon, A. T., et al. (2017). Management of *Helicobacter pylori* infection—the maastricht V/Florence consensus report. *Gut* 66, 6–30. doi: 10.1136/gutjnl-2016-312288

Nishizawa, T., and Suzuki, H. (2014). Mechanisms of *Helicobacter pylori* antibiotic resistance and molecular testing. *Front. Mol. Biosci.* 24:19. doi: 10.3389/fmolb.2014.00019

Peleteiro, B., Bastos, A., Ferro, A., and Lunet, N. (2014). Prevalence of *Helicobacter pylori* infection worldwide: a systematic review of studies with national coverage 2014;59(8):1698-709. *Dig. Dis. Sci.* 59, 1698–1709. doi: 10.1007/s10620-014-3063-0

Redondo, J. J., Keller, P. M., Zbinden, R., and Wagner, K. (2018). A novel RT-PCR for the detection of *Helicobacter pylori* and identification of clarithromycin resistance mediated by mutations in the 23S rRNA gene. *Diagn. Microbiol. Infect. Dis.* 90, 1–6. doi: 10.1016/j.diagmicrobio.2017.09.014

Rimbara, E., Noguchi, N., Kawai, T., and Sasatsu, M. (2012). Fluoroquinolone resistance in *Helicobacter pylori*: role of mutations at position 87 and 91 of GyrA on the level of resistance and identification of a resistance conferring mutation in GyrB. *Helicobacter* 17, 36–42. doi: 10.1111/j.1523-5378.2011.00912.x

Sayed, M. M., Ibrahim, W. A., Abdel-bary, S. A., Abdelhakam, S. M., El-Masry, S. A., and Ghoraba, D. (2011). Salivary PCR detection of *Helicobacter pylori* DNA in Egyptian patients with dyspepsia. *Egypt. J. Med. Hum. Genet.* 12, 211–216.

Šeligová, B., Lukáè, Ľ, Bábelová, M., Vávrová, S., and Sulo, P. (2020). Diagnostic reliability of nested PCR depends on the primer design and threshold abundance of *Helicobacter pylori* in biopsy, stool, and saliva samples. *Helicobacter* 25:12680. doi: 10.1111/hel.12680

Shukla, S., Prasad, K. N., Tripathi, A., Ghoshal, U. C., Krishnani, N., Nuzhat, H., et al. (2011). Quantitation of *Helicobacter pylori* ureC gene and its comparison with different diagnostic techniques and gastric histopathology. *J. Microbiol. Methods* 86, 231–237. doi: 10.1016/j.mimet.2011.05.012

Sirous, M., Mehrabadi, J. F., Daryani, N. E., Eshraghi, S., Hajikhani, S., and Shirazi, M. H. (2011). Prevalence of antimicrobial resistance in *Helicobacter pylori* isolates from Iran. *African J. Biotechnol.* 9, 5962–5965.

Sulo, P., and Šipková, B. (2021). DNA diagnostics for reliable and universal identification of *Helicobacter pylori*. *World J. Gastroenterol.* 27:7100. doi: 10.3748/wjg.v27.i41.7100

Thung, I., Aramin, H., Vavinskaya, V., Gupta, S., Park, J. Y., Crowe, S. E., et al. (2016). Review article: the global emergence of *Helicobacter pylori* antibiotic resistance. *Aliment. Pharmacol. Ther.* 43, 514–533. doi: 10.1111/apt.13497

Wang, G. E., and Taylor, D. E. (1998). Site-specific mutations in the 23S rRNA gene of *Helicobacter pylori* confer two types of resistance to macrolide-lincosamide-streptogramin B antibiotics. *Antimicrob. Agents Chemother.* 42, 1952–1958. doi: 10.1128/AAC.42.8.1952

Wang, Y.-K., Kuo, F. C., Liu, C. J., Wu, M. C., Shih, H. Y., Wang, S. S., et al. (2015). Diagnosis of *Helicobacter pylori* infection: current options and developments. *Orld J. Gastroenterol.* 21, 11221–11235.

Wongphutorn, P., Chomvarin, C., Sripa, B., Namwat, W., and Faksri, K. (2018). Detection and genotyping of *Helicobacter pylori* in saliva versus stool samples from asymptomatic individuals in Northeastern Thailand reveals intra-host tissue-specifc *H. pylori* subtypes. *BMC Microbiol.* 18:10. doi: 10.1186/s12866-018-1150-7

frontiers | Frontiers in Microbiology

TYPE Review
PUBLISHED 18 October 2022
DOI 10.3389/fmicb.2022.998240

OPEN ACCESS

EDITED BY
Paula Roszczenko-Jasinska,
University of Warsaw, Poland

REVIEWED BY
Giuseppe Losurdo,
University of Bari Medical School, Italy
Daphne Ang,
Changi General Hospital, Singapore

*CORRESPONDENCE
Yin Zhu
zhuyin27@sina.com

SPECIALTY SECTION
This article was submitted to Infectious Agents and Disease, a section of the journal Frontiers in Microbiology

RECEIVED 21 July 2022
ACCEPTED 20 September 2022
PUBLISHED 18 October 2022

CITATION
Xu X, He C and Zhu Y (2022) Treatment of refractory *Helicobacter pylori* infection: A new challenge for clinicians.
Front. Microbiol. 13:998240.
doi: 10.3389/fmicb.2022.998240

Treatment of refractory *Helicobacter pylori* infection: A new challenge for clinicians

XinBo Xu, Cong He and Yin Zhu*

Department of Gastroenterology, Digestive Disease Hospital, The First Affiliated Hospital of Nanchang University, Nanchang, China

Patients who have failed two or more attempts to eradicate *Helicobacter pylori* are commonly referred to as refractory. Although the incidence of refractory *Helicobacter pylori* infection is only 10–20%, with the increasing rate of antibiotic resistance in various regions, the treatment of refractory *Helicobacter pylori* infection has gradually become a difficult problem faced by clinicians. When choosing a rescue therapy, the physician must consider numerous factors. A longer treatment duration, higher doses of proton pump inhibitors (PPIs), or the use of potassium-competitive acid blocker (P-CAB) may increase the efficacy of triple therapy or bismuth quadruple therapy. Rescue treatment based on bismuth quadruple therapy usually achieves better results. At the same time, treatment based on drug susceptibility tests or genotypic resistance is recommended where available. Of course, appropriate empiric treatment can also be selected according to local drug resistance, a patient's previous medication history and compliance. It is the best choice if it can improve the success rate of the first treatment and reduce the occurrence of refractory *Helicobacter pylori* infection. This review aims to summarize the articles related to refractory *Helicobacter pylori* in recent years and to explore a better remedial treatment plan for clinicians.

KEYWORDS

refractory *Helicobacter pylori* infection, rescue therapy, antibiotic resistance, antibiotic susceptibility testing, empirical treatments

Introduction

Eradication with *Helicobacter pylori* can reduce the recurrence rate of peptic ulcers, reduce the incidence of *Helicobacter pylori*-associated gastritis, cure patients with mucosa-associated lymphoid tissue lymphoma (MALT), and reduce the risk of gastric cancer (Lee et al., 2016; Malfertheiner et al., 2017; Liou et al., 2019). Currently, the eradication rate of clarithromycin triple therapy, a commonly used first-line treatment regimen, is less than 80% (Malfertheiner et al., 2017; Liou et al., 2020), and quadruple

therapy with levofloxacin and bismuth agents is often selected as the second-line treatment (Liou et al., 2010; Fallone et al., 2016). However, approximately 10–20% of patients still fail treatment (Liou et al., 2011, 2016). Patients who fail two or more treatments are often referred to as patients with refractory *Helicobacter pylori* infection, and treating these patients is still a difficult problem in the clinic (Losurdo et al., 2022a). Therefore, we reviewed the evidence from previous studies to identify more appropriate treatment options.

Status of refractory *Helicobacter pylori* infection

Helicobacter pylori is a major carcinogen that can cause gastric cancer, with 1–3% of *Helicobacter pylori* patients eventually developing stomach cancer (Blaser, 2016). Therefore, the eradication of *Helicobacter pylori* plays a very important role in the prevention and control of gastric cancer. Current first-line treatment regimens have good eradication rates. However, antibiotic resistance rates have risen around the world. The success rate of initial eradication is challenged by multiple resistant bacteria (Savoldi et al., 2018; Lin et al., 2021). Accordingly, the occurrence of refractory *Helicobacter pylori* infection is increasing, becoming a concern that cannot be ignored (Liou et al., 2011, 2016). Therefore, it is necessary to perform in-depth research on refractory *Helicobacter pylori* infection to explore its causes and potential treatment modalities.

The causes of treatment failure

Antibiotic resistance

Antibiotic resistance is currently the main cause of refractory *Helicobacter pylori* infection, and antibiotic resistance is mainly a concern for clarithromycin, metronidazole and levofloxacin (Sugano et al., 2015; Malfertheiner et al., 2017). A report published in 2018 looked at antibiotic resistance in 65 countries and territories around the world. The primary and secondary drug resistance rates of clarithromycin, metronidazole and levofloxacin in other regions of the world were $\geq$ 15%, except for the Americas, Southeast Asia and some parts of Europe. However, due to the large heterogeneity of studies in different regions, the results need to be discussed and analyzed separately by region (Kuo et al., 2017; Savoldi et al., 2018; Hulten et al., 2021; Megraud et al., 2021). In the Asia-Pacific region, the drug resistance of clarithromycin, metronidazole and levofloxacin is also serious, and the drug resistance rate of metronidazole is as high as 44% (**Table 1**). In China, studies have shown that secondary resistance to clarithromycin, metronidazole and levofloxacin is greater than 50% and even greater than 90% in some areas. Not only has the prevalence of single-resistant strains increased, but that of double- and multiple-resistant strains has also increased. This has become an important reason for the annual increase in *Helicobacter pylori* eradication failure. In these highly resistant areas, eradication therapies containing clarithromycin, metronidazole and levofloxacin are clearly no longer suitable (Baylina et al., 2019; Li et al., 2020, 2021; Kuo et al., 2021; Resina and Gisbert, 2021). How to choose antibiotics to eradicate *Helicobacter pylori* is a new challenge for clinicians (Savoldi et al., 2018).

Helicobacter pylori-related factors

Helicobacter pylori can increase its resistance to antibiotics through mutation of drug resistance genes. Studies have shown that *Helicobacter pylori* can increase its resistance to metronidazole by upregulating the expression of hefA, a key gene of the drug efflux pump, and mutation of rdxA (Lee et al., 2018a). Mutations in the A2142G and A2143G loci may lead to increased clarithromycin resistance (Hamza et al., 2018). Other studies have also shown that gyrA, 23S rRNA and 16S rRNA mutations in *Helicobacter pylori* are also responsible for other increased resistance (Nezami et al., 2019). In addition, *Helicobacter pylori* can also escape the effects of antibiotics through internalization. Research by Apolinaria Garcia-Cancino revealed that *Helicobacter pylori* can hide in Candida albicans under clarithromycin and amoxicillin and avoid their effects (Sánchez-Alonzo et al., 2021). At the same time, another study revealed that *Helicobacter pylori* entered the gastric mucosal tissues of patients in whom *Helicobacter pylori* eradication had failed, mainly in the gastric body (95.2%). Standard clarithromycin-containing triple therapy failed even though the internalized *Helicobacter pylori* was mostly clarithromycin-sensitive, suggesting that cellular internalization of *Helicobacter pylori* may have contributed to the failure (Beer et al., 2021). In addition, *Helicobacter pylori* will activate the chromosomal type I toxin antitoxin system (AapA1 IsoA1) under the oxidative stress, and further express AapA1 toxin to induce the formation of coccoids, so as to avoid the influence of antibiotics. This process did not destroy the integrity of *Helicobacter pylori* biofilm and did not produce changes in membrane potential, which may be related to the interference of cell elongation/division interference. But the specific mechanism still needs more research and discussion (El Mortaji et al., 2020).

Host factors

Host factors are also important causes of refractory *Helicobacter pylori* infection. Most proton pump inhibitors (PPIs) need to be metabolized through the CYP2C19 pathway, and the metabolic type of CYP2C19 can affect the eradication effect of *Helicobacter pylori* by affecting the metabolism of PPIs. Patients with the fast metabolic type need to increase the

TABLE 1 Antibiotics resistance of *Helicobacter pylori*.

References	Region	Antibiotic resistance		
		Clarithromycin	Metronidazole	Levofloxacin
Megraud et al. (2021)	European	21.4%	38.9%	15.8%
Hulten et al. (2021)	The United States	17.4%	43.9%	57.8%
Kuo et al. (2017)	Asia	17%	44%	18%
Camargo et al. (2014)	Latin America	12%	53%	15%
Savoldi et al. (2018)	Africa	15%	91%	14%

dose of PPIs to maintain a high eradication rate (Fontes et al., 2019). Studies have shown that vitamin D can affect *Helicobacter pylori* colonization and eradication by affecting the autophagy pathway, and the eradication rate of *Helicobacter pylori* is low in patients with vitamin D deficiency (Hu et al., 2019; Shatla et al., 2021). The family environment is also one of the possible causes of eradication failure. *Helicobacter pylori* is easily transmitted among family members. Studies have shown that there is a significant correlation between a history of eradication failure in parents and eradication failure in offspring (Deguchi et al., 2019; Ding et al., 2022). Therefore, emphasis should be placed on the eradication of *Helicobacter pylori* in the home. Older age, prior eradication treatment, and a history of PPI use also increased the risk of eradication failure (Yan et al., 2020). Otherwise, studies have suggested that smoking, non-alcoholic fatty liver disease, and human immunodeficiency virus (HIV) infection may have contributed to the failure of eradication, but more research is needed to confirm these results (Itskoviz et al., 2017; Hanafy and Seleem, 2019; Takara et al., 2019; Nkuize et al., 2021).

Options for rescue treatment: Antibiotic-susceptibility testing or empirical treatment

Antibiotic-susceptibility testing

How should rescue treatment be chosen? We generally have two options: experiential treatment and drug sensitivity-guided regimens, both of which have their own advantages. With the increase in antibiotic resistance rates in various regions of the world, drug sensitivity-guided regimens are increasingly being chosen by more clinicians. The advantage of drug sensitivity guidance is to be able to know the individual's sensitivity to antibiotics and to use sensitive antibiotics specifically to increase the success rate of eradication. Not only is this approach recommended in the guidelines, but many regional studies provide strong evidence to support this view (Lee et al., 2016; Malfertheiner et al., 2017; Liou et al., 2019). The study revealed that in patients with more than two eradication failures, the eradication rate of both the triple and quadruple regimens guided by drug sensitivity reached more than 90%, especially in patients with penicillin allergy. The treatment guided by drug sensitivity achieved almost perfect results, with an eradication rate as high as 99% (Huang et al., 2018; Yu et al., 2019; Luo et al., 2020; Gingold-Belfer et al., 2021; Lee et al., 2021). However, not all hospitals meet the criteria necessary to carry out drug sensitivity testing because it requires great laboratories and professional testing personnel. This is the reason why drug-sensitive guided treatment is not widely available (Gisbert, 2020).

Empirical treatment

Empirical treatment is more acceptable because it does not require additional testing to evaluate drug sensitivities. However, clinicians need to predict the effectiveness of treatment options based on local epidemiology, population resistance, and whether patients have been previously exposed to antibiotics for any reason (Gisbert, 2020). Although empirical therapy cannot provide individualized precision treatment compared with drug sensitivity therapy, it is an alternative in areas lack of medical facilities for laboratory testing. Moreover, there are also more studies showing that empirical treatment of refractory *Helicobacter pylori* infection has a good effect, with an eradication rate of 75–90% (Gisbert, 2020; Ji et al., 2020; Nyssen et al., 2021). Since the main resistant antibiotics are clarithromycin, levofloxacin and metronidazole, more studies are needed to investigate the efficacy of other antibiotics as an empirical treatment option.

Dosage and selection of proton pump inhibitors

Due to polymorphism in the CYP2C19 gene among patients, the dose of PPIs will affect the efficacy of eradication therapy. In clinical trials, 20 mg (low dose) and 40 mg (high dose) are usually used for comparison (Graham et al., 2019). High doses of PPI significantly improved the outcome of standard triple therapy (Katelaris and Katelaris, 2017;Ierardi et al., 2019;

TABLE 2 Eradication rate of tetracycline-containing rescue therapy.

References	Dosing frequency	Duration of therapy	Eradication rate %
Nyssen et al. (2020)	Tetracycline 500 mg qid; metronidazole 500 mg tid; bismuth 240 bid; PPI 20 mg bid	10/14	Over all: 77%; PP:NA ITT:NA
Kim et al. (2022)	Tetracycline 1 g bid; metronidazole 500 mg tid; bismuth 600 mg bid; PPI 20 mg bid	14	Over all: 92.5% PP:NA ITT:NA
Hsu et al. (2021)	Tetracycline 500 mg qid; levofloxacin 500 mg qd; bismuth 300 mg qid; PPI 40 mg bid	10	Over all:NA ITT:89.3% PP:89.1%
Shin et al. (2021)	Tetracycline 500 mg qid; metronidazole 500 mg tid; bismuth 120 mg qid; PPI 20 mg bid	7/10/14	Over all:NA ITT:80.7% PP:93.3%
Losurdo et al. (2022b)	Pylera (Tetracycline/ metronidazole/bismuth) bid; PPI 20 mg bid	10	Over all:NA ITT:84.9% PP:86.1%
De Francesco et al. (2021)	Pylera (Tetracycline/ metronidazole/bismuth) bid; PPI 20 mg bid	–	Over all:NA ITT:90.6% PP:94%
Fiorini et al. (2017)	Pylera (Tetracycline/ metronidazole/bismuth) bid; PPI 20 mg bid	10	Over all:NA ITT:81% PP:87%

Losurdo et al., 2022b). Therefore, a double dose of PPIs is recommended for rescue therapy. In addition, the selection of new-generation PPIs to replace existing drugs is also an option to improve treatment effectiveness. Such as Rabeprazole, Esomperazole, they are less affected by CYP2C19 polymorphisms. A Japanese study showed that a 7-day triple therapy based on vonoprazan proved superior to lansoprazole-based triple therapy for 7 days. This is especially true in patients infected with clarithromycin-resistant strains (Murakami et al., 2016). Another Japanese study showed that the annual eradication rates of second-line therapy between 2013 and 2018 were 90, 82.6, 88.8, 87.5, 91.8, and 90.1%, respectively. The use of vanorazan was an independent factor in the success of second-line treatment (Mori et al., 2019).

New antibiotics

It is very important to optimize the treatment plan and choose more efficient antibiotics for rescue treatment. We need to find some antibiotics that are more effective as rescue treatment and in how they are administered. In past reports of rescue treatment, tetracycline and rifabutin were assessed in many studies, and both achieved good results. In recent years, many studies have reported the role of tetracycline in remedial therapy. Two studies from Taiwan, China, compared the efficacy of tetracycline regimens in rescue therapy. The first study compared the 10-day TL regimen (tetracycline plus levofloxacin bismuth quadruple regimen) with the AL triple regimen (amoxicillin plus levofloxacin triple regimen) in remedial therapy. The eradication rate in the TL group was 98% higher than that in the AL group (69.2%) (Hsu et al., 2017). Another study compared the 10-day TL regimen with the AL regimen as a remedial treatment for *Helicobacter pylori*. The eradication rate of 89.3% in the TL group was only 69.6% in the AL group, and the eradication rate of levofloxacin-resistant strains in the TL group was also higher than that in the AL group (Hsu et al., 2021). The 10–14-day regimen was associated with a higher eradication rate than the 7-day regimen with tetracycline (Shin et al., 2021). Studies have shown that the minimum inhibitory concentration (MIC) of tetracycline can achieve a better effect as long as it reaches 0.094 mg/L (Hsieh et al., 2020). At the same time, the Korean study compared the eradication rate of the tetracycline regimen with different dosing methods, and the dosage of 2,000 mg tetracycline per day, whether 500 mg qid or 1,000 mg bid, had a good eradication effect (Kim et al., 2022). Otherwise, many studies have reported that the Pylera three-in-one capsule combined with PPI achieved a good curative effect in remedial treatment.

In addition to tetracycline, many studies have reported the role of other antibiotics in rescue treatment (**Table 2**). A meta-analysis showed that quinolones are the best second-line treatment option in Western countries (Yeo et al., 2019). Antofloxacin is a new quinolone drug. A Chinese study compared antofloxacin with a 14-day triple therapy with levofloxacin. The eradication rate of the levofloxacin group was higher than that of the antofloxacin group (87.6 vs. 68.5%) when the levofloxacin resistance rate was over 40%. Antofloxacin has both good efficacy and safety (Mori et al., 2020; He et al., 2022). Second, previous reports have

TABLE 3 Eradication rate of rifabutin-containing rescue therapy.

References	Dosing frequency	Duration of therapy	Eradication rate %
Kuo et al. (2020)	Rifabutin 150 mg bid; amoxicillin 1 g bid; PPI 40 mg bid	10	Over all:79.5% ITT:NA PP:NA
Fiorini et al. (2018)	Rifabutin 150 mg bid; amoxicillin 1 g bid; PPI 40 mg bid	12	Over all:NA ITT:82.9% PP:88.7%
Hirata et al. (2020)	Rifabutin 150 mg bid; amoxicillin 750 mg bid; PPI 20 mg bid	10	Over all:NA ITT:100% PP:100%
Saracino et al. (2020)	Rifabutin 150 mg bid; amoxicillin 1 g bid; PPI 40 mg bid	12	Over all:NA ITT:51.9% PP:61.9%
Ribaldone et al. (2019)	Rifabutin 150 mg bid; amoxicillin 1 g bid; PPI 20 mg bid	14	Over all:NA ITT:71.5% PP:72.7%

demonstrated that furazolidone has a good eradication effect in first-line treatment. It also had a significant effect on rescue therapy in patients who had failed previous clarithromycin or levofloxacin quadruple therapy. The 14-day quadruple furazolidone regimen achieved 90% eradication in patients with clarithromycin and levofloxacin resistance rates of more than 40% (Kong et al., 2020; Resina and Gisbert, 2021). However, some countries do not allow the use of furazolidone for safety reasons, so more studies are needed to explore the safety of furazolidone use. Otherwise, a large number of studies have reported the efficacy of rifabutin in rescue therapy (Ierardi et al., 2014; Nyssen et al., 2022; **Table 3**). Studies have shown that rifabutin triple therapy has an obvious antibacterial effect on multiple drug-resistant *Helicobacter pylori*, and the eradication rate can reach more than 80% (Fiorini et al., 2018; Siavoshi et al., 2018; Ribaldone et al., 2019; Kuo et al., 2020). At present, the main rescue therapy contains rifabutin, amoxicillin and PPIs. More studies are needed to compare the efficacy of other antibiotics combined with rifabutin in rescue therapy. In conclusion, in the absence of drug sensitivity guidance, clinicians should consider the use of the above antibiotics to address refractory *Helicobacter pylori* infection.

Duration of therapy

Insufficient time is also an important factor in eradication failure. A treatment duration extended by 14 days with triple therapy was superior to the same regimen of 7 or 10 days with first-line therapy (Yuan et al., 2013). Therefore, various guidelines recommend a duration of 14 days for first-line treatment, unless shorter durations are locally proven to be non-inferior and yield reliably high success rates (Fallone et al., 2016; Liou et al., 2018). Among second- or third-line treatments, the cure rates of levofloxacin triple therapy at 7, 10, and 14 days were 58.3, 68.2, and 93.3%, respectively (Noh et al., 2016). However, the benefit of extending treatment to 14 days was minimal in susceptible strains (Liou et al., 2018). In strains resistant to clarithromycin, the eradication rate can be increased due to the effect of PPI-amoxicillin dual therapy. In summary, we recommend 14 days of treatment for refractory *Helicobacter pylori*.

Other treatments

Does the addition of adjunctive agents on a triple or quadruple basis increase the efficacy of remedial therapy? In recent years, many studies have combined probiotics, biological extracts, traditional Chinese medicine and other adjuvant drugs with traditional therapy to increase the eradication effect of rescue treatment. A study from China treated patients with refractory *Helicobacter pylori* with Lactobacillus for 2 weeks followed by 10-day quadruplex therapy with tetracycline and furazolidone as rescue treatment. The overall eradication rate was 92% in the intention-to-treat (ITT) analysis and 91.8% in the Per-Protocol (PP) analysis, with fewer adverse reactions and a good safety profile (Liu et al., 2020). The Iranian study also found that in patients in whom eradication had failed, quadruple therapy containing Lactobacillus was more effective as a rescue therapy than non-probiotic treatment (Karbalaei and Keikha, 2021). In addition, there are also studies on the role of traditional Chinese medicine as an adjuvant therapy in remedial therapy. A Chinese meta-analysis revealed that integrated traditional Chinese and Western medicine treatment had a higher eradication rate and fewer adverse reactions than Western medicine alone (OR 2.21, 95% CI: 1.74, 2.81) (Zhong et al., 2022). Other studies demonstrated that the combination of berberine or WUZHUYUTANG combined with the antibiotic

bismuth can improve the eradication effect of rescue treatment (Nagata et al., 2018; Zhang et al., 2020). However, these studies were only conducted in China, and more Western studies are needed to confirm whether this treatment is suitable for patients in other parts of the world. It was also found that the extracts of lime could inhibit the growth and urease activity of clarithromycin, metronidazole and levofloxacin triple-drug-resistant strains; therefore, these extracts could have therapeutic potential (Lee et al., 2018b).

Conclusion

In conclusion, in the remedial treatment of refractory *Helicobacter pylori* infection, it is recommended to use a higher dose of PPI quadruple therapy for 14 days, and vonoprazan is a better choice when necessary. When conditions permit, it is recommended to use drug sensitivity tests or genotype resistance guidance therapy. Of course, taking into account the economy, compliance and feasibility of patients, appropriate empiric treatment can be an acceptable alternative to drug sensitivity treatment based on previous drug use and prevailing drug resistance in the region. Tetracycline, furazolidone, rifambutin, or a new generation of quinolone-based therapy or bismuth quadruple therapy may be a good option. Further large randomized studies are needed to determine the best treatment for refractory *Helicobacter pylori* infection.

Author contributions

CH: give the idea. XX: write the article. YZ: offer a suggestion. All authors contributed to the article and approved the submitted version.

Funding

This work was supported by the National Natural Science Foundation of China (81860106 and 82170580).

Conflict of interest

The authors declare that the research was conducted in the absence of any commercial or financial relationships that could be construed as a potential conflict of interest.

Publisher's note

All claims expressed in this article are solely those of the authors and do not necessarily represent those of their affiliated organizations, or those of the publisher, the editors and the reviewers. Any product that may be evaluated in this article, or claim that may be made by its manufacturer, is not guaranteed or endorsed by the publisher.

References

Baylina, M., Muñoz, N., Sánchez-Delgado, J., López-Góngora, S., Calvet, X., and Puig, I. (2019). Systematic review: Would susceptibility-guided treatment achieve acceptable cure rates for second-line *Helicobacter pylori* therapy as currently practiced? *Helicobacter* 24:e12584. doi: 10.1111/hel.12584

Beer, A., Hudler, H., Hader, M., Kundi, M., Hudler, S., Täuber, V., et al. (2021). Apparent intracellular *Helicobacter pylori* detected by immunohistochemistry: The missing link in eradication failure. *Clin. Infect. Dis.* 73, e1719–e1726. doi: 10.1093/cid/ciaa839

Blaser, M. J. (2016). Antibiotic use and its consequences for the normal microbiome. *Science* 352, 544–545.

Camargo, M. C., García, A., Riquelme, A., Otero, W., Camargo, C. A., Hernandez-García, T., et al. (2014). The problem of *Helicobacter pylori* resistance to antibiotics: A systematic review in Latin America. *Am. J. Gastroenterol.* 109, 485–495.

De Francesco, V., Zullo, A., Gatta, L., Manta, R., Pavoni, M., Saracino, I. M., et al. (2021). Rescue therapies for *H. pylori* infection in Italy. *Antibiotics* 10:525.

Deguchi, H., Yamazaki, H., Yamamoto, Y., and Fukuhara, S. (2019). Association between parental history of *Helicobacter pylori* treatment failure and treatment failure in the offspring. *J. Gastroenterol. Hepatol.* 34, 2112–2117.

Ding, S. Z., Du, Y. Q., Lu, H., Wang, W. H., Cheng, H., Chen, S. Y., et al. (2022). Chinese consensus report on family-based *Helicobacter pylori* infection control and management (2021 Edition). *Gut* 71, 238–253. doi: 10.1136/gutjnl-2021-325630

El Mortaji, L., Tejada-Arranz, A., Rifflet, A., Boneca, I. G., Pehau-Arnaudet, G., Radicella, J. P., et al. (2020). A peptide of a type I toxin-antitoxin system induces *Helicobacter pylori* morphological transformation from spiral shape to coccoids. *Proc. Natl. Acad. Sci. U.S.A.* 117, 31398–31409. doi: 10.1073/pnas.2016195117

Fallone, C. A., Chiba, N., van Zanten, S. V., Fischbach, L., Gisbert, J. P., Hunt, R. H., et al. (2016). The Toronto consensus for the treatment of *Helicobacter pylori* infection in adults. *Gastroenterology* 151, 51–69.e14.

Fiorini, G., Saracino, I. M., Zullo, A., Gatta, L., Pavoni, M., and Vaira, D. (2017). Rescue therapy with bismuth quadruple regimen in patients with *Helicobacter pylori* -resistant strains. *Helicobacter* 22, 113–130. doi: 10.1111/hel.12448

Fiorini, G., Zullo, A., Vakil, N., Saracino, I. M., Ricci, C., Castelli, V., et al. (2018). Rifabutin triple therapy is effective in patients with multidrug-resistant strains of *Helicobacter pylori*. *J. Clin. Gastroenterol.* 52, 137–140. doi: 10.1097/MCG.0000000000000540

Fontes, L. E. S., Martimbianco, A. L. C., Zanin, C., and Riera, R. (2019). N-acetylcysteine as an adjuvant therapy for *Helicobacter pylori* eradication. *Cochrane Database Syst. Rev.* 2:CD012357.

Gingold-Belfer, R., Niv, Y., Schmilovitz-Weiss, H., Levi, Z., and Boltin, D. (2021). Susceptibility-guided versus empirical treatment for *Helicobacter pylori* infection: A systematic review and meta-analysis. *J. Gastroenterol. Hepatol.* 36, 2649–2658.

Gisbert, J. P. (2020). Empirical or susceptibility-guided treatment for *Helicobacter pylori* infection? A comprehensive review. *Ther. Adv. Gastroenterol.* 13:175628482096873 6.

Graham, D. Y., Lu, H., and Dore, M. P. (2019). Relative potency of proton-pump inhibitors, *Helicobacter pylori* therapy cure rates, and meaning of double-dose PPI. *Helicobacter* 24:e12554. doi: 10.1111/hel.12554

Hamza, D., Elhelw, R., Elhariri, M., and Ragab, E. (2018). Genotyping and antimicrobial resistance patterns of *Helicobacter pylori* in human and dogs associated with A2142G and A2143G point mutations in clarithromycin resistance. *Microb. Pathog.* 123, 330–338. doi: 10.1016/j.micpath.2018.07.016

Hanafy, A. S., and Seleem, W. M. (2019). Refractory *Helicobacter pylori* gastritis: The hidden predictors of resistance. *J. Glob. Antimicrob. Resist.* 19, 194–200. doi: 10.1016/j.jgar.2019.05.015

He, X. J., Zeng, X. P., Jiang, C. S., Liu, G., Li, D. Z., and Wang, W. (2022). Efficacy and safety of antofloxacin-based triple therapy for *Helicobacter pylori* eradication failure in China. *Dig. Dis. Sci.* 67, 208–215. doi: 10.1007/s10620-021-06856-z

Hirata, Y., Yamada, A., Niikura, R., Shichijo, S., Hayakawa, Y., and Koike, K. (2020). Efficacy and safety of a new rifabutin-based triple therapy with vonoprazan for refractory *Helicobacter pylori* infection: A prospective single-arm study. *Helicobacter* 25:e12719. doi: 10.1111/hel.12719

Hsieh, M. T., Chang, W. L., Wu, C. T., Yang, H. B., Kuo, H. Y., Lin, M. Y., et al. (2020). Optimizing the MIC breakpoints of amoxicillin and tetracycline for antibiotic selection in the rescue therapy of *H. pylori* with bismuth quadruple regimen. *Eur. J. Clin. Pharmacol.* 76, 1581–1589. doi: 10.1007/s00228-020-02938-5

Hsu, P. I., Tsai, F. W., Kao, S. S., Hsu, W. H., Cheng, J. S., Peng, N. J., et al. (2017). Ten-day quadruple therapy comprising proton pump inhibitor, bismuth, tetracycline, and levofloxacin is more effective than standard levofloxacin triple therapy in the second-line treatment of *Helicobacter pylori* infection: A randomized controlled trial. *Am. J. Gastroenterol.* 112, 1374–1381. doi: 10.1038/ajg.2017.195

Hsu, P. I., Tsay, F. W., Kao, J. Y., Peng, N. J., Chen, Y. H., Tang, S. Y., et al. (2021). Tetracycline-levofloxacin versus amoxicillin-levofloxacin quadruple therapies in the second-line treatment of *Helicobacter pylori* infection. *Helicobacter* 26:e12840. doi: 10.1111/hel.12840

Hu, W., Zhang, L., Li, M. X., Shen, J., Liu, X. D., Xiao, Z. G., et al. (2019). Vitamin D3 activates the autolysosomal degradation function against *Helicobacter pylori* through the PDIA3 receptor in gastric epithelial cells. *Autophagy* 15, 707–725. doi: 10.1080/15548627.2018.1557835

Huang, H. T., Wang, H. M., Yang, S. C., Tai, W. C., Liang, C. M., Wu, K. L., et al. (2018). Efficacy of a 14-day quadruple-therapy regimen for third-line *Helicobacter pylori* eradication. *Infect. Drug Resist.* 11, 2073–2080. doi: 10.2147/IDR.S185511

Hulten, K. G., Lamberth, L. B., Kalfus, I. N., and Graham, D. Y. (2021). National and regional US antibiotic resistance to *Helicobacter pylori*: Lessons from a clinical trial. *Gastroenterology* 161, 342–344e341. doi: 10.1053/j.gastro.2021.03.045

Ierardi, E., Giangaspero, A., Losurdo, G., Giorgio, F., Amoruso, A., De Francesco, V., et al. (2014). Quadruple rescue therapy after first and second line failure for *Helicobacter pylori* treatment: Comparison between two tetracycline-based regimens. *J. Gastrointestin. Liver Dis.* 23, 367–370. doi: 10.15403/jgld.2014.1121.234.qrth

Ierardi, E., Losurdo, G., Fortezza, R. F., Principi, M., Barone, M., and Leo, A. D. (2019). Optimizing proton pump inhibitors in *Helicobacter pylori* treatment: Old and new tricks to improve effectiveness. *World J. Gastroenterol.* 25, 5097–5104. doi: 10.3748/wjg.v25.i34.5097

Itskoviz, D., Boltin, D., Leibovitzh, H., Tsadok Perets, T., Comaneshter, D., Cohen, A., et al. (2017). Smoking increases the likelihood of *Helicobacter pylori* treatment failure. *Dig. Liver Dis.* 49, 764–768. doi: 10.1016/j.dld.2017.03.010

Ji, C. R., Liu, J., Li, Y. Y., Qiao, C., Qu, J. Y., Hu, J. N., et al. (2020). Susceptibility-guided quadruple therapy is not superior to medication history-guided therapy for the rescue treatment of *Helicobacter pylori* infection: A randomized controlled trial. *J. Dig. Dis.* 21, 549–557.

Karbalaei, M., and Keikha, M. (2021). Rescue effects of *Lactobacillus*-containing bismuth regimens after *Helicobacter pylori* treatment failure. *New Microbes New Infect.* 42:100904. doi: 10.1016/j.nmni.2021.100904

Katelaris, P. H., and Katelaris, A. L. (2017). A prospective evaluation of levofloxacin-based triple therapy for refractory *Helicobacter pylori* infection in Australia. *Intern. Med. J.* 47, 761–766. doi: 10.1111/imj.13432

Kim, J., Gong, E. J., Seo, M., Seo, H. I., Park, J. K., Lee, S. J., et al. (2022). Efficacy of twice a day bismuth quadruple therapy for second-line treatment of *Helicobacter pylori* infection. *J. Pers. Med.* 12:56.

Kong, S., Huang, K., Wang, J., Wang, X., Yang, N., Dong, Y., et al. (2020). Efficacy of tailored second-line therapy of *Helicobacter pylori* eradication in patients with clarithromycin-based treatment failure: A multicenter prospective study. *Gut Pathog.* 12:39. doi: 10.1186/s13099-020-00378-1

Kuo, C. J., Lee, C. H., Chang, M. L., Lin, C. Y., Lin, W. R., Su, M. Y., et al. (2021). Multidrug resistance: The clinical dilemma of refractory *Helicobacter pylori* infection. *J. Microbiol. Immunol. Infect.* 54, 1184–1187. doi: 10.1016/j.jmii.2021.03.006

Kuo, C. J., Lin, C. Y., Le, P. H., Chang, P. Y., Lai, C. H., Lin, W. R., et al. (2020). Rescue therapy with rifabutin regimen for refractory *Helicobacter pylori* infection with dual drug-resistant strains. *BMC Gastroenterol.* 20:218. doi: 10.1186/s12876-020-01370-4

Kuo, Y. T., Liou, J. M., El-Omar, E. M., Wu, J. Y., Leow, A. H. R., Goh, K. L., et al. (2017). Primary antibiotic resistance in *Helicobacter pylori* in the Asia-Pacific region: A systematic review and meta-analysis. *Lancet Gastroenterol. Hepatol.* 2, 707–715.

Lee, J. W., Kim, N., Nam, R. H., Jang, J. Y., Choi, Y., and Lee, D. H. (2021). Favorable outcomes of rescue second- or third-line culture-based *Helicobacter pylori* eradication treatment in areas of high antimicrobial resistance. *Helicobacter* 26:e12844.

Lee, S. M., Kim, N., Kwon, Y. H., Nam, R. H., Kim, J. M., Park, J. Y., et al. (2018a). rdxA, frxA, and efflux pump in metronidazole-resistant *Helicobacter pylori*: Their relation to clinical outcomes. *J. Gastroenterol. Hepatol.* 33, 681–688. doi: 10.1111/jgh.13906

Lee, S. M., Park, S. Y., Kim, M. J., Cho, E. A., Jun, C. H., Park, C. H., et al. (2018b). Key lime (*Citrus aurantifolia*) inhibits the growth of triple drug resistant *Helicobacter pylori*. *Gut Pathog.* 10:16. doi: 10.1186/s13099-018-0244-y

Lee, Y. C., Chiang, T. H., Chou, C. K., Tu, Y. K., Liao, W. C., Wu, M. S., et al. (2016). Association between *Helicobacter pylori* eradication and gastric cancer incidence: A systematic review and meta-analysis. *Gastroenterology* 150, 1113–1124.e5.

Li, J., Deng, J., Wang, Z., Li, H., and Wan, C. (2020). Antibiotic resistance of *Helicobacter pylori* strains isolated from pediatric patients in Southwest China. *Front. Microbiol.* 11:621791. doi: 10.3389/fmicb.2020.621791

Li, S. Y., Li, J., Dong, X. H., Teng, G. G., Zhang, W., Cheng, H., et al. (2021). The effect of previous eradication failure on antibiotic resistance of *Helicobacter pylori*: A retrospective study over 8 years in Beijing. *Helicobacter* 26:e12804. doi: 10.1111/hel.12804

Lin, Y., Zheng, Y., Wang, H. L., and Wu, J. (2021). Global patterns and trends in gastric cancer incidence rates (1988-2012) and predictions to 2030. *Gastroenterology* 161, 116–127.e8. doi: 10.1053/j.gastro.2021.03.023

Liou, J. M., Bair, M. J., Chen, C. C., Lee, Y. C., Chen, M. J., Chen, C. C., et al. (2016). Levofloxacin sequential therapy vs levofloxacin triple therapy in the second-line treatment of *Helicobacter pylori*: A randomized trial. *Am. J. Gastroenterol.* 111, 381–387. doi: 10.1038/ajg.2015.439

Liou, J. M., Chen, C. C., Chen, M. J., Chang, C. Y., Fang, Y. J., Lee, J. Y., et al. (2011). Empirical modified sequential therapy containing levofloxacin and high-dose esomeprazole in second-line therapy for *Helicobacter pylori* infection: A multicentre clinical trial. *J. Antimicrob. Chemother.* 66, 1847–1852. doi: 10.1093/jac/dkr217

Liou, J. M., Chen, P. Y., Kuo, Y. T., and Wu, M. S. (2018). Toward population specific and personalized treatment of *Helicobacter pylori* infection. *J. Biomed. Sci.* 25:70. doi: 10.1186/s12929-018-0471-z

Liou, J. M., Lee, Y. C., El-Omar, E. M., and Wu, M. S. (2019). Efficacy and long-term safety of *H. pylori* eradication for gastric cancer prevention. *Cancers* 11:593.

Liou, J. M., Lin, J. T., Chang, C. Y., Chen, M. J., Cheng, T. Y., Lee, Y. C., et al. (2010). Levofloxacin-based and clarithromycin-based triple therapies as first-line and second-line treatments for *Helicobacter pylori* infection: A randomised comparative trial with crossover design. *Gut* 59, 572–578. doi: 10.1136/gut.2009.198309

Liou, J. M., Malfertheiner, P., Lee, Y. C., Sheu, B. S., Sugano, K., Cheng, H. C., et al. (2020). Screening and eradication of *Helicobacter pylori* for gastric cancer prevention: The Taipei global consensus. *Gut* 69, 2093–2112. doi: 10.1136/gutjnl-2020-322368

Liu, A., Wang, Y., Song, Y., and Du, Y. (2020). Treatment with compound *Lactobacillus acidophilus* followed by a tetracycline- and furazolidone-containing quadruple regimen as a rescue therapy for *Helicobacter pylori* infection. *Saudi J. Gastroenterol.* 26, 78–83. doi: 10.4103/sjg.SJG_589_19

Losurdo, G., D'Abramo, F. S., Piazzolla, M., Rima, R., Continisio, A., Pricci, M., et al. (2022a). Second line therapy for *Helicobacter pylori* eradication: State of art. *Mini Rev. Med. Chem.* 22, 2430–2437.

Losurdo, G., Lacavalla, I., Russo, F., Riezzo, G., Brescia, I. V., Rendina, M., et al. (2022b). Empiric "Three-in-One" bismuth quadruple therapy for second-line *Helicobacter pylori* eradication: An intervention study in Southern Italy. *Antibiotics* 11:78. doi: 10.3390/antibiotics11010078

Luo, L., Huang, Y., Liang, X., Ji, Y., Yu, L., and Lu, H. (2020). Susceptibility-guided therapy for *Helicobacter pylori*-infected penicillin-allergic patients: A prospective clinical trial of first-line and rescue therapies. *Helicobacter* 25:e12699. doi: 10.1111/hel.12699

Malfertheiner, P., Megraud, F., O'Morain, C. A., Gisbert, J. P., Kuipers, E. J., Axon, A. T., et al. (2017). Management of *Helicobacter pylori* infection-the Maastricht V/Florence consensus report. *Gut* 66, 6–30. doi: 10.1136/gutjnl-2016-312288

Megraud, F., Bruyndonckx, R., Coenen, S., Wittkop, L., Huang, T. D., Hoebeke, M., et al. (2021). *Helicobacter pylori* resistance to antibiotics in Europe in 2018 and its relationship to antibiotic consumption in the community. *Gut* 70, 1815–1822. doi: 10.1136/gutjnl-2021-324032

Mori, H., Suzuki, H., Matsuzaki, J., Masaoka, T., and Kanai, T. (2020). 10-year trends in *Helicobacter pylori* eradication rates by sitafloxacin-based third-line rescue therapy. *Digestion* 101, 644–650. doi: 10.1159/000501610

Mori, H., Suzuki, H., Omata, F., Masaoka, T., Asaoka, D., Kawakami, K., et al. (2019). Current status of first- and second-line *Helicobacter pylori* eradication therapy in the metropolitan area: A multicenter study with a large number of patients. *Ther. Adv. Gastroenterol.* 12:1756284819858511. doi: 10.1177/1756284819858511

Murakami, K., Sakurai, Y., Shiino, M., Funao, N., Nishimura, A., and Asaka, M. (2016). Vonoprazan, a novel potassium-competitive acid blocker, as a component of first-line and second-line triple therapy for *Helicobacter pylori* eradication: A phase III, randomised, double-blind study. *Gut* 65, 1439–1446. doi: 10.1136/gutjnl-2015-311304

Nagata, Y., Nagasaka, K., Koyama, S., Murase, M., Saito, M., Yazaki, T., et al. (2018). Successful eradication of *Helicobacter pylori* with a herbal medicine, goshuyuto (Wu Zhu Yu Tang), plus rabeprazole after failure of triplet therapy with Vonoprazan: A report of three cases. *J. Dig. Dis.* 19, 439–442. doi: 10.1111/1751-2980.12537

Nezami, B. G., Jani, M., Alouani, D., Rhoads, D. D., and Sadri, N. (2019). *Helicobacter pylori* mutations detected by next-generation sequencing in formalin-fixed, paraffin-embedded gastric biopsy specimens are associated with treatment failure. *J. Clin. Microbiol.* 57:e01834-18. doi: 10.1128/JCM.01834-18

Nkuize, M., Vanderpas, J., Buset, M., Delforge, M., Cadière, G. B., and De Wit, S. (2021). Failure to eradicate *Helicobacter pylori* infection is more frequent among HIV-positive patients. *HIV Med.* 22, 547–556. doi: 10.1111/hiv.13083

Noh, H. M., Hong, S. J., Han, J. P., Park, K. W., Lee, Y. N., Lee, T. H., et al. (2016). Eradication rate by duration of third-line rescue therapy with levofloxacin after *Helicobacter pylori* treatment failure in clinical practice. *Korean J. Gastroenterol.* 68, 260–264. doi: 10.4166/kjg.2016.68.5.260

Nyssen, O. P., Perez-Aisa, A., Rodrigo, L., Castro, M., Mata Romero, P., Ortuño, J., et al. (2020). Bismuth quadruple regimen with tetracycline or doxycycline versus three-in-one single capsule as third-line rescue therapy for *Helicobacter pylori* infection: Spanish data of the European *Helicobacter pylori* registry (Hp-EuReg). *Helicobacter* 25:e12722.

Nyssen, O. P., Vaira, D., Pérez Aísa, Á., Rodrigo, L., Castro-Fernandez, M., Jonaitis, L., et al. (2021). Empirical second-line therapy in 5000 patients of the European registry on *Helicobacter pylori* management (Hp-EuReg). *Clin. Gastroenterol. Hepatol.* 20, 2243–2257. doi: 10.1016/j.cgh.2021.12.025

Nyssen, O. P., Vaira, D., Saracino, I. M., Fiorini, G., Caldas, M., Bujanda, L., et al. (2022). Experience with rifabutin-containing therapy in 500 patients from the European registry on *Helicobacter pylori* management (Hp-EuReg). *J. Clin. Med.* 11:1658. doi: 10.3390/jcm11061658

Resina, E., and Gisbert, J. P. (2021). Rescue therapy with furazolidone in patients with at least five eradication treatment failures and multi-resistant *H. pylori* infection. *Antibiotics* 10:1028. doi: 10.3390/antibiotics10091028

Ribaldone, D. G., Fagoonee, S., Astegiano, M., Durazzo, M., Morgando, A., Sprujevnik, T., et al. (2019). Rifabutin-based rescue therapy for *Helicobacter pylori* eradication: A long-term prospective study in a large cohort of difficult-to-treat patients. *J. Clin. Med.* 8:199. doi: 10.3390/jcm8020199

Sánchez-Alonzo, K., Belmar, L., Parra-Sepúlveda, C., Bernasconi, H., Campos, V. L., Smith, C. T., et al. (2021). Antibiotics as a stressing factor triggering the harboring of *Helicobacter pylori* J99 within *Candida albicans* ATCC10231. *Pathogens* 10:382. doi: 10.3390/pathogens10030382

Saracino, I. M., Pavoni, M., Zullo, A., Fiorini, G., Saccomanno, L., Lazzarotto, T., et al. (2020). Rifabutin-based triple therapy or bismuth-based quadruple regimen as rescue therapies for *Helicobacter pylori* infection. *Eur. J. Intern. Med.* 81, 50–53.

Savoldi, A., Carrara, E., Graham, D. Y., Conti, M., and Tacconelli, E. (2018). Prevalence of antibiotic resistance in *Helicobacter pylori*: A systematic review and meta-analysis in World Health Organization regions. *Gastroenterology* 155, 1372–1382.e17. doi: 10.1053/j.gastro.2018.07.007

Shatla, M. M., Faisal, A. S., and El-Readi, M. Z. (2021). Is vitamin D deficiency a risk factor for *Helicobacter pylori* eradication failure? *Clin. Lab.* 67. doi: 10.7754/Clin.Lab.2020.200118

Shin, K., Cho, M. J., Oh, J. H., and Lim, C. H. (2021). Second-line bismuth-containing quadruple therapy for *Helicobacter pylori* infection: A 12-year study of annual eradication rates. *J. Clin. Med.* 10:3273. doi: 10.3390/jcm10153273

Siavoshi, F., Saniee, P., and Malekzadeh, R. (2018). Effective antimicrobial activity of rifabutin against multidrug-resistant *Helicobacter pylori*. *Helicobacter* 23:e12531. doi: 10.1111/hel.12531

Sugano, K., Tack, J., Kuipers, E. J., Graham, D. Y., El-Omar, E. M., Miura, S., et al. (2015). Kyoto global consensus report on *Helicobacter pylori* gastritis. *Gut* 64, 1353–1367.

Takara, Y., Endo, H., Nakano, R., Kawachi, K., Hidaka, H., Matsunaga, T., et al. (2019). Smoking and drinking did not increase the failure of therapeutic *Helicobacter pylori* eradication by vonoprazan, clarithromycin, and amoxicillin. *Digestion* 99, 172–178.

Yan, T. L., Gao, J. G., Wang, J. H., Chen, D., Lu, C., and Xu, C. F. (2020). Current status of *Helicobacter pylori* eradication and risk factors for eradication failure. *World J. Gastroenterol.* 26, 4846–4856.

Yeo, Y. H., Hsu, C. C., Lee, C. C., Ho, H. J., Lin, J. T., Wu, M. S., et al. (2019). Systematic review and network meta-analysis: Comparative effectiveness of therapies for second-line *Helicobacter pylori* eradication. *J. Gastroenterol. Hepatol.* 34, 59–67. doi: 10.1111/jgh.14462

Yu, L., Luo, L., Long, X., Liang, X., Ji, Y., Chen, Q., et al. (2019). Susceptibility-guided therapy for *Helicobacter pylori* infection treatment failures. *Ther. Adv. Gastroenterol.* 12:1756284819874922. doi: 10.1177/1756284819874922

Yuan, Y., Ford, A. C., Khan, K. J., Gisbert, J. P., Forman, D., Leontiadis, G. I., et al. (2013). Optimum duration of regimens for *Helicobacter pylori* eradication. *Cochrane Database Syst. Rev.* CD008337.

Zhang, J., Han, C., Lu, W. Q., Wang, N., Wu, S. R., Wang, Y. X., et al. (2020). A randomized, multicenter and noninferiority study of amoxicillin plus berberine vs tetracycline plus furazolidone in quadruple therapy for *Helicobacter pylori* rescue treatment. *J. Dig. Dis.* 21, 256–263. doi: 10.1111/1751-2980.12870

Zhong, M. F., Li, J., Liu, X. L., Gong, P., and Zhang, X. T. (2022). TCM–based therapy as a rescue therapy for re-eradication of *Helicobacter pylori* infection: A systematic review and meta-analysis. *Evid. Based Complement. Alternat. Med.* 2022:5626235. doi: 10.1155/2022/5626235

frontiers | Frontiers in Microbiology

TYPE Original Research
PUBLISHED 07 November 2022
DOI 10.3389/fmicb.2022.1019666

OPEN ACCESS

EDITED BY
Rao Narasimha Desirazu,
Indian Institute of Science (IISc), India

REVIEWED BY
Hiroshi Asakura,
National Institute of Health Sciences (NIHS), Japan
Liping Wang,
Nanjing Agricultural University, China

*CORRESPONDENCE
Mona T. Kashef
mona.kashef@pharma.cu.edu.eg

†These authors have contributed equally to this work and share first authorship

SPECIALTY SECTION
This article was submitted to Antimicrobials, Resistance and Chemotherapy, a section of the journal Frontiers in Microbiology

RECEIVED 15 August 2022
ACCEPTED 19 October 2022
PUBLISHED 07 November 2022

CITATION
Ibrahim KA, Kashef MT, Elkhamissy TR, Ramadan MA and Helmy OM (2022) Aspartate α-decarboxylase a new therapeutic target in the fight against *Helicobacter pylori* infection. *Front. Microbiol.* 13:1019666. doi: 10.3389/fmicb.2022.1019666

Aspartate α-decarboxylase a new therapeutic target in the fight against *Helicobacter pylori* infection

Kareem A. Ibrahim[1†], Mona T. Kashef[2*†], Tharwat R. Elkhamissy[1], Mohammed A. Ramadan[2] and Omneya M. Helmy[2]

[1]Department of Microbiology and Immunology, Faculty of Pharmacy, Egyptian Russian University, Cairo, Egypt, [2]Department of Microbiology and Immunology, Faculty of Pharmacy, Cairo University, Cairo, Egypt

Effective eradication therapy for *Helicobacter pylori* is a worldwide demand. Aspartate α-decarboxylase (ADC) was reported as a drug target in *H. pylori*, in an *in silico* study, with malonic acid (MA) as its inhibitor. We evaluated eradicating *H. pylori* infection through ADC inhibition and the possibility of resistance development. MA binding to ADC was modeled *via* molecular docking. The minimum inhibitory concentration (MIC) and minimum bactericidal concentration (MBC) of MA were determined against *H. pylori* ATCC 43504, and a clinical *H. pylori* isolate. To confirm selective ADC inhibition, we redetermined the MIC in the presence of products of the inhibited enzymatic pathway: β-alanine and pantothenate. HPLC was used to assay the enzymatic activity of *H. pylori* 6x-his tagged ADC in the presence of different MA concentrations. *H. pylori* strains were serially exposed to MA for 14 passages, and the MICs were determined. Cytotoxicity in different cell lines was tested. The efficiency of ADC inhibition in treating *H. pylori* infections was evaluated using a Sprague–Dawley (SD) rat infection model. MA spectrum of activity was determined in different pathogens. MA binds to *H. pylori* ADC active site with a good docking score. The MIC of MA against *H. pylori* ranged from 0.5 to 0.75mg/mL with MBC of 1.5mg/mL. Increasing β-alanine and pantothenate concentrations proportionally increased MA MIC. The 6x-his tagged ADC activity decreased by increasing MA concentration. No resistance to ADC inhibition was recorded after 14 passages; MA lacked cytotoxicity in all tested cell lines. ADC inhibition effectively eradicated *H. pylori* infection in SD rats. MA had MIC between 0.625 to 1.25mg/mL against the tested bacterial pathogens. In conclusion, ADC is a promising target for effectively eradicating *H. pylori* infection that is not affected by resistance development, besides being of broad-spectrum presence in different pathogens. MA provides a lead molecule for the development of an anti-helicobacter ADC inhibitor. This provides hope for saving the lives of those at high risk of infection with the carcinogenic *H. pylori*.

KEYWORDS

Helicobacter pylori, aspartate α-decarboxylase, broad-spectrum, malonic acid, drug target

Introduction

Helicobacter pylori is the primary cause of peptic ulcer, besides being classified as a class I carcinogen by the World Health Organization. Infection with *H. pylori* is associated with both intra-gastric and extra-gastric disorders. Despite the extensive research during the last three decades, no effective vaccine against *H. pylori* is available (Robinson and Atherton, 2021). Antibiotics are used for the clinical management of *H. pylori* infections (Xu et al., 2021). However, poor patients' compliance to the long and complex treatment regimens and the fast-paced antibiotic resistance development magnified by the stalled development of new anti-helicobacter agents have posed a global threat (Ventola, 2015; Abadi, 2016). This requires an urgent intervention to propose new treatments for *H. pylori* infections (Xu et al., 2021).

The availability of the genomic sequences of pathogenic bacteria has provided huge data that can be used for identifying potential drug and vaccine targets through subtractive genomic, proteomic or transcriptomic approaches (Nandode et al., 2012; Yan and Gao, 2020). Using a subtractive proteomic approach, we previously identified 17 essential targets in *H. pylori* with 42 possible Drugbank ligands, of which several small organic acids were potential ligands for many of the retrieved essential targets (Ibrahim et al., 2020). These molecules have a well-known antibacterial activity, such as (S)-3-phenyllactic acid (Mu et al., 2012), citric acid (Adamczak et al., 2020), malonic acid (Feng et al., 2010), dipicolinic acid (Jadamus et al., 2005), and D-tartaric acid (Hu et al., 2019; Coban, 2020).

Aspartate α-decarboxylase (ADC) enzyme was proposed as an essential drug target, conserved in *H. pylori* and more than 200 common pathogens (Ibrahim et al., 2020), suggesting it as broad-spectrum target. ADC catalyzes the bacterial alpha decarboxylation of L-aspartate into β-alanine, required for pantothenate production (the ionized form of pantothenic acid or vitamin B5). Pantothenate is the precursor of CoA (Song et al., 2015; Zhang et al., 2015), which is an essential cofactor for many enzymes in almost all living organisms. Nearly 9% of the 3,500 enzymatic activities identified in the Braunschweig enzyme database use CoA as a cofactor in the metabolism of fats, carbohydrates, and proteins, as well as energy production (Spry et al., 2008). Disruption of the genes/enzymes in CoA biosynthesis can lead to lethal phenotypes (Walia et al., 2009). ADC was identified as a *Mycobacterium tuberculosis* drug target inhibited by pyrazinamide (Gopal et al., 2020). Malonic acid was proposed as a potential inhibitor of the *H. pylori* ADC enzyme (Ibrahim et al., 2020).

In this study, we confirmed ADC as a promising drug target for eradicating *H. pylori* infections. Besides being conserved in many pathogenic species, no resistance development to ADC inhibition was detected in *H. pylori* following 14 serial passages. The possible utilization of malonic acid as an ADC inhibitor is also proposed, where malonic acid can be used as a lead molecule for developing ADC inhibitors.

Materials and methods

Bacterial strains and culture conditions

Helicobacter pylori ATCC 43504 and a clinical *H. pylori* isolate (HPM001) from the culture collection of the Department of Clinical Pathology, Faculty of Medicine (Kasr El-Aini), Cairo University, Cairo, Egypt, were used in the study. *H. pylori* strains were stored in brain heart infusion broth (MAST, United Kingdom) containing 10% fetal bovine serum (FBS) (Sigma-Aldrich, Germany) and 20% glycerol at −70°C. When needed, and unless otherwise stated, *H. pylori* was subcultured on Columbia agar base (LabM, United Kingdom) containing 5% sheep blood and DENT supplement (Oxoid, United Kingdom), and incubated at 37°C for 72 h under microaerophilic conditions (5% O_2, 10% CO_2, and 85% N_2 at 95% humidity) using CampyGen paper sachets (Oxoid, United Kingdom; Piccolomini et al., 1997) or a candle jar (Sudhakar et al., 2008).

Escherichia coli DH5α and *E. coli* BL21 were used in cloning and expression experiments. *Acinetobacter baumannii* ATCC 19606, *Burkholderia cenocepacia* ATCC BAA-245, *E. coli* ATCC 25922, *Enterococcus faecium* ATCC 27270, *Enterococcus faecalis* ATCC 19433, *Klebsiella pneumoniae* ATCC 10031, *Pseudomonas aeruginosa* ATCC 27856, and *Staphylococcus aureus* ATCC 25923 were used in testing the spectrum of activity. They were stored in Muller-Hinton broth (Oxoid, United Kingdom) containing 20% glycerol at −70°C. When needed, they were subcultured on Lauria Bertani (LB) agar (LabM, United Kingdom) and incubated at 37°C for 18 h. The culture media were supplemented with 50 μg/mL ampicillin if required.

Molecular docking of malonic acid to the active site of ADC enzyme

Before performing the modeling study, the amino acid sequences of the ADC enzyme (about 50 sequences) from *H. pylori* 26695 (PDB ID: 1UHE; used in docking study), *H. pylori*

ATCC 43504 (the standard strain used in this study) and from randomly selected *H. pylori* strains were downloaded from the National Center for Biotechnology Information (NCBI) and analyzed by multiple sequence alignment, using Clustal Omega (Madeira et al., 2022). The molecular docking study of malonic acid to the binding site of ADC was done at the Micro-analytical Unit, Molecular Modelling Laboratory, Faculty of Pharmacy, Cairo University, Cairo, Egypt. The modeling studies were performed using Molecular Operating Environment (MOE, 2015.10). All minimizations were performed with MOE until a root mean squared distance gradient of 0.05 kcal.mol^{-1} Å^{-1} was reached using MMFF94x force field, and the partial charges were automatically calculated. The X-ray crystallographic structure of the *H. pylori* ADC enzyme (PDB ID: 1UHE) was downloaded from the Protein Data Bank. Ligands not involved in binding and water molecules were removed from each co-crystallized enzyme. The protein was prepared for the docking study using Protonate 3D protocol in MOE with default options. The co-crystalized ligand (N-2-(2-amino-1-methyl-2-oxoethylidene) asparaginate) was used to define the binding site for docking. Triangle Matcher placement method and London ΔG scoring function were used for docking.

Docking setup was first validated by self-docking the co-crystallized ligand in the vicinity of the enzyme's binding site. The docking of the enzyme's natural ligand (aspartate) was performed to expose its intermolecular interactions with the active binding site. The validated setup was then used to predict the malonate-receptor interactions at the ADC binding site.

Determination of malonic acid minimum inhibitory concentration

The MIC of malonic acid was determined by agar dilution and broth microdilution methods, against *H. pylori* ATCC 43504 and *H. pylori* HPM001 strains. Malonic acid (Loba, India) was dissolved in distilled water to the desired concentration, sterilized by a 0.22 µM syringe filter, and used within 72 h of preparation. Inocula for MIC testing were prepared by suspending colonies in saline to reach an optical density equivalent to 2.0 McFarland turbidity standard (approximately 1×10^7 to 1×10^8 CFU/mL) (CLSI, 2015). The culture media used in MIC determination were freshly prepared, according to the manufacturer's instruction, and supplemented with 1% yeast extract (LabM, United Kingdom) to enhance bacterial growth (Walsh and Moran, 1997).

Agar dilution method

Determination of MIC by the agar dilution method was performed according to the clinical and laboratory standards institute (CLSI) guidelines (CLSI, 2015). Briefly, 2 µL of the inoculum (containing 1×10^4 CFU) was spotted on the surface of Muller-Hinton agar (Oxoid, United Kingdom) plates supplemented with 5% sheep blood and containing the specified concentration of malonic acid (6 to 0.19 mg/mL) followed by incubation at 37°C for 72 h, under microaerophilic conditions. The MIC was the lowest concentration of malonic acid that completely inhibited visible bacterial growth (CLSI, 2015). The experiment was done in triplicates.

Broth microdilution method

MIC determination by broth microdilution method was carried out in 96-well round-bottom micro-titre plates. Each well contained 100 µL of brucella broth (Conda, Spain) containing 10% FBS. Malonic acid solution (12 mg/mL) was two-fold serially diluted in the broth-FBS mixture to get concentrations ranging from 6 to 0.19 mg/mL. The bacterial inoculum was diluted 1:10, and 10 µL of the diluted inoculum was transferred to each well to contain 5×10^5 CFU/mL followed by incubation at 37°C for 72 h under microaerophilic conditions. The MIC was the lowest concentration of malonic acid completely inhibiting the visible growth of the tested organism. The experiment was carried out in triplicates.

Determination of the minimum bactericidal concentration of malonic acid

The MBC of malonic acid against both *H. pylori* ATCC 43504 and *H. pylori* HPM001 was determined, according to Moraes and colleagues (Moraes et al., 2021). Briefly, following MIC determination by broth microdilution method, 10 µL were transferred from wells showing no visible growth onto the surface of Muller-Hinton agar plate supplemented with 5% sheep blood and incubated at 37°C for 72 h, under microaerophilic conditions. The MBC was the lowest concentration that failed to show bacterial growth on the agar plate.

Evaluation of ADC inhibition by malonic acid

Determination of the MIC of malonic acid in presence of β-alanine and pantothenate

β-alanine and pantothenate, the downstream products of the enzymatic pathway (EC: 4.1.1.11) potentially inhibited by malonic acid, were used to confirm the selective inhibition of *H. pylori* ADC enzyme by malonic acid. The MIC of β-alanine (Sigma-Aldrich, Germany) and pantothenate (Loba Chemie, India) against *H. pylori* ATCC 43504 and *H. pylori* HPM001 were determined by agar dilution and broth microdilution methods, as described earlier. The MIC of malonic acid against *H. pylori* ATCC 43504 and *H. pylori* HPM001 was determined in the absence and presence of increasing sub-inhibitory concentrations of β-alanine (0.6–560 mM) or pantothenate (0.25–228 mM). Experiments were done in triplicates.

Assessment of recombinant *Helicobacter pylori* 6xHis-tagged ADC activity in presence of malonic acid

Cloning and expression of *Helicobacter pylori* ADC enzyme

The genomic DNA of *H. pylori* ATCC 43504 was extracted using GeneJet Genomic DNA Purification Kit (Thermo Fisher Scientific, Lithuania). Primers used in the study were supplied by Macrogen, Korea, and are listed in Supplementary Table S1. The *pan*D gene was amplified using KI001 and KI002 primers; The polymerase chain reaction (PCR) products were digested by *Eco*RI/*Xho*I enzymes (Puregene, Genetix, India) and ligated using T4 DNA ligase (Takara, Japan) with the similarly digested pET-22b(+) plasmid (Merck, Germany). The recombinant plasmid (RecPl) was transformed into chemically competent *E. coli* DH5α cells (Sambrook and Russel, 2001). Clones were selected on LB agar plates containing 50 μg/mL ampicillin; the LB agar plates were incubated at 37°C for 24 h, and the obtained colonies were screened by PCR using combinations of the following primers; KI001, KI002, KI003 (Yang et al., 2020), and KI004 (Yang et al., 2020).

RecPl from successful clones was extracted using QIAprep Spin Miniprep kit (Qiagen, Germany) and transformed into chemically competent *E. coli* BL21. Overnight culture of *E. coli* BL21/RecPl was subcultured in LB broth containing 50 μg/mL ampicillin and incubated at 37°C with shaking (250 rpm) to reach an optical density of approximately 0.6 at 600 nm. Protein expression was induced by using 0.75 mM isopropyl β-D-1-thiogalactopyranoside (IPTG) (Scharlau, Spain), and incubation at 37°C for 4 h with shaking at 200 rpm. Cells were harvested by centrifugation at 6000 rpm for 10 min at 4°C and resuspended in binding buffer (50 mM sodium phosphate buffer, 500 mM NaCl and 100 mM imidazole, pH = 7.4). The crude extract, of IPTG-induced *E. coli* BL21/RecPl in binding buffer, was prepared by sonication for 30 min on ice, followed by centrifugation at 6000 rpm for 20 min at 4°C and filtered using 0.45 μM syringe filter (Mo et al., 2018). 6xHis-tagged ADC protein purification was performed using Ni-NTA spin columns (Qiagen, Germany), according to the manufacturer's instructions. The purified protein was analyzed using sodium dodecyl sulphate-polyacrylamide gel electrophoresis (SDS-PAGE) and its concentration was determined by BCA protein assay kit (Novagen, Germany), according to the manufacturer's instructions.

Assay of *Helicobacter pylori* 6xHis-tagged ADC enzymatic activity

Aspartate α-decarboxylase activity was determined in the crude extract of IPTG-induced *E. coli* BL21/RecPl and the purified recombinant *H. pylori* 6xHis-tagged ADC protein, according to Pei et al. (Pei et al., 2017). The reaction mixture contained either 500 μL of the crude extract and 536 μL of a 60 g/l L-aspartate solution (adjusted to pH 7.0 with NaOH) or 25 μg/mL of the purified 6xHis-tagged ADC and 1 mL of a 6.66 mg/mL L-aspartate solution (adjusted to pH 7.0 with NaOH). The assay was repeated in presence of increasing concentrations of malonic acid (0.1875, 0.375, 0.75, 1.5, 3, and 6 mg/mL equivalent to 1.8, 3.75, 7.5, 15, 30 and 60 mM). After incubating the reaction mixture at 37°C for 20 min, the reaction was stopped by adding 0.1 mL of 1 M NaOH. The production of β-alanine was measured by high performance liquid chromatography (HPLC) using Waters 2,690 Alliance HPLC system equipped with a Waters 996 photodiode array detector, Column C18 Inertsil ODS 4.6 mm × 250 mm, 5 μM Mobile phase: Acetate buffer pH 7.5: Methanol (80,20%); Mode of elution: Isocratic; Flow rate: 1 mL/min; Temperature: Ambient and Wavelength: 210 nm.

Assessment of resistance development to ADC inhibition

Helicobacter pylori ATCC 43504 and *H. pylori* HPM001 strains were subjected to 14 consecutive serial passages in increasing malonic acid concentrations. Similarly, serial passage in increasing clarithromycin (Abbott, United States) concentrations as a comparator (Abadi, 2016) was performed according to Haas and colleagues with modifications (Haas et al., 1990). Briefly, broth microdilution testing was performed for malonic acid and clarithromycin against the tested *H. pylori* strains. Following incubation, a subculture from the well-containing ½ of the MIC of each drug onto Columbia agar plates supplemented with 5% sheep blood, and DENT supplement was done. The plates were incubated for 72 h at 37°C under microaerophilic conditions. At the end of incubation period, colonies (considered as P0) were suspended in saline to reach an optical density equivalent to 2.0 McFarland turbidity standard, and the process of MIC determination was repeated using P0 colonies as inoculum. The process was repeated for 14 consecutive serial passages.

In vitro cytotoxicity of malonic acid

The cytotoxicity of malonic acid was assessed using sulforhodamine B (SRB) colorimetric assay against normal oral epithelial and human skin fibroblast cell lines. Cell lines were maintained in Dulbecco's Modified Eagle Medium (DMEM); the medium for culturing cell lines was supplemented with 100 mg/mL streptomycin, 100 units/mL penicillin, and 10% FBS. Briefly, 100 μL aliquots of cell suspension (5×10^3 cells) were treated in triplicates with 100 μL culture medium containing malonic acid at concentrations: 6 and 60 mg/mL and incubated for 2 h at 37°C in a humidified incubator with 5% CO_2. Cells were fixed with 10% trichloroacetic acid and incubated at 4°C for 1 h. The trichloroacetic acid solution was removed, and the cells were washed with sterile distilled water. SRB solution (70 μL of 0.4% w/v solution) was added and incubated in a dark place at room temperature for 10 min. Plates were washed with 1% acetic acid

and allowed to air-dry overnight. Tris (150 μL of 10 mM) was added to dissolve the protein-bound SRB stain, and the absorbance was measured at 540 nm using a microplate reader (Allam et al., 2018; Hosny et al., 2020). The half maximal inhibitory concentration (IC_{50}) was calculated as the concentration of the test compound that inhibited the viability of the tested cells by 50% (Mahavorasirikul et al., 2010).

In vivo efficiency of ADC inhibition in treatment of *Helicobacter pylori* infections

We developed a rat infection model to test the efficiency of ADC inhibition by malonic acid in treating *H. pylori* infections. Male Sprague–Dawley (SD) rats (10 weeks) weighing 160–200 grams, purchased from the New veterinary center (Cairo, Egypt), were used in the study (Li et al., 2018). The sample size was calculated according to the equation: $2(Z^{\alpha}_{/2}+Z^{\beta})^2 \times P\ (1-P)/(p_1 - p_2)^2$, where $Z^{\alpha}_{/2} = Z_{0.05/2} = 1.96$ (from Z table) at type 1 error of 5%; $Z^{\beta} = Z_{0.20} = 0.842$ (from Z table) at 80% power; pooled prevalence = (0.8 + 1)/2, and the value was adjusted for 5% attrition (Charan and Kantharia, 2013).

Rats were randomly assigned to Makrolon cages (3-4/cage). Environmental conditions were maintained at a temperature of 22–25°C and a 12-h light/dark cycle with food and water *ad libitum* unless fasting was required. The rats were allowed to acclimatize for 1 week prior to the experiment. All procedures involving the use of animals were performed following the recommendations of the National Institutes of Health Guide for Care and Use of Laboratory Animals (National Research Council, 2010), and were approved by the Ethics Committee of the Faculty of Pharmacy, Cairo University, Cairo, Egypt [Approval no. MI (1894)].

Infecting rats by *Helicobacter pylori*

Before the infection, all rats received vancomycin once daily (25 mg/kg/day), by oral gavage, for 1 week to reduce the gastric microbial load and facilitate *H. pylori* colonization (Stahl et al., 2014). Forty-eight rats were randomly distributed into two infection groups, each composed of 24 rats. *H. pylori* ATCC 43504 and *H. pylori* HPM001 were each used to infect the corresponding group of rats, starting from day 8 of the experiment in five infection cycles. For each infection cycle, rats were forced to fast for 18–24 h before receiving the infection dose. Three hours prior to infection, omeprazole (25 mg/kg/day), dissolved in sterile distilled water, was administered orally to reduce gastric acidity and augment the colonization process (Li et al., 1998). Infection was carried out by administering 5×10^8 CFU/mL of *H. pylori* strain in 1 mL sterile water within 30 min of preparation, using an oro-gastric tube attached to a 3-cc or 5-cc syringe, without anaesthesia. Infection was done on days 8, 10, 12, 14, and 16 of the experiment (Werawatganon, 2014). Feeding was resumed 2 h following each infection dose (Supplementary Figure S1). An uninfected negative control group ($n = 4$) received sterile water instead of the bacterial inoculum throughout the infection process.

Confirmation of successful *Helicobacter pylori* infection

Successful infection of rats was confirmed using the *H. pylori* stool antigen (HpSA) test (ACON, United States; Asgari et al., 2020). The test was carried out according to the manufacturer's instructions at room temperature immediately after collecting the fecal samples. The result was read within 10–20 min, where any shade of color in the test line region was considered positive. The test was performed on days 16, 23, and 30 of the experiment.

On day 30 of the experiment, we further confirmed successful infection by sacrificing three rats from each infection group and four from the negative control group. According to Li and colleagues (Li et al., 1998), with modifications, the rats were euthanized by decapitation under anesthesia using thiopental (EIPICO, Egypt). The stomach was dissected, and immediately homogenized in 20 mL brucella broth using Witeg® HG-15D homogenizer at 1500 rpm for 20 s, or until it yielded a homogenous suspension. The CLO rapid urease test (Kimberly-Clark, United States) was performed to confirm urease activity (Cai et al., 2014), following the manufacturer's instructions, where the test result was read at room temperature within 72 h. Any change in color, from deep orange to magenta red color, was considered positive.

In addition, a sterile swab was soaked in the homogenized stomach suspension and spread in triplicates onto the surface of Columbia agar plates, supplemented with 5% sheep blood and DENT supplement. The plates were incubated for 72 h at 37°C under microaerophilic conditions. Colonies of *H. pylori* were identified by the characteristic morphological appearance (small translucent to pale colonies), microscopical characters (Gram negative spiral, curved or coccoid bacilli) (Andersen and Wadström, 2001), and positive oxidase (HIMEDIA, India), catalase, and urease tests (Kadkhodaei et al., 2020).

Malonic acid treatment

On day 38 of the experiment, each infected group ($n = 21$ rats; infected with either *H. pylori* ATCC 43504 or *H. pylori* HPM001) was subdivided into three subgroups (Supplementary Figure S2); an untreated group ($n = 7$) receiving only sterile water, group A receiving ¼ LD_{50} (327.5 mg/kg) of malonic acid once daily ($n = 7$), and group B receiving ¼ LD_{50} (327.5 mg/kg) of malonic acid twice daily ($n = 7$), by oral gavage for 3 weeks. The used LD_{50} was specified in the malonic acid manufacturer's safety data sheet and was equivalent to 1,310 mg/kg.

Follow-up of the treatment efficiency was performed on days 7, 14, and 21 from the beginning of treatment (days 45, 52, and 59 of the experiment) using HpSA. At the end of treatment, all rats were euthanized as described earlier. The stomach was dissected, weighed, and homogenized in brucella broth. As mentioned earlier, the presence of *H. pylori* was determined by the CLO rapid urease test, culturing,

microscopical and biochemical characteristics of the recovered isolates from stomach homogenates. The count in stomach was determined by the plate count method; the stomach's homogenate of each rat was serially diluted (1,10, 1:100, and 1:1000), and 50 µL of each dilution was spread onto Columbia blood agar plates supplemented with 5% sheep blood, and DENT supplement and incubated for 72 h at 37°C, under microaerophilic conditions (Li et al., 1998). Following incubation, the number of *H. pylori* colonies was counted, and the total *H. pylori* count per mg stomach was calculated (Li et al., 1998).

Assessment of the spectrum of activity of malonic acid

The spectrum of activity of malonic acid was assessed by determining malonic acid MIC against eight other pathogenic bacterial species (*A. baumannii* ATCC 19606, *B. cenocepacia* ATCC BAA-245, *E. coli* ATCC 25922, *E. faecium* ATCC 27270, *E. faecalis* ATCC 19433, *K. pneumoniae* ATCC 10031, *P. aeruginosa* ATCC 27856, and *S. aureus* ATCC 25923) using broth microdilution method, according to the CLSI guidelines (CLSI, 2018). Malonic acid solution was serially diluted in Muller-Hinton broth (100 µL) to get concentrations ranging from 6 to 0.19 mg/mL. The inoculum was prepared to be equivalent to 0.5 McFarland standard (containing approximately $1–2 \times 10^8$ CFU/mL with most species) and was further diluted 1:10 (to get a concentration of 10^7 CFU/mL). 10 µL of the diluted inoculum was transferred to each well to contain 5×10^5 CFU/mL. Plates were incubated at 37°C for 20 h. The MIC was the lowest concentration that completely inhibited the visible growth of the tested organism. The experiment was carried out in triplicates.

Statistical analysis

All statistical analyses were performed using GraphPad Prism 8.0.1. Two-way ANOVA and the unpaired t-test were used to evaluate the results of determining the MIC of malonic acid. Two-way ANOVA and multiple t tests, using the Holm-Sidak method, were used to analyse the results of *in vitro* confirmation of ADC inhibition by malonic acid, treatment follow-up using HpSA test, and the results of the *H. pylori* total plate count. The difference was significant at $p < 0.05$ in all tests. *Post hoc* test using Dunnett's method was used to evaluate the significance of the results of *H. pylori* total plate count in treated and untreated groups. Pearson correlation coefficient was used to evaluate the correlation between different concentrations of β-alanine and pantothenate and the MIC of malonic acid as well as the correlation between different malonic acid concentrations and ADC enzymatic activity.

Results

Successful docking of malonic acid to ADC binding site

Multiple sequence alignment of the sequences of ADC enzyme from *H. pylori* 26695 (PDB ID: 1UHE), *H. Pylori* ATCC 43504, and from other randomly selected *H. Pylori* strains showed high level of conservation (Supplementary Figure S3). Malonic acid interaction with the ADC binding site was modeled *via* molecular docking. The docking setup was first validated by self-docking the co-crystallized potential ligand [N-2-(2-amino-1-methyl-2-oxoethylidene) asparaginate] in the vicinity of the binding site of the ADC. It bound the amino acids: Isoleucine (Ile) 26, Threonine (Thr) 57, Asparagine (Asp) 71, and Alanine (Ala) 74 through ionic, hydrogen bond, and hydrophobic interactions, with a docking score of −4.4312 kcal/mol (Figure 1A). Docking of aspartate (ADC substrate) with ADC was used to identify its intermolecular interactions with the active binding site. Aspartate interacted with the amino acids Thr57 and Ala74 through hydrogen bonding and hydrophobic interactions, with a docking score of −3.9130 kcal/mol (Figures 1B,C). The validated setup was then used to predict the ligand-receptor interactions for malonate with the ADC binding site. Malonate interacted with the key amino acids in the binding site (Thr57 and Ala74) through hydrogen bonding and hydrophobic interactions, with a docking score of −3.5542 kcal/mol (Figures 1D,E).

In vitro anti-helicobacter activity of malonic acid

The MIC of malonic acid was determined by agar dilution and broth microdilution methods against *H. pylori* ATCC 43504 and *H. pylori* HPM001. The MIC against both strains was 0.75 mg/mL when using the agar dilution method. Upon using the broth microdilution method, the MIC was 0.5 ± 0.17 and 0.75 mg/mL against *H. pylori* ATCC 43504 and *H. pylori* HPM001. The MBC of malonic acid was 1.5 mg/mL for both strains. No significant difference was recorded between the MIC of malonic acid against *H. pylori* ATCC 43504 and *H. pylori* HPM001 using either the agar ($p = 0.8529$) or the broth microdilution methods ($p = 0.8784$). There was also no significant difference between the mean MIC of malonic acid recorded against the tested strains by both methods ($p = 0.54$).

ADC inhibition by malonic acid

Confirmation of ADC inhibition by malonic acid was carried out by determining the MIC of malonic acid in the presence of increasing sub-inhibitory concentrations of β-alanine and pantothenate (the products of the inhibited enzymatic reaction). The MIC of β-alanine and pantothenate were 1.12 M (100 mg/mL)

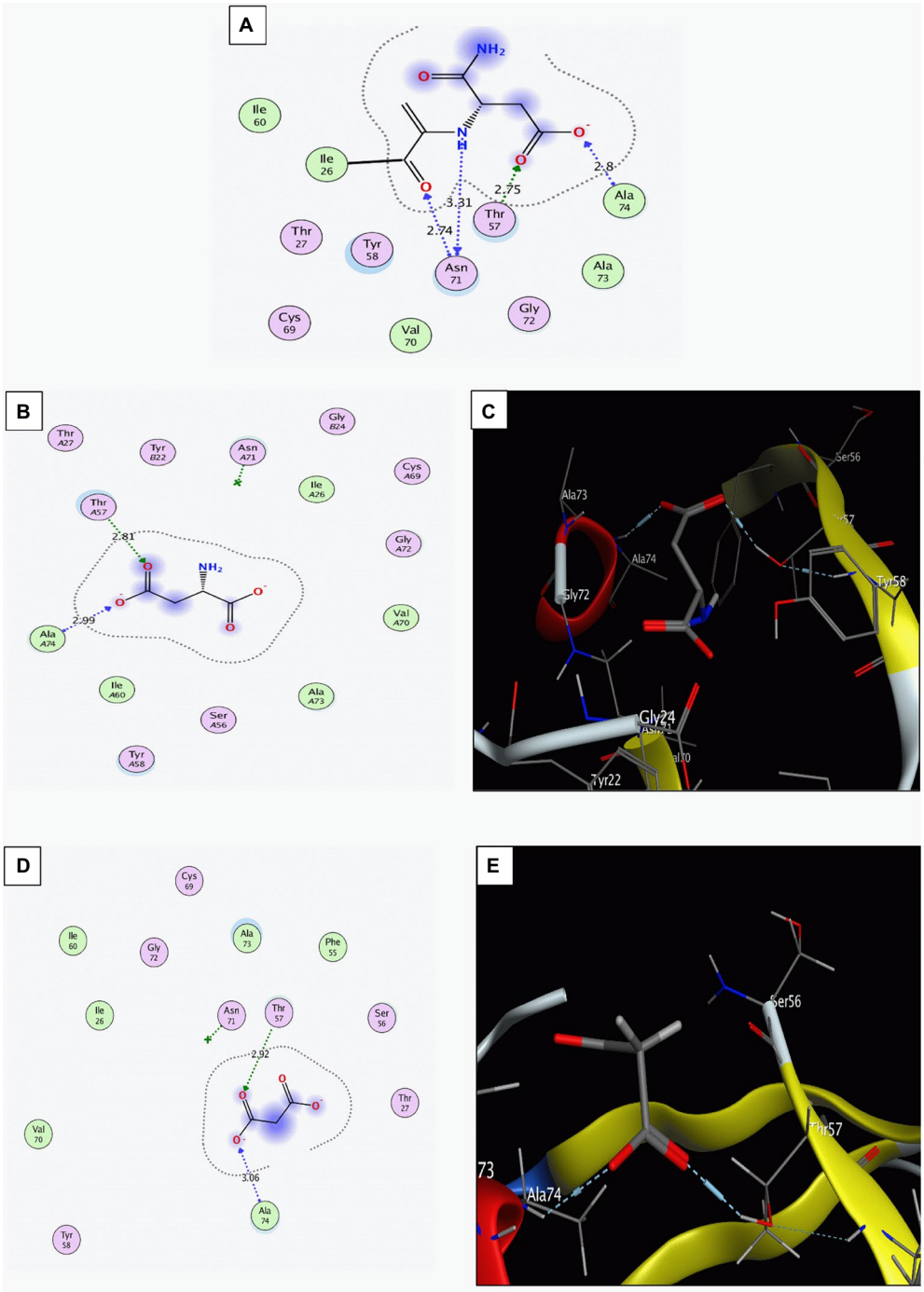

FIGURE 1
Interaction of the binding site of aspartate α-decarboxylase with different ligands. **(A)** The co-crystalized ligand ((N-2-(2-amino-1-methyl-2-oxoethylidene)asparaginate)). **(B,C)** Aspartate (Two-D structures and three-D structures). **(D,E)** Malonate (Two-D structures and three-D structures). Images were generated by Molecular Operating Environment (MOE, 2015.10) software.

and 456 mM (100 mg/mL), respectively. Supplementing the growth media with increasing concentrations of β-alanine or pantothenate resulted in a significant increase in the mean malonic acid MIC (Figures 2A,B) determined using the agar dilution and broth microdilution methods. A strong uphill linear relationship between β-alanine (r = 0.6857) or pantothenate (r = 0.7670) concentrations and the MIC of malonic acid was observed (Figures 2C,D).

Further confirmation of ADC inhibition by malonic acid was carried out by assaying β-alanine, the product of the enzymatic action of recombinant *H. pylori* 6x-His-tagged ADC on aspartate, in the presence of an increasing concentration of malonic acid

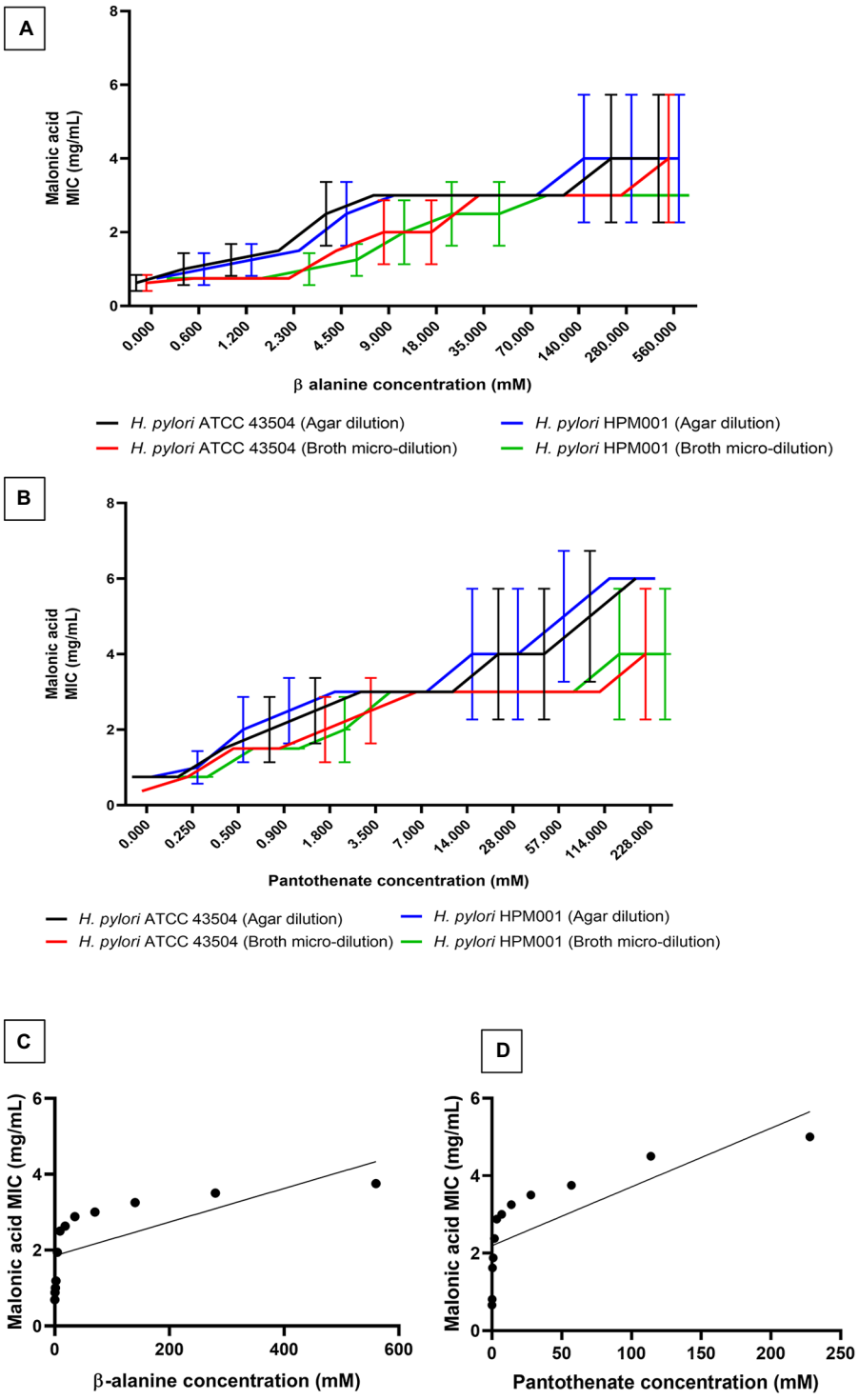

FIGURE 2
Minimum inhibitory concentration (MIC) of malonic acid in presence of the products of aspartate α-decarboxylase catalyzed enzymatic reaction. MIC of malonic acid in the presence of increasing concentrations of **(A)** β-alanine and **(B)** pantothenate, using both agar dilution and broth microdilution methods, against both *Helicobacter pylori* ATCC 43504 and the clinical *H. pylori* isolate (HPM001). The correlation between the MIC of malonic acid and the concentrations of **(C)** β-alanine, and **(D)** pantothenate.

using HPLC. The *pan*D gene, encoding ADC, was amplified from *H. pylori* ATCC 43504 genome, resulting in a DNA fragment of 375 bp; the DNA fragment was inserted in the pET22b + plasmid. The constructed recombinant RecP1 plasmid (pET22b + with *panD* insert) was transformed into *E. coli* DH5α. Clones were confirmed by PCR using different combinations of primers

(Figures 3A,B). The cloned DNA fragment encoded 123 amino acids polypeptide, 117 amino acids for ADC, and six amino acids for the His-tag. The whole fragment was predicted to have a size of 13.8 kDa using (Bioinformatics.Org/sms/prot_mw.html). The recombinant plasmid RecP1 was transformed into *E. coli* BL21, and the recombinant protein was purified using Ni-NTA columns. A single intense band (37% of the elute) with the expected size of 13.8 KDa was visualized on SDS-PAGE (Figures 3C,D). A standard curve for β-alanine was constructed using HPLC (Supplementary Figure S4). The ADC activity of the crude extract of IPTG-induced *E. coli* BL21/RecPl and the purified 6x-his tagged ADC was measured. There was a decrease in the concentration of the produced β-alanine by increasing malonic acid concentration. A strong downhill linear relationship between β-alanine and malonic acid concentrations was recorded in crude and purified enzyme preparations ($r = -0.8605$ and -0.6575, respectively; Figure 4).

Lack of resistance development in *Helicobacter pylori* by repeated ADC inhibition using malonic acid

Helicobacter pylori ATCC 43504 and *H. pylori* HPM001 were subjected to serial passage in the presence of increasing concentrations of either malonic acid or clarithromycin (comparator). No increase in the MIC of malonic acid against both strains was recorded after 14 serial passages. However, there was an increase in the MIC of clarithromycin against both strains. The MIC of clarithromycin against *H. pylori* ATCC 43504 and *H. pylori* HPM001 was 6 and 48 μg/mL and increased by 16-fold, following 14 serial passages (Figure 5).

Malonic acid is not cytotoxic

The *in vitro* cytotoxicity of malonic acid was evaluated in oral epithelial and human skin fibroblast cell lines using two concentrations, 6 mg/mL (equivalent to 10X the average MIC) and 60 mg/mL (approximately the *in vivo* used dose per rat). The IC_{50} was higher than 60 mg/mL, with recorded cell viability of 82.13% ± 2.13 and 61.36% ± 2.25 in oral epithelial cells and 85.91 ± 1.1% and 79.03 ± 0.94% in human skin fibroblast for 6 and 60 mg/mL, respectively.

Successful treatment of *Helicobacter pylori* infection by ADC inhibition

Helicobacter pylori ATCC 43504 and *H. pylori* HPM001were used to infect SD male rats ($n = 48$). An uninfected group that received only sterile water served as a negative control ($n = 4$). The HpSA test was used to monitor infection; on day 16 (the day of the last infection cycle), all rats ($n = 52$) tested negative. The following week (day 23), 87.5% ($n = 21$) and 83.3% ($n = 20$) of *H. pylori* ATCC 43504 and *H. pylori* HPM001 infected rats tested positive, and by day 30, all infected rats tested positive. Rats in the uninfected control group remained negative throughout the experiment.

Successful infection was further confirmed by sacrificing three rats from each infected group, besides the four uninfected rats, to validate the HpSA test results. The rapid urease CLO test was performed on the homogenized stomachs of the sacrificed rats. Homogenized stomachs of all infected rats tested positive for urease, while those of uninfected rats tested negative. Colonies resulting from culturing the homogenized stomachs of infected rats were positive for urease, oxidase, and catalase. Microscopically examining the Gram-stained colonies under 1,000× magnification revealed the characteristic spiral-shaped Gram-negative single rods indicative of *H. pylori*. No growth was observed when culturing the stomachs of uninfected rats.

Infected rats with *H. pylori* ATCC 43505 and *H. pylori* HPM001 ($n = 21$ each) were treated with malonic acid (¼ LD_{50} once ($n = 7$) and twice ($n = 7$) daily); in addition to two control untreated groups ($n = 7$ each) that received sterile water once and twice daily (Supplementary Figure S5). All rats survived the entire treatment period. The untreated rats ($n = 14$) tested positive for *H. pylori* by the HpSA test throughout the 3-weeks treatment period. All treated rats ($n = 42$) tested positive for *H. pylori* after the first week of treatment. The number of rats that tested negative in the HpSA test increased by the end of the second week of treatment to reach 15% ($n = 4$). This includes three rats treated with ¼ LD_{50} twice daily and one treated with ¼ LD_{50} once daily. By the end of the 3 weeks treatment period, 93% of the infected rats in the treatment groups ($n = 26$) tested negative in the HpSA test. Only two rats failed to clear the infection; they were treated with ¼ LD_{50} ($n = 2$) once daily (Supplementary Figure S5). Follow-up of the number of rats clearing the infection following each week of treatment is shown in Figure 6A.

By the end of the treatment period, all rats ($n = 42$) were sacrificed, and the stomachs were dissected, weighed, and homogenized. Performing the rapid urease CLO test on homogenized stomachs confirmed the HpSA test results. Upon culturing the homogenized stomachs, no visible growth was observed in rats testing negative with the HpSA test; the total *H. pylori* plate count of the untreated group ($n = 14$) ranged from 2,850 to 3,400 CFU/mg stomach. However, the homogenized stomachs of the two rats that failed to clear the infection (treated with ¼ LD_{50} once daily and tested positive with the HpSA test at the end of the treatment period) had a mean total *H. pylori* plate count of 1,030 CFU/mg stomach. There is a significant difference between the mean of the total *H. pylori* counts in the stomachs of rats that failed to clear the infection (treated with ¼ LD_{50} of malonic acid once daily) and the mean of the total *H. pylori* counts in the stomachs of the untreated group ($p < 0.0001$; Figure 6B).

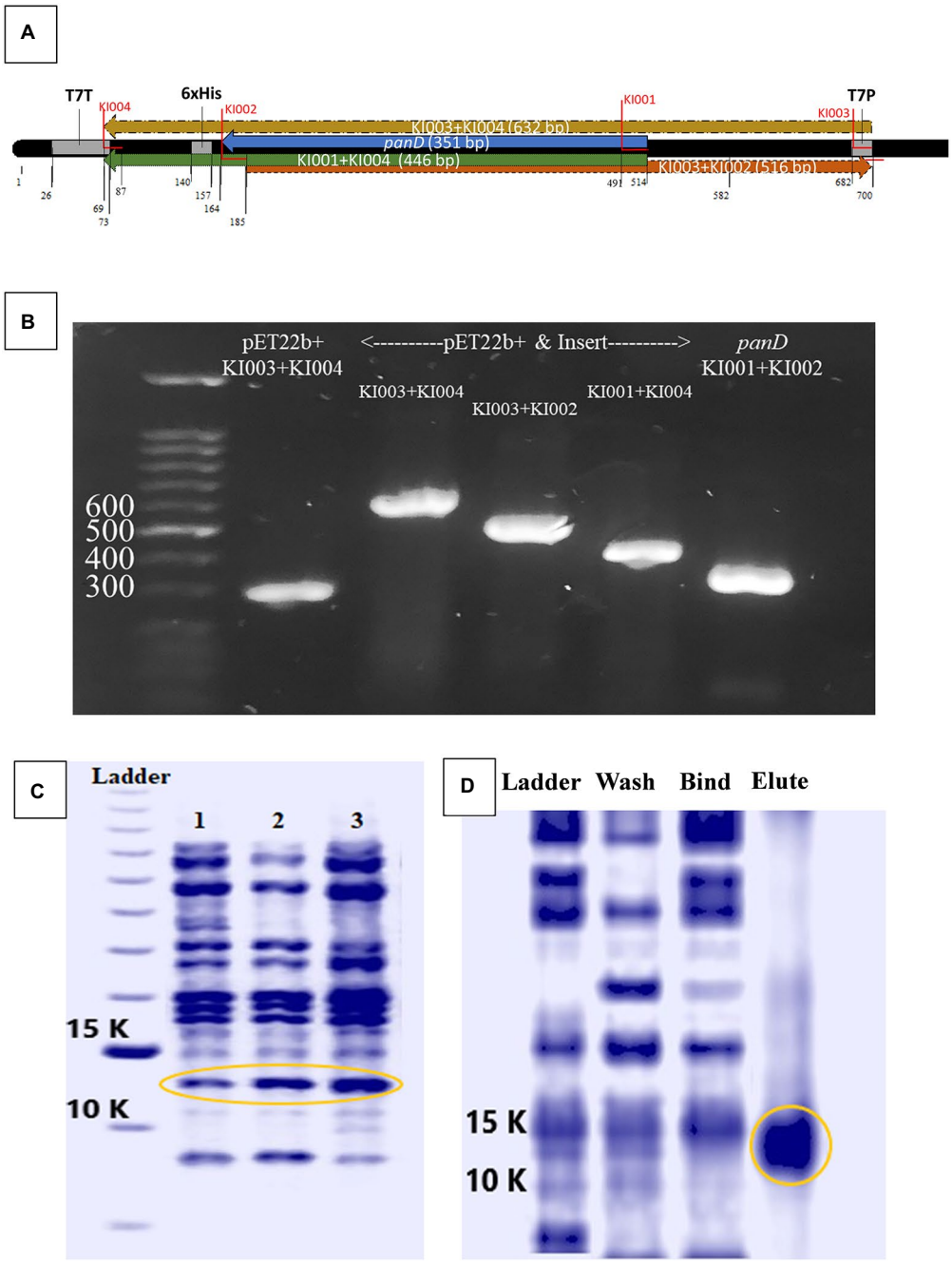

FIGURE 3
Cloning and expression of *Helicobacter pylori* ATCC 43504 aspartate α-decarboxylase. **(A)** Schematic diagram generated by BioEdit (7.2.5., 2015) of pET22b+vector containing the *pan*D insert with the positions of different primers highlighted. **(B)** Polymerase chain reaction (PCR) amplicons produced by different primer combinations performed on *H. pylori* ATCC 43504 DNA (*pan*D), empty pET22b(+) plasmid vector and the recombinant plasmid vector pET22b(+) containing the insert *pan*D, **(C)** Crude protein extract from: lane 1: *Escherichia coli* BL21, lane 2: *E.coli* BL21/RecPl induced by 0.5mM Isopropyl β-D-1-thiogalactopyranoside (IPTG), lane 3: *E. coli* BL21/RecPl induced by 0.75mM IPTG **(D)** The wash, bind and elute of Ni-NTA columns purification of the recombinant protein from *E. coli* BL21/RecPl.

The broad-spectrum of MA as an ADC inhibitor

Malonic acid MIC was determined against other pathogenic species (*A. baumannii* ATCC 19606, *B. cenocepacia* ATCC BAA-245, *E. coli* ATCC 25922, *E. faecium* ATCC 27270, *E. faecalis* ATCC 19433, *K. pneumoniae* ATCC 10031, *P. aeruginosa* ATCC 27856, and *S. aureus* ATCC 25923) by the broth microdilution method. The MIC of malonic acid ranged from 0.625 to 1.25 mg/mL in the tested species (Supplementary Table S2).

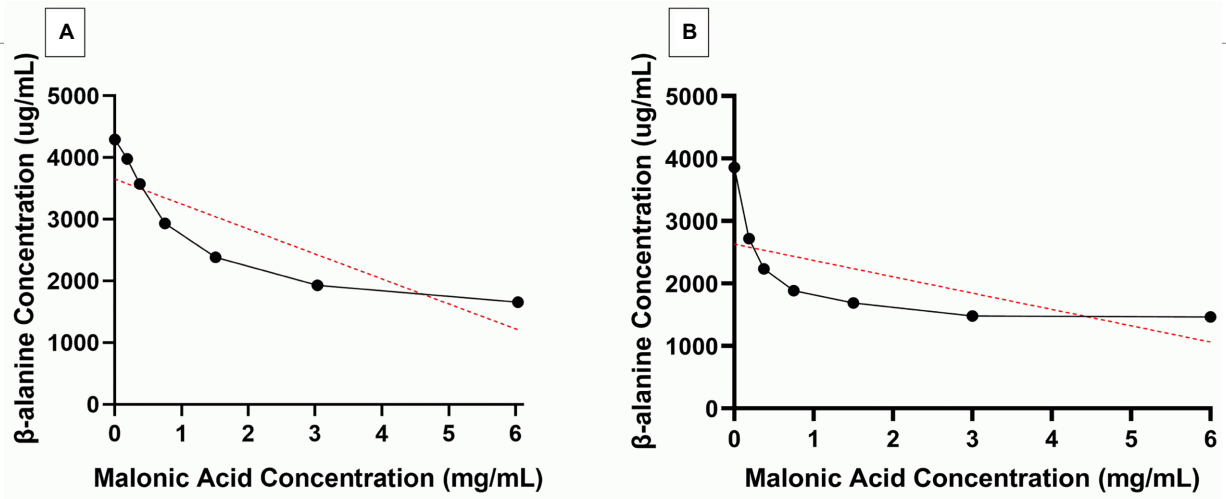

FIGURE 4
Selective inhibition of *Helicobacter pylori* aspartate α-decarboxylase (ADC) by malonic acid. β-alanine (Black line) produced from the action of **(A)** crude enzyme extract and **(B)** purified 6x-His tagged ADC, of Isopropyl β-D-1-thiogalactopyranoside induced *Escherichia coli* BL21/RecPl, in the presence of increasing concentrations of malonic acid. The red lines depict the correlation between the two variables.

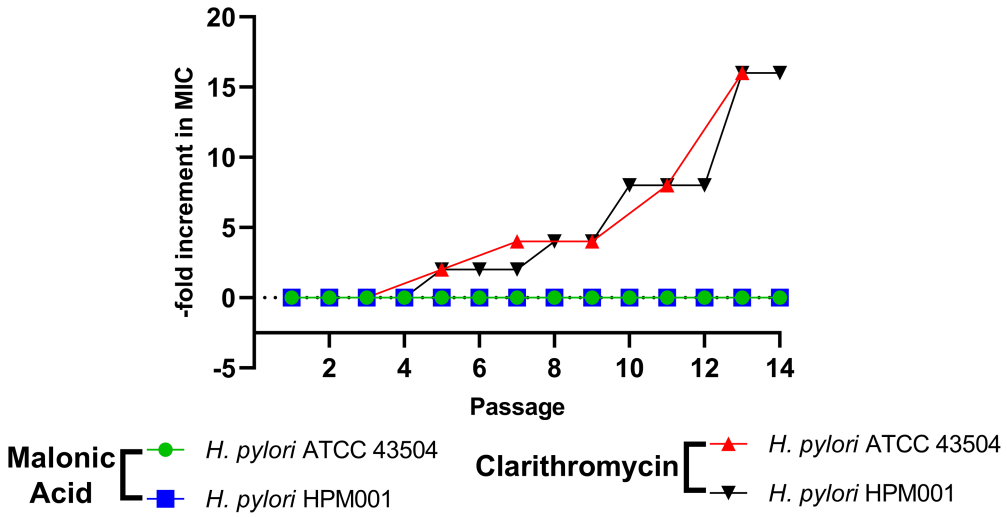

FIGURE 5
Lack of resistance development in *Helicobacter pylori* by repeated exposure to aspartate α-decarboxylase inhibition using malonic acid. Fold increase in minimum inhibitory concentration (MIC) of malonic acid and clarithromycin against *H. pylori* ATCC 43504 and the clinical *H. pylori* HPM001 isolate, following 14 serial passages.

Discussion

Aspartate α-decarboxylase was previously reported, using *in silico* proteomic approaches, as a promising conserved drug target in *H. pylori* with malonic acid as the proposed inhibitor (Ibrahim et al., 2020). Here, the conservation of ADC in 50 non-redundant *H. pylori* strains, including the strain for which the crystallographic structure of ADC enzyme was available in the protein databank (*H. pylori* 26695) and the standard *H. pylori* ATCC 43504 strain, was confirmed. We modeled the interaction of malonic acid to *H. pylori* ADC *via* molecular docking, which resulted in a docking score (−3.5542) similar to that of its natural substrate, aspartate (−3.9130). Both interacted with the key amino acids in the ADC binding site using similar bonds (hydrogen bonding and hydrophobic interactions); these key amino acids (Thr57 and Ala74) are totally conserved in the aligned ADC sequences. Aspartic acid (2-amino-butanedioic acid, $C_4H_7NO_4$) and malonic

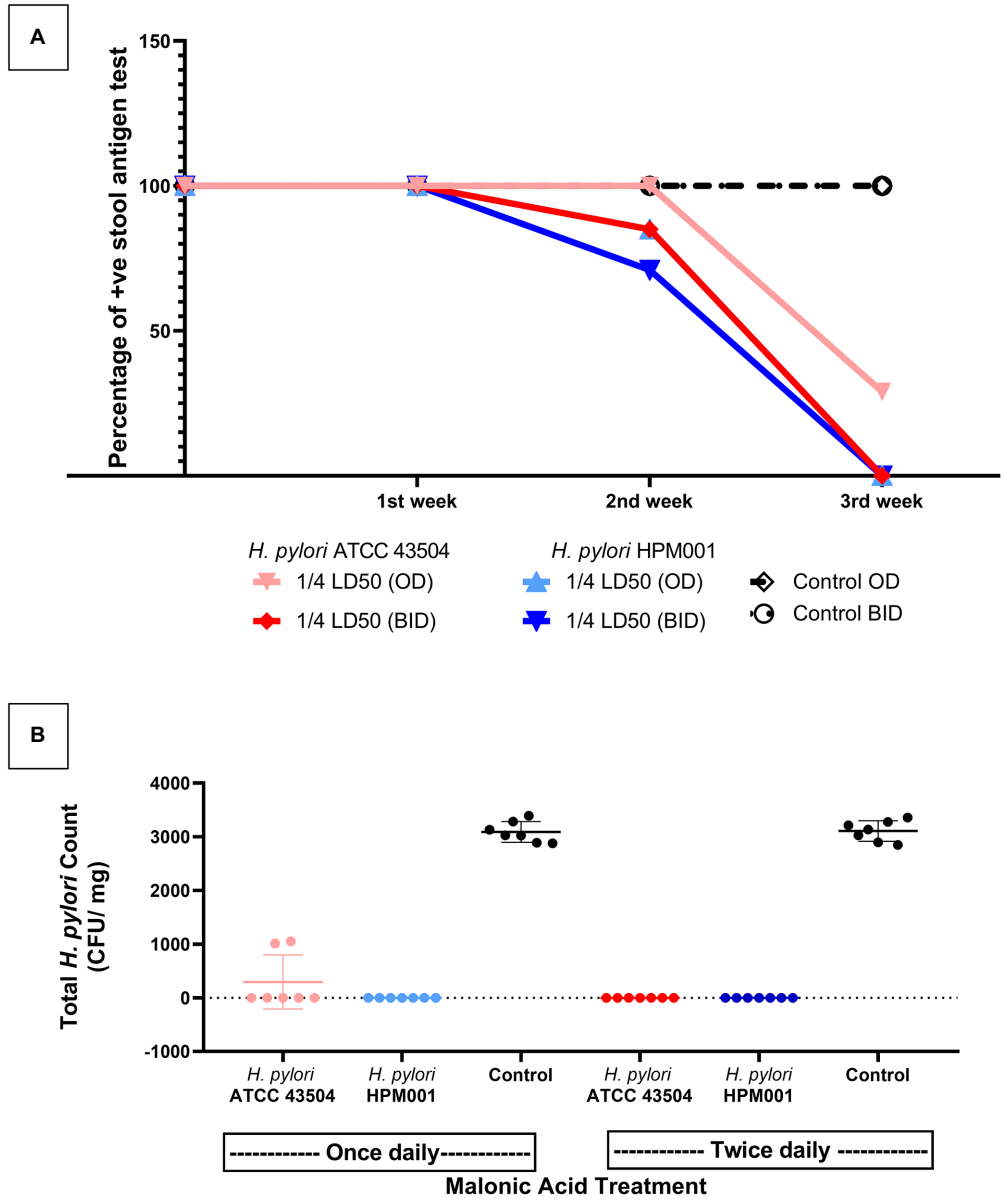

FIGURE 6
Inhibition of aspartate-α-decarboxylase successfully treated *Helicobacter pylori* infected rats. **(A)** Weekly follow up of the number of rats that cleared infection with either *H. pylori* ATCC 43504 or the clinical *H. pylori* HPM001 strains as indicated by *H. pylori* Stool Antigen (HpSA) test during the 3 weeks treatment period. **(B)** The total *H. pylori* count in the stomachs of malonic acid treated and untreated (control) groups of rats at the end of the 3 weeks treatment period. OD, once daily; BID, twice daily; LD_{50}, lethal dose 50; Control, rat groups that received sterile water instead of malonic acid.

acid (propanedioic acid, $C_3H_4O_4$) are structurally similar, with the latter being one carbon less. A low docking score with good interaction results reveals the stability of the ligands and receptors interactions (Syahri et al., 2017). Interaction of the inhibitor with weak bonds to the enzyme's binding site suggests reversible competitive inhibition (Kwon et al., 2022). ADC enzyme was reported as a drug target in *M. tuberculosis* and could be inhibited by pyrazinamide (Gopal et al., 2020).

The MIC of malonic acid against *H. pylori* ranged from 0.5 to 0.75 mg/mL. This is the first report about the anti-helicobacter activity of malonic acid. Few studies have reported the antibacterial activity of malonic acid as a component of the pine needles extract (Feng et al., 2010), and in ternary complexes (El-Sherif, 2010). Several studies reported using short-chain acids as antimicrobial agents (Dittoe et al., 2018; El Baaboua et al., 2018; Gómez-García et al., 2019; Kovanda et al., 2019), besides the prolonged use of organic acids as food preservatives (Ricke, 2003). Malonic acid and its salts are known inhibitors of succinate dehydrogenase enzyme, involved in the cellular respiration as a part of Kreb's cycle, of different bacterial species including *H. pylori* (Chen et al., 1999;

Minato et al., 2013; Meylan et al., 2017; Matsumoto et al., 2020). Inhibition of succinate dehydrogenase was reported to be responsible for the antimicrobial activity of many natural compounds (Keohane et al., 2018; Guo et al., 2021). However, in our previous *in silico* study on druggable targets in *H. pylori*, succinate dehydrogenase was not retrieved among the list of essential or choke points proteins of *H. pylori* (Ibrahim et al., 2020).

The results of the agar dilution and broth microdilution methods, used for MIC determination, were comparable, with no significant difference. This agrees with other studies comparing both methods against *H. pylori* (Piccolomini et al., 1997), and *H. cinaedi* (Tomida et al., 2013). The agar dilution method, the CLSI approved method for antimicrobial susceptibility testing (CLSI, 2015), is time-consuming and tedious compared to the broth microdilution method. Therefore, the broth microdilution method can be an alternative to the agar dilution method for determining MIC in *H. pylori*. Moreover, the difference in the MIC value between *H. pylori* ATCC 43504 and the clinical *H. pylori* HPM001 strain, determined by both methods, was non-significant.

The MBC of malonic acid was almost only two-fold its MIC, confirming the bactericidal nature of ADC inhibition in *H. pylori* by malonic acid. Antimicrobial agents are bactericidal if the MBC is not more than four-fold the MIC (French, 2006).

The selective ADC inhibition by malonic acid was further confirmed by the significant dose-dependent increase in malonic acid MIC ($p < 0.05$) in presence of increasing sub-inhibitory concentrations of β-alanine and pantothenate (the end products of the enzymatic reaction catalyzed by ADC enzyme), with a strong uphill positive relationship between either β-alanine ($r = 0.6857$) or pantothenate ($r = 0.767$) concentrations and malonic acid MIC. Similarly, pyrazinamide, the first-line anti-tuberculosis agent, interferes with CoA biosynthesis in *M. tuberculosis* by inhibiting the ADC enzyme (Shi et al., 2014; Gopal et al., 2020). β-alanine and pantothenate also antagonize the activity of pyrazinamide in *M. tuberculosis* (Shi et al., 2014). Pantothenate auxotrophic strains of *M. tuberculosis* are insensitive to pyrazinamide, while prototrophic strains are sensitive (Dillon et al., 2014). Similarly, *Zymomonas mobilis* pantothenate auxotrophs grow well in media supplemented with β-alanine (Gliessman et al., 2017). Several natural and synthetic pantothenic acid analogues possess anti-bacterial activity (Spry et al., 2008). Humans depend on the exogenous uptake of pantothenic acid, while some bacteria, plants, and fungi are capable of *de novo* synthesis of pantothenic acid from β-alanine (Webb et al., 2004). The absence of ADC enzyme in humans makes it a specific promising drug target (Sharma et al., 2012).

The activity of the recombinant 6x-His-tagged ADC enzyme was assayed in presence of increasing concentrations of malonic acid to further confirm ADC inhibition by malonic acid. Direct measurement of the β-alanine concentration, by HPLC, in the enzymatic reaction catalyzed by either the crude extract of IPTG-induced *E. coli* BL21/RecPl or the purified recombinant 6x-His-tagged ADC showed a significant reduction in enzymatic activity with increasing malonic acid concentration ($p < 0.000001$).

Repeated exposure to ADC inhibition by malonic acid did not develop resistance in any of the tested *H. pylori* strains. In contrast, clarithromycin-resistant and susceptible *H. pylori* strains readily developed resistance following 14 serial passages, with the MIC increasing by 16-fold at the end of the passages. Similar studies reported an increased MIC of clarithromycin against *H. pylori* isolates following repeated exposure (Kobayashi et al., 2002). This confirms the superiority of ADC inhibition as a drug target in *H. pylori*, where the relapse of *H. pylori* infection usually occurs due to incomplete eradication or the emergence of resistant strains (Abadi, 2016).

Malonic acid had no cytotoxic effect on the tested oral epithelial or human skin fibroblast cells, even at the highest tested concentration (60 mg/mL). According to the US national cancer institute guidelines, any compound is considered to lack cytotoxic activity if it has an $IC_{50} > 4$ μg/mL (Kroll, 2001; Ramasamy et al., 2012).

The effectiveness of ADC inhibition in treating *H. pylori* infection was tested in a SD rat infection model. Developing a successful *H. pylori* infection model is challenging as the infection models take a long time with high failure rates (Taylor and Fox, 2012; Werawatganon, 2014). Infection with *H. pylori* Sydney strain remains the most successful animal model for *H. pylori* infection (Taylor and Fox, 2012). However, infection with other strains like *H. pylori* B128 and *H. pylori* ATCC 43504 was also successful (Israel et al., 2001; Hahm et al., 2002; Fox et al., 2003). Non-toxigenic *H. pylori* strains often fail to induce successful animal infection compared to the *cag*A-positive and *vac*A-positive strains (Werawatganon, 2014). We used *H. pylori* ATCC 43504 and a clinical *cag*A-positive and *vac*A-positive *H. pylori* isolate (*H. pylori* HPM001) to infect SD male rats.

Our model was successful, as *H. pylori* colonized ~85.4% of rats by the end of first week post-infection and 100% by the end of the second week. The HpSA test was used to monitor infection throughout the study; it has been used previously to detect *H. pylori* infection in C57BL/6 mice and the results were validated by PCR and rapid urease test (Sjunnesson et al., 2003; Moon et al., 2013). We validated the HpSA test results using the rapid urease test and culture techniques. The results of oxidase, catalase, and urease tests performed on colonies from cultured stomachs of infected and non-infected rats matched the HpSA test.

Aspartate α-decarboxylase Inhibition by malonic acid was effective in the complete eradication of *H. pylori* infection when ¼ LD_{50} (327.5 mg/kg) of malonic acid was administered twice daily for 3 weeks. This dosing regimen was optimum in terms of safety and effectiveness against *H. pylori*. Administering malonic acid at ¼ LD_{50} (327.5 mg/ kg) once daily for 3 weeks resulted in a 100% survival rate and 85.7% curing following the 3 weeks treatment period. However, the average *H. pylori* plate count of the homogenized stomachs from the non-cured rats showed a significant difference ($p < 0.0001$) from the average *H. pylori* plate count of untreated infected rats. Prolonging the treatment period with the once-daily dose regimen could cause complete curing. This is evidenced by the significant difference ($p < 0.0001$) in the

percentage of the HpSA positive results recorded in the first and second week of treatment and that recorded in the second and third week of treatment. The percentage of positive HpSA test results following each week of treatment declined slowly in the group receiving ¼ LD_{50} (327.5 mg/ kg) once daily (mean positive results following each week of treatment were 100, 92.8, and 14.2%, respectively). However, this decline was moderate and steady in the group treated with ¼ LD_{50} (327.5 mg/ kg) twice daily (mean positive test results following each week of treatment were 100, 78.6, and 0%, respectively). This agrees with previous studies about the significant impact of prolonging treatment, either from seven to 10 days or from 10 to 14 days, on eradicating *H. pylori* infection in man (Lee et al., 2010; Fallone et al., 2013; Yuan et al., 2017).

The inhibition of succinate dehydrogenase by malonate in different models (mice and rats) is known to modulate tissue inflammation (Yang et al., 2019; Jespersen et al., 2020); however, whether the use of malonate derivatives in treatment of *H. pylori* infection will also result in modulating gastric tissue inflammation needs to be tested.

Aspartate α-decarboxylase was confirmed as a broad-spectrum target, with comparable malonic acid MIC, in eight bacterial species other than *H. pylori*. *P. aeruginosa* and *E. faecalis* had the lowest MIC (0.625 mg/mL), similar to the mean MIC recorded against *H. pylori* (0.6875 mg/mL). This agrees with our previous *in silico* results regarding the possible broad-spectrum of ADC as a drug target (Ibrahim et al., 2020).

The high MIC values recorded with malonic acid will hinder its applicability in treatment of patients with *H. pylori* infections. Nevertheless, we present malonic acid as a non-toxic lead molecule that can be structurally modified to produce an effective anti-helicobacter agent. Future studies will then be required to determine the kinetics of enzyme inhibition of the newly-developed inhibitors and whether these inhibitors will have an inhibitory effect on succinate dehydrogenase.

The successful use of *in silico* approach in prediction of novel therapeutic targets in microbial species was described previously (Kaplan et al., 2012; Serral et al., 2021). This study is another example of using *in silico* approach in predicting druggable targets in pathogenic species and their possible ligands that can be utilized as lead molecule for the development of novel antimicrobial agents.

Conclusion

Aspartate α-decarboxylase is a promising drug target in *H. pylori*, with low tendency for resistance development by repeated exposure. Malonic acid can be a lead molecule for developing effective anti-helicobacter compounds functioning through ADC inhibition. This offers new hope for saving the lives of those at high risk of infection with the carcinogenic *H. pylori* pathogen.

The determination of *H. pylori* MIC by broth microdilution method is comparable to the gold standard agar dilution method. The broth dilution method is much easier to perform and more efficient in terms of cost and time. Additionally, we successfully developed *H. pylori* infection model by strains other than the Sydney strain in SD rats that can be used for further *in vivo* testing.

Data availability statement

The original contributions presented in the study are included in the article/supplementary material, further inquiries can be directed to the corresponding author.

Ethics statement

The animal study was reviewed and approved by Ethics Committee of the Faculty of Pharmacy, Cairo University, Cairo, Egypt [Approval no. MI (1894)].

Author contributions

MK, MR, and OH contributed to the study conception and design. KI performed the experiment and wrote the first draft of the manuscript. KI, MK, and OH contributed to data analysis and provided the required resources for the work. MK, TE, MR, and OH supervised the work. MK and OH contributed in the preparation of the final article. All authors approved the submitted version.

Funding

Publication fees are partially covered by Cairo University.

Conflict of interest

The authors declare that the research was conducted in the absence of any commercial or financial relationships that could be construed as a potential conflict of interest.

Publisher's note

Supplementary material

The Supplementary material for this article can be found online at: https://www.frontiersin.org/articles/10.3389/fmicb.2022.1019666/full#supplementary-material

References

Abadi, A. T. B. (2016). Vaccine against *Helicobacter pylori*: inevitable approach. *World J. Gastroenterol.* 22, 3150–3157. doi: 10.3748/wjg.v22.i11.3150

Adamczak, A., Ożarowski, M., and Karpiński, T. M. (2020). Antibacterial activity of some flavonoids and organic acids widely distributed in plants. *J. Clin. Med.* 9:109. doi: 10.3390/jcm9010109

Allam, R. M., Al-Abd, A. M., Khedr, A., Sharaf, O. A., Nofal, S. M., Khalifa, A. E., et al. (2018). Fingolimod interrupts the cross talk between estrogen metabolism and sphingolipid metabolism within prostate cancer cells. *Toxicol. Lett.* 291, 77–85. doi: 10.1016/j.toxlet.2018.04.008

Andersen, L. P., and Wadström, T. (2001). "Basic bacteriology and culture," in *Helicobacter pylori: Physiology and genetics*.. eds. H. L. T. Mobley, G. L. Mendz and S. L. Hazell (Washington, DC: ASM press), 132–154.

Asgari, B., Kermanian, F., Yaghoobi, M. H., Vaezi, A., Soleimanifar, F., and Yaslianifard, S. J. V. M. (2020). The anti-*helicobacter pylori* effects of *lactobacillus acidophilus*, *L. plantarum*, and *L. rhamnosus* in stomach tissue of C57BL/6 mice. *Visceral Medecine* 36, 137–143. doi: 10.1159/000500616

Cai, J., Kim, T.-S., Jang, J. Y., Kim, J., Shin, K., Lee, S.-P., et al. (2014). *In vitro* and *in vivo* anti-*Helicobacter pylori* activities of FEMY-R7 composed of fucoidan and evening primrose extract. *Lab.Anim. Res.* 30, 28–34. doi: 10.5625/lar.2014.30.1.28

Charan, J., and Kantharia, N. (2013). How to calculate sample size in animal studies? *J. Pharmacol. Pharmacother.* 4, 303–306. doi: 10.4103/0976-500X.119726

Chen, M., Andersen, L. P., Zhai, L., and Kharazmi, A. (1999). Characterization of the respiratory chain of *Helicobacter pylori*. *FEMS Immunol. Med. Microbiol.* 24, 169–174. doi: 10.1111/j.1574-695X.1999.tb01278.x

CLSI (2015). *Methods for antimicrobial dilution and disk susceptibility testing of infrequently isolated or fastidious bacteria. CLSI guideline M45*: Wayne, PA: Clinical and Laboratory Standards Institute.

CLSI (2018). *Methods for dilution antimicrobial susceptibility tests for bacteria that grow aerobically; CLSI standard M07*. Wayne, PA: Clinical and Laboratory Standards Institute.

Coban, H. B. (2020). Organic acids as antimicrobial food agents: applications and microbial productions. *Bioprocess Biosyst. Eng.* 43, 569–591. doi: 10.1007/s00449-019-02256-w

Dillon, N. A., Peterson, N. D., Rosen, B. C., and Baughn, A. D. (2014). Pantothenate and pantetheine antagonize the antitubercular activity of pyrazinamide. *Antimicrob. Agents Chemother.* 58, 7258–7263. doi: 10.1128/AAC.04028-14

Dittoe, D. K., Ricke, S. C., and Kiess, A. S. (2018). Organic acids and potential for modifying the avian gastrointestinal tract and reducing pathogens and disease. *Front. Vet. Sci.* 5:216. doi: 10.3389/fvets.2018.00216

El Baaboua, A., El Maadoudi, M., Bouyahya, A., Belmehdi, O., Kounnoun, A., Zahli, R., et al. (2018). Evaluation of antimicrobial activity of four organic acids used in chicks feed to control *salmonella Typhimurium*: suggestion of amendment in the search standard. *Int. J. Microbiol.* 2018:7352593. doi: 10.1155/2018/7352593

El-Sherif, A. A. (2010). Synthesis, solution equilibria and antibacterial activity of co (II) with 2-(aminomethyl)-benzimidazole and dicarboxylic acids. *J. Solut. Chem.* 39, 1562–1581. doi: 10.1007/s10953-010-9593-y

Fallone, C. A., Barkun, A. N., Szilagyi, A., Herba, K. M., Sewitch, M., Martel, M., et al. (2013). Prolonged treatment duration is required for successful *Helicobacter pylori* eradication with proton pump inhibitor triple therapy in Canada. *Can. J. Gastroenterol.* 27, 397–402. doi: 10.1155/2013/801915

Feng, S., Zeng, W., Luo, F., Zhao, J., Yang, Z., and Sun, Q. (2010). Antibacterial activity of organic acids in aqueous extracts from pine needles (*Pinus massoniana lamb.*). *Food Sci. Biotechnol.* 19, 35–41. doi: 10.1007/S10068-010-0005-2

Fox, J. G., Wang, T. C., Rogers, A. B., Poutahidis, T., Ge, Z., Taylor, N., et al. (2003). Host and microbial constituents influence *helicobacter pylori*-induced cancer in a murine model of hypergastrinemia. *Gastroenterology* 124, 1879–1890. doi: 10.1016/s0016-5085(03)00406-2

French, G. (2006). Bactericidal agents in the treatment of MRSA infections—the potential role of daptomycin. *J. Antimicrob. Chemother.* 58, 1107–1117. doi: 10.1093/jac/dkl393

Gliessman, J. R., Kremer, T. A., Sangani, A. A., Jones-Burrage, S. E., and McKinlay, J. B. (2017). Pantothenate auxotrophy in *Zymomonas mobilis* ZM4 is due to a lack of aspartate decarboxylase activity. *FEMS Microbiol. Lett.* 364:fnx136. doi: 10.1093/femsle/fnx136

Gómez-García, M., Sol, C., de Nova, P. J., Puyalto, M., Mesas, L., Puente, H., et al. (2019). Antimicrobial activity of a selection of organic acids, their salts and essential oils against swine enteropathogenic bacteria. *Porcine Health Manag.* 5, 32–38. doi: 10.1186/s40813-019-0139-4

Gopal, P., Sarathy, J. P., Yee, M., Ragunathan, P., Shin, J., Bhushan, S., et al. (2020). Pyrazinamide triggers degradation of its target aspartate decarboxylase. *Nat. Commun.* 11, 1661–1610. doi: 10.1038/s41467-020-15516-1

Guo, F., Chen, Q., Liang, Q., Zhang, M., Chen, W., Chen, H., et al. (2021). Antimicrobial activity and proposed action mechanism of linalool against *Pseudomonas fluorescens*. *Front. Microbiol.* 12:562094. doi: 10.3389/fmicb.2021.562094

Haas, C., Nix, D. E., and Schentag, J. (1990). *In vitro* selection of resistant *helicobacter pylori*. *Antimicrob. Agents Chemother.* 34, 1637–1641. doi: 10.1128/aac.34.9.1637

Hahm, K. B., Lee, K., Kim, Y., Hong, W., Lee, W., Han, S., et al. (2002). Conditional loss of TGF-β signalling leads to increased susceptibility to gastrointestinal carcinogenesis in mice. *Aliment. Pharmacol. Ther.* 16 Suppl 2, 115–127. doi: 10.1046/j.1365-2036.16.s2.3.x

Hosny, Y., Abutaleb, N. S., Omara, M., Alhashimi, M., Elsebaei, M. M., Elzahabi, H. S., et al. (2020). Modifying the lipophilic part of phenylthiazole antibiotics to control their drug-likeness. *Eur. J. Med. Chem.* 185:111830. doi: 10.1016/j.ejmech.2019.111830

Hu, C. H., Ren, L. Q., Zhou, Y., and Ye, B. C. (2019). Characterization of antimicrobial activity of three *lactobacillus plantarum* strains isolated from Chinese traditional dairy food. *Food Sci. Nutr.* 7, 1997–2005. doi: 10.1002/fsn3.1025

Ibrahim, K. A., Helmy, O. M., Kashef, M. T., Elkhamissy, T. R., and Ramadan, M. A. (2020). Identification of potential drug targets in *helicobacter pylori* using in silico subtractive proteomics approaches and their possible inhibition through drug repurposing. *Pathogens* 9:747. doi: 10.3390/pathogens9090747

Israel, D. A., Salama, N., Arnold, C. N., Moss, S. F., Ando, T., Wirth, H.-P., et al. (2001). *Helicobacter pylori* strain-specific differences in genetic content, identified by microarray, influence host inflammatory responses. *J. Clin. Investig.* 107, 611–620. doi: 10.1172/JCI11450

Jadamus, A., Vahjen, W., and Simon, O. (2005). Studies on the mode of action of probiotics: effects of the spore-specific dipicolinic acid on selected intestinal bacteria. *J. Agric. Sci.* 143, 529–535. doi: 10.1017/S0021859605005666

Jespersen, N. R., Hjortbak, M. V., Lassen, T. R., Støttrup, N. B., Johnsen, J., Tonnesen, P. T., et al. (2020). Cardioprotective effect of succinate dehydrogenase inhibition in rat hearts and human myocardium with and without diabetes mellitus. *Sci. Rep.* 10, 10344–10315. doi: 10.1038/s41598-020-67247-4

Kadkhodaei, S., Siavoshi, F., and Akbari Noghabi, K. (2020). Mucoid and coccoid *helicobacter pylori* with fast growth and antibiotic resistance. *Helicobacter* 25:e12678. doi: 10.1111/hel.12678

Kaplan, N., Albert, M., Awrey, D., Bardouniotis, E., Berman, J., Clarke, T., et al. (2012). Mode of action, *in vitro* activity, and *in vivo* efficacy of AFN-1252, a selective antistaphylococcal FabI inhibitor. *Antimicrob. Agents Chemother.* 56, 5865–5874. doi: 10.1128/aac.01411-12

Keohane, C. E., Steele, A. D., Fetzer, C., Khowsathit, J., Van Tyne, D., Moynié, L., et al. (2018). Promysalin elicits species-selective inhibition of *Pseudomonas aeruginosa* by targeting succinate dehydrogenase. *J. Am. Chem. Soc.* 140, 1774–1782. doi: 10.1021/jacs.7b11212

Kobayashi, I., Muraoka, H., Hasegawa, M., Saika, T., Nishida, M., Kawamura, M., et al. (2002). *In vitro* anti-*helicobacter pylori* activity of BAS-118, a new benzamide derivative. *J. Antimicrob. Chemother.* 50, 129–132. doi: 10.1093/jac/dkf106

Kovanda, L., Zhang, W., Wei, X., Luo, J., Wu, X., Atwill, E. R., et al. (2019). *In vitro* antimicrobial activities of organic acids and their derivatives on several species of gram-negative and gram-positive bacteria. *Molecules* 24:3770. doi: 10.3390/molecules24203770

Kroll, D. J. (2001). Natural compounds in cancer therapy: promising nontoxic antitumor agents from plants and other natural sources. *J. Nat. Prod.* 64, 1605–1606. doi: 10.1021/np000765k

Kwon, C. W., Yeo, S., and Chang, P.-S. (2022). Characterization and molecular docking study of cathepsin L inhibitory peptides (SnuCalCpIs) from *Calotropis procera* R. *Br. Scient. Rep.* 12:5825. doi: 10.1038/s41598-022-09854-x

Lee, B. H., Kim, N., Hwang, T. J., Lee, S. H., Park, Y. S., Hwang, J. H., et al. (2010). Bismuth-containing quadruple therapy as second-line treatment for *Helicobacter pylori* infection: effect of treatment duration and antibiotic resistance on the eradication rate in Korea. *Helicobacter* 15, 38–45. doi: 10.1111/j.1523-5378.2009.00735.x

Li, H., Kalies, I., Mellgård, B., and Helander, H. (1998). A rat model of chronic *helicobacter pylori* infection: studies of epithelial cell turnover and gastric ulcer healing. *Scand. J. Gastroenterol.* 33, 370–378. doi: 10.1080/00365529850170991

Li, H., Liang, X., Chen, Q., Zhang, W., and Lu, H. (2018). Inappropriate treatment in *helicobacter pylori* eradication failure: a retrospective study. *Scand. J. Gastroenterol.* 53, 130–133. doi: 10.1080/00365521.2017.1413132

Madeira, F., Pearce, M., Tivey, A. R. N., Basutkar, P., Lee, J., Edbali, O., et al. (2022). Search and sequence analysis tools services from EMBL-EBI in 2022. *Nucleic Acids Res.* 50, W276–W279. doi: 10.1093/nar/gkac240

Mahavorasirikul, W., Viyanant, V., Chaijaroenkul, W., Itharat, A., and Na-Bangchang, K. (2010). Cytotoxic activity of Thai medicinal plants against human cholangiocarcinoma, laryngeal and hepatocarcinoma cells *in vitro*. *BMC Complement. Altern. Med.* 10, 55–64. doi: 10.1186/1472-6882-10-55

Matsumoto, Y., Nakashima, T., Cho, O., Ohkubo, T., Kato, J., and Sugita, T. (2020). Pyruvate-triggered TCA cycle regulation in *Staphylococcus aureus* promotes tolerance to betamethasone valerate. *Biochem. Biophys. Res. Commun.* 528, 318–321. doi: 10.1016/j.bbrc.2020.05.035

Meylan, S., Porter, C. B. M., Yang, J. H., Belenky, P., Gutierrez, A., Lobritz, M. A., et al. (2017). Carbon sources tune antibiotic susceptibility in *Pseudomonas aeruginosa* via tricarboxylic acid cycle control. *Cell Chem. Biol.* 24, 195–206. doi: 10.1016/j.chembiol.2016.12.015

Minato, Y., Fassio, S. R., and Häse, C. C. (2013). Malonate inhibits virulence gene expression in *vibrio cholerae*. *PLoS One* 8:e63336. doi: 10.1371/journal.pone.0063336

Mo, Q., Li, Y., Wang, J., and Shi, G. (2018). Identification of mutations restricting autocatalytic activation of bacterial l-aspartate α-decarboxylase. *J. Amino Acids* 50, 1433–1440. doi: 10.1007/s00726-018-2620-9

Moon, D.-I., Shin, E.-H., Oh, H.-G., Oh, J.-S., Hong, S., Chung, Y., et al. (2013). Usefulness of a *helicobacter pylori* stool antigen test for diagnosing *H. pylori* infected C57BL/6 mice. *Lab. Anim. Res.* 29, 27–32. doi: 10.5625/lar.2013.29.1.27

Moraes, T. D. S., Lima, L. K. D., Veneziani, R. C. S., Ambrósio, S. R., Santos, R. A. D., Silva, J. J. M. D., et al. (2021). *In vitro* antibacterial potential of the oleoresin, leaf crude hydroalcoholic extracts and isolated compounds of the *Copaifera* spp. against *helicobacter pylori*. Journal of biologically active products from. *Nature* 11, 183–189. doi: 10.1080/22311866.2021.1914730

Mu, W., Yu, S., Zhu, L., Zhang, T., and Jiang, B. (2012). Recent research on 3-phenyllactic acid, a broad-spectrum antimicrobial compound. *Appl. Microbiol. Biotechnol.* 95, 1155–1163. doi: 10.1007/s00253-012-4269-8

Nandode, S., Damale, M., and Harke, S. (2012). *In silico* comparative analysis of metabolic pathways of *Heamophilus influenzae* and *helicobacter pylori* to identify potential drug targets. *Int J Pharm. Bio. Sci* 3, 412–420.

National Research Council (2010). *Guide for the care and use of laboratory animals. 8th Edn*. Washington, D.C: National Academies Press.

Pei, W., Zhang, J., Deng, S., Tigu, F., Li, Y., Li, Q., et al. (2017). Molecular engineering of L-aspartate-α-decarboxylase for improved activity and catalytic stability. *Appl. Microbiol. Biotechnol.* 101, 6015–6021. doi: 10.1007/s00253-017-8337-y

Piccolomini, R., Di Bonaventura, G., Catamo, G., Carbone, F., and Neri, M. (1997). Comparative evaluation of the E test, agar dilution, and broth microdilution for testing susceptibilities of *helicobacter pylori* strains to 20 antimicrobial agents. *J. Clin. Microbiol.* 35, 1842–1846. doi: 10.1128/jcm.35.7.1842-1846.1997

Ramasamy, S., Wahab, N. A., Abidin, N. Z., Manickam, S., and Zakaria, Z. (2012). Growth inhibition of human gynecologic and colon cancer cells by *Phyllanthus watsonii* through apoptosis induction. *PLoS One* 7:e34793. doi: 10.1371/journal.pone.0034793

Ricke, S. (2003). Perspectives on the use of organic acids and short chain fatty acids as antimicrobials. *Poult. Sci.* 82, 632–639. doi: 10.1093/ps/82.4.632

Robinson, K., and Atherton, J. C. (2021). The Spectrum of *helicobacter*-mediated diseases. *Annu. Rev. Pathol.* 16, 123–144. doi: 10.1146/annurev-pathol-032520-024949

Sambrook, J., and Russel, D. W. (2001). "*Molecular Cloning: A Laboratory Manual*. New York: Cold Spring Harbor.

Serral, F., Castello, F. A., Sosa, E. J., Pardo, A. M., Palumbo, M. C., Modenutti, C., et al. (2021). From genome to drugs: new approaches in antimicrobial discovery. *Front. Pharmacol.* 12:647060. doi: 10.3389/fphar.2021.647060

Sharma, R., Kothapalli, R., Van Dongen, A. M., and Swaminathan, K. (2012). Chemoinformatic identification of novel inhibitors against *mycobacterium tuberculosis* L-aspartate α-decarboxylase. *PLoS One* 7:e33521. doi: 10.1371/journal.pone.0033521

Shi, W., Chen, J., Feng, J., Cui, P., Zhang, S., Weng, X., et al. (2014). Aspartate decarboxylase (PanD) as a new target of pyrazinamide in *mycobacterium tuberculosis*. *Emerg. Microb. Infect.* 3, 1–8. doi: 10.1038/emi.2014.61

Sjunnesson, H., Fält, T., Sturegård, E., Al-Soud, W. A., and Wadström, T. (2003). PCR-denaturing gradient gel electrophoresis and two feces antigen tests for detection of *helicobacter pylori* in mice. *Curr. Microbiol.* 47, 278–0285. doi: 10.1007/s00284-002-3952-x

Song, C. W., Lee, J., Ko, Y.-S., and Lee, S. Y. (2015). Metabolic engineering of *Escherichia coli* for the production of 3-aminopropionic acid. *Metab. Eng.* 30, 121–129. doi: 10.1016/j.ymben.2015.05.005

Spry, C., Kirk, K., and Saliba, K. J. (2008). Coenzyme a biosynthesis: an antimicrobial drug target. *FEMS Microbiol. Rev.* 32, 56–106. doi: 10.1111/j.1574-6976.2007.00093.x

Stahl, M., Ries, J., Vermeulen, J., Yang, H., Sham, H. P., Crowley, S. M., et al. (2014). A novel mouse model of *campylobacter jejuni* gastroenteritis reveals key pro-inflammatory and tissue protective roles for toll-like receptor signaling during infection. *PLoS Pathog.* 10:e1004264. doi: 10.1371/journal.ppat.1004264

Sudhakar, U., Anusuya, C., Ramakrishnan, T., and Vijayalakshmi, R. (2008). Isolation of *helicobacter pylori* from dental plaque: a microbiological study. *J. Ind. Soc. Periodontol.* 12, 67–72. doi: 10.4103/0972-124X.44098

Syahri, J., Yuanita, E., Nurohmah, B. A., Armunanto, R., and Purwono, B. (2017). Chalcone analogue as potent anti-malarial compounds against *plasmodium falciparum*: synthesis, biological evaluation, and docking simulation study. *Asian Pac. J. Trop. Biomed.* 7, 675–679. doi: 10.1016/j.apjtb.2017.07.004

Taylor, N. S., and Fox, J. G. (2012). Animal models of Helicobacter-induced disease: methods to successfully infect the mouse. *Methods Mol. Biol.* 921, 131–142. doi: 10.1007/978-1-62703-005-2_18

Tomida, J., Oumi, A., Okamoto, T., Morita, Y., Okayama, A., Misawa, N., et al. (2013). Comparative evaluation of agar dilution and broth microdilution methods for antibiotic susceptibility testing of *helicobacter cinaedi*. *Microbiol. Immunol.* 57, 353–358. doi: 10.1111/1348-0421.12044

Ventola, C. L. (2015). The antibiotic resistance crisis: part 1: causes and threats. *Pharm. Therap.* 40, 277–283.

Walia, G., Kumar, P., and Surolia, A. (2009). The role of UPF0157 in the folding of *M. tuberculosis* dephosphocoenzyme a kinase and the regulation of the latter by CTP. *PLoS One* 4:e7645. doi: 10.1371/journal.pone.0007645

Walsh, E., and Moran, A. (1997). Influence of medium composition on the growth and antigen expression of *helicobacter pylori*. *J. Appl. Microbiol.* 83, 67–75. doi: 10.1046/j.1365-2672.1997.00164.x

Webb, M. E., Smith, A. G., and Abell, C. (2004). Biosynthesis of pantothenate. *Nat. Prod. Rep.* 21, 695–721. doi: 10.1039/B316419P

Werawatganon, D. (2014). Simple animal model of *helicobacter pylori* infection. *World J. Gastroenterol.* 20, 6420–6424. doi: 10.3748/wjg.v20.i21.6420

Xu, D., Zhao, S., Dou, J., Xu, X., Zhi, Y., and Wen, L. (2021). Engineered endolysin-based "artilysins" for controlling the gram-negative pathogen *helicobacter pylori*. *AMB Express* 10, 1–9. doi: 10.3390/antibiotics10111277

Yan, F., and Gao, F. (2020). A systematic strategy for the investigation of vaccines and drugs targeting bacteria. *Comput. Struct. Biotechnol. J.* 18, 1525–1538. doi: 10.1016/j.csbj.2020.06.008

Yang, Y., Shao, R., Tang, L., Li, L., Zhu, M., Huang, J., et al. (2019). Succinate dehydrogenase inhibitor dimethyl malonate alleviates LPS/d-galactosamine-induced acute hepatic damage in mice. *Innate Immun.* 25, 522–529. doi: 10.1177/1753425919873042

Yang, Y., Wang, J., Xu, J., Liu, Q., Wang, Z., Zhu, X., et al. (2020). Characterization of IL-22 bioactivity and IL-22-positive cells in grass carp *Ctenopharyngodon idella*. *Front. Immunol.* 11:586889. doi: 10.3389/fimmu.2020.586889

Yuan, X.-Y., Yan, J.-J., Yang, Y.-C., Wu, C.-M., Hu, Y., and Geng, J.-I. (2017). *Helicobacter pylori* with east Asian-type cagPAI genes is more virulent than strains with Western-type in some cagPAI genes. *Braz. J. Microbiol.* 48, 218–224. doi: 10.1016/j.bjm.2016.12.004

Zhang, X.-S., Tegtmeyer, N., Traube, L., Jindal, S., Perez-Perez, G., Sticht, H., et al. (2015). A specific a/T polymorphism in Western tyrosine phosphorylation B-motifs regulates *helicobacter pylori* CagA epithelial cell interactions. *PLoS Pathog.* 11:e1004621. doi: 10.1371/journal.ppat.1004621

frontiers | Frontiers in Microbiology

TYPE Original Research
PUBLISHED 08 December 2022
DOI 10.3389/fmicb.2022.1033201

OPEN ACCESS

EDITED BY
Lucinda Janete Bessa,
Egas Moniz – Cooperativa de Ensino Superior, CRL, Portugal

REVIEWED BY
Norma Velazquez-Guadarrama,
Federico Gómez Children's Hospital, Mexico
Sasikala Muthusamy,
Academia Sinica, Taiwan

*CORRESPONDENCE
Lei Li
htlilei@163.com

SPECIALTY SECTION
This article was submitted to Antimicrobials, Resistance and Chemotherapy, a section of the journal Frontiers in Microbiology

RECEIVED 31 August 2022
ACCEPTED 23 November 2022
PUBLISHED 08 December 2022

CITATION
Zhang Y, Wang C, Zhang L, Yu J, Yuan W and Li L (2022) Vitamin D_3 eradicates *Helicobacter pylori* by inducing VDR-CAMP signaling. *Front. Microbiol.* 13:1033201. doi: 10.3389/fmicb.2022.1033201

Vitamin D_3 eradicates *Helicobacter pylori* by inducing VDR-CAMP signaling

Ye Zhang[1], Chunya Wang[1], Li Zhang[1], Jie Yu[2], Wenjie Yuan[1] and Lei Li[1]*

[1]Department of Gastroenterology, Affiliated Hospital of Weifang Medical University, Weifang, China, [2]Department of Hepatobiliary Surgery, The First Affiliated Hospital, Kunming Medical University, Kunming, China

Background: Vitamin D_3 [$VitD_3$, 1,25 $(OH)_2D_3$] is known to have immunomodulatory and anti-microbial properties; however, its activity against *Helicobacter pylori* is unclear. In this study, we established *H. pylori* infection models in wild-type and $VitD_3$ receptor (VDR) knockdown mice and analyzed the effects of $VitD_3$ and their underlying mechanisms.

Methods: $VDR^{+/+}$ and $VDR^{+/-}$ mice were intragastrically infected with the *H. pylori* SS1 strain. After confirmation of *H. pylori* infection, mice were treated with different doses of $VitD_3$. The infection levels in stomach tissues were quantified using the colony-forming assay, and the expression levels of the VDR and cathelicidin antimicrobial peptide (CAMP) in the gastric mucosa were analyzed by immunohistochemistry and western blotting.

Results: The gastric mucosa of $VDR^{+/-}$ mice was more susceptible to *H. pylori* colonization and had lower levels of VDR and CAMP expression than that of $VDR^{+/+}$ mice. *H. pylori* infection upregulated VDR and CAMP expression in the stomach of both wild-type and mutant mice, and $VitD_3$ treatment resulted in further increase of VDR and CAMP levels, while significantly and dose-dependently decreasing the *H. pylori* colonization rate in both mouse groups, without affecting blood calcium or phosphorus levels.

Conclusion: Our data indicate that oral administration of $VitD_3$ reduces the *H. pylori* colonization rate and upregulates VDR and CAMP expression in the gastric mucosa, suggesting a role for $VitD_3$/VDR/CAMP signaling in the eradication of *H. pylori* in the stomach. These findings provide important insights into the mechanism underlying the anti-*H. pylori* activity of $VitD_3$ and should be useful in the development of measures to eradicate *H. pylori*.

KEYWORDS

1α, 25-dihydroxyvitamin D_3, *H. pylori*, vitamin D receptor, cathelicidin antimicrobial peptide, inflammation

Introduction

Helicobacter pylori colonizes the gastric epithelium of approximately half of the world's population and is classified as a class I carcinogen by the World Health Organization (Malfertheiner et al., 2017). Both sanitary conditions and socio-economic status are important factors in the prevalence of *H. pylori* infection, which is higher in developing than in developed countries. The pathogenic activity of *H. pylori* can result in such diseases as chronic gastritis and peptic ulcer, and individuals carrying the bacteria for many years have an increased risk of gastric cancer and gastric mucosa-associated lymphoid tissue lymphoma. Furthermore, in users of non-steroidal anti-inflammatory drugs, *H. pylori* infection may increase the risk of gastric bleeding (Mitchell and Katelaris, 2016). *H. pylori* may also play a role in many extragastric diseases, including idiopathic thrombocytopenic purpura, unexplained iron deficiency anemia, and vitamin B12 deficiency (Huang et al., 2010). The eradication of *H. pylori* can effectively prevent the occurrence of these pathological conditions; however, it is difficult for the host to clear the infection through the innate immune system. Proton pump inhibitor (PPI)-based triple therapy was once the first-line approach to *H. pylori* eradication (Malfertheiner et al., 2007), but the widespread use of antibiotics has led to the emergence of single- and multiple-drug-resistant *H. pylori* strains, making its eradication more difficult (Malfertheiner et al., 2012; Savoldi et al., 2018). At present, quadruple therapy is considered to be an effective alternative regimen, especially in developing countries where the population has high resistance to clarithromycin or metronidazole (Kim et al., 2014). Our previous research indicates that bismuth in a compound preparation, Wei Bi Mei, has higher efficacy and safety in eradicating *H. pylori* compared to commonly used bismuth medicines: it can significantly reduce *H. pylori* colonization, while showing the fastest clearance and the lowest accumulation rates in organs (Li et al., 2018). However, new drug-resistant strains continue to emerge, while safe and effective vaccines are still under development (Stubljar et al., 2018; Walduck and Raghavan, 2019). Therefore, there is an urgent need for new antibacterial agents with fewer adverse effects to improve on the current status of *H. pylori* eradication.

Vitamin D (VitD) is a steroid hormone necessary for bone mineralization. Obtained from food or through solar exposure, VitD is inactive and is transported to the liver, where 25-hydroxyvitamin D (calcidiol) is produced through the activity of microsomal VitD-25-hydroxylase and is then either stored in the liver or released into the bloodstream. In the kidney, calcidiol is catalyzed by mitochondrial 1a-hydroxylase (CYP27B1), produced by the renal proximal tubule epithelial cells, into 1α,25-dihydroxyvitamin D_3 ($VitD_3$), the activated hormonal form of VitD (Reeve et al., 1983) which regulates calcium and phosphorus absorption in the intestine, mobilizes bone calcium, and maintains the balance of calcium and phosphorus in serum (Christakos et al., 2012).

Now, it is increasingly recognized that $VitD_3$ is not only related to the diseases of the skeletal system but is also associated with many other physiological processes in the human body. $VitD_3$ exerts its functional effects through binding to the VitD receptor (VDR), a transcription factor that belongs to the nuclear receptor superfamily and is found in almost all cell types of the human organism (Carlberg, 2014). The VDR not only controls the expression of genes related to mineral metabolism but also interacts with other intracellular signaling pathways such as those regulating immune reactions, cell cycle progression, and apoptosis. The effects of $VitD_3$ on immune responses to bacterial infections, especially to *Mycobacterium tuberculosis*, have been documented in many studies. VitD3 has been shown to promote autophagy in *M. tuberculosis*-infected macrophages and induce the activation of Toll-like receptors (TLRs), thus inducing VDR, CYP27B1, and CYP27B1 expression and the synthesis of biologically active $VitD_3$; the latter in turn binds to the VDR and upregulates the expression of cathelicidin antimicrobial peptide (CAMP), ultimately enhancing immune response and promoting the eradication of intracellular *M. tuberculosis* (Hmama et al., 2004; Schauber et al., 2007; Hewison, 2011). VitD can also reduce the incidence of respiratory tract infections. A previous study found that serum VitD levels were negatively correlated with the rate of recent upper respiratory infections among 19,000 participants, who had been followed for an average of more than 12 years (Ginde et al., 2009). In a cohort study including 800 participants, it was found that the number of days of absence from duty due to respiratory infection was significantly higher for the participants with serum VitD levels <40 nmol/L than for the control group (Laaksi et al., 2007). As $VitD_3$ is a direct inducer of CAMP, which is known to mount immune response against a variety of pathogenic microorganisms, including gram-positive and gram-negative bacteria, viruses, and fungi (Liu et al., 2006; Wang et al., 2019), we hypothesize that the $VitD_3$–CAMP axis may be involved in the immune defense against *H. pylori*.

Accumulating evidence indicates that VitD is associated with the risk of *H. pylori* infection and failure of its eradication. Specifically, serum VitD levels are higher in patients successfully treated for *H. pylori* infection than in those with treatment failure (Yildirim et al., 2017). Serum VitD levels also have a significant positive correlation with *H. pylori* infection in uremic patients (Nasri and Baradaran, 2007). VitD deficiency can promote the development of *H. pylori*-related chronic gastritis and increase the severity of gastric mucosal damage, whereas VitD supplementation can improve disease status (Zhang et al., 2016). It has been documented that *H. pylori* infection in children is significantly associated with VitD deficiency (Gao et al., 2020) and that its prevalence in elderly patients is decreased by VitD supplementation. Cumulatively,

these findings indicate that VitD administration may improve the efficiency of *H. pylori* eradication and reduce drug-related adverse effects.

It has been shown that in human GES-1 cells, the expression of the VDR and CAMP is increased after *H. pylori* infection, whereas in mice, the inhibition of VDR expression leads to significant downregulation of CAMP mRNA and protein expression but upregulation of inflammatory factors (Guo et al., 2014). A previous study indicates that compared with wild-type mice, CAMP knockout mice have increased susceptibility to *H. pylori* colonization of the gastric mucosa and aggravated mucosal inflammation, whereas supplementation with exogenous CAMP can reduce *H. pylori* colonization and inflammation in the mucosa and decrease the production of inflammatory cytokines (Zhang et al., 2013). These results suggest that CAMP plays an important role in the prevention of gastric mucosa colonization by *H. pylori*.

In this study, we tested a hypothesis that the VDR/CAMP pathway may be involved in the inhibitory effect of $VitD_3$ on *H. pylori* infection. For this test, we established *H. pylori* infection models in C57BL/6J wild-type and VDR knockdown mice and investigated the effect of $VitD_3$ gavage. Our findings indicate that $VitD_3$ can, in a concentration-dependent manner, eradicate *H. pylori* and induce the expression of VDR and CAMP *in vivo*, suggesting the mechanism underlying the anti-*H. pylori* activity of $VitD_3$.

Materials and methods

Bacterial culture and strain adaptation

The *H. pylori* Sydney strain 1 (SS1) (kindly provided by Professor Chun-Jie Liu, Academy of Military Medical Sciences of the Chinese People's Liberation Army (PLA), Beijing, China) was stored at −80°C. After thawing at room temperature, the bacterial suspension was dropped onto Campylobacter Base Agar plates containing three antibiotics (0.38 mg/L polymyxin B, 10 mg/L vancomycin, and 2 mg/L amphotericin B) and cultured for 36–72 h at 37°C under microaerobic conditions (5% O_2, 10% CO_2, and 85% N_2). A small amount of cultured *H. pylori* was picked, evenly spread on slides dripped with Double Distilled Water, dried, and stained with flagellar staining solution (alkalescent carbolfuchsin; DM0031, Beijing Leagene Biotechnology Co., Ltd., Beijing, China) to assess bacterial growth status. Bacterial suspensions were prepared by adding sterile saline to *H. pylori*-containing plates and collecting for subsequent use.

Specific-pathogen-free (SPF) C57BL/6J mice (10-week-old males weighting 19–22 g) were purchased from Beijing Vital River Laboratory (Beijing Vital River Laboratory Animal Technology Co., Ltd., Beijing, China) and housed in the Animal Experiment Center of the Chinese Center for Disease Control and Prevention under a 12:12 h light-dark cycle in a standard environment of 23 ± 2°C and 50–60% relative humidity; distilled water and standard sterile mouse feed (Beijing Keao Xieli Feed Co., Ltd., Beijing, China) were provided *ad libitum*. The adapted *H. pylori* strains capable of mouse colonization were obtained by serial passage *in vivo* and used to establish infection models. Mice were administered bacterial suspension [10^8 colony forming units (CFU)/L] orally and euthanized 4 weeks later. Stomachs were removed, washed, and cut longitudinally into halves along the greater curvature; one half of the gastric mucosa was suspended, transferred to plates, and cultured for 36–72 h to reveal the presence or absence of *H. pylori*, whereas the other half was used for direct smear microscopy. After confirmation of successful infection, the *H. pylori* isolate with the highest number of colonies was selected as the first-generation adapted strain. The next-generation strain was obtained after infecting new mice with the first-generation strain as described above. The procedure was repeated until stable infection in mice was achieved. All animal experiments were approved by the Laboratory Animal Ethics Committee of Beijing Friendship Hospital, Affiliated to Capital Medical University, and were performed in accordance with institutional guidelines.

Mouse models of *Helicobacter pylori* infection

Before infection, mice were fasted for 12 h and deprived of water for 4 h; then, they received 300 μL of 3% $NaHCO_3$ by gavage to increase the pH in the stomach. Mice were then divided into control and *H. pylori* infection groups and intragastrically inoculated with 300 μL of sterile saline or the suspension of the adapted *H. pylori* strain (10^8 CFU/L), respectively. Inoculation was performed twice in each subject, once 30 min after $NaHCO_3$ treatment and once after 4 h. Mice were allowed free access to food and water 2 h after the last dose and were fed normally until the end of the experiment. Three months later, fecal genetic testing was performed to confirm *H. pylori* infection in the gastrointestinal tract. Mice were euthanized by spinal cord dislocation, and their gastric tissues were removed and stained with hematoxylin–eosin to analyze the inflammatory response. Warthin-Starry staining (SBJ-0548, Nanjing SenBeiJia Co., Ltd., Nanjing, China) and a *H. pylori* rapid detection kit (HPUT-H104, Fujian Sanqiang Biochemical Co., Ltd., Fujian, China) were used to observe *H. pylori* colonization.

$VitD_3$ intervention

Male 3–12 week-old C57BL/6J mice of the wild type ($VDR^{+/+}$) and VDR knockout homozygous type ($VDR^{-/-}$; B6.129S4-Vdr^{TM1Mbd}/J, SPF) were purchased from Jackson Laboratory (Bar Harbor, ME, USA). VDR knockdown

($VDR^{+/-}$) mice were obtained by *in vitro* fertilization in Beijing Biocytogen Co., Ltd.

$VDR^{+/+}$ and $VDR^{+/-}$ mice were randomly divided into five groups (n = 6 mice per group): control and *H. pylori* infection (HP) groups, and three HP + $VitD_3$ groups. Mice in the control group were intragastrically inoculated with sterile saline and those in HP/HP + $VitD_3$ groups with *H. pylori* suspension as described above. After 3 months, the control and HP groups were orally administered equal volumes (300 μL) of corn oil, whereas the three HP + $VitD_3$ groups were orally administered 0.1, 0.4, and 1.6 μg/kg of 1α,25-Dihydroxyvitamin D_3 (D1530, Sigma Aldrich, St Louis, MO, USA) and designated as HP+$VitD_3$*1, HP+$VitD_3$*4, and HP+$VitD_3$*16, respectively. All treatments were performed once a day for 14 consecutive days. Then, blood was collected from the eye, and mice were euthanized by spinal cord dislocation. Gastric tissue was removed under sterile conditions, washed, and cut longitudinally into halves along the greater curvature. One half was fixed in 10% formalin, embedded in paraffin, cut into 4 μm-thick sections, baked for 1 h at 60°C, deparaffinized in xylene, and rehydrated in graded ethanol for subsequent staining. The other half was used for the colony-forming assay and other tests.

Warthin-starry staining

Deparaffinized tissue sections were washed three times for 1 min with distilled water, incubated in acidic silver nitrate solution for 1 h in the dark at 56°C, and immersed in Warthin-Starry solution for 3–8 min. After soaking in distilled water at 56°C and rinsing once with distilled water, sections were dehydrated in 100% ethanol, cleared with xylene for transparency, sealed with neutral gel, and analyzed by light microscopy. *H. pylori* appeared tan or black on a light yellow background.

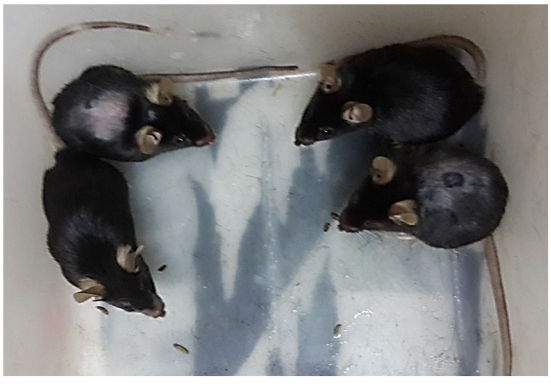

FIGURE 1
Mouse strains. $VDR^{+/-}$ C57BL/6J mice (upper left and lower right) and $VDR^{+/+}$ C57BL/6J mice (lower left and upper right).

Rapid urease reaction

Fresh gastric mucosal tissue was placed into the liquid medium of the enzyme-labeled strip (enzymatic reaction solution) from the *H. pylori* detection kit, according to the manufacturer's instructions, and incubated at 10–30°C for 5 min. The results were visually observed and interpreted according to color change of the liquid at the edge of gastric mucosal tissue: yellow (no chromogenic reaction) was treated as negative and light or rose red as positive for *H. pylori*.

Determination of serum calcium and phosphorus levels

Blood samples were centrifuged at 3,000 rpm for 10 min, and about 100–300 μL of supernatant was collected to measure serum calcium and phosphorus contents using an automatic biochemical analyzer.

Colony-forming assay

The level of *H. pylori* infection in mouse gastric tissue was quantified by the colony-forming assay. Approximately half of the stomach tissue was weighed, homogenized in 1 mL Brucella broth, serially 10-fold diluted, and spread on agar plates containing Campylobacter Base Agar, 10% fetal calf serum, 0.38 mg/L polymyxin B, 10 mg/L vancomycin, 2 mg/L amphotericin B, 5 mg/L trimethoprim, and 50 mg/L bacitracin (Merck KGaA, Darmstadt, Germany). After 72 h of incubation, the number of colonies per plate and CFUs per gram of stomach tissue were calculated.

Immunohistochemistry

Paraffin sections were rehydrated through graded alcohol solutions and washed with distilled water. Antigen retrieval was performed by heating sections in 0.01 M sodium citrate buffer (pH 6.0) in a pressure cooker at 130°C for 3 min, and endogenous peroxidase activity was quenched by incubation in 3% hydrogen peroxide for 15 min. Then, tissue sections were incubated with anti-VDR C-20 or anti-CAMP antibodies (Santa Cruz Biotechnology, Santa Cruz, CA, USA) at 4°C overnight. After washing in PBS three times, sections were incubated with horseradish peroxidase-conjugated secondary anti-rabbit Ig (ZSGB-BIO, Beijing, China) for 1 h at room temperature, washed, and immersed in diaminobenzidine (ZSGB-BIO) for 1–2 min to develop color reaction. Finally, sections were counterstained with hematoxylin, dehydrated, and mounted in resin mounting medium.

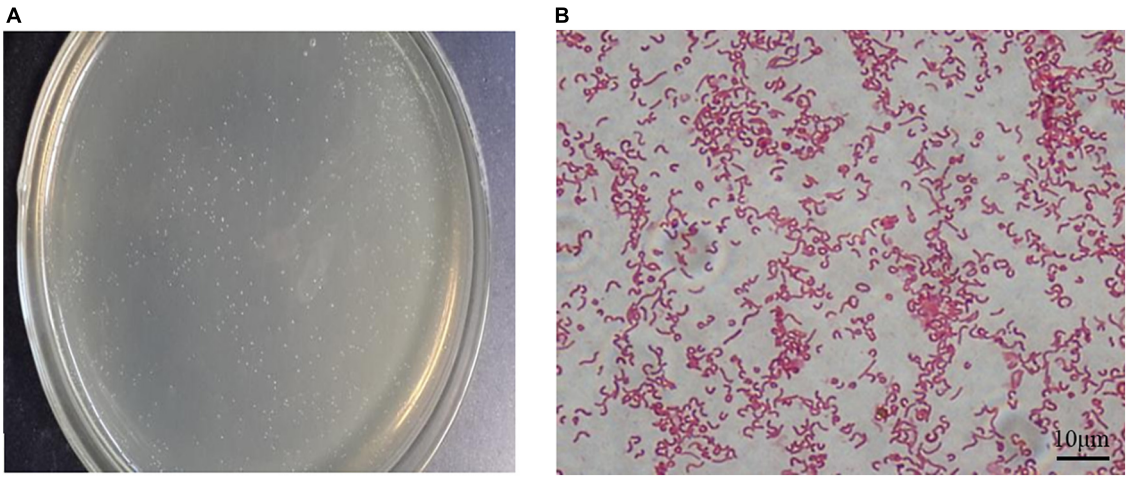

FIGURE 2
Cultivation of the *Helicobacter pylori* Sydney strain 1 (SS1) strain *in vitro*. **(A)** Typical white needle tip colonies could be seen on the plates after 72 h of incubation. **(B)** Bacterial flagella were observed after alkalescent carbolfuchsin staining. Scale bar = 10 μm.

Western blotting

Total protein was extracted from gastric mucosal tissue using RIPA lysis buffer, and protein concentration was quantified using the Pierce BCA Protein Quantification kit (Thermo Fisher Scientific, Waltham, MA, USA). Proteins were separated by SDS/PAGE in 10% gels and transferred to polyvinylidene fluoride (PVDF) membranes, which were then blocked with 5% non-fat milk for 3 h at room temperature and incubated with antibodies against VDR (Santa Cruz Biotechnology, Santa Cruz, CA, USA), CAMP (Santa Cruz Biotechnology, Santa Cruz, CA, USA), or β-actin (Sigma, USA) at 4°C overnight. After three 10 min washes with Tris-buffered saline containing 0.1% Tween 20, the membranes were incubated with horseradish peroxidase-conjugated secondary antibodies at room temperature for 1 h, and signals were developed using the enhanced chemiluminescence kit (Bio-Rad, California, USA).

Statistical analysis

The data are presented as the mean ± standard deviation (SD). Differences between groups were assessed by analysis of variance and standalone *t*-test. $P < 0.05$ was considered to indicate statistical significance.

Results

The mouse tail genotype test showed that $VDR^{+/-}$ C57BL/6J mice were successfully created and met the requirements of the experiment. Compared with wild-type $VDR^{+/+}$ C57BL/6J mice, $VDR^{+/-}$ C57BL/6J mice had less hair in the back, clearly showing the skin (Figure 1).

Characteristics of the *Helicobacter pylori* Sydney strain 1 strain cultured *in vitro*

After 72 h of culture, the resuscitated *H. pylori* SS1 strain formed typical spiculate translucent colonies (Figure 2A). In most smears, morphologically intact *H. pylori*, typically with flagella, were revealed after carbolfuchsin staining (Figure 2B), indicating good activity, and strong colonization ability of the adapted strain.

Helicobacter pylori successfully colonized mouse stomachs

It is known that *H. pylori* has urease genes and can produce large amounts of urease, which is necessary for its colonization of the human gastric mucosa and is used for routine diagnosis of *H. pylori* infection. Three months after *H. pylori* intragastric administration, the urease reaction test was positive in infected mice and negative in control mice (Figure 3A), indicating *H. pylori* colonization of gastric tissues. Several black rod-shaped structures were observed after Warthin-Starry silver staining (Figure 3B), confirming that *H. pylori* was present in the gastric mucosa. Compared with the gastric tissue of uninfected mice (Figure 3C), that of infected mice showed massive lymphocyte infiltration and increased presence of inflammatory cells (Figure 3D). These results indicated that the

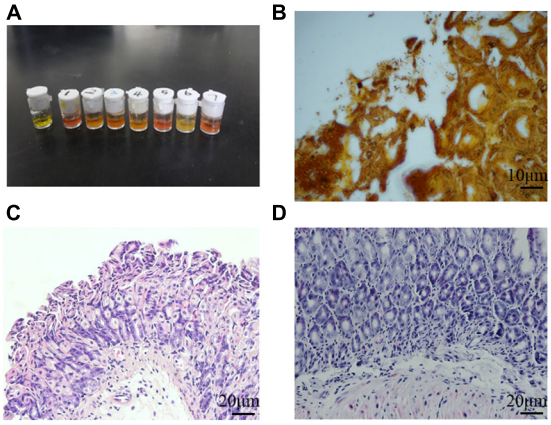

FIGURE 3
Helicobacter pylori successfully colonized mouse stomach tissue. **(A)** Rapid urease reaction showed positive results in infected mice and negative results in control mice. **(B)** Several black rod-shaped structures were observed after Warthin-Starry silver staining. Scale bar = 10 μm. **(C,D)** Hematoxylin-eosin staining of the gastric mucosa of uninfected **(C)** and infected **(D)** mice. Chronic gastric mucosal inflammation could be observed in the infected group. Scale bar = 20 μm.

one-time oral gavage of the *H. pylori* SS1 strain resulted in the successful establishment of a mouse model of *H. pylori* infection, which produced chronic gastric inflammation after 3 months.

Helicobacter pylori eradication efficacy of $VitD_3$ in infected mice

The results of the colony-forming assay performed 3 months after intragastric administration of *H. pylori* indicated that $VDR^{+/-}$ mice were more susceptible to *H. pylori* colonization than $VDR^{+/+}$ mice ($P < 0.05$, Figure 4). In both wild-type and mutant mice, $VitD_3$ administration significantly reduced *H. pylori* colonization compared with corn oil-treated control groups, and the number of *H. pylori* showed a gradual dose-dependent decrease (Figure 4A). There were no significant changes in food intake or body weight throughout the experiment, and all mice showed no abnormalities. After $VitD_3$ intervention, serum calcium and phosphorus concentrations were still in the normal range in all mice (Figure 4B, $P > 0.05$).

$VitD_3$ upregulated VitD3 receptor expression in the mouse gastric mucosa

To further investigate the mechanism of *H. pylori* clearance by $VitD_3$, we analyzed VDR expression in control and infected mice, treated or not with $VitD_3$. VDR protein expression was significantly upregulated in the gastric mucosa of $VitD_3$-treated

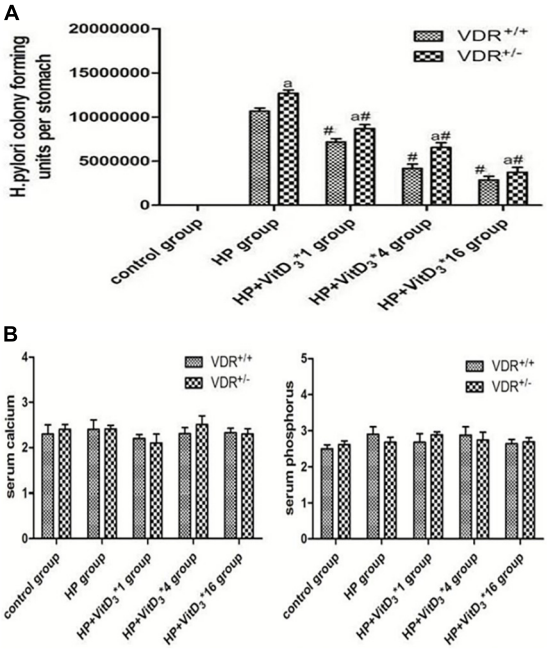

FIGURE 4
Helicobacter pylori eradication efficacy of $VitD_3$ at different doses in infected mice. **(A)** Colony-forming assay results showing increased susceptibility of $VDR^{+/-}$ mice to *H. pylori* colonization compared to $VDR^{+/+}$ mice ($P < 0.05$). In both mouse strains, *H. pylori* colonization was significantly reduced after $VitD_3$ administration and *H. pylori* numbers decreased in a dose-dependent manner ($n = 6$; $^{\#}P < 0.05$ vs. HP group and $^{a}P < 0.05$ vs. $VDR^{+/+}$ group). **(B)** Serum calcium and phosphorus levels were comparable in $VDR^{+/+}$ and $VDR^{+/-}$ mice and remained in the normal range after $VitD_3$ administration ($n = 6$; $P > 0.05$). HP, *H. pylori* infection.

mice compared with that of corn oil-treated mice, and the effect was dose-dependent ($P < 0.05$; Figures 5A,B). Furthermore, after $VitD_3$ treatment VDR protein expression in $VDR^{+/-}$ mice was consistently weaker than that in $VDR^{+/+}$ mice ($P < 0.05$). Immunohistochemistry analysis showed that the intensity of VDR staining increased with the $VitD_3$ dose (Figure 5C), confirming the upregulation of VDR expression by $VitD_3$. Collectively, these results indicate that $VitD_3$ can induce VDR expression *in vivo*.

$VitD_3$ stimulated cathelicidin antimicrobial peptide expression in the mouse gastric mucosa

Cathelicidin antimicrobial peptide has a broad spectrum of antibacterial activities and can induce immune responses to a variety of pathogenic microorganisms. As $VitD_3$ has been shown to upregulate CAMP expression, we hypothesized that CAMP could be involved in the clearance of *H. pylori* through the $VitD_3$–VDR interaction. In agreement with the VDR expression

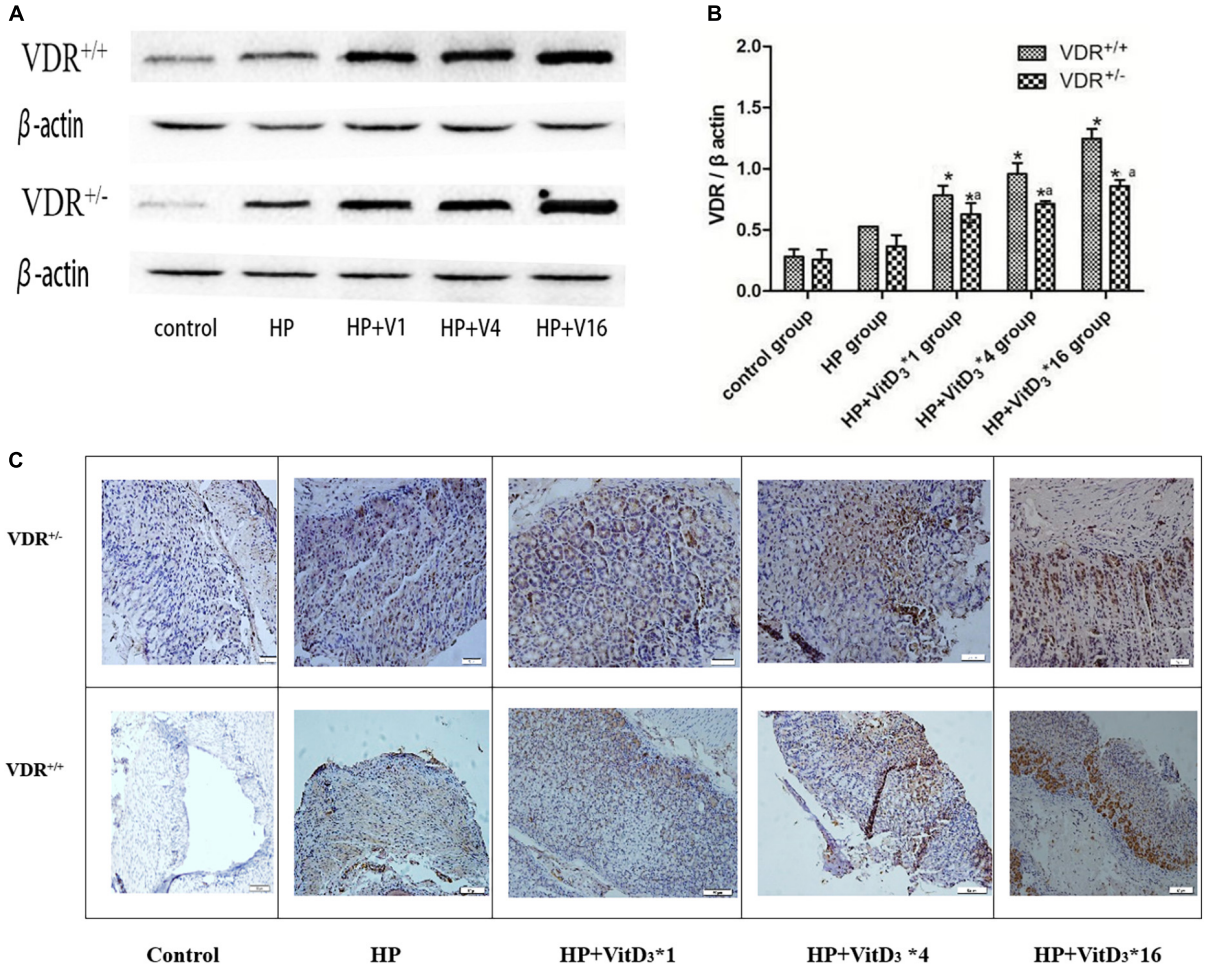

FIGURE 5
$VitD_3$ increased $VitD_3$ receptor (VDR) protein expression in mouse gastric tissues. **(A)** Western blotting analysis revealed a significant, dose-dependent increase of VDR expression by $VitD_3$ in mouse gastric tissues. VDR protein expression was consistently lower in $VDR^{+/-}$ mice than in $VDR^{+/+}$ mice after $VitD_3$ treatment ($n = 6$; $P < 0.05$). **(B)** Histogram showing quantitative analysis of the results presented in panel **(A)**. **(C)** Immunohistochemistry analysis of VDR expression in gastric tissues of infected mice treated or not with different doses of $VitD_3$. $^*P < 0.05$ vs. HP group and $^aP < 0.05$ vs. $VDR^{+/+}$ group. HP, *Helicobacter pylori* infection. Upper row, scale bar = 20 μm. Bottom row, scale bar = 50 μm.

results described above, the intragastric administration of $VitD_3$ resulted in significant dose-dependent upregulation of CAMP expression in the gastric mucosa of *H. pylori*-infected mice, compared with that in the control HP group ($P < 0.05$; Figures 6A,B). CAMP expression was consistently lower in $VDR^{+/-}$ mice than in $VDR^{+/+}$ mice ($P < 0.05$). These results were consistent with the immunohistochemistry analysis (Figure 6C). Thus, CAMP may be involved in the anti-*H. pylori* activity of $VitD_3$.

Discussion

In this study, we bred VDR knockdown ($VDR^{+/-}$) mice and compared their reaction to *H. pylori* infection and $VitD_3$ administration with that of wild-type ($VDR^{+/+}$) mice. Treatment with $VitD_3$ decreased, in a dose-dependent manner, *H. pylori* colonization of the gastric mucosa, especially in wild-type mice, without causing abnormalities in body weight, food intake, or serum calcium or phosphorus levels, indicating that $VitD_3$ could efficiently eradicate *H. pylori* infection *in vivo*. The expression of both VDR and CAMP was higher in the gastric tissues of wild-type mice than in those of VDR knockdown mice and was further increased after $VitD_3$ administration. Our findings suggest that $VitD_3$ could eradicate *H. pylori* through activation of the VDR/CAMP pathway.

As a spiral microaerophilic gram-negative bacterium, *H. pylori* was first isolated from gastric mucosal specimens of a patient with chronic active gastritis, in 1983 (Warren and Marshall, 1983). At present, *H. pylori* has a global infection rate over 50% and is implicated not only in various gastrointestinal diseases but also in other systemic disorders. Regardless of the

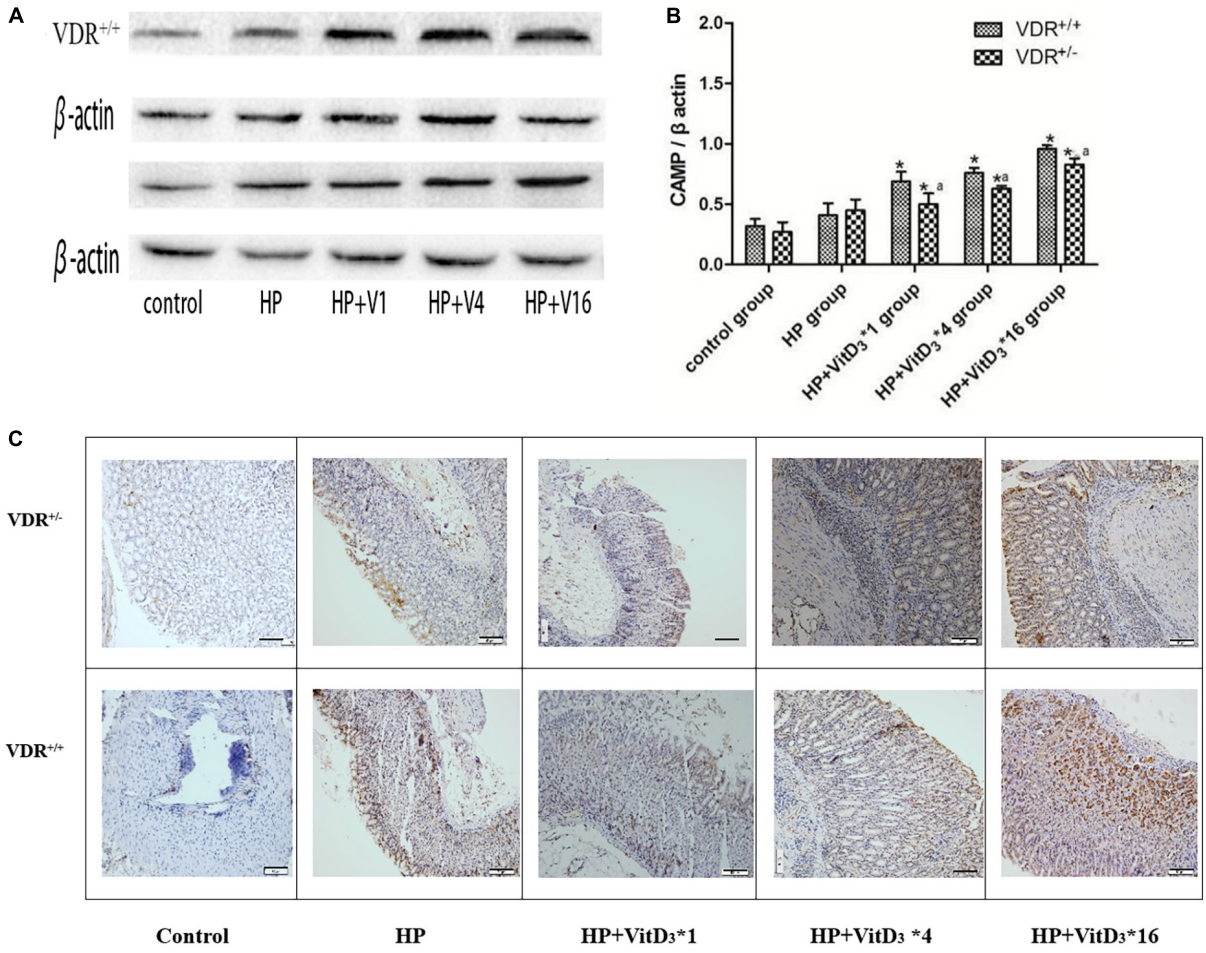

FIGURE 6
$VitD_3$ upregulated cathelicidin antimicrobial peptide (CAMP) expression in the mouse gastric mucosa. **(A)** CAMP expression in the gastric mucosa was analyzed by western blotting. $VitD_3$ gavage increased CAMP protein expression in a dose-dependent manner. The CAMP expression level was consistently lower in $VDR^{+/-}$ than in $VDR^{+/+}$ mice ($n = 6$; $P < 0.05$). **(B)** Histogram showing quantitative analysis of the results presented in panel **(A)**. **(C)** Immunohistochemistry analysis showing $VitD_3$ dose-dependent increase of CAMP staining intensity in the mouse mucosa. *$P < 0.05$ vs. HP group and $^{a}P < 0.05$ vs. $VDR^{+/+}$ group. HP, *Helicobacter pylori* infection. Scale bar = 50 μm.

presence of alarm symptoms, *H. pylori* eradication is considered a necessary measure. The increased resistance to classical antibiotics limits the application of globally recognized triple and bismuth-containing quadruple therapies in developing countries (Malfertheiner et al., 2017). In addition, *H. pylori* has evolved autophagy evasion strategies to support its survival in host cells. Thus, *H. pylori* vacuolating cytotoxin A (VacA) can induce autophagy in several gastric cell lines (Allen et al., 2000) and, together with other virulence factors, has a suppressive role in the autolysosome maturation process. VacA has been found to interfere with lysosome acidification and induce autophagosome formation, leading to massive replication of *H. pylori* in cells (Raju et al., 2012). Therefore, there is an urgent need to develop anti-*H. pylori* agents whose activity would not be compromised by antibiotic resistance or damaging to host cells.

Accumulating evidence indicates that $VitD_3$ has anti-inflammatory and anti-microbial effects on *H. pylori* infection and can be used for its eradication. $VitD_3$ mainly regulates calcium and phosphate metabolism and the associated physiological processes by activating VDR-dependent signaling. $VitD_3$ at high doses has been shown to significantly reduce the risk of autoimmune diseases such as inflammatory bowel disease, type 1 diabetes, and rheumatic disorders (Holick, 2004). Recently, $VitD_3$ has been found to protect the gastric mucosal epithelium from *H. pylori* infection, and, by signaling through the VDR, to promote c-Raf/MEK/ERK phosphorylation and prevent apoptosis in *H. pylori*-infected GES-1 cells (Zhao et al., 2022). Interestingly, $VitD_3$ has been reported to exert an antibacterial effect through the protein disulfide isomerase A3 (PDIA3) receptor and the downstream STAT3–MCOLN3–Ca^{2+} signaling pathway,

thus promoting the recovery of damaged lysosomes and their degradation function, which leads to *H. pylori* clearance (Hu et al., 2019). Therefore, the $VitD_3$-PDIA3 pathway emerges as a novel pathway to reactivate autolysosomal degradation, which is critical for $VitD_3$ antibacterial activity. Furthermore, $VitD_3$ decomposition product 1 and its derivatives can specifically inhibit *H. pylori* (Hosoda et al., 2015; Wanibuchi et al., 2018, 2020). These findings indicate that VitD exerts its anti-*H. pylori* activity *via* various molecular mechanisms.

$VitD_3$ biological functions are mediated by VDR, a member of the nuclear hormone receptor superfamily and a ligand-activated transcription factor (Schauber et al., 2007) which is expressed in various tissues, including the intestinal tract, liver, kidneys, muscle, and prostate (Provvedini et al., 1983). VDR is also present in many immune cells, including monocytes, macrophages, natural killer cells, and activated B and T cells. VDR–$VitD_3$ signaling is involved in the regulation of cell growth, gene transcription, calcium and phosphorus metabolism, and the activity of the immune system (Amrein et al., 2014). It has been found that $VitD_3$ inhibits *H. pylori* through the VDR/CAMP pathway (Zhou et al., 2020). However, the effect of $VitD_3$ on *H. pylori* infection *in vivo* has rarely been investigated. Our findings indicate that $VitD_3$ reduces *H. pylori* colonization of the gastrointestinal tract through activation of the VDR/CAMP pathway, thus paving the way for the development of novel approaches to *H. pylori* eradication, which could address the problem of antibiotic resistance in this pathogen.

Data availability statement

The raw data supporting the conclusions of this article will be made available by the authors, without undue reservation.

Ethics statement

This animal study was reviewed and approved by the Beijing Friendship Hospital Affiliated to Capital Medical University.

Author contributions

YZ conducted the statistical analysis and drafted the manuscript. CW and LZ critically revised and finalized the manuscript. JY performed the data analysis and interpretation. WY reviewed and edited the manuscript. LL designed the study and performed all experiments. All authors have approved the final version of the manuscript.

Funding

This study was supported by the Weifang Science and Technology Development Plan for 2021 (University part) (2021GX063).

Acknowledgments

We would like to thank Liu Chunjie, Institute of Biomedical Engineering, Academy of Military Medical Sciences of the Chinese PLA, Beijing, for the gift of *H. pylori* Sydney strain.

Conflict of interest

The authors declare that the research was conducted in the absence of any commercial or financial relationships that could be construed as a potential conflict of interest.

Publisher's note

References

Allen, L. A., Schlesinger, L. S., and Kang, B. (2000). Virulent strains of *Helicobacter pylori* demonstrate delayed phagocytosis and stimulate homotypic phagosome fusion in macrophages. *J. Exp. Med.* 191, 115–128. doi: 10.1084/jem.191.1.115

Amrein, K., Schnedl, C., Holl, A., Riedl, R., Christopher, K. B., Pachler, C., et al. (2014). Effect of high-dose vitamin D3 on hospital length of stay in critically ill patients with vitamin D deficiency: The VITdAL-ICU randomized clinical trial. *JAMA* 312, 1520–1530. doi: 10.1001/jama.2014.13204

Carlberg, C. (2014). The physiology of vitamin D-far more than calcium and bone. *Front. Physiol.* 5:335. doi: 10.3389/fphys.2014.00335

Christakos, S., Ajibade, D. V., Dhawan, P., Fechner, A. J., and Mady, L. J. (2012). Vitamin D: Metabolism. *Rheum. Dis. Clin. North Am.* 38, 1–11. doi: 10.1016/j.rdc.2012.03.003

Gao, T., Zhao, M. W., Zhang, C., Wang, P. P., Zhou, W. J., Tan, S., et al. (2020). Association of *Helicobacter pylori* infection with vitamin D deficiency in infants and toddlers. *Am. J. Trop. Med. Hyg.* 102, 541–546. doi: 10.4269/ajtmh.19-0523

Ginde, A. A., Mansbach, J. M., and Camargo, C. A. (2009). Association between serum 25-hydroxyvitamin D level and upper respiratory tract infection in the third national health and nutrition examination survey. *Arch. Intern. Med.* 169, 384–390. doi: 10.1001/archinternmed.2008.560

Guo, L. H., Chen, W. G., Zhu, H. T., Chen, Y., Wan, X. Y., Yang, N. M., et al. (2014). *Helicobacter pylori* induces increased expression of the vitamin D receptor in immune responses. *Helicobacter* 19, 37–47. doi: 10.1111/hel.12102

Hewison, M. (2011). Antibacterial effects of vitamin D. *Nat. Rev. Endocrinol.* 7, 337–345. doi: 10.1038/nrendo.2010.226

Hmama, Z., Sendide, K., Talal, A., Garcia, R., Dobos, K., and Reiner, N. E. (2004). Quantitative analysis of phagolysosome fusion in intact cells: Inhibition by mycobacterial lipoarabinomannan and rescue by an 1alpha,25-dihydroxyvitamin D3-phosphoinositide 3-kinase pathway. *J. Cell Sci.* 117, 2131–2140. doi: 10.1242/jcs.01072

Holick, M. F. (2004). Vitamin D: Importance in the prevention of cancers, type 1 diabetes, heart disease, and osteoporosis. *Am. J. Clin. Nutr.* 79, 362–371. doi: 10.1093/ajcn/79.3.362

Hosoda, K., Shimomura, H., Wanibuchi, K., Masui, H., Amgalanbaatar, A., Hayashi, S., et al. (2015). Identification and characterization of a vitamin D_3 decomposition product bactericidal against *Helicobacter pylori*. *Sci. Rep.* 5:8860. doi: 10.1038/srep08860

Hu, W., Zhang, L., Li, M. X., Shen, J., Liu, X. D., Xiao, Z. G., et al. (2019). Vitamin D3 activates the autolysosomal degradation function against *Helicobacter pylori* through the PDIA3 receptor in gastric epithelial cells. *Autophagy* 15, 707–725. doi: 10.1080/15548627.2018.1557835

Huang, X., Qu, X., Yan, W., Huang, Y., Cai, M., Hu, B., et al. (2010). Iron deficiency anaemia can be improved after eradication of *Helicobacter pylori*. *Postgrad. Med. J.* 86, 272–278. doi: 10.1136/pgmj.2009.089987

Kim, S. G., Jung, H.-K., Lee, H. L., Jang, J. Y., Lee, H., Kim, C. G., et al. (2014). Guidelines for the diagnosis and treatment of *Helicobacter pylori* infection in Korea, 2013 revised edition. *J. Gastroenterol. Hepatol.* 29, 1371–1386. doi: 10.1111/jgh.12607

Laaksi, I., Ruohola, J.-P., Tuohimaa, P., Auvinen, A., Haataja, R., Pihlajamäki, H., et al. (2007). An association of serum vitamin D concentrations < 40 nmol/L with acute respiratory tract infection in young Finnish men. *Am. J. Clin. Nutr.* 86, 714–717. doi: 10.1093/ajcn/86.3.714

Li, L., Meng, F., Zhu, S., Guo, S., Wang, Y., Zhao, X., et al. (2018). Efficacy and safety of Wei Bi Mei, a Chinese herb compound, as an alternative to bismuth for eradication of *Helicobacter pylori*. *Evid. Based Complement. Alternat. Med.* 2018:4320219. doi: 10.1155/2018/4320219

Liu, P. T., Stenger, S., Li, H., Wenzel, L., Tan, B. H., Krutzik, S. R., et al. (2006). Toll-like receptor triggering of a vitamin D-mediated human antimicrobial response. *Science* 311, 1770–1773. doi: 10.1126/science.1123933

Malfertheiner, P., Megraud, F., O'Morain, C. A., Atherton, J., Axon, A. T. R., Bazzoli, F., et al. (2012). Management of *Helicobacter pylori* infection–the Maastricht IV/ Florence consensus report. *Gut* 61, 646–664. doi: 10.1136/gutjnl-2012-302084

Malfertheiner, P., Megraud, F., O'Morain, C. A., Gisbert, J. P., Kuipers, E. J., Axon, A. T., et al. (2017). Management of *Helicobacter pylori* infection-the Maastricht V/Florence consensus report. *Gut* 66, 6–30. doi: 10.1136/gutjnl-2016-312288

Malfertheiner, P., Megraud, F., O'Morain, C., Bazzoli, F., El-Omar, E., Graham, D., et al. (2007). Current concepts in the management of *Helicobacter pylori* infection: The Maastricht III consensus report. *Gut* 56, 772–781. doi: 10.1136/gut.2006.101634

Mitchell, H., and Katelaris, P. (2016). Epidemiology, clinical impacts and current clinical management of *Helicobacter pylori* infection. *Med. J. Aust.* 204, 376–380. doi: 10.5694/mja16.00104

Nasri, H., and Baradaran, A. (2007). The influence of serum 25-hydroxy vitamin D levels on *Helicobacter pylori* infections in patients with end-stage renal failure on regular hemodialysis. *Saudi J. Kidney Dis. Transpl.* 18, 215–219.

Provvedini, D. M., Tsoukas, C. D., Deftos, L. J., and Manolagas, S. C. (1983). 1,25-dihydroxyvitamin D3 receptors in human leukocytes. *Science* 221, 1181–1183. doi: 10.1126/science.6310748

Raju, D., Hussey, S., Ang, M., Terebiznik, M. R., Sibony, M., Galindo-Mata, E., et al. (2012). Vacuolating cytotoxin and variants in Atg16L1 that disrupt autophagy promote *Helicobacter pylori* infection in humans. *Gastroenterology* 142, 1160–1171. doi: 10.1053/j.gastro.2012.01.043

Reeve, L., Tanaka, Y., and DeLuca, H. F. (1983). Studies on the site of 1,25-dihydroxyvitamin D3 synthesis in vivo. *J. Biol. Chem.* 258, 3615–3617.

Savoldi, A., Carrara, E., Graham, D. Y., Conti, M., and Tacconelli, E. (2018). Prevalence of antibiotic resistance in *Helicobacter pylori*: A systematic review and meta-analysis in world health organization regions. *Gastroenterology* 155, 1372–1382.e17. doi: 10.1053/j.gastro.2018.07.007

Schauber, J., Dorschner, R. A., Coda, A. B., Büchau, A. S., Liu, P. T., Kiken, D., et al. (2007). Injury enhances TLR2 function and antimicrobial peptide expression through a vitamin D-dependent mechanism. *J. Clin. Invest.* 117, 803–811. doi: 10.1172/JCI30142

Stubljar, D., Jukic, T., and Ihan, A. (2018). How far are we from vaccination against *Helicobacter pylori* infection? *Expert Rev. Vaccines* 17, 935–945. doi: 10.1080/14760584.2018.1526680

Walduck, A. K., and Raghavan, S. (2019). Immunity and vaccine development against *Helicobacter pylori*. *Adv. Exp. Med. Biol.* 1149, 257–275. doi: 10.1007/5584_2019_370

Wang, J., Dou, X., Song, J., Lyu, Y., Zhu, X., Xu, L., et al. (2019). Antimicrobial peptides: Promising alternatives in the post feeding antibiotic era. *Med. Res. Rev.* 39, 831–859. doi: 10.1002/med.21542

Wanibuchi, K., Hosoda, K., Ihara, M., Tajiri, K., Sakai, Y., Masui, H., et al. (2018). Indene compounds synthetically derived from vitamin D have selective antibacterial action on *Helicobacter pylori*. *Lipids* 53, 393–401. doi: 10.1002/lipd.12043

Wanibuchi, K., Takezawa, M., Hosoda, K., Amgalanbaatar, A., Tajiri, K., Koizumi, Y., et al. (2020). Antibacterial effect of indene on *Helicobacter pylori* correlates with specific interaction between its compound and dimyristoyl-phosphatidylethanolamine. *Chem. Phys. Lipids* 227:104871. doi: 10.1016/j.chemphyslip.2020.104871

Warren, J. R., and Marshall, B. (1983). Unidentified curved bacilli on gastric epithelium in active chronic gastritis. *Lancet* 1, 1273–1275.

Yildirim, O., Yildirim, T., Seckin, Y., Osanmaz, P., Bilgic, Y., and Mete, R. (2017). The influence of vitamin D deficiency on eradication rates of *Helicobacter pylori*. *Adv. Clin. Exp. Med.* 26, 1377–1381. doi: 10.17219/acem/65430

Zhang, L., Wu, W. K. K., Gallo, R. L., Fang, E. F., Hu, W., Ling, T. K. W., et al. (2016). Critical role of antimicrobial peptide cathelicidin for controlling *Helicobacter pylori* survival and infection. *J. Immunol.* 196, 1799–1809. doi: 10.4049/jimmunol.1500021

Zhang, L., Yu, J., Wong, C. C. M., Ling, T. K. W., Li, Z. J., Chan, K. M., et al. (2013). Cathelicidin protects against *Helicobacter pylori* colonization and the associated gastritis in mice. *Gene Ther.* 20, 751–760. doi: 10.1038/gt.2012.92

Zhao, S., Wan, D., Zhong, Y., and Xu, X. (2022). 1α, 25-dihydroxyvitamin D3 protects gastric mucosa epithelial cells against -infected apoptosis through a vitamin D receptor-dependent c-Raf/MEK/ERK pathway. *Pharm. Biol.* 60, 801–809. doi: 10.1080/13880209.2022.2058559

Zhou, A., Li, L., Zhao, G., Min, L., Liu, S., Zhu, S., et al. (2020). Vitamin D3 inhibits infection by activating the VitD3/VDR-CAMP pathway in mice. *Front. Cell. Infect. Microbiol.* 10:566730. doi: 10.3389/fcimb.2020.566730

frontiers | Frontiers in Microbiology

TYPE Original Research
PUBLISHED 23 December 2022
DOI 10.3389/fmicb.2022.1065462

OPEN ACCESS

EDITED BY
Alain Pierre Gobert,
Vanderbilt University Medical Center,
United States

REVIEWED BY
Lydia E. Wroblewski,
Vanderbilt University Medical Center,
United States
Océane C. B. Martin,
Université de Bordeaux,
France

*CORRESPONDENCE
Yin Zhu
✉ zhuyin27@sina.com
Nianshuang Li
✉ zyyalns@126.com

SPECIALTY SECTION
This article was submitted to Infectious Agents and Disease, a section of the journal Frontiers in Microbiology

RECEIVED 10 October 2022
ACCEPTED 08 December 2022
PUBLISHED 23 December 2022

CITATION
Xu X, Shu C, Wu X, Ouyang Y, Cheng H, Zhou Y, Wang H, He C, Xie C, He X, Hong J, Lu N, Ge Z, Zhu Y and Li N (2022) A positive feedback loop of the TAZ/β-catenin axis promotes *Helicobacter pylori*-associated gastric carcinogenesis.
Front. Microbiol. 13:1065462.
doi: 10.3389/fmicb.2022.1065462

A positive feedback loop of the TAZ/β-catenin axis promotes *Helicobacter pylori*-associated gastric carcinogenesis

Xinbo Xu[1,2], Chunxi Shu[1,2], Xidong Wu[3], Yaobin Ouyang[1,2], Hong Cheng[1,2], Yanan Zhou[1,2], Huan Wang[1,2], Cong He[1,2,4], Chuan Xie[1,2], Xingxing He[1,2,4], Junbo Hong[1,2], Nonghua Lu[1,2], Zhongming Ge[5], Yin Zhu[1,2]* and Nianshuang Li[1,2,4]*

[1]Digestive Disease Hospital, The First Affiliated Hospital of Nanchang University, Nanchang, China, [2]Department of Gastroenterology, The First Affiliated Hospital of Nanchang University, Nanchang, China, [3]Department of Drug Safety Evaluation, Jiangxi Testing Center of Medical Instruments, Nanchang, China, [4]Jiangxi Institute of Digestive Disease, The First Affiliated Hospital of Nanchang University, Nanchang, China, [5]Division of Comparative Medicine, Massachusetts Institute of Technology, Cambridge, MA, United States

Background: *Helicobacter pylori* infection is the strongest known risk factor for gastric cancer. The Hippo signaling pathway controls organ size and maintains tissue homeostasis by coordinately regulating cell growth and proliferation. Here, we demonstrate the interactive role of TAZ, the transcriptional coactivator of the Hippo pathway, and beta-catenin in promoting the pathogenesis of *H. pylori* infection.

Methods: TAZ expression was evaluated in human gastric tissues and *H. pylori*-infected insulin–gastrin (INS-GAS) mice. Western blot, immunofluorescence, immunohistochemistry, and RT–PCR assays were performed. Coimmunoprecipitation was performed to examine the interaction between TAZ and β-catenin. TAZ and β-catenin were silenced using small interfering RNAs. HA-β-catenin and Flag-TAZ were constructed.

Results: Increased TAZ was noted in human gastric cancer tissues compared to chronic gastritis tissues and in *H. pylori*-positive gastritis tissues compared to *H. pylori*-negative gastritis tissues. In addition, *H. pylori* infection induced TAZ expression and nuclear accumulation in the gastric tissue of INS-GAS mice and cultured gastric epithelial cells, which was dependent on the virulence factor CagA. Moreover, TAZ or β-catenin knockdown significantly suppressed *H. pylori* infection-induced cell growth, survival, and invasion. Furthermore, the interactive regulation of TAZ and β-catenin activation was revealed. Finally, β-catenin was required for *H. pylori*-induced TAZ activation.

Conclusion: These findings suggest the existence of a positive feedback loop of activation between TAZ and β-catenin that could play an important role in CagA+ *H. pylori* infection-induced gastric carcinogenesis. TAZ inhibition represents a potential target for the prevention of *H. pylori* infection-associated gastric cancer.

KEYWORDS

Helicobacter Pylori, CagA, TAZ, β-catenin, gastric carcinogenesis

Background

Helicobacter pylori infection is the strongest known risk factor for the development of gastric cancer and the fourth leading cause of cancer death worldwide, particularly in East Asian populations Approximately half of the world's population is infected with *H. pylori* (Sung et al., 2021). *H. pylori* infection can cause chronic active gastritis that can progress through Correa's cascade to intestinal metaplasia, dysplasia, and finally gastric adenocarcinoma (Correa and Piazuelo, 2011). CagA is the most well-characterized virulence factor that links *H. pylori* infection to gastric carcinogenesis (Ansari and Yamaoka, 2019). Patients infected with CagA-positive *H. pylori* strains are suggested to have an increased risk of gastric carcinoma compared to CagA-negative subjects (Park et al., 2018). Accumulating data suggest that the interaction between bacterial virulence factors and host gastric epithelial cells induces aberrant activation of multiple oncogenic signaling pathways (PI3K/AKT, Wnt/β-catenin, etc) and subsequently results in gastric carcinogenesis (Xie et al., 2018; Cao et al., 2022). Another bacterial virulence factor, VacA, is also linked to clinical phenotypes, such as cellular vacuolation of *H. pylori* infection. Numerous studies have shown that eradication of *H. pylori* based on regiments including systematic PPI and antibiotics could significantly reduce gastric cancer risk before the development of atrophic gastritis and intestinal metaplasia (Liou et al., 2020; Yan et al., 2022). However, it remains unclear whether *H. pylori* eradication therapy reduces the incidence of gastric cancer once premalignant gastric lesions develop. Therefore, the identification of novel and reliable biomarkers is essential for the prediction and prevention of gastric cancer associated with *H. pylori* infection.

The Hippo signaling pathway maintains organ size and tissue homeostasis *via* the regulation of cell proliferation, survival, and differentiation (Russell and Camargo, 2022). YAP and its paralogue TAZ (also known as WWTR1) act as transcriptional coactivators and effectors of the Hippo signaling cascade. Activation of the upstream kinases LATS1/2 and MST1/2 leads to the phosphorylation and inactivation of YAP and TAZ due to cytoplasmic retention and degradation (Totaro et al., 2018; Mohajan et al., 2021). Inhibition of the Hippo kinase cascade increases the nuclear localization of YAP and TAZ, which are responsible for the activation of downstream genes, such as *CTGF*, *CYR61,* and *c-MYC* (Pobbati and Hong, 2020). It is increasingly evident that the dysregulation of the Hippo signaling pathway plays a vital role in *H. pylori* infection-induced gastric tumorigenesis (Molina-Castro et al., 2020). We previously reported that *H. pylori* infection promotes total YAP levels and nuclear localization, which is also dependent on virulence CagA. As a result, neoplastic transformation is initiated in gastric epithelial cells through the epithelial-mesenchymal transition (EMT), a process by which epithelial cells lose their cell polarity and cell–cell adhesion and subsequently acquire migratory and invasive characteristics (Yang et al., 2020). We also found higher TAZ expression levels in gastric carcinoma tissues compared with adjacent normal tissues (Li et al., 2018). However, the role of YAP paralogue TAZ in the pathogenesis of *H. pylori* infection has not been explored.

Independent of the Hippo cascade, β-catenin is the core effector of the canonical Wnt signaling pathway (Liu et al., 2022). The nuclear accumulation of β-catenin upon the activation of the Wnt pathway accounts for the upregulation of target genes such as *c-MYC* and *cyclin D1* (Zhang and Wang, 2020). Accumulating data suggest that the Hippo and Wnt signaling pathways regulate overlapping biological processes, including tissue growth, development, and homeostasis (Sylvester and Colnot, 2014; Li et al., 2019). TAZ is defined as the downstream element of the Wnt/β-catenin signaling cascade. β-catenin phosphorylation leads to TAZ degradation by bridging TAZ to the E3 ubiquitin ligase β-TrCP. In Wnt-ON cells, β-catenin dissociation from the destruction complex impairs TAZ degradation, allowing the nuclear accumulation of TAZ and β-catenin (Azzolin et al., 2012). It has been reported that infection with carcinogenic *H. pylori* strains induces nuclear translocation of β-catenin in a rodent model and gastric cells (Franco et al., 2005). It remains unclear whether the intersection of TAZ and the β-catenin pathway is implicated in *H. pylori*-mediated carcinogenesis.

In the present study, we elucidated a mechanism by which the activation of TAZ promotes the β-catenin pathway to trigger gastric epithelial malignant transformation in response to *H. pylori* infection. Here, we showed that *H. pylori* strains expressing high levels of CagA significantly upregulated TAZ expression and nuclear accumulation in gastric epithelial cells and transgenic INS-GAS mice. TAZ knockdown reduced *H. pylori* infection-induced expression, nuclear translocation and transcriptional activity of β-catenin. Interestingly, TAZ and β-catenin were mainly located in the cellular cytoplasm and plasma membrane in human specimens with chronic gastritis, whereas partial nuclear colocalization of TAZ with β-catenin was observed in human gastric cancer tissues. *In vitro* studies revealed that *H. pylori* infection augmented the direct

Abbreviations: *H. pylori*, *Helicobacter pylori*; CagA, Cytotoxin-associated gene A; PPI, proton pump inhibitor; YAP, Yes-associated protein; TAZ, PDZ-binding motif; EMT, epithelial-mesenchymal transition; INS-GAS, Insulin–gastrin; FBS, fetal bovine serum; BSA, bovine serum albumin; CCK-8, Cell counting kit-8; SD, standard deviation; ADPKD, autosomal-dominant polycystic kidney disease; DVL, Disheveled.

interaction of TAZ with β-catenin *via* the CagA-dependent mechanism. Furthermore, β-catenin knockdown significantly suppressed the activation of TAZ and its downstream genes following *H. pylori* infection. Moreover, TAZ knockdown by siRNA reduced *H. pylori* infection-triggered neoplastic transformation including cell viability, proliferation, and invasion. These findings suggest that aberrant activation of TAZ is a marker of gastric carcinoma risk and that the feedback loop of the TAZ/β-catenin axis plays a crucial role in *H. pylori* infection-induced carcinogenesis.

Materials and methods

Cell culture and reagents

Human gastric epithelial cell lines, HFE-145 (immortalized, non-cancerous) and AGS (human diffuse type of gastric cancer) were cultured in DMEM and DMEM/F12, containing 10% FBS (Gibco), 100 U/ml penicillin, and 100 μg/ml streptomycin at 37°C in an atmosphere of 5% CO2.

Helicobacter pylori strains

CagA + *VacA*+ *H. pylori* strain PMSS1 (pre-mouse Sydney strain 1) and its isogenic *cagA* mutant were established in our previous research. *CagA* + *VacA* + *H. pylori* strains 7.13 and an isogenic cagA were also included in this study, which were kindly provided by Dr. Richard Peek Jr. from the Vanderbilt Digestive Disease Research Center. All *H. pylori* strains were cultured on Campylobacter agar plates containing 10% sheep serum at 37°C under microaerophilic conditions. The measure methods of *H. pylori* bacterial density were as same as the previous study (Hu et al., 2019). Gastric epithelial cells were cocultured with *H. pylori* strains at MOI of 100.

Human gastric specimens

A total of 40 human chronic non-atrophic gastritis ($n = 20$) and gastric carcinoma ($n = 20$) tissues were acquired from The First Affiliated Hospital of Nanchang University. Each group were divided into two subgroups: *H. pylori*-positive ($n = 10$) and *H. pylori*-negative ($n = 10$) individuals. The study protocol and exemption of informed consent were approved by the Ethics Committee of The First Affiliated Hospital of Nanchang University. Status of *H. pylori* infection for these clinical specimens was determined with a rapid urease test or Giemsa staining. Immunohistochemical staining was performed to examine expression profiles of TAZ on these samples, which were evaluated and scored for intensity (scaled 0–3) and frequency (scaled 0–4) by two pathologists blinded to sample identity. For statistical analysis, expression levels of TAZ proteins were illustrated by an expression score in range of 0 to 12 using the formula intensity × frequency (Li et al., 2018).

Infection of mice with *Helicobacter pylori*

Animal care and experimental protocols were in accordance with guidelines established by the Institutional Animal Care and Use Committee of Nanchang University. The INS-GAS transgenic mice overexpressed pancreatic gastrin were purchased from Jackson Laboratory (Bar Harbor, ME). INS-GAS mice were orogastrically challenged with Brucella Broth ($n = 6$) or with 2×10^9 CFU/ml *H. pylori* strain PMSS1 ($n = 8$) once every other day for a total of 5 times (Arnold et al., 2011; Li et al., 2020). Mice were euthanized at 4 months post infection, and gastric tissues were collected.

Expression vectors, siRNAs, and transfection

The recombinant plasmids such as TAZ, β-catenin cDNAs were designed and synthesized by hitrobio (Beijing, China). The recombinant CagA plasmid was a generous gift from Prof. Shiming Yang, Third Military Medical University of China. Small interfering (si) RNA duplexes were obtained from GenePharma (Shanghai, China). Cells were transfected with appropriate plasmid or siRNA using Lipofectamine 3,000 (Thermo Scientific, Waltham, MA, United States) according to manufacturer's instructions.

Immunohistochemistry

Immunohistochemistry analysis was performed for gastric tissues from human and INS-GAS mice as previously described (22). These specimens were incubated with rabbit polyclonal anti-TAZ (Proteintech, Wuhan, China) at dilution of 1:400, followed by incubation with secondary antibody (PV6000, Zhongshan Golden-bridge, Beijing, China). Immunostained tissue slides were imaged on an upright confocal microscope (Nikon ECLIPSE Ni). Tissue sections were imaged at 200× and 400× magnification.

Western blotting

Western blotting analysis was conducted as described previously (Xie et al., 2020). Primary anti-TAZ (#83669), anti-β-catenin (#37447), anti-β-tubulin (#2128), anti-Histone 3 (#4499), anti-GAPDH (#2118), anti-HA-Tag (#3724), anti-Myc (#9402), anti-Cyclin D1(#2978), anti-CYR61(#14479), anti-CTGF (#86641) antibodies were purchased from Cell Signal Technology (Beverly, MA, United States); anti-CagA (sc-28,368) were from

Santa Cruz (Dallas, TX, United States), anti-β-actin (#20536-1-AP) from proteintech (Wuhan, China); anti-Flag (F1804) was purchased from Sigma-Aldrich. All primary antibodies were used at a dilution of 1:1000, except for the internal control antibodies including GAPDH and β-actin which were diluted at 1:2000. Briefly, the proteins were extracted after adding lysis buffer supplemented with protease inhibitors (Invitrogen, GA, United States). Equal amounts of the sample proteins were separated on SDS-PAGE gels and transferred to nitrocellulose membranes. After blocking with 5% milk, the membranes were incubated with the primary antibodies overnight at 4°C, and then incubated with HRP-conjugated secondary antibodies (Invitrogen, GA, United States) for 1 h at room temperature. The protein bands were visualized using Super Signal West Pico stable peroxide solution (Thermo Scientific) and collected using iBright imaging system (Thermo Scientific). β-actin and GAPDH were used as internal control to normalize protein expression in cells sample and animal tissues sample, respectively.

Quantitative real-time PCR analysis

The qRT-PCR analysis was performed as described in our previous studies (Xie et al., 2020). Briefly, total RNA was extracted using TRIzol reagent (Invitrogen, GA, United States). The primer sequences are presented in Supplementary Table S1. The qPCR assays were performed with a QuantStudio 5 Real-time PCR system (Life Technologies) according to the manufacturer's protocol. The GAPDH gene was used as an internal control.

Luciferase assay

The TCF/LEF reported plasmid for β-catenin activity (M50 Super 8 × TOPFlash; plasmid#12456; Addgene, Cambridge, MA, United States) was a gift from Randall Moon (Veeman et al., 2003). For dual luciferase assay, cells were seeded into 12-well plates. The cells were transfected with 8 × TOPFlash plasmid and indicated siRNA. After transfection for 48 h, cells were co-cultured with *H. pylori* strain. The cell lysates were collected and subjected to a dual luciferase assay system (Yeasen Biotech, Shanghai, China) according to the manufacturer's protocol.

Immunofluorescence

For immunofluorescence staining, cells were washed with ice-cold PBS and fixed with 4% formaldehyde in PBS for 15 min. Then, the cells were permeabilized with 0.5% Triton X-100 for 10 min at room temperature. After blocking with 3% BSA for 30 min, the cells were incubated with primary antibodies against TAZ (dilution 1:100) or β-catenin (dilution 1:200) overnight at 4°C, and then incubated with Secondary Antibody (Alexa Fluor Plus 488 and Alexa Fluor Plus 555; Thermo Scientific). Cell nuclei were counters with DAPI. All images were acquired using a confocal fluorescence microscope (Leica Stellaris).

Immunoprecipitation

For immunoprecipitation assay, cells were transfected with the indicated plasmids, and then collected with lysis buffer. In brief, the cell lysates were incubated overnight with the mixture of 1 ug of antibodies and beads at 4°C. Then the beads were washed three times with 1 ml of lysis buffer and then boiled in loading buffer. The samples were subjected to western blot analysis as described above.

CCK8 and EDU assays

Cells were transfected with indicated plasmid vector or siRNA, and then seeded into 96-well plates at a density of 2×10^3 cells/100 μl per well. The cells were infected with *H. pylori* strain at an MOI of 50 for the indicated time. The CCK-8 assay (TransGen Biotech, Beijing, China) was performed according to the manufacturer's instructions. The optical density values were measured at a wavelength of 450 nm using a Molecular Devices SpectraMax M2e. For EDU assay, the relative viability of cells was determined by Cell-Light EDU Apollo 488 *in Vitro* imaging kit (RiboBio) following the kit protocol. All images were acquired and quantified using the high-content screening platform In-Cell Analyzer 2,200 (GE Healthcare).

Boyden chamber assay

Boyden chamber assay is useful tool to study cell migration and invasion. For cell invasion detection, about 2×10^5 cells were plated into the upper Boyden chamber (8 μm pore size, Corning, NY, United States) with Matrigel-precoated inserts (BD Science, United States). For cell migration detection, Matrigel was not required. DMEM/F12 medium supplemented with 20% FBS was added in the lower chamber. After transfection and *H. pylori* infection, Cells adhering to the lower surface were fixed with methanol for 30 min, stained with 1% crystal violet for 15 min. The cells on the upper surface of the filters were gently wiped and counted under the inverted microscope (Nikon, ECLIPSE Ti).

Statistical analyses

All the statistical analysis was performed using SPSS 21.0 software. Data are presented as mean ± SD of three independent experiments. Studies for continuous variables were statistically analyzed using Student's *t*-test or One-way ANOVA. The immunohistochemical data from human clinical specimens was statistically analyzed using Mann–Whitney test. The results were considered statistically significant at $p < 0.05$ (***, $p < 0.001$; **, $p < 0.01$; *, $p < 0.05$).

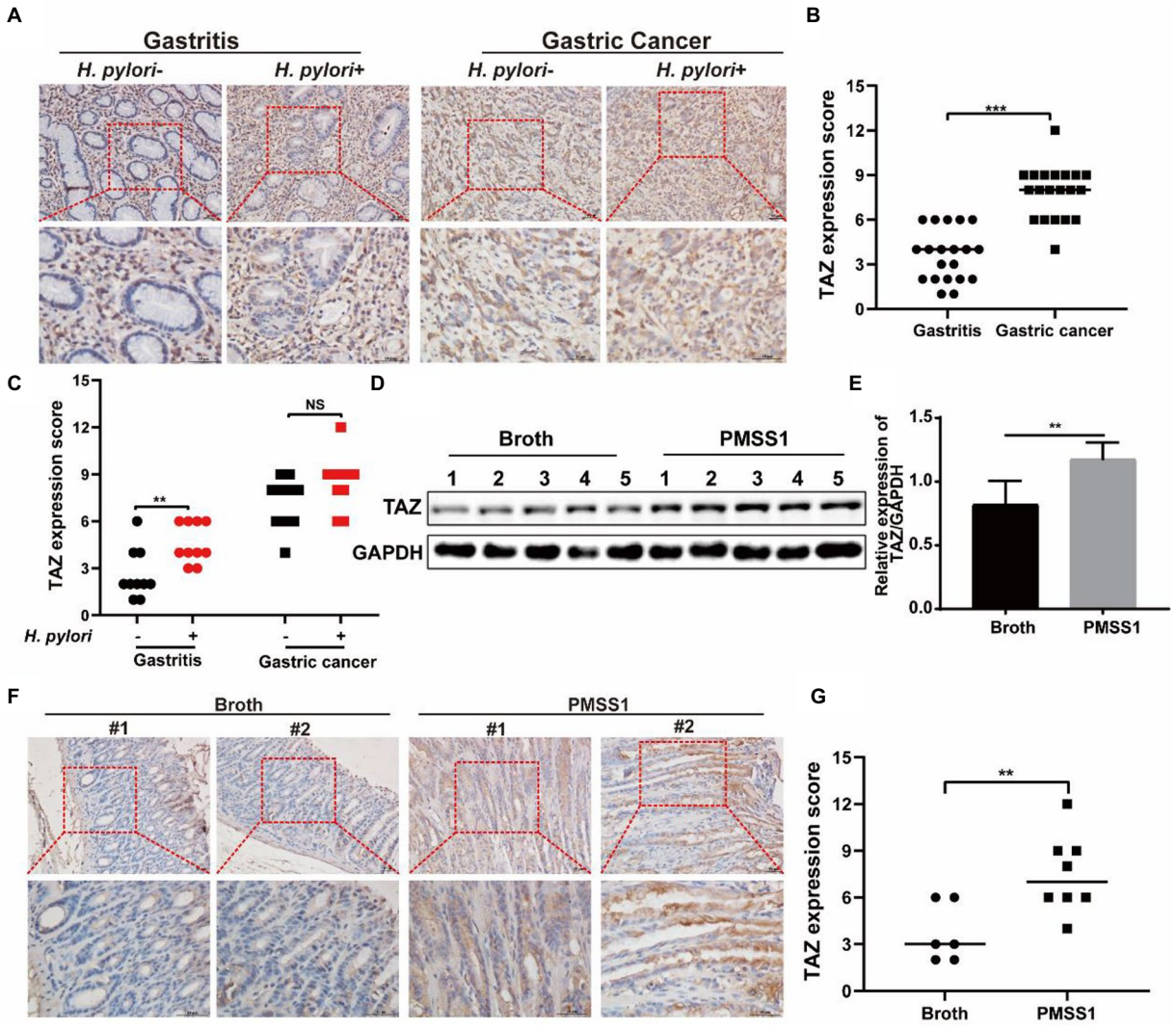

FIGURE 1
TAZ expression levels in human gastric tissues and INS-GAS mice infected with *H. pylori* PMSS1. **(A)** Immunohistochemistry for TAZ expression in human chronic gastritis and gastric cancer tissues. Representative images of TAZ (magnification 200× and 400×, scale bars =50μm). **(B)** Quantitative analysis of TAZ expression in all cell types in gastritis and gastric cancer tissues from both *H. pylori*-negative and *H. pylori*-positive subjects. **(C)** Quantitative immunohistochemistry analysis of TAZ levels in *H. pylori*-positive or *H. pylori*-negative gastric tissues. **(D)** Western blot of TAZ protein expression in gastric tissues of INS-GAS mice infected with *H. pylori* PMSS1 strain or Brucella broth treatment. **(E)** Statistical analysis of the intensity of western blot bands. **(F)** Immunohistochemistry staining for TAZ expression in the *H. pylori*-infected INS-GAS mice. Representative images of TAZ (magnification 200× and 400×, scale bars =50μm). **(G)** Quantitative analysis of TAZ levels. $^{**}p<0.01$, $^{***}p<0.001$, *NS, not significant.* Scare bars in **(A,E)**, 10μm.

Results

Expression of gastric TAZ was elevated in *Helicobacter pylori*+human gastritis tissues and *Helicobacter pylori*-infected INS-GAS mice

We previously reported augmented YAP expression in preneoplastic lesions of human gastric tissues (Li et al., 2018). In this study, we first examined the expression patterns of the YAP homologue TAZ in clinical specimens. As shown in Figures 1A,B, the expression of gastric TAZ was strongly increased in human gastric cancer tissues compared to that observed in chronic nonatrophic gastritis tissues. *H. pylori* infection is linked to the initiation of chronic active gastritis and significantly increases the risk of gastric adenocarcinoma (Crowe, 2019). Therefore, the TAZ expression levels were further compared between *H. pylori*-positive and *H. pylori*-negative subjects. Interestingly, *H. pylori*-positive gastritis tissues tended to have higher levels of TAZ than *H.*

pylori-negative gastritis tissues. However, no significant difference in TAZ expression was noted between *H. pylori*-infected and -uninfected gastric cancer individuals (Figures 1A,C). Next, we utilized INS-GAS mice, which overexpress human pancreatic gastrin and have been widely used for studying the pathogenesis of *H. pylori* infection (14), to characterize the effects of *H. pylori* on TAZ. Western blot analysis showed that gastric TAZ expression was significantly increased in *H. pylori*-infected mice compared with sham controls (Figures 1D,E). In addition, a significant increase in gastric TAZ expression was noted in *H. pylori*-infected mice compared to uninfected animals based on immunohistochemistry analysis (Figure 1F) and quantitative image analysis (Figure 1G). These results indicated that *H. pylori* infection triggers TAZ activation, which may be implicated in the initiation of gastric neoplastic lesions.

Helicobacter pylori infection led to TAZ upregulation and nuclear accumulation in a CagA-dependent manner

To recapitulate the effects of *H. pylori* infection on gastric TAZ expression in human gastric tissues and INS-GAS mice, human gastric epithelial AGS cells were cocultured with the CagA+ *H. pylori* strain NCTC11637 or 7.13. *H. pylori* infection significantly increased TAZ protein expression in both an MOI-dependent (50, 100, 200 and 400 MOI) (Figure 2A) and a time-dependent manner (2 h, 4 h, 6 h, and 8 h) (Figure 2B). Similarly, an increase was noted in total TAZ expression in normal human gastric epithelial HFE145 cells infected with *H. pylori* (Figure 2C). In addition, the intracellular localization of TAZ was increased after treatment with *H. pylori* strains, as shown by immunofluorescence staining. Importantly, the increase of *H. pylori* MOIs was correlated with the promotion of TAZ translocation from the cytoplasm to the nucleus (Figure 2D). These *in vitro* data clearly indicated that *H. pylori* infection leads to TAZ upregulation and activation.

CagA, which is delivered into gastric epithelial cells *via* the type IV secretion system (T4SS), has been considered an oncoprotein that induces gastric carcinogenesis (30). To determine the role of CagA in *H. pylori*-induced activation of TAZ, AGS cells were cultured alone or cocultured with *H. pylori* PMSS1 wild-type or its CagA-deficient isogenic mutant strain. We found that CagA knockout significantly inhibited the induction of TAZ in response to *H. pylori* infection (Figure 2E). Furthermore, transient overexpression of CagA *via* plasmid transfection into AGS cells strongly increased TAZ expression (Figure 2F). Furthermore, the recombinant CagA overexpression caused an marked increase in the nuclear localization of TAZ. These findings suggest that bacterial CagA is integral for *H. pylori*-induced TAZ activation.

TAZ knockdown significantly inhibited *Helicobacter pylori* infection-induced gastric epithelial cell malignant transformation

Given that TAZ activation promotes cell survival, proliferation, and metastasis by stimulating its downstream transcription factors (Pocaterra et al., 2020), we next dissected the role of TAZ in the *H. pylori* infection-induced malignant transformation of gastric epithelial cells. Knockdown of endogenous TAZ by siRNA inhibited cell proliferation (Figures 3A,B, EDU assay) and cell viability (Figure 3C, CCK8 assay) induced by CagA+ *H. pylori* strain NCTC11637 or 7.13. compared with *H. pylori* infection alone in AGS cells. Similarly, the number of AGS cell clones was diminished after treatment with TAZ siRNA in combination with the *H. pylori* strain compared to *H. pylori* infection alone (Figure 3D). To explore how TAZ mediates cell invasion and migration induced by *H. pylori* infection, AGS cells were transfected with TAZ siRNA for 48 h and then cocultured with the *H. pylori* strain for a transwell assay. The siRNA-mediated knockdown of YAP in combination with CagA+ *H. pylori* NCTC11637 infection significantly decreased invasion and migration capacities (Figures 3E–G). These findings suggest that impaired TAZ activation abolishes *H. pylori* infection-induced malignant transformation including cell survival, proliferation, invasion and migration.

Helicobacter pylori promoted the Wnt/β-catenin pathway through regulation of TAZ expression

YAP/TAZ are closely linked to the Wnt/β-catenin pathway because they share some target genes and biological processes (Li et al., 2019). Given that our data indicated that *H. pylori* infection led TAZ overexpression and nuclear accumulation, we next investigated whether TAZ induction promotes β-catenin pathway activation in response to *H. pylori* infection. TAZ knockdown significantly downregulated the β-catenin protein levels induced by *H. pylori* (Figure 4A). In addition, qRT-PCR data showed that *H. pylori* infection upregulated the transcription of β-catenin-targeted genes including *Lgr5* and *Myc* which were then downregulated after treatment with TAZ siRNA (Figure 4B). Given that β-catenin activation is correlated with increased nuclear β-catenin abundance, we examined the effect of TAZ knockdown on the subcellular expression of β-catenin following *H. pylori* infection in AGS cells by separating the nuclear and cytoplasmic proteins. As shown in Figure 4C, *H. pylori* infection promoted nuclear TAZ and β-catenin compartmentalization, which was significantly suppressed by TAZ knockdown. Consistent with these findings, immunofluorescence assay showed that *H. pylori* infection-induced nuclear translocation was significantly suppressed by

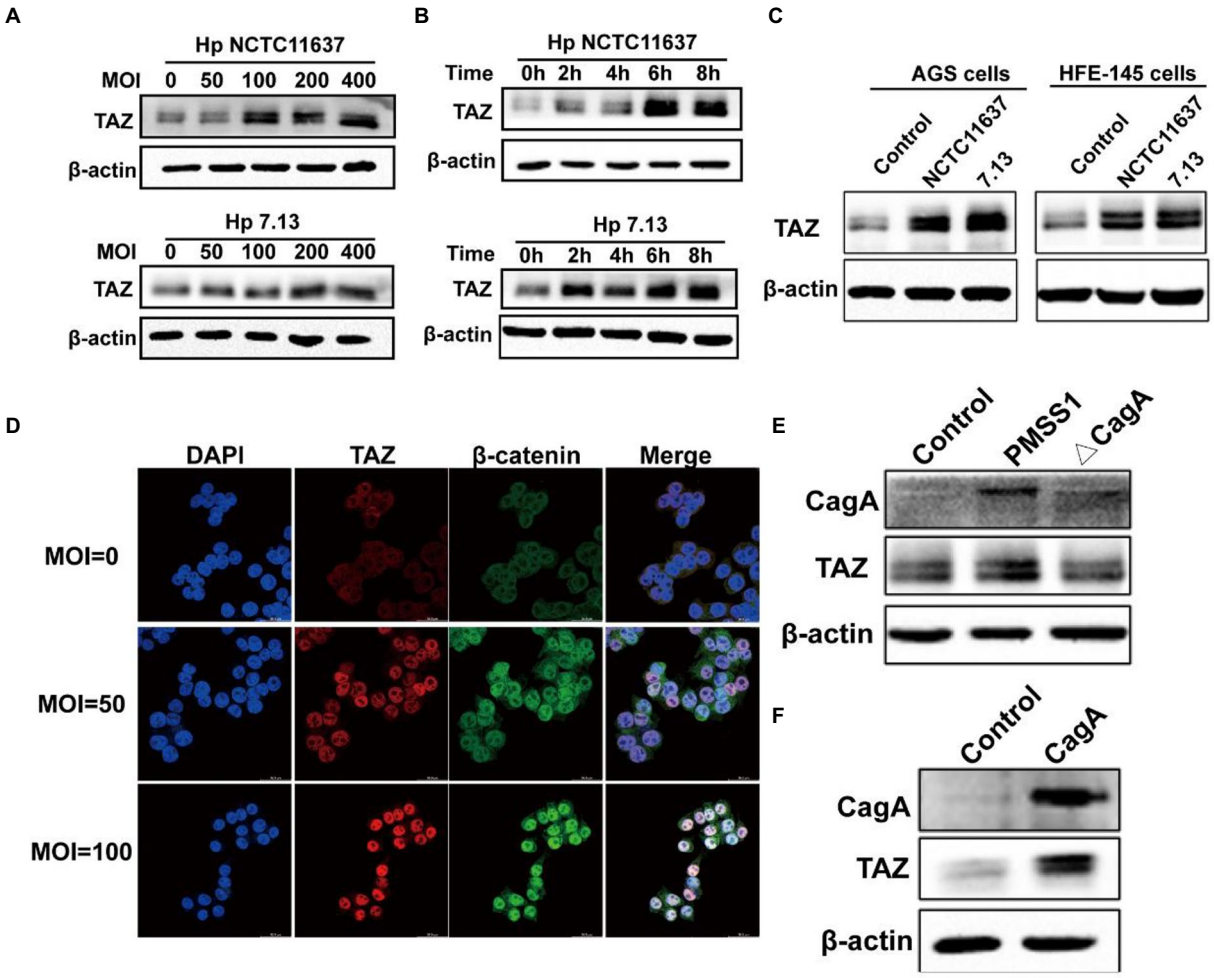

FIGURE 2
Helicobacter pylori infection promoted TAZ expression and nuclear localization. **(A)** Western blot for TAZ protein levels in human gastric epithelial cells infected with *H. pylori* NCTC11637 or 7.13 at different MOI for 6h. **(B)** Western blot for TAZ levels in AGS cells treated with *H. pylori* strains at different time points at MOI of 100. **(C)** Western blot for TAZ levels in different gastric epithelial cells (AGS and HFE145) following infection with different *H. pylori* strains at MOI of 100 for 6h. **(D)** Immunofluorescence staining for TAZ and β-catenin cellular localization after *H. pylori* NCTC11637 infection at different MOI for 6h. (Magnification 400×, scale bars =30μm) **(E)** Western blot for TAZ expression in gastric epithelial cells infected with PMSS1 or its isogenic CagA- mutant. **(F)** Western blot for TAZ expression in gastric cells after transfection with the CagA expression vector.

inhibition of TAZ activation (Figure 4D). Moreover, we performed a TOP/FOP flash luciferase reporter assay to detect β-catenin transcriptional activity. As shown in Figure 4E, *H. pylori* infection increased TCF/β-catenin reporter activity, and this effect was significantly inhibited by siRNA-mediated TAZ knockdown. To further confirm the effect of TAZ on the β-catenin pathway, AGS cells were transiently transfected with a TAZ overexpression plasmid. Exogenous TAZ overexpression increased the protein levels of Myc and Cyclin D1, the downstream targets of the Wnt/β-catenin pathway (Figure 4F). Consistent with these results, TAZ overexpression led to significant transcriptional induction of the downstream genes of Wnt signaling, such as *Lgr5*, *Cyclin D1*, and *Myc*, which was remarkably blocked following β-catenin knockdown by siRNA (Figure 4G). Collectively, these findings suggest that *H. pylori* infection leads to β-catenin activation and target gene expression through TAZ upregulation.

TAZ activation in response to *Helicobacter pylori* infection was abrogated by β-catenin knockdown

We next explored the molecular mechanism of TAZ activation in response to *H. pylori* infection. Given the close relationship between the Hippo and Wnt signaling pathways, we hypothesized that *H. pylori* infection activates the TAZ pathway through the regulation of β-catenin. To test this hypothesis, gastric epithelial AGS cells were transfected with β-catenin siRNA and then cocultured with the *H. pylori* NCTC11637 strain. Knockdown of

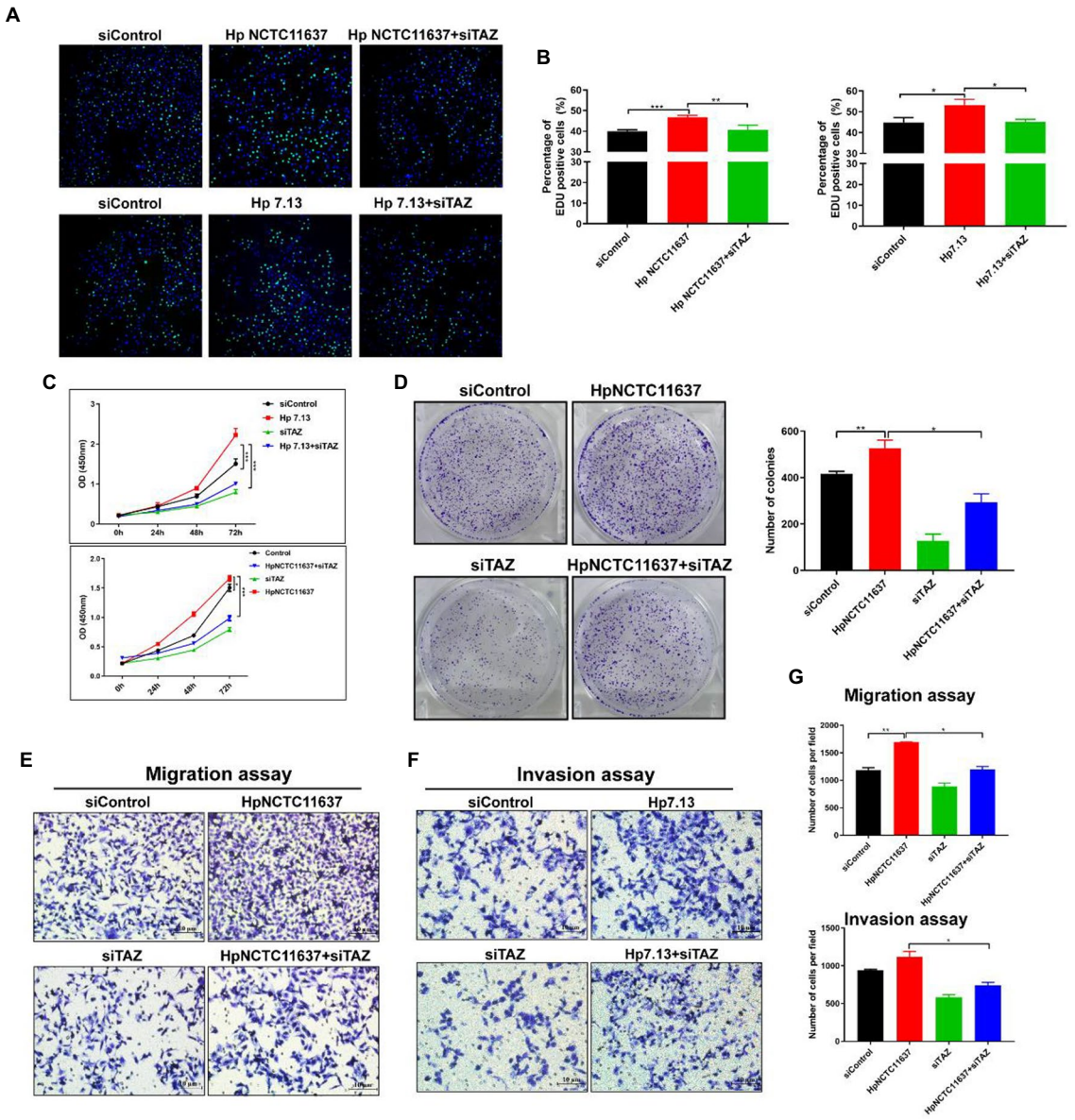

FIGURE 3
TAZ knockdown significantly inhibited *H. pylori* infection-induced cell proliferation, invasion and migration. **(A)** EdU assay for cell proliferation in AGS cells following infection with *H. pylori* (MOI=100) and transfection with TAZ siRNA. Representative confocal images of EdU staining. **(B)** Quantification of the percentage of EdU-positive cells. **(C)** CCK8 viability assay for cell proliferation in AGS cells treated with *H. pylori* alone or in combination with TAZ siRNA. **(D)** Colony formation assay for the assessment of cell survival in the groups treated as described above. **(E–G)** Transwell migration and invasion assays were performed in the groups treated as described above. *p< 0.05, **p<0.01, ***p<0.001.

β-catenin significantly suppressed TAZ expression induced by *H. pylori* (Figure 5A). Moreover, cytoplasmic and nuclear proteins were effectively separated for the detection of the intracellular TAZ expression. Notably, *H. pylori* infection promoted the nuclear accumulation of TAZ and β-catenin, whereas β-catenin knockdown by siRNA remarkably inhibited this induction (Figure 5B). Immunofluorescence staining for TAZ and β-catenin confirmed that *H. pylori*-induced nuclear translocation of TAZ was inhibited by knockdown of β-catenin (Figure 5C). Furthermore, transient overexpression of β-catenin upregulated the protein levels of CTGF and CYR61 downstream of the Hippo signaling pathway (Figure 5D). Taken together, these findings suggest that a positive feedback loop exists between TAZ and the Wnt/β-catenin pathway in *H. pylori*-induced gastric tumorigenesis.

CagA+ *Helicobacter pylori* infection enhanced the interaction of TAZ with β-catenin

It has been reported that TAZ is associated with the destruction complex in the Wnt/β-catenin pathway, including

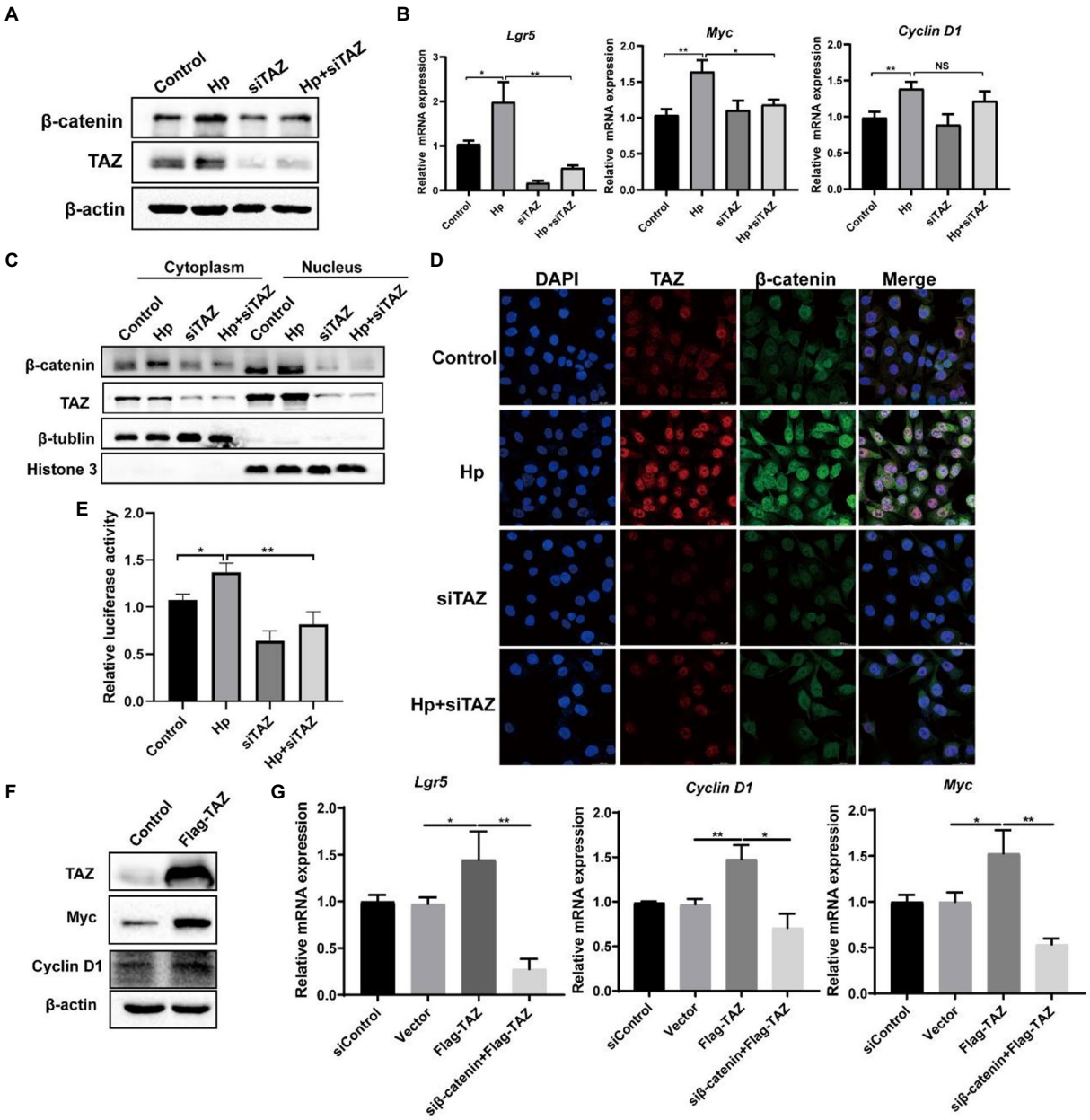

FIGURE 4
Helicobacter pylori infection promoted the β-catenin pathway *via* TAZ. **(A)** Western blot for total β-catenin and TAZ expression in gastric AGS cells transfected with TAZ siRNA and subsequently infected with *H. pylori*. **(B)** RT-PCR assay for mRNA levels of downstream genes of Wnt/β-catenin pathway in the groups treated as described above. **(C)** After transfection with TAZ siRNA and infection with *H. pylori*, cytoplasmic and nuclear protein fractions were isolated. Western blotting was performed to determine the protein levels of TAZ and beta-catenin. β-Tubulin and histone H3 served as loading controls for cytoplasmic and nuclear proteins, respectively. **(D)** Immunofluorescence staining for TAZ and β-catenin cellular localization in the groups treated as described above. **(E)** TOP-Flash luciferase reporter assay for β-catenin transcriptional activity in AGS cells transfected with TAZ siRNA and infected with the *H. pylori* strain. **(F)** Western blot analysis of the protein levels Myc and Cyclin D1, which are downstream effectors of β-catenin, in AGS cells transiently transfected with Flag-TAZ or empty vector. **(G)** RT–PCR analysis of the mRNA levels of downstream effectors of β-catenin, such as Lgr5, Cyclin D1 and Myc, in AGS cells transfected with Flag-TAZ alone or in combination with β-catenin siRNA. *H. pylori* strains in all experiments were used at an MOI of 100. *$p<0.05$, **$p<0.01$.

Axin1, β-TrCP, β-catenin and GSK3β (Azzolin et al., 2014; Lee et al., 2020). Therefore, we delineated the possible interaction between TAZ and β-catenin in *H. pylori*-associated gastric carcinogenesis. The immunofluorescence assay was first performed to determine the expression and cellular localization of TAZ and β-Catenin in human gastric tissues. β-catenin was normally expressed in the membrane of epithelial cells of gastric mucosa with chronic gastritis, and TAZ was present in the plasma membrane and cytoplasm. In contrast, increased overall expression of gastric TAZ was observed, and TAZ

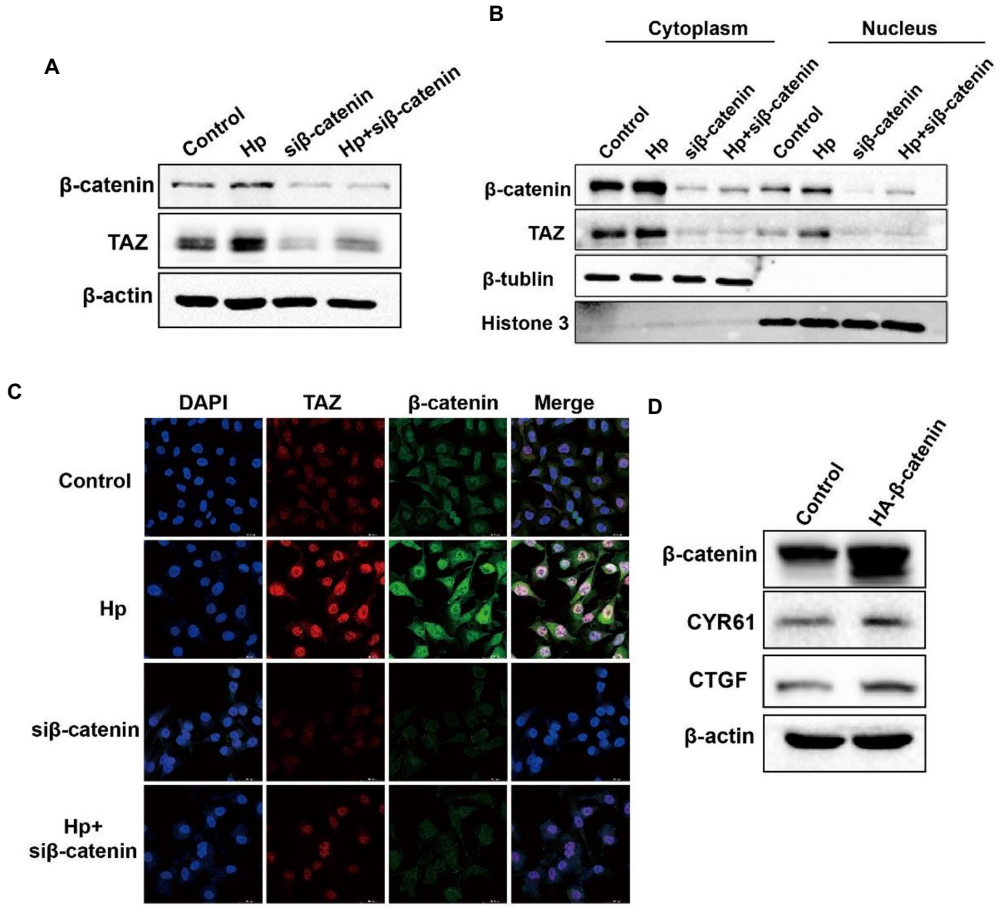

FIGURE 5
β-Catenin also acted as the upstream factor for TAZ activation and exhibited enhanced interaction with TAZ in response to *H. pylori* infection. **(A)** After knocking downβ-catenin by siRNA, AGS cells were cocultured with the *H. pylori* strain. Western blot analysis of TAZ total expression. **(B)** Western blot analysis of TAZ and β-catenin expression in the cytoplasmic and nuclear fractions after treatment with β-catenin siRNA and the *H. pylori* strain. β-Tubulin and histone H3 served as loading controls for cytoplasmic and nuclear proteins, respectively. **(C)** Immunofluorescence staining for TAZ and β-catenin subcellular localization in the groups treated as described above. **(D)** Western blot analysis of the protein levels of CTGF and CYR61 in AGS cells expressing HA-β-catenin plasmid or empty vector. *H. pylori* strains in all experiments were used at an MOI of 100.

colocalization with β-catenin was noted in human gastric cancer tissues but not gastritis tissues (Figure 6A). The interaction of endogenous TAZ with β-catenin was further demonstrated using the co-immunoprecipitation assay (Figure 6B). These data suggest that TAZ may be translocated from the plasma membrane and cytoplasm to the cellular nucleus, and directly interact with β-catenin in gastric tumorigenesis. Moreover, HA-tagged β-catenin was transiently coexpressed with Flag-tagged TAZ in gastric AGS cells, and the cell lysates were subjected to immunoprecipitation with an anti-HA antibody, demonstrating the strong exogenous interaction between HA-β-catenin and Flag-TAZ (Figure 6C). This interaction was significantly enhanced by coinfection with CagA+ *H. pylori* strain NCTC11637 or 7.13 (Figure 6D). Our data and recent studies have indicated that CagA is required for *H. pylori*-induced TAZ and β-catenin (Yong et al., 2016); w therefore, we investigated whether CagA is involved in the interaction between TAZ and β-catenin in response to *H. pylori* infection. Coimmunoprecipitation of TAZ with β-catenin in wild-type *H. pylori*-infected cells was stronger than that in CagA-deficient mutant strain-infected cells (Figure 6E). These data collectively indicated that *H. pylori* CagA plays an important role in the *H. pylori*-enhanced interaction between TAZ and β-catenin.

Knockdown of β-catenin significantly suppressed TAZ-induced gastric cancer cell proliferation, migration, and invasion

As our data indicated that *H. pylori* infection promotes the Wnt/β-catenin signaling pathway *via* the activation of TAZ, we next investigated whether β-catenin plays a role in regulating TAZ-mediated phenotypic alterations of gastric cancer cells. TAZ overexpression induced gastric cell proliferation, which was blocked by β-catenin siRNA (Figure 7A). Furthermore, β-catenin

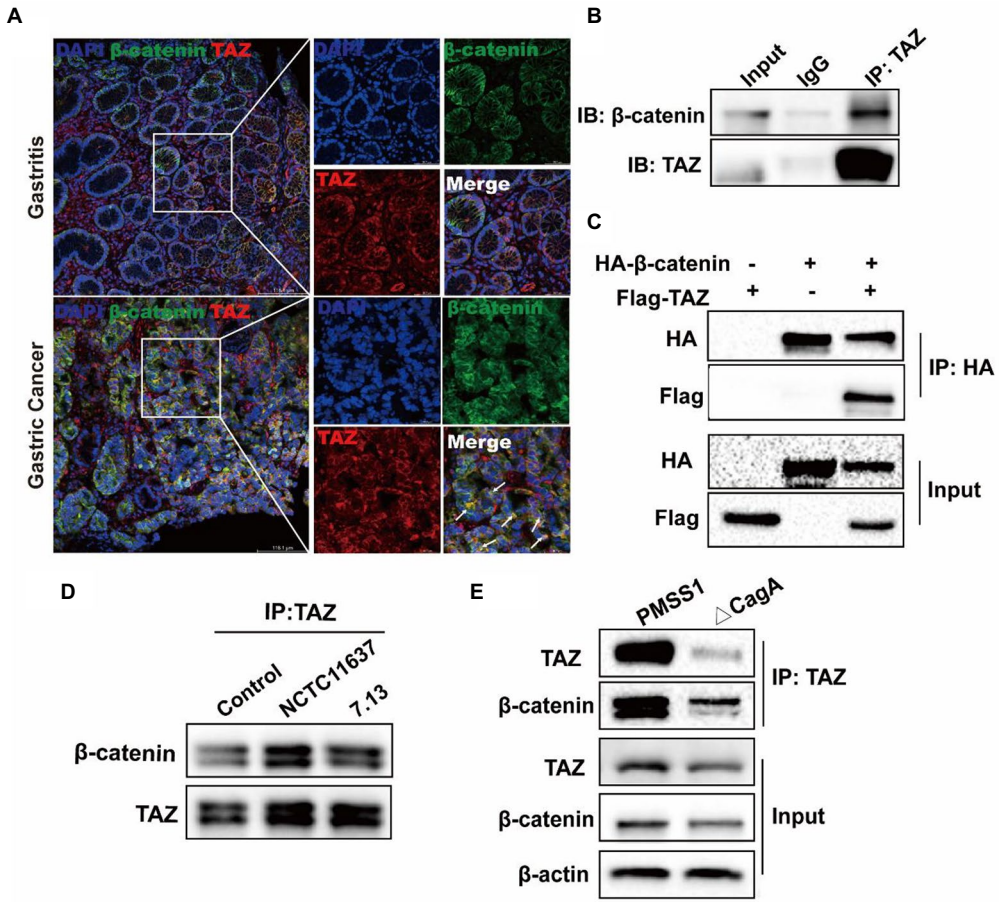

FIGURE 6
CagA+ *H. pylori* infection enhances the interaction of TAZ with β-catenin. **(A)** Immunofluorescence staining for TAZ and β-catenin colocalization in human gastritis and gastric cancer tissues (Magnification 200×, scale bars =116.1μm; and digital zoom, scale bars=38.7μm). **(B)** Interaction between endogenous TAZ and β-catenin. Immunoprecipitation was performed with an anti-TAZ antibody followed by immunoblotting with the indicated antibodies. **(C)** Interaction between HA-β-catenin and Flag-TAZ. Immunoprecipitation was performed with an anti-HA antibody, followed by immunoblotting with the indicated antibodies. **(D)** AGS cells were cocultured with *H. pylori* NCTC11637 or 7.13 strain at an MOI of 100 for 6h. Cell lysates were collected and then immunoprecipitated with anti-TAZ antibody. Western blotting was performed to assess TAZ and β-catenin expression. **(E)** After infection with the *H. pylori* wild-type strain or CagA- mutant for 6h, cell lysates were collected. Infection with the *H. pylori* CagA- mutant resulted in a weak interaction of TAZ with β-catenin, compared with that treatment with wild-type *H. pylori* strain.

knockdown alleviated TAZ-induced gastric cancer cell migration and invasion (Figures 7B,C). Taken together, knockdown of β-catenin suppressed TAZ-mediated cell proliferation, migration and invasion.

Discussion

H. pylori is generally acquired during childhood and remains in the stomach for a lifetime if untreated (Suerbaum and Michetti, 2002; Crowe, 2019). It has been documented that gastrointestinal diseases, particularly gastric adenocarcinoma, are closely associated with *H. pylori* infection (Crowe, 2019). The prevalence of *H. pylori* infection varies greatly among geographic regions. Notably, East Asian countries have a high incidence of gastric carcinoma, which is mainly attributed to the high prevalence of *H. pylori* infection (Inoue, 2017; Wong et al., 2021). At present, the molecular mechanisms underlying *H. pylori* infection-induced gastric carcinogenesis are not completely understood. We previously reported that *H. pylori* infection induces the epithelial-mesenchymal transition and contributes to gastric malignant transformation *via* activation of the YAP pathway (Li et al., 2018). We reported increased TAZ expression in human gastric cancer tissues compared with chronic gastritis tissues as well as *H. pylori*-positive gastritis patients compared with *H. pylori*-negative patients. In addition, *H. pylori* infection significantly elevated TAZ expression and its nuclear translocation in a CagA-dependent manner both in the INS-GAS mouse model and cultured human gastric cells. In addition, our results indicated that TAZ is required for *H. pylori*-induced activation of the Wnt/β-catenin pathway, and the reverse is true for β-catenin. These effects likely occur *via* their direct interaction. Furthermore, *H. pylori* CagA plays an important role in enhancing the interaction between TAZ and β-catenin. Finally, we showed that the

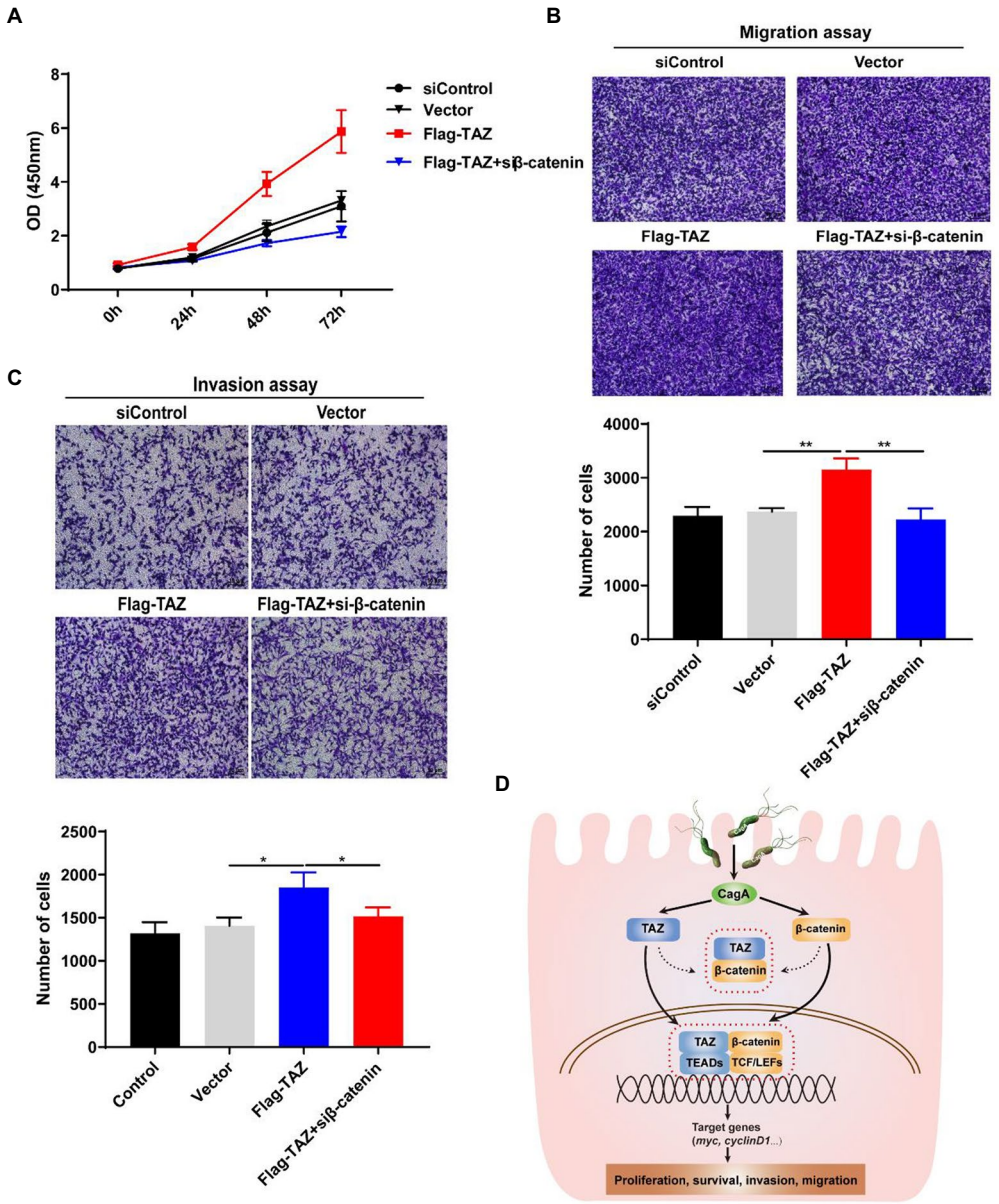

FIGURE 7
Knockdown of β-catenin significantly suppressed TAZ-induced cell proliferation, invasion, and migration. **(A)** CCK8 assay for cell proliferation in AGS cells treated as described for *A*. **(B,C)** Transwell assays for migration **(B)** and invasive **(C)** ability of AGS cells treated as described above. (Magnification 100×, scale bars =10μm). **(D)** Schematic representation of the regulation of the TAZ/β-catenin axis by *H. pylori* infection in gastric carcinogenesis.

interactive regulation of activation between TAZ and β-catenin is integral in *H. pylori* infection-associated gastric epithelial cell malignant transformation as demonstrated by increased cell proliferation, invasion and migration. Taken together, our data reveal a positive feedback loop mechanism between the YAP orthologue TAZ and the β-catenin pathway in *H. pylori* infection-induced gastric tumorigenesis (Figure 7D), providing new insights into the mechanism of *H. pylori* pathogenicity.

As core effectors of the Hippo pathway, TAZ and its related protein YAP have been widely characterized in the regulation of cell growth, tissue regeneration and organ size (Mohajan et al., 2021). Although TAZ and YAP share similarities in amino acid sequences, TAZ can be clearly distinguished based on its structure, function and regulatory network (Jeong et al., 2021; Reggiani et al., 2021). Our previous studies have identified the role of YAP in the pathogenesis of *H. pylori* infection. Supporting this role, *Molina-Catro* et al. also demonstrated the relationship between *H. pylori* and YAP (Molina-Castro et al., 2020). Subsequently, this research team found that *H. pylori* increased TAZ expression and nuclear

accumulation. Additionally, TAZ was overexpressed in human gastric cancer tissues (Tiffon et al., 2020). We further indicated that the increase in TAZ expression seems to be dependent of *H. pylori* infection in gastritis tissues rather than gastric cancer tissues. A significant induction of TAZ expression was also observed in *H. pylori*-infected mice, which developed gastric inflammation after infection. This result further supports the role of *H. pylori* as the initiation factor in precancerous lesions. A lower abundance of *H. pylori* was previously observed in human gastric cancer (Ozbey et al., 2020). This study showed for the first time that *H. pylori* infection-induced TAZ activation was dependent on the virulence factor CagA. Furthermore, TAZ activation is required for *H. pylori* infection-induced gastric cell proliferation, invasion, and migration, as demonstrated by CCK8, EdU, colony formation, and transwell assays. Notably, our data showed that *H. pylori*-positive gastritis tissues had higher TAZ levels than *H. pylori*-negative tissues. Therefore, we hypothesized that TAZ upregulation may occur in the early stages of *H. pylori* infection.

Given the overlapping roles in several biological functions, recent studies have explored the molecular interplay between the YAP/TAZ and β-catenin pathways. Tripath et al. indicated that TAZ directly inhibited β-catenin transcriptional activity in muscle cells and further affected skeletal muscle differentiation (Tripathi et al., 2022). TAZ exhibited entirely different regulatory effects on β-catenin in other diseases. *Lee* et al. clarified the regulatory mechanism of TAZ on the Wnt/β-catenin signaling pathway in ADPKD caused by genetic mutation of PKD1 or PKD2. TAZ strongly interacts with AXIN1, the core component of destruction complex, thereby increasing β-catenin activity and downstream c-MYC expression (Lee et al., 2020). This study innovatively revealed the crosstalk between TAZ and Wnt/β-catenin in *H. pylori*-associated gastric carcinogenesis. Our experiments first indicated that TAZ knockdown significantly inhibited the expression, nuclear translocation and transcriptional activity of β-catenin in response to *H. pylori* infection. Additionally, β-catenin knockdown suppressed *H. pylori*-induced TAZ expression. These data suggest a positive feedback loop between TAZ and β-catenin in the pathogenesis of *H. pylori* infection. Consistent with these findings, some evidence supports the synergistic effect of YAP/TAZ and the Wnt/β-catenin signaling pathway. TAZ acts in concert with β-catenin to promote hepatoblastoma development (Zhang et al., 2020). YAP and TAZ are transcriptionally activated upon β-catenin activation, thereby promoting liver tumorigenesis (Bisso et al., 2020). Silencing of the Hippo upstream kinases Mst1 and Mst2 could activate the activity of YAP/TAZ and Wnt/β-catenin signaling, resulting in rapid hepatocellular carcinoma formation. Additionally, the positive feedback loop between Notch signaling and YAP/TAZ could be inhibited by the Wnt/β-catenin pathway (Kim et al., 2017).

Some evidence in support of the relationship between the other components of Hippo signaling and the Wnt/β-catenin pathway has been reported. Wnt3a and Wnt5a were identified as potent activators of YAP/TAZ (Park et al., 2015). The Wnt scaffolding protein DVL interacts with YAP in a phosphorylation-dependent manner (Lee et al., 2018). A recent study reported that YAP/TAZ physically interacts with β-catenin. In the "Wnt-off" state, YAP/TAZ could be sequestered in the β-catenin destruction complex and associated with Axin1, β-catenin, GSK3, and β-TrCP (Azzolin et al., 2014). Likewise, our observation suggested that both endogenous and exogenous TAZ interacted with β-catenin. Furthermore, infection with two *H. pylori* strains, NCTC11637 and 7.13, enhanced the interaction between TAZ and β-catenin. Intriguingly, we found that CagA plays an important role in their interaction by employing the PMSS1 strain and its CagA- isogenic mutant. VacA, another important virulence factor, is responsible for *H. pylori*-induced cellular vacuolation and gastric injury (Chauhan et al., 2019). Further studies will investigate the role of VacA in the interaction between TAZ and β-catenin by constructing an *H. pylori* VacA- isogenic mutant. In summary, these findings also indicated that β-catenin was responsible for ectopic TAZ-induced gastric cell proliferation, migration and invasion. Based on our findings, we established a regulatory feedback loop underlying the relationship between TAZ and β-catenin, which promotes *H. pylori* infection-induced gastric tumorigenesis.

Conclusion

In summary, our data demonstrated that *H. pylori* infection triggers gastric epithelial cell malignant transformation *via* the promotion of TAZ activation. Mechanistically, *H. pylori* infection leads toβ-catenin pathway activation *via* TAZ, which contributes to gastric carcinogenesis. In turn, β-catenin functions as an upstream regulator and is involved in TAZ activation following *H. pylori* infection. Moreover, we implicated the important role of CagA in TAZ regulation by *H. pylori*. Studies further confirmed the clinical evidence that *H. pylori* positive gastritis tissues contain higher TAZ expression levels than *H. pylori*-negative tissues. This study effectively linked *H. pylori* infection and the bacterial protein CagA to TAZ and the β-catenin pathway, thereby elucidating a new pathogenic mechanism of *H. pylori* and suggesting novel targets for the prevention and early detection of gastric cancer.

Data availability statement

The original contributions presented in the study are included in the article/Supplementary material, further inquiries can be directed to the corresponding authors.

Ethics statement

The studies involving human participants were reviewed and approved by the Ethics Committees of The First Affiliated Hospital of Nanchang University. The patients/participants provided their written informed consent to participate in this study. The animal study was reviewed and approved by the ethics committees of The First Affiliated Hospital of Nanchang University.

Author contributions

XX, NLi, and YZh: contributed to the design of this study, performance of the experiments, and analysis of data. CS, XW, YO, HW, and YZho: conducted various portions of the experiments. XH, CH, and NLu: analyzed immunohistochemical data. NLi, XX, and ZG: drafted the manuscript. CX, CH, JH, NLu, YZh, and NLi: contributed to the study supervision and coordination. NLi, CH, and YZh: obtained funding support. All the authors critically revised the manuscript and provided intellectual content.

Funding

This work was supported by the National Natural Science Foundation of China (81900500, 81870395, and 82170580), Natural Science Foundation of Jiangxi Province (20212BAB216016), Doctoral Research Initiation Funding (701221002), and Young Medical Teacher Training Fund of Nanchang University (4209-16100009-PY201923).

Acknowledgments

We thank Richard Peek (Vanderbilt University Medical Center, Nashville, TN, United States) for kindly providing the *H. pylori* strain 7.13.

Conflict of interest

The authors declare that the research was conducted in the absence of any commercial or financial relationships that could be construed as a potential conflict of interest.

Publisher's note

All claims expressed in this article are solely those of the authors and do not necessarily represent those of their affiliated organizations, or those of the publisher, the editors and the reviewers. Any product that may be evaluated in this article, or claim that may be made by its manufacturer, is not guaranteed or endorsed by the publisher.

Supplementary material

The Supplementary material for this article can be found online at: https://www.frontiersin.org/articles/10.3389/fmicb.2022.1065462/full#supplementary-material

References

Ansari, S., and Yamaoka, Y. (2019). *Helicobacter pylori* virulence factors exploiting gastric colonization and its pathogenicity. *Toxins (Basel)* 11. doi: 10.3390/toxins11110677

Arnold, I. C., Lee, J. Y., Amieva, M. R., Roers, A., Flavell, R. A., Sparwasser, T., et al. (2011). Tolerance rather than immunity protects from *Helicobacter pylori*-induced gastric preneoplasia. *Gastroenterology* 140, 199–209.e8. doi: 10.1053/j.gastro.2010.06.047

Azzolin, L., Panciera, T., Soligo, S., Enzo, E., Bicciato, S., Dupont, S., et al. (2014). YAP/TAZ incorporation in the beta-catenin destruction complex orchestrates the Wnt response. *Cells* 158, 157–170. doi: 10.1016/j.cell.2014.06.013

Azzolin, L., Zanconato, F., Bresolin, S., Forcato, M., Basso, G., Bicciato, S., et al. (2012). Role of TAZ as mediator of Wnt signaling. *Cells* 151, 1443–1456. doi: 10.1016/j.cell.2012.11.027

Bisso, A., Filipuzzi, M., Gamarra Figueroa, G. P., Brumana, G., Biagioni, F., et al. (2020). Cooperation between MYC and beta-catenin in liver tumorigenesis requires yap/Taz. *Hepatology* 72, 1430–1443. doi: 10.1002/hep.31120

Cao, L., Zhu, S., Lu, H., Soutto, M., Bhat, N., Chen, Z., et al. (2022). *Helicobacter pylori*-induced RASAL2 through activation of nuclear factor-kappaB promotes gastric tumorigenesis via beta-catenin signaling Axis. *Gastroenterology* 162:e1717, 1716–1731.e17. doi: 10.1053/j.gastro.2022.01.046

Chauhan, N., Tay, A. C. Y., Marshall, B. J., and Jain, U. (2019). *Helicobacter pylori* VacA, a distinct toxin exerts diverse functionalities in numerous cells: an overview. *Helicobacter* 24:e12544. doi: 10.1111/hel.12544

Correa, P., and Piazuelo, M. B. (2011). *Helicobacter pylori* infection and gastric adenocarcinoma. *US Gastroenterol. Hepatol. Rev.* 7, 59–64. doi: 10.1128/CMR.00011-10

Crowe, S. E. (2019). *Helicobacter pylori* infection. *N. Engl. J. Med.* 380, 1158–1165. doi: 10.1056/NEJMcp1710945

Franco, A. T., Israel, D. A., Washington, M. K., Krishna, U., Fox, J. G., Rogers, A. B., et al. (2005). Activation of beta-catenin by carcinogenic *Helicobacter pylori*. *Proc. Natl. Acad. Sci. U. S. A.* 102, 10646–10651. doi: 10.1073/pnas.0504927102

Hu, Y., Liu, J. P., Li, X. Y., Cai, Y., He, C., Li, N. S., et al. (2019). Downregulation of tumor suppressor RACK1 by *Helicobacter pylori* infection promotes gastric carcinogenesis through the integrin beta-1/NF-kappaB signaling pathway. *Cancer Lett.* 450, 144–154. doi: 10.1016/j.canlet.2019.02.039

Inoue, M. (2017). Changing epidemiology of *Helicobacter pylori* in Japan. *Gastric Cancer* 20, 3–7. doi: 10.1007/s10120-016-0658-5

Jeong, M. G., Kim, H. K., and Hwang, E. S. (2021). The essential role of TAZ in normal tissue homeostasis. *Arch. Pharm. Res.* 44, 253–262. doi: 10.1007/s12272-021-01322-w

Kim, W., Khan, S. K., Gvozdenovic-Jeremic, J., Kim, Y., Dahlman, J., Kim, H., et al. (2017). Hippo signaling interactions with Wnt/beta-catenin and Notch signaling repress liver tumorigenesis. *J. Clin. Invest.* 127, 137–152. doi: 10.1172/JCI88486

Lee, E. J., Seo, E., Kim, J. W., Nam, S. A., Lee, J. Y., Jun, J., et al. (2020). TAZ/Wnt-beta-catenin/c-MYC axis regulates cystogenesis in polycystic kidney disease. *Proc. Natl. Acad. Sci. U. S. A.* 117, 29001–29012. doi: 10.1073/pnas.2009334117

Lee, Y., Kim, N. H., Cho, E. S., Yang, J. H., Cha, Y. H., Kang, H. E., et al. (2018). Dishevelled has a YAP nuclear export function in a tumor suppressor context-dependent manner. *Nat. Commun.* 9:2301. doi: 10.1038/s41467-018-04757-w

Li, N., Feng, Y., Hu, Y., He, C., Xie, C., Ouyang, Y., et al. (2018). *Helicobacter pylori* CagA promotes epithelial mesenchymal transition in gastric carcinogenesis via triggering oncogenic YAP pathway. *J. Exp. Clin. Cancer Res.* 37:280. doi: 10.1186/s13046-018-0962-5

Li, N., Lu, N., and Xie, C. (2019). The hippo and Wnt signalling pathways: crosstalk during neoplastic progression in gastrointestinal tissue. *FEBS J.* 286, 3745–3756. doi: 10.1111/febs.15017

Li, N., Ouyang, Y., Chen, S., Peng, C., He, C., Hong, J., et al. (2020). Integrative analysis of differential lncRNA/mRNA expression profiling in *Helicobacter pylori* infection-associated gastric carcinogenesis. *Front. Microbiol.* 11:880. doi: 10.3389/fmicb.2020.00880

Liou, J. M., Malfertheiner, P., Lee, Y. C., Sheu, B. S., Sugano, K., Cheng, H. C., et al. (2020). Screening and eradication of *Helicobacter pylori* for gastric cancer prevention: the Taipei global consensus. *Gut* 69, 2093–2112. doi: 10.1136/gutjnl-2020-322368

Liu, J., Xiao, Q., Xiao, J., Niu, C., Li, Y., Zhang, X., et al. (2022). Wnt/beta-catenin signalling: function, biological mechanisms, and therapeutic opportunities. *Signal Transduct. Target. Ther.* 7:3. doi: 10.1038/s41392-021-00762-6

Mohajan, S., Jaiswal, P. K., Vatanmakarian, M., Yousefi, H., Sankaralingam, S., Alahari, S. K., et al. (2021). Hippo pathway: regulation, deregulation and potential therapeutic targets in cancer. *Cancer Lett.* 507, 112–123. doi: 10.1016/j.canlet.2021.03.006

Molina-Castro, S. E., Tiffon, C., Giraud, J., Boeuf, H., Sifre, E., Giese, A., et al. (2020). The hippo kinase LATS2 controls *Helicobacter pylori*-induced epithelial-mesenchymal transition and intestinal metaplasia in gastric mucosa. *Cell. Mol. Gastroenterol. Hepatol.* 9, 257–276. doi: 10.1016/j.jcmgh.2019.10.007

Ozbey, G., Sproston, E., and Hanafiah, A. (2020). *Helicobacter pylori* infection and gastric microbiota. *Euro. J. Hepatogastroenterol.* 10, 36–41. doi: 10.5005/jp-journals-10018-1310

Park, H. W., Kim, Y. C., Yu, B., Moroishi, T., Mo, J. S., Plouffe, S. W., et al. (2015). Alternative Wnt signaling activates YAP/TAZ. *Cells* 162, 780–794. doi: 10.1016/j.cell.2015.07.013

Park, J. Y., Forman, D., Waskito, L. A., Yamaoka, Y., and Crabtree, J. E. (2018). Epidemiology of *Helicobacter pylori* and CagA-positive infections and global variations in gastric cancer. *Toxins (Basel)* 10. doi: 10.3390/toxins10040163

Pobbati, A. V., and Hong, W. (2020). A combat with the YAP/TAZ-TEAD oncoproteins for cancer therapy. *Theranostics* 10, 3622–3635. doi: 10.7150/thno.40889

Pocaterra, A., Romani, P., and Dupont, S. (2020). YAP/TAZ functions and their regulation at a glance. *J. Cell Sci.* 133. doi: 10.1242/jcs.230425

Reggiani, F., Gobbi, G., Ciarrocchi, A., and Sancisi, V. (2021). YAP and TAZ are not identical twins. *Trends Biochem. Sci.* 46, 154–168. doi: 10.1016/j.tibs.2020.08.012

Russell, J. O., and Camargo, F. D. (2022). Hippo signalling in the liver: role in development, regeneration and disease. *Nat. Rev. Gastroenterol. Hepatol.* 19, 297–312. doi: 10.1038/s41575-021-00571-w

Suerbaum, S., and Michetti, P. (2002). *Helicobacter pylori* infection. *N. Engl. J. Med.* 347, 1175–1186. doi: 10.1056/NEJMra020542

Sung, H., Ferlay, J., Siegel, R. L., Laversanne, M., Soerjomataram, I., Jemal, A., et al. (2021). Global cancer statistics 2020: GLOBOCAN estimates of incidence and mortality worldwide for 36 cancers in 185 countries. *CA Cancer J. Clin.* 71, 209–249. doi: 10.3322/caac.21660

Sylvester, K. G., and Colnot, S. (2014). Hippo/YAP, beta-catenin, and the cancer cell: a "menage a trois" in hepatoblastoma. *Gastroenterology* 147, 562–565. doi: 10.1053/j.gastro.2014.07.026

Tiffon, C., Giraud, J., Molina-Castro, S. E., Peru, S., Seeneevassen, L., et al. (2020). TAZ controls *Helicobacter pylori*-induced epithelial-mesenchymal transition and cancer stem cell-like invasive and tumorigenic properties. *Cells* 9. doi: 10.3390/cells9061462

Totaro, A., Panciera, T., and Piccolo, S. (2018). YAP/TAZ upstream signals and downstream responses. *Nat. Cell Biol.* 20, 888–899. doi: 10.1038/s41556-018-0142-z

Tripathi, S., Miyake, T., Kelebeev, J., and McDermott, J. C. (2022). TAZ exhibits phase separation properties and interacts with Smad7 and beta-catenin to repress skeletal myogenesis. *J. Cell Sci.* 135. doi: 10.1242/jcs.259097

Veeman, M. T., Slusarski, D. C., Kaykas, A., Louie, S. H., and Moon, R. T. (2003). Zebrafish prickle, a modulator of noncanonical Wnt/Fz signaling, regulates gastrulation movements. *Curr. Biol.* 13, 680–685. doi: 10.1016/s0960-9822(03)00240-9

Wong, M. C. S., Huang, J., Chan, P. S. F., Choi, P., Lao, X. Q., Chan, S. M., et al. (2021). Global incidence and mortality of gastric cancer, 1980-2018. *JAMA Netw. Open* 4:e2118457. doi: 10.1001/jamanetworkopen.2021.18457

Xie, C., Li, N., Wang, H., He, C., Hu, Y., Peng, C., et al. (2020). Inhibition of autophagy aggravates DNA damage response and gastric tumorigenesis via Rad51 ubiquitination in response to H. pylori infection. *Gut Microbes* 11, 1567–1589. doi: 10.1080/19490976.2020.1774311

Xie, C., Yi, J., Lu, J., Nie, M., Huang, M., Rong, J., et al. (2018). N-acetylcysteine reduces ROS-mediated oxidative DNA damage and PI3K/Akt pathway activation induced by *Helicobacter pylori* infection. *Oxidative Med. Cell. Longev.* 2018:1874985. doi: 10.1155/2018/1874985

Yan, L., Chen, Y., Chen, F., Tao, T., Hu, Z., Wang, J., et al. (2022). Effect of *Helicobacter pylori* eradication on gastric cancer prevention: updated report from a randomized controlled trial with 26.5 years of follow-up. *Gastroenterology* 163, 154–162.e3. doi: 10.1053/j.gastro.2022.03.039

Yang, J., Antin, P., Berx, G., Blanpain, C., Brabletz, T., Bronner, M., et al. (2020). Guidelines and definitions for research on epithelial-mesenchymal transition. *Nat. Rev. Mol. Cell Biol.* 21, 341–352. doi: 10.1038/s41580-020-0237-9

Yong, X., Tang, B., Xiao, Y. F., Xie, R., Qin, Y., Luo, G., et al. (2016). *Helicobacter pylori* upregulates Nanog and Oct4 via Wnt/beta-catenin signaling pathway to promote cancer stem cell-like properties in human gastric cancer. *Cancer Lett.* 374, 292–303. doi: 10.1016/j.canlet.2016.02.032

Zhang, S., Zhang, J., Evert, K., Li, X., Liu, P., Kiss, A., et al. (2020). The hippo effector transcriptional coactivator with PDZ-binding motif cooperates with oncogenic beta-catenin to induce Hepatoblastoma development in mice and humans. *Am. J. Pathol.* 190, 1397–1413. doi: 10.1016/j.ajpath.2020.03.011

Zhang, Y., and Wang, X. (2020). Targeting the Wnt/beta-catenin signaling pathway in cancer. *J. Hematol. Oncol.* 13:165. doi: 10.1186/s13045-020-00990-3

frontiers | Frontiers in Microbiology

TYPE Original Research
PUBLISHED 13 January 2023
DOI 10.3389/fmicb.2022.999564

OPEN ACCESS

EDITED BY
Susana Fuentes,
National Institute for Public Health and the Environment (Netherlands), Netherlands

REVIEWED BY
Ignacio Rangel,
Örebro University,
Sweden
Qinbo Cai,
The First Affiliated Hospital of Sun Yat-sen University, China

*CORRESPONDENCE
Feng Gao
✉ xjgf@sina.com

†These authors share first authorship

SPECIALTY SECTION
This article was submitted to Infectious Agents and Disease, a section of the journal Frontiers in Microbiology

RECEIVED 21 July 2022
ACCEPTED 21 December 2022
PUBLISHED 13 January 2023

CITATION
Liu W, Kong W, Hui W, Wang C, Jiang Q, Shi H and Gao F (2023) Characteristics of different types of *Helicobacter pylori*: New evidence from non-amplified white light endoscopy.
Front. Microbiol. 13:999564.
doi: 10.3389/fmicb.2022.999564

Characteristics of different types of *Helicobacter pylori*: New evidence from non-amplified white light endoscopy

Weidong Liu[1†], Wenjie Kong[2,3†], Wenjia Hui[2,3], Chun Wang[4], Qi Jiang[2,3], Hong Shi[5] and Feng Gao[2,3*]

[1]College of Life Science and Technology, Xinjiang University, Urumqi, China, [2]Department of Gastroenterology, People's Hospital of Xinjiang Uygur Autonomous Region, Urumqi, China, [3]Xinjiang Clinical Research Center for Digestive Diseases, Urumqi, China, [4]Department of Pathology, People's Hospital of Xinjiang Uygur Autonomous Region, Urumqi, China, [5]Department of Gastroenterology, ZhongShan Hospital, Fudan University, Shanghai, China

Background: Different types of *Helicobacter pylori (H. pylori)* were analyzed to determine their infection characteristics using serology, pathology, and non-magnification white light endoscopy combined with the Kimura–Takemoto classification, and the regular arrangement of collecting venules (RAC) as well.

Materials and methods: A retrospective analysis of 685 inpatients who have completed the ^{14}C-urea breath test, the *H. pylori* antibody typing classification, the serum gastric function tests (PGI/PGII/G-17), the endoscope detection, and the pathological examinations.

Results: The levels of PGI, PGII, and G-17 were in descending order from the type I *H. pylori* infection group to the type II *H. pylori* infection group than the control group (F=14.31; 26.23; 9.12, P<0.01). Using the Kimura–Takemoto classification, there were significant differences among the three groups of different degrees of atrophy (χ^2 =29.81; 482.78; 292.5, P< 0.01). Based on the characteristics of RAC, the *H. pylori* infection rates were in descending order from the type I *H. pylori* infection group to the type II *H. pylori* infection group than the control group (χ^2 =200.39; 174.72; 143.51, P<0.01). The type I *H. pylori* infection group had higher grades than those of the type II *H. pylori* infection group in the OLGA and OLGIM staging systems, while the differences are statistically significant only in the OLGA staging system (χ^2 =10.63, P<0.05).

Conclusion: With the aid of non-amplified white light endoscopy, we found new evidence of type I *H. pylori* infection accelerating the progression of gastric mucosal atrophy through the degree of atrophy and the range of infection, whereas type II *H. pylori* infection has a low ability of migration and atrophy progression. Individual virulence factor-based eradication therapy may be a better choice in future.

KEYWORDS

endoscopy, *Helicobacter pylori*, CagA Ab, gastritis—microbiology, urea breath test

1. Introduction

The major sites of *Helicobacter pylori* (*H. pylori*) infection are the stomach and duodenal bulbs, which are significantly associated with chronic gastritis, gastric mucosa atrophy and erosion, peptic ulcer, MALT lymphoma, and gastric cancer (Smith et al., 2017). In 1994, *H. pylori* were classified as a class I biological carcinogen by the World Health Organization (Ferreira et al., 2014). In 2015, the *Kyoto Global Consensus Report on Helicobacter pylori* identified *H. pylori* as an infectious disease (Sugano et al., 2015). In 2022, the United States Department of Health and Human Services listed *H. pylori* as a definite carcinogen. *Helicobacter pylori* are a highly heterogeneous bacterium, from which many virulence factors have been isolated and identified. Cytotoxin-associated gene A (*CagA*) and Vacuolating cytotoxin gene A (*VacA*) have been extensively studied as the virulence markers of *H. pylori*, since carrying these two genes has made *H. pylori* closely associated with the occurrence and development of many gastric diseases (Chey et al., 2017; Lee et al., 2021). Recent studies have shown that the CagA of *H. pylori* can cause genomic instability induced by BRCNESS. Moreover, *H. pylori*'s CagA can cause gastric cancer through a "hit and run" mechanism in the absence of p53 (Imai et al., 2021).

Clinically, based on the antibody expression of CagA and VacA, *H. pylori* can be classified into type I *H. pylori* infection ($CagA^+/VacA^+$) and type II *H. pylori* infection ($CagA^-/VagA^-$). Previous studies have found that type I *H. pylori* infection may contribute to the progression of gastric mucosal atrophy through its higher virulence factors and migration ability; however, there is no direct evidence to support this in the real gastric condition (Liu et al., 2021; Zhang et al., 2022). In this study, different types of *H. pylori* were analyzed to determine their infection characteristics using serology, pathology, and non-magnification white light endoscopy combined with Kimura–Takemoto classification, and the regular arrangement of collecting venules (RAC) as well. We have explored characteristics of different types of *H. pylori* causing gastric mucosa atrophy through virulence factors and migration ability in a specific population (50–60 years old), which may provide a new theoretical basis for clinical individual eradication therapy.

2. Materials and methods

2.1. Subject investigated

A retrospective analysis of 745 inpatients in the Department of Gastroenterology of Xinjiang Urumqi People's Hospital from March 2019 to January 2022, and 685 cases were eventually included given the exclusion criteria. All inpatients were Han Chinese, aged 50–60 years, and have completed the ^{14}C-urea breath test, the *H. pylori* antibody typing classification, the serum gastric function tests (PGI/PGII/G-17), and the endoscope detection and the pathological examinations. The exclusion criteria included the following: previous history of gastric cancer and gastric cancer surgery; active bleeding and other serious systemic diseases; previous eradication of *H. pylori*; discordant results from the ^{14}C-urea breath test and the *H. pylori* antibody typing classification; and incomplete endoscopic data. G*Power was used to calculate the sample size: select tests—Goodness-of-fit tests: Contingency tables, effect size = 0.3, $\alpha = 0.05$, $1-\beta = 0.95$. The results of pre-investigation were taken as parameters, and the minimum sample size required for calculation was 342 cases. The sample size of the study was 685 cases, which could ensure reliable results. The study was approved by the ethics committee of the People's Hospital of Xinjiang Uygur Autonomous Region (KY2019051528).

2.2. ^{14}C-urea breath test

The inpatients were required to take a ^{14}C urea capsule on an empty stomach or 2 h after meals and sit for 25 min, and then blow into the gas collector for about 3 min until the liquid indicator color became colorless. Then, 4.5 ml scintillation solution to the gas collector was added and mixed upside down three times before being sent to the *H. pylori* detector (HUBT01) for 1 min. The sample was determined as positive for *H. pylori* infection if the detection value ≥100 dpm, and negative for the detection value <100 dpm.

2.3. *Helicobacter pylori* antibody typing classification

To type and classify *H. pylori* antibodies, 2–3 ml venous blood was collected from hospitalized patients, and then the serum was obtained by centrifugation at 3,500 rpm/10 min. The *H. pylori* antibody typing classification kit (immunoblotting method) was provided by Shenzhen Blot Biological Products, Shenzhen, China, Co., Ltd. The imprinting membrane strip was qualitatively compared with the standard strip after binding to serum antibodies, enzyme-linked reaction, color reaction, and termination of the reaction. Positive for type I *H. pylori* infection: either or both of the CagA and VacA zones appeared simultaneously. Positive for type II *H. pylori* infection: either or both of urease A (UreA) and UreB zones but no CagA or VacA zone were found. Negative results: no positive zone was found in the color zone.

2.4. Serum gastric function tests

For the serum gastric function test, serum was obtained by centrifugation of 3 ml venous blood at a rate of 3,500 rpm/10 min. The serum gastric function assay kit (Biohit, Hefei, China) was used to follow its instructions: 80 μl serum was added into the sample hole of the test card and kept for 15 min, then it was detected by fluorescence immunoassay (HIT-9A). The normal reference range of PGI was

70–165 μg/L, the normal reference range of PGII was 3–11 μg/L, the normal reference range of PGI/PGII was >7, and the normal reference range of G-17 was 1–7 pmol/L.

2.5. Endoscope detection

To assess the status and extent of *H. pylori* infection, an endoscopy was performed. All patients underwent endoscopy performed by an endoscopist with 5 years of standardized training, using either GIF-H260 or GIF-HQ290 from Olympus, Japan, and biopsies were performed according to the new Sydney standard. The range and degree of endoscopic atrophy were classified according to the Kimura–Takemoto classification, and the mucosal lesions were divided into 0, C1, C2, C3, O1, O2, and O3, and two senior endoscopists were responsible for determining the degree of atrophy (see Appendant.1). The status and range of *H. pylori* infection were evaluated in conjunction with the characteristics of endoscopic RAC (see Appendant.2).

2.6. Pathological examinations

Endoscopic biopsies were formalin overnight, paraffin-embedded the next day, sectioned with a sectioning machine, HE stained by an automated immunohistochemical machine, and biopsied by a pathologist based on the most common chronic gastritis; five histological changes (*H. pylori*, chronic inflammatory lesions, motility, atrophy, and intestinal metaplasia) were assessed and the degree of each histological change was assessed as nil, mild, moderate, and severe. The grading method was based on the *consensus of pathological diagnosis for biopsy of chronic gastritis and epithelial tumor of the gastric mucosa* (2017), combined with the updated Sydney System's visual analog scales. The pathological diagnosis report included histological changes in biopsy specimens from each site. The OLGA and OLGIM staging systems were used to assess chronic gastritis with gastric atrophy. The OLGA staging system ranks the degree of pathological atrophy as stage 0, stage1, stage 2, stage 3, and stage 4 (see Appendant.3A); and the OLGIM staging system ranks the degree of pathological intestinal metaplasia as stage 0, stage1, stage 2, stage 3, and stage 4 (see Appendant.3B).

2.7. Statistical analysis

All data were analyzed by SPSS 19.0. The metering data were presented as $\bar{x} \pm S$, variance analysis or non-parametric tests were used for the mean value among groups, and the Mann–Whitney U-test was used for the comparison between the two groups. The counting data were represented by the number of cases and percentage. Pearson Chi-Square and Fisher's exact test were used for comparison between groups. The difference was considered statistically significant at $P < 0.05$.

3. Results

3.1. Analyses of general data

The study included 745 Han Chinese inpatients aged 50–60 years, and 685 patients were finally enrolled given the exclusion criteria. There were 355 male and 330 female patients with an average age of 55.4 ± 3.3 years. According to the *H. pylori* antibody typing classification, these inpatients were divided into three groups. Among the 291 patients with type I *H. pylori* infection, 148 were male and 143 were female patients, and the average age was 55.3 ± 3.2 years. Among the 110 patients with type II *H. pylori* infection, there were 54 male and 56 female patients with an average age of 55.4 ± 3.3 years. The control group was made of 153 male and 131 female patients, 284 in total with an average age of 55.5 ± 3.3 years. There was no significant difference in sex and age between groups ($x^2 = 0.91$, $p = 0.63$; $x^2 = 0.45$, $P = 0.80$, P all > 0.05).

3.2. Expression of serum gastric function tests levels in different types of *Helicobacter pylori*

Serum gastric function tests revealed that expression levels of PGI were higher in the type I *H. pylori* infection group (181.0 ± 79.9 μg/L) than those in the type II *H. pylori* infection group (148.8 ± 62.9 μg/L) and the control group (153 ± 63.8 μg/L), and the differences were statistically significant ($F = 14.1$, $P < 0.01$), as shown in Figure 1A. The expression levels of PGII were higher in the type I *H. pylori* infection group (11.3 ± 8.3 μg/L) than those in the type II *H. pylori* infection group (7.4 ± 8.4 μg/L) and the control group (6.7 ± 7.4 μg/L), and the differences were statistically significant ($F = 26.2$, $P < 0.01$), as shown in Figure 1B. The expression levels of PGR were lower in the type I *H. pylori* infection group (22 ± 14.5) than those in the type II *H. pylori* infection group (29.5 ± 15.2) and the control group (32.3 ± 16.6), and the differences were statistically significant ($F = 33.2$, $P < 0.01$), as shown in Figure 1C. The expression levels of G-17 were higher in the type I *H. pylori* infection group (8 ± 11.4 pmol/L) than those in the type II *H. pylori* infection group (5.9 ± 10.4 pmol/L) and the control group (4.2 ± 9.8 pmol/L), and the differences were statistically significant only between the type I *H. pylori* infection group and the control group ($F = 9.1$, $P < 0.01$), as shown in Figure 1D.

3.3. Characteristic analysis of atrophy of different types of *Helicobacter pylori* infection under endoscopy

The composition ratio of different degrees of atrophy in the Kimura–Takemoto classification was statistically different among the type I *H. pylori* infection group, the type II *H. pylori* infection

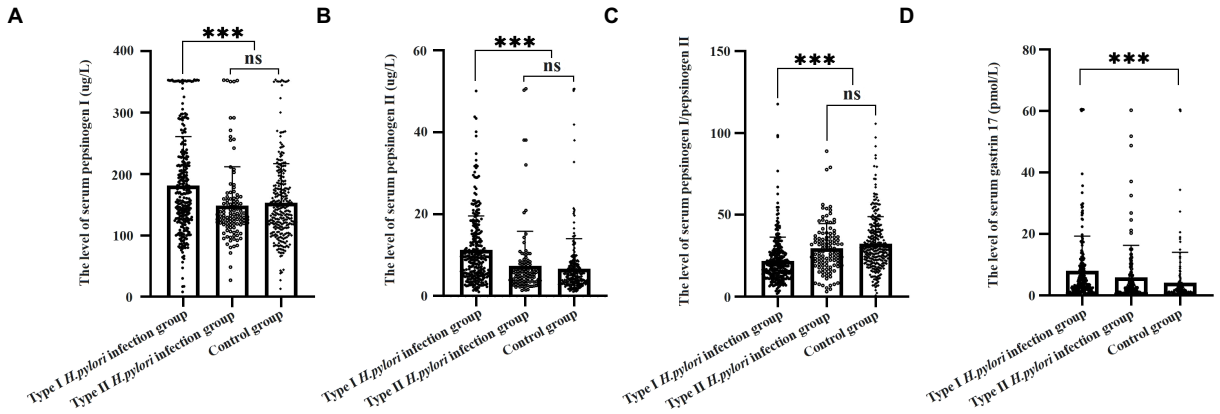

FIGURE 1
Serum gastric function of different types of *Helicobacter pylori* infection.

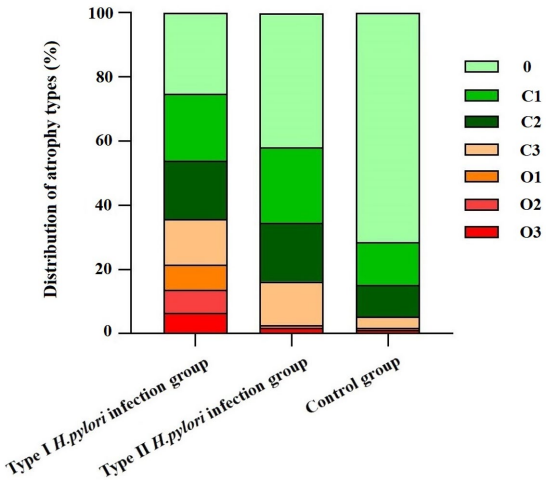

FIGURE 2
Distribution of different types of *Helicobacter pylori* infection in Kimura–Takemoto classification.

group, and the control group (x^2 =29.81; 482.78; 292.5, P< 0.01). Intergroup comparison has shown that only the composition ratio of C1 had no significant difference between the type I *H. pylori* infection group and the type II *H. pylori* infection group (x^2 =0.34, P>0.05), as shown in Figure 2.

3.4. Distribution of different types of *Helicobacter pylori* infection under endoscopy

Regular arrangement of collecting venules is mainly distributed in the gastric angle and gastricum, and the site and range of *H. pylori* infection can be located and evaluated by the absence of RAC; therefore, the status of *H. pylori* infection is mainly estimated by the characteristics of RAC under endoscopy. The results showed that the type I *H. pylori* infection group and the type II *H. pylori* infection group expressed higher characteristics of infection in gastric antrum (x^2 =2, P>0.05). According to the characteristics of RAC, the *H. pylori* infection rates in the angular lesser curvature of the stomach and the greater curvature of the stomach were in descending order from the type I *H. pylori* infection group to the type II *H. pylori* infection group than the control group, and the differences were statistically significant (x^2 =200.39; 174.72; 143.51, P<0.01), as shown in Figure 3.

3.5. Different types of *Helicobacter pylori* infection in OLGA and OLGIM staging system

In the OLGA and OLGIM staging systems, the composition ratio of the type I *H. pylori* infection group, the type II *H. pylori* infection group, and the control group is shown in Figure 4. Specifically, the type I *H. pylori* infection group graded higher in the OLGA and OLGIM staging systems than those in the control group, and the differences were statistically significant (x^2 =95.45; 70.23, P<0.01). The type II *H. pylori* infection group graded higher in the OLGA and OLGIM staging systems than those in the control group, and the differences were statistically significant (x^2 =26.62; 30.05, P<0.01). The type I *H. pylori* infection group graded higher in the OLGA and OLGIM staging systems than those in the type II *H. pylori* infection group, and the differences were statistically significant only in the OLGA staging system (x^2 =10.63, P<0.05).

4. Discussion

Helicobacter pylori have a high intraspecific genetic diversity, and most studies have focused on the identification

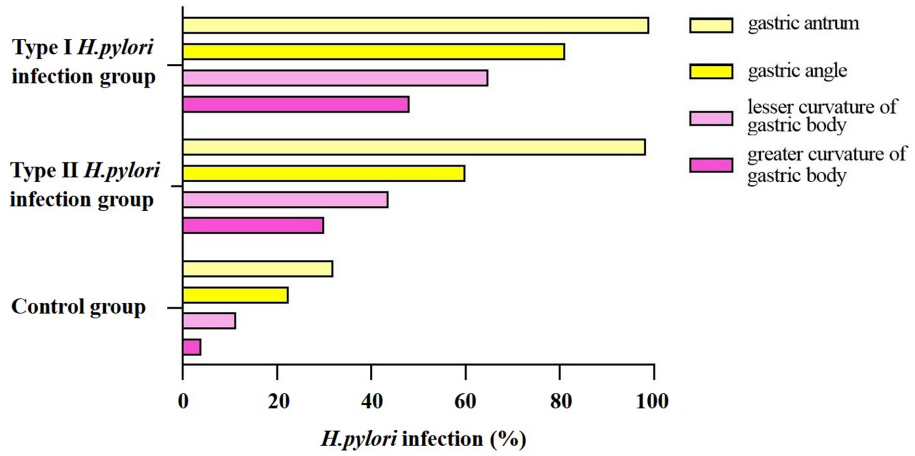

FIGURE 3
Distribution of different types of *Helicobacter pylori* infection in different parts of the stomach.

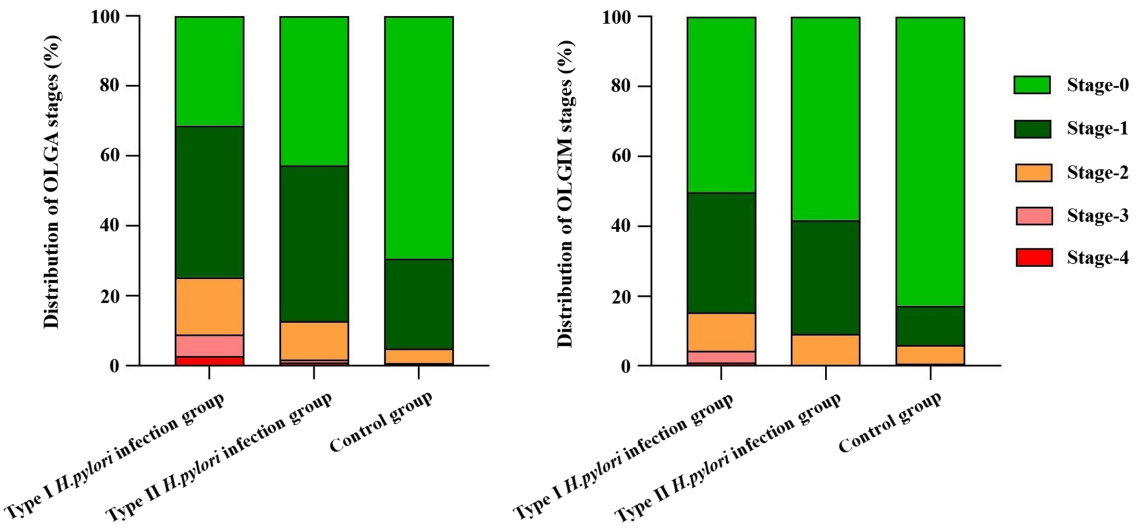

FIGURE 4
Different types of *Helicobacter pylori* infection in OLGA and OLGIM staging system.

of strain specificity related to gastric cancer (Tissera et al., 2022). The pathogenic mechanism of *H. pylori* may be related to many pathogenic factors of the bacteria, such as genes encoding outer membrane proteins (babA, oipA, sabA, and hopQ), exercise genes (flaA and flaB), and iceA, of which the CagA, VacA, activating protein A of peptic ulcer, and adhesins are particularly important (Da Costa et al., 2015). The CagA may interact with several host proteins after being transmitted to the cytoplasm, by either EPIYA phosphorylation-dependent or non-dependent, to regulate key cellular functions such as proliferation, apoptosis, inflammation, and genome integrity (Knorr et al., 2019; Kontizas et al., 2020). At present, clinical studies of type I *H. pylori* infection are closely related to the severity of many diseases, such as atrophic gastritis, ulcers, gastritis cancer, arteriosclerosis, and myasthenia gravis (El Khadir et al., 2021; Li et al., 2021; Wu and Chen, 2021). Atrophic gastritis is led by *H. pylori* infection and has a high risk of gastric cancer (Kato et al., 2019). Although eradication of *H. pylori* may reduce the risk of gastric cancer in the general population, nevertheless, it does exist and is associated with the degree of atrophy and intestinal metaplasia (Shibagaki et al., 2021). Specific *H. pylori* antibodies and CagA may act together on the progression of intestinal metaplasia in non-atrophic gastritis (Song et al., 2022). A large cohort of the study found an increased risk of cascade in patients positive for *H. pylori*, and they progressed from chronic gastritis to atrophic gastritis, eventually leading to intestinal metaplasia (Ohata et al., 2004). It takes about 10 years for atrophic gastritis to progress to

atrophy or intestinal metaplasia, but 11.6 years to atrophic gastritis and 11.4 years to intestinal metaplasia for 95% of those people in precancerous conditions (Kodama et al., 2012). At the age of 60 years, the gastric mucosa will undergo atrophy and intestinal metaplasia, and the eradication of *H. pylori* at the right time can slow down the atrophic gastritis process (Chey et al., 2017).

Pepsin is an inactive precursor of pepsin in gastric juice, which can be divided into PGI and PGII subpopulations according to their biochemical properties, immunogenicity, cell origin, and tissue distribution. The serum gastric function tests can be used as an index for gastric diseases (Chen et al., 2018; Yuan et al., 2020). The PGI is secreted by the principal cells of the gastricum and gastric fundus and the PGII is secreted by the pyloric gland, fundus gland, Brunner gland, and cardiac gland. The G-17 is secreted by the G cells of the antrum. Serum PGI, PGII, and G-17 levels are related to one's living habits, environment, *H. pylori* infection, sex, age, smoking, as well as alcohol consumption (Sjomina et al., 2018). The PGI, PGII, and G-17 levels are positively correlated with the activity and degree of inflammation of chronic gastritis in the antrum and gastricum, while PGR was negatively correlated with inflammation (Li et al., 2022). Serum PGI, PGII, PGR, and G-17 may indirectly reflect the secretory site of gastric mucosal lesions. To eliminate the influence of confounding factors on serum PGI, PGII, and G-17, we defined the nationality (Han Chinese) and age range (50–60 years). From the serological level, the PGI and PGII levels were significantly higher in the type I *H. pylori* infection group than those in the type II *H. pylori* infection group, which suggested that type I *H. pylori* infection may involve more extensive PGI and PGII cells (gastricum) in the stomach. The PGR level of the type I *H. pylori* infection group was significantly lower than those in the type II *H. pylori* infection group, which suggested that the type I *H. pylori* infection may have a high level of inflammatory activity. There was no significant difference in serum G-17 levels between the type I *H. pylori* infection group and the type II *H. pylori* infection group, which suggested that different types of *H. pylori* infection may have the same range of infection in the antrum. Serological studies suggested that the type I *H. pylori* infection may have a higher ability to cause atrophy and a larger infection range.

In 2005, the international atrophy research group proposed the OLGA staging system for chronic gastritis; and in 2010, the OLGIM staging system was proposed for intestinal metaplasia to replace atrophy. This is a semi-quantitative scoring method based on the updated Sydney system for chronic gastritis for inflammation and atrophy, which represents the range and degree of gastric mucosal atrophy (Capelle et al., 2010). In this study, to further explore if type I *H. pylori* infection has a higher ability to cause atrophy and a larger infection range or not, different types of *H. pylori* infection were analyzed to determine their ability to cause atrophy and infection range using pathology, non-magnification white light endoscopy combined with Kimura–Takemoto classification, and the absence of RAC (Ebigbo et al., 2021; Xiao et al., 2021). The type I *H. pylori* infection was graded higher than the type II *H. pylori* infection in the Kimura–Takemoto classification, which suggested that the type I *H. pylori* infection may be apt to cause atrophic lesions in the gastricum. Based on the lack of RAC, the type I *H. pylori* infection involved a wider loss of the gastricum than that in the type II *H. pylori* infection, suggesting that the type I *H. pylori* infection had a higher expression level in the gastricum. In the OLGA/OLGIM staging systems, the type I *H. pylori* infection graded higher than the type II *H. pylori* infection in the OLGA staging system, but no significant difference in the OLGIM staging system. The endoscopic and histopathologic data presented earlier provide us with more intuitive evidence. The type I *H. pylori* infection has a higher ability to cause atrophy and a larger infection range than that of the type II *H. pylori* infection, while the type II *H. pylori* infection is limited to the antrum with weaker atrophy progression (as shown in Figures 5, 6).

There are limitations to this study. First, this research did not conduct a prospective study, nor did include different ethnic groups, genders, and ages for follow-up study. Second, the identification of different types of *H. pylori* was determined only by ^{14}C-urea Breath Test and *H. pylori* antibody typing classification, lacking gene characteristic information. Third, although the characteristics of *H. pylori* with different virulence from clinical samples are supported by serum gastric function tests, pathological examinations, and endoscope detection, basic experimental verification is still lacking. Based on this, type II *H. pylori* is less toxic, and it causes a slow progression of gastric mucosa atrophy. The support of long-term clinical follow-up data is needed to determine whether asymptomatic patients with type II *H. pylori* infection need eradication therapy or not.

The virulence factors of *H. pylori* not only participate in the induction of inflammatory responses but also control and regulate these responses, maintain chronic inflammation, and most importantly facilitate the interaction among the host, gastric microenvironment, and bacterial virulence factors (Baj et al., 2020). At present, the cancer-promoting mechanism of the CagA protein has been revealed, and only with the earlier eradication of *H. pylori* can we prevent the occurrence of gastric cancer (Takahashi-Kanemitsu et al., 2020). While about 4.4 billion people worldwide have been infected with *H. pylori*, less than 20% of them have developed serious gastric problems and 1% of them have developed gastric cancer (Sharndama and Mba, 2022). Nowadays, numerous *H. pylori*-related guidelines recommend the national eradication of *H. pylori*; yet, there are still many countries that are under great pressure on public health, and eradicating *H. pylori* nationally may pose a potential risk of antibiotic abuse (Kato et al., 2019; Jung et al., 2021; National Clinical Research Center for Digestive Diseases (Shanghai) et al., 2021). Eradicating *H. pylori* infection is still controversial in inflammatory bowel disease, gastroesophageal reflux disease, asthma, and other diseases (He et al., 2022). Moreover, the benefits and risks of eradicating *H. pylori* vary among individuals

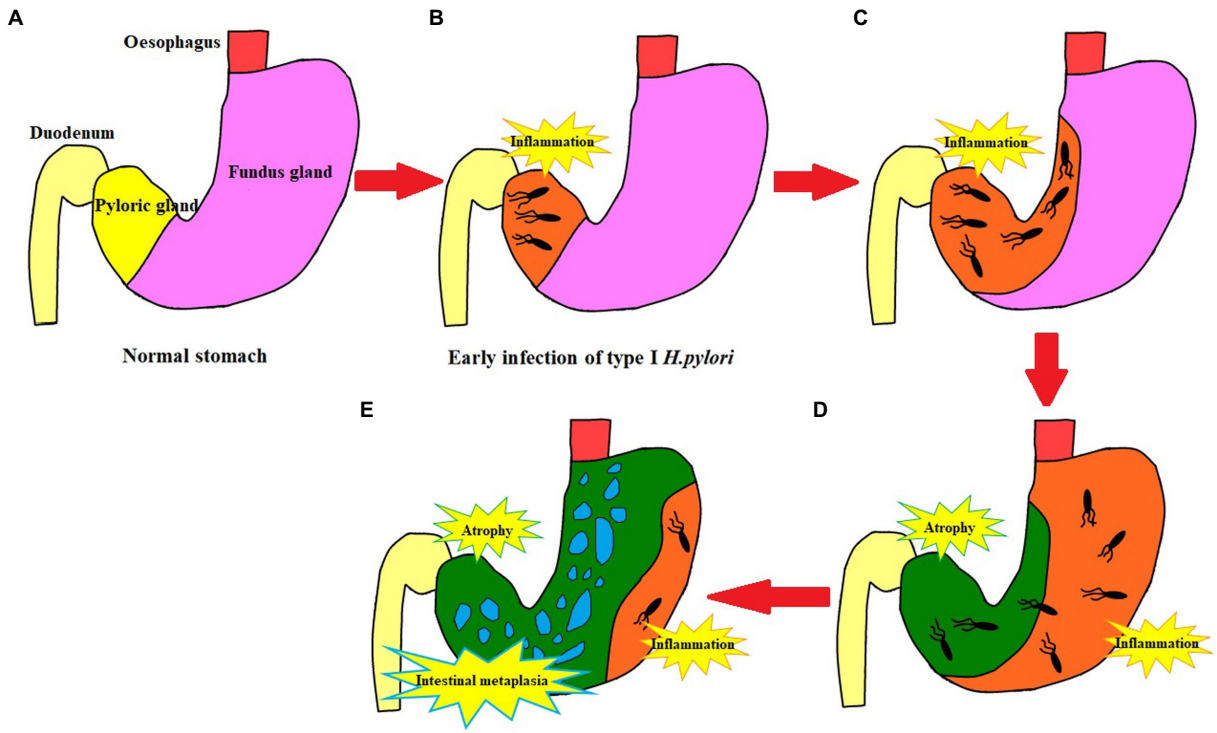

FIGURE 5
Schematic diagram of type I *H. pylori* infection. **(A)** Normal stomach structure. **(B)** The initial stage of type I *Helicobacter pylori* infection is limited to the gastric antrum. **(C)** Type I *H. pylori* infection progresses to the lesser curvature of the stomach. **(D)** Lesser curvature atrophy; Type I *H. pylori* infection extends from lesser curvature to greater curvature; Inflammation affects the whole stomach. **(E)** With the lesser curvature as the center, the atrophy extends to the periphery, accompanied by intestinal metaplasia and persistent active inflammation in the greater curvature.

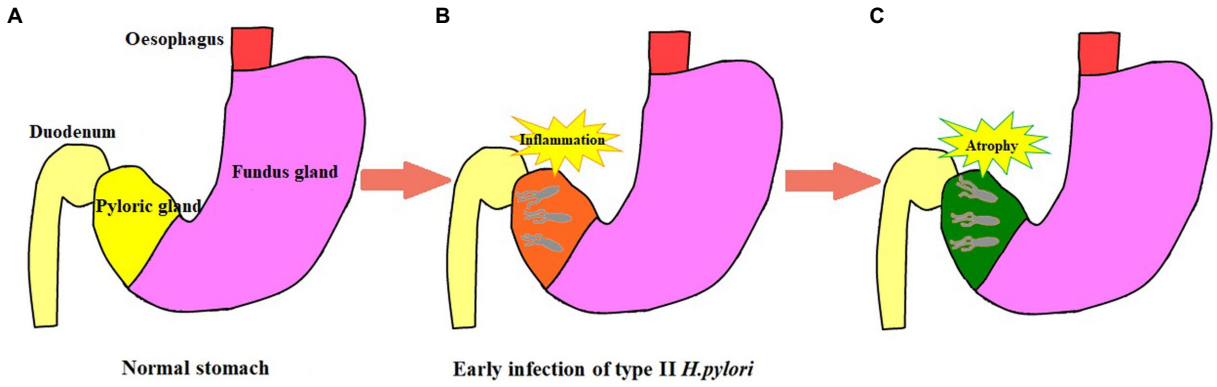

FIGURE 6
Schematic diagram of type II *H. pylori* infection. **(A)** Normal stomach structure. **(B)** The initial stage of type II *H. pylori* infection is limited to the gastric antrum. **(C)** Type II *H. pylori* infection in gastric antrum progresses to atrophy and it is difficult to advance to the stomach body.

(Helicobader pylori Study Group, Chinese Society of Gastroenterology, Chinese Medical Association, 2022). In addition, the virulence factor of *H. pylori* plays a key role in its pathogenicity, so individual virulence factor-based eradication therapy may be a better choice in future.

Data availability statement

The raw data supporting the conclusions of this article will be made available by the authors, without undue reservation.

Ethics statement

The studies involving human participants were reviewed and approved by Ethics Committee of People's Hospital of Xinjiang Uygur Autonomous Region. The patients/participants provided their written informed consent to participate in this study.

Author contributions

WL and WK: conceptualization, data analysis, and manuscript preparation. WH and QJ: data collection. CW, HS, and FG: critical manuscript review. All authors contributed to the article and approved the submitted version.

Funding

This study was sponsored by the Natural Science Foundation of Xinjiang Uygur Autonomous Region (2019D01C110).

Conflict of interest

The authors declare that the research was conducted in the absence of any commercial or financial relationships that could be construed as a potential conflict of interest.

Publisher's note

All claims expressed in this article are solely those of the authors and do not necessarily represent those of their affiliated organizations, or those of the publisher, the editors and the reviewers. Any product that may be evaluated in this article, or claim that may be made by its manufacturer, is not guaranteed or endorsed by the publisher.

Supplementary material

The Supplementary material for this article can be found online at: https://www.frontiersin.org/articles/10.3389/fmicb.2022.999564/full#supplementary-material

References

Baj, J., Forma, A., Sitarz, M., Portincasa, P., Garruti, G., Krasowska, D., et al. (2020). *Helicobacter pylori* virulence factors-mechanisms of bacterial pathogenicity in the gastric microenvironment. *Cells* 10:27. doi: 10.3390/cells10010027

Capelle, L. G., de Vries, A. C., Haringsma, J., ter Borg, F., de Vries, R. A., Bruno, M. J., et al. (2010). The staging of gastritis with the OLGA system by using intestinal metaplasia as an accurate alternative for atrophic gastritis. *Gastrointest. Endosc.* 71, 1150–1158. doi: 10.1016/j.gie.2009.12.029

Chen, X. Z., Huang, C. Z., Hu, W. X., Liu, Y., and Yao, X. Q. (2018). Gastric cancer screening by combined determination of serum *helicobacter pylori* antibody and pepsinogen concentrations: ABC method for gastric cancer screening. *Chin. Med. J.* 131, 1232–1239. doi: 10.4103/0366-6999.231512

Chey, W. D., Leontiadis, G. I., Howden, C. W., and Moss, S. F. (2017). ACG clinical guideline: treatment of *helicobacter pylori* infection. *Am. J. Gastroenterol.* 112, 212–239. doi: 10.1038/ajg.2016.563

Da Costa, D. M., Pereira Edos, S., and Rabenhorst, S. H. (2015). What exists beyond cagA and vacA? *Helicobacter pylori* genes in gastric diseases. *World J. Gastroenterol.* 21, 10563–10572. doi: 10.3748/wjg.v21.i37.10563

Ebigbo, A., Marienhagen, J., and Messmann, H. (2021). Regular arrangement of collecting venules and the Kimura-Takemoto classification for the endoscopic diagnosis of *helicobacter pylori* infection: evaluation in a western setting. *Dig. Endosc.* 33, 587–591. doi: 10.1111/den.13808

el Khadir, M., Boukhris, S. A., Zahir, S. O., Benajah, D. A. L. L. A. H., Ibrahimi, S. A., Chbani, L., et al. (2021). CagE, cagA and cagA 3′ region polymorphism of *helicobacter pylori* and their association with the intra-gastric diseases in Moroccan population. *Diagn. Microbiol. Infect. Dis.* 100:115372. doi: 10.1016/j.diagmicrobio.2021.115372

Ferreira, R. M., Machado, J. C., and Figueiredo, C. (2014). Clinical relevance of *Helicobacter pylori* vacA and cagA genotypes in gastric carcinoma. *Best Pract. Res. Clin. Gastroenterol.* 28, 1003–1015. doi: 10.1016/j.bpg.2014.09.004

He, J., Liu, Y., Ouyang, Q., Li, R., Li, J., Chen, W., et al. (2022). Helicobacter pylori and unignorable extragastric diseases: mechanism and implications. *Front. Microbiol.* 13:972777. doi: 10.3389/fmicb.2022.972777

Helicobader pylori Study Group, Chinese Society of Gastroenterology, Chinese Medical Association (2022). Sixth Chinese national consensus report on the management of helicobacter pylori infection (treatment excluded). *Chin. J. Dig.* 42, 289–303. doi: 10.3760/cma.j.cn311367-20220206-00057

Imai, S., Ooki, T., Murata-Kamiya, N., Komura, D., Tahmina, K., Wu, W., et al. (2021). *Helicobacter pylori* CagA elicits BRCAness to induce genome instability that may underlie bacterial gastric carcinogenesis. *Cell Host Microbe* 29, 941–958.e10. doi: 10.1016/j.chom.2021.04.006

Jung, H. K., Kang, S. J., Lee, Y. C., Yang, H. J., Park, S. Y., Shin, C. M., et al. (2021). Evidence-based guidelines for the treatment of *helicobacter pylori* infection in Korea 2020. *Gut Liver* 15, 168–195. doi: 10.5009/gnl20288

Kato, M., Ota, H., Okuda, M., Kikuchi, S., Satoh, K., Shimoyama, T., et al. (2019). Guidelines for the management of *helicobacter pylori* infection in Japan: 2016 revised edition. *Helicobacter* 24:e12597. doi: 10.1111/hel.12597

Knorr, J., Ricci, V., Hatakeyama, M., and Backert, S. (2019). Classification of *Helicobacter pylori* virulence factors: is CagA a toxin or not? *Trends Microbiol.* 27, 731–738. doi: 10.1016/j.tim.2019.04.010

Kodama, M., Murakami, K., Okimoto, T., Sato, R., Uchida, M., Abe, T., et al. (2012). Ten-year prospective follow-up of histological changes at fve points on the gastric mucosa as recommended by the updated Sydney system afer helicobacter pylori eradication. *J. Gastroenterol.* 47, 394–403. doi: 10.1007/s00535-011-0504-9

Kontizas, E., Tastsoglou, S., Karamitros, T., Karayiannis, Y., Kollia, P., Hatzigeorgiou, A. G., et al. (2020). Impact of *helicobacter pylori* infection and its major virulence factor CagA on DNA damage repair. *Microorganisms* 8:2007. doi: 10.3390/microorganisms8122007

Lee, D. H., Ha, J. H., Shin, J. I., Kim, K. M., Choi, J. G., Park, S., et al. (2021). Increased risk of severe gastric symptoms by virulence factors vacAs1c, alpA, babA2, and hopZ in *Helicobacter pylori* infection. *J. Microbiol. Biotechnol.* 31, 368–379. doi: 10.4014/jmb.2101.01023

Li, X., Feng, M., and Yuan, G. (2022). Clinical efficacy of Weisu granule combined with Weifuchun tablet in the treatment of chronic atrophic gastritis and its effect on serum G-17, PG I and PG II levels. *Am. J. Transl. Res.* 14, 275–284. PMID: 35173844

Li, B. W., Liu, Y., Zhang, L., Guo, X. Q., Wen, C., Zhang, F., et al. (2021). Cytotoxin-associated gene a (CagA) promotes aortic endothelial inflammation and accelerates atherosclerosis through the NLRP3/caspase-1/IL-1β axis. *FASEB J.* 35:e21942. doi: 10.1096/fj.202100695RR

Liu, W., Tian, J., Hui, W., Kong, W., Feng, Y., Si, J., et al. (2021). A retrospective study assessing the acceleration effect of type I *helicobacter pylori* infection on the progress of atrophic gastritis. *Sci. Rep.* 11:4143. doi: 10.1038/s41598-021-83647-6

National Clinical Research Center for Digestive Diseases (Shanghai), Astrointestinal Early Cancer Prevention & Treatment Alliance of China, and Helicobacter pylori and Peptic Ulcer roup of Chinese Society of Gastroenterology (2021). Chinese consensus on family based-*helicobacter pylori* infection control and management. *Chin. J. Dig.* 41, 221–233.

Ohata, H., Kitauchi, S., Yoshimura, N., Mugitani, K., Iwane, M., Nakamura, H., et al. (2004). Progression of chronic atrophic gastritis associated with *helicobacter pylori* infection increases risk of gastric cancer. *Int. J. Cancer* 109, 138–143. doi: 10.1002/ijc.11680

Sharndama, H. C., and Mba, I. E. (2022). *Helicobacter pylori*: an up-to-date overview on the virulence and pathogenesis mechanisms. *Braz. J. Microbiol.* 53, 33–50. doi: 10.1007/s42770-021-00675-0

Shibagaki, K., Itawaki, A., Miyaoka, Y., Kishimoto, K., Takahashi, Y., Kotani, S., et al. (2021). Intestinal-type gastric dysplasia in *helicobacter pylori*-naïve patients. *Virchows Arch.* 480, 783–792. doi: 10.1007/s00428-021-03237-9

Sjomina, O., Pavlova, J., Daugule, I., Janovic, P., Kikuste, I., Vanags, A., et al. (2018). Pepsinogen test for the evaluation of precancerous changes in gastric mucosa: a population-based study. *J. Gastrointest. Liver Dis.* 27, 11–17. doi: 10.15403/jgld.2014.1121.271.pep

Smith, S., Boyle, B., Brennan, D., Buckley, M., Crotty, P., Doyle, M., et al. (2017). The Irish *helicobacter pylori* working group consensus for the diagnosis and treatment of H. pylori infection in adult patients in Ireland. *Eur. J. Gastroenterol. Hepatol.* 29, 552–559. doi: 10.1097/MEG.0000000000000822

Song, L., Song, M., Rabkin, C. S., Chung, Y., Williams, S., Torres, J., et al. (2022). Identification of anti-helicobacter pylori antibody signatures in gastric intestinal metaplasia. *J. Gastroenterol.*, 1–13. doi: 10.1007/s00535-022-01933-0

Sugano, K., Tack, J., Kuipers, J. E., Graham, D. Y., El-Omar, E. M., Miura, S., et al. (2015). Kyoto global consensus report on *helicobacter pylori* gastritis. *Gut* 64, 1353–1367. doi: 10.1136/gutjnl-2015-309252

Takahashi-Kanemitsu, A., Knight, C. T., and Hatakeyama, M. (2020). Molecular anatomy and pathogenic actions of *helicobacter pylori* CagA that underpin gastric carcinogenesis. *Cell. Mol. Immunol.* 17, 50–63. doi: 10.1038/s41423-019-0339-5

Tissera, K., Kim, M. A., Lai, J., Angulmaduwa, S., Kim, A., Merrell, D. S., et al. (2022). Characterization of east-Asian *helicobacter pylori* encoding Western EPIYA-ABC CagA. *J. Microbiol.* 60, 207–214. doi: 10.1007/s12275-022-1483-7

Wu, S. E., and Chen, W. L. (2021). Detrimental relevance of *helicobacter pylori* infection with sarcopenia. *Gut Pathog.* 13:67. doi: 10.1186/s13099-021-00464-y

Xiao, S., Fan, Y., Yin, Z., and Zhou, L. (2021). Endoscopic grading of gastric atrophy on risk assessment of gastric neoplasia: a systematic review and meta-analysis. *J. Gastroenterol. Hepatol.* 36, 55–63. doi: 10.1111/jgh.15177

Yuan, L., Zhao, J. B., Zhou, Y. L., Qi, Y. B., Guo, Q. Y., Zhang, H. H., et al. (2020). Type I and type II *helicobacter pylori* infection status and their impact on gastrin and pepsinogen level in a gastric cancer prevalent area. *World J. Gastroenterol.* 26, 3673–3685. doi: 10.3748/wjg.v26.i25.3673

Zhang, X., Li, C., Chen, D., He, X. F., Zhao, Y., Bao, L. Y., et al. (2022). H. Pylori CagA activates the NLRP3 inflammasome to promote gastric cancer cell migration and invasion. *Inflamm. Res.* 71, 141–155. doi: 10.1007/s00011-021-01522-6

frontiers | Frontiers in Microbiology

TYPE Original Research
PUBLISHED 09 February 2023
DOI 10.3389/fmicb.2023.1083330

OPEN ACCESS

EDITED BY
Zhongming Ge,
Massachusetts Institute of Technology,
United States

REVIEWED BY
Norma Velazquez-Guadarrama,
Federico Gómez Children's Hospital, Mexico
Utkarsh Jain,
Amity University,
India

*CORRESPONDENCE
Mohammad Hossein Haddadi
✉ haddadi-m@medilam.ac.ir;
✉ haddadi841@gmail.com

SPECIALTY SECTION
This article was submitted to Infectious Agents and Disease, a section of the journal Frontiers in Microbiology

RECEIVED 16 November 2022
ACCEPTED 24 January 2023
PUBLISHED 09 February 2023

CITATION
Khoshnood S, Negahdari B, Kaviar VH, Sadeghifard N, Abdullah MA, El-Shazly M and Haddadi MH (2023) Amoxicillin-docosahexaenoic acid encapsulated chitosan-alginate nanoparticles as a delivery system with enhanced biocidal activities against *Helicobacter pylori* and improved ulcer healing. *Front. Microbiol.* 14:1083330. doi: 10.3389/fmicb.2023.1083330

Amoxicillin-docosahexaenoic acid encapsulated chitosan-alginate nanoparticles as a delivery system with enhanced biocidal activities against *Helicobacter pylori* and improved ulcer healing

Saeed Khoshnood[1], Babak Negahdari[2], Vahab Hassan Kaviar[1], Nourkhoda Sadeghifard[1], Mohd Azmuddin Abdullah[3], Mohamed El-Shazly[4] and Mohammad Hossein Haddadi[1]*

[1]Clinical Microbiology Research Centre, Ilam University of Medical Sciences, Ilam, Iran, [2]Department of Medical Biotechnology, School of Advanced Technologies in Medicine, Tehran University of Medical Sciences, Tehran, Iran, [3]Department of Toxicology, Advanced Medical and Dental Institute, Universiti Sains Malaysia, Penang, Malaysia, [4]Department of Pharmacognosy, Faculty of Pharmacy, Ain-Shams University, Cairo, Egypt

Encapsulation of amoxicillin (AMX) for drug delivery against *Helicobacter pylori* infection and aspirin-induced ulcers in rat's stomachs was performed using docosahexaenoic acid (DHA)-loaded chitosan/alginate (CA) nanoparticles (NPs) developed by ionotropic gelation method. The physicochemical analyses of the composite NPs were performed by scanning electron microscopy, Fourier transform infrared spectroscopy, zeta potential, X-ray diffraction, and atomic force microscopy. The encapsulation efficiency of AMX was increased to 76% by incorporating DHA, which resulted in a reduction in the particle size. The formed CA-DHA-AMX NPs effectively adhered to the bacteria and rat gastric mucosa. Their antibacterial properties were more potent than those of the single AMX and CA-DHA NPs as demonstrated by the *in vivo* assay. The composite NPs attained higher mucoadhesive potential during food intake than during fasting ($p = 0.029$). At 10 and 20 mg/kg AMX, the CA-AMX-DHA showed more potent activities against *H. pylori* than the CA-AMX, CA-DHA, and single AMX. The *in vivo* study showed that the effective dose of AMX was lower when DHA was included, indicating better drug delivery and stability of the encapsulated AMX. Both mucosal thickening and ulcer index were significantly higher in the groups receiving CA-DHA-AMX than in the groups receiving CA-AMX and single AMX. The presence of DHA declines the pro-inflammatory cytokines including IL-1β, IL-6, and IL-17A. The synergistic effects of AMX and the CA-DHA formulation increased the biocidal activities against *H. pylori* infection and improved ulcer healing properties.

KEYWORDS

chitosan-DHA nanoparticles, *Helicobacter pylori*, biocidal activities, amoxicillin, encapsulation, chitosan, docosahexaenoic

Introduction

Stomach infection with *Helicobacter pylori*, a Gram-negative bacterium with carcinogenic potential, is a major cause of gastric malignancies such as MALT lymphoma and gastric adenocarcinoma (Kim and Wang, 2021). Successful *H. pylori* eradication could reduce the risk of metachronous gastric cancer by 50% (Choi et al., 2020). In the majority of cases (89.4%), the first line of treatment against *H. pylori* infection is clarithromycin (CLA) and amoxicillin (AMX) or metronidazole (MET) in combination with a proton pump inhibitor (PPI) (Suzuki and Matsuzaki, 2018). However, antibiotic resistance emerged in recent years and gastric acid was found to inactivate some antibacterial agents (Qin et al., 2021). As the clinical isolates of *H. pylori* have become increasingly resistant to antibiotics worldwide, there is an urgent need to improve therapeutic strategies with more effective antibiotic regimens to reduce treatment failures (Krzyżek et al., 2020).

H. pylori showed resistance to MET and CLA and a less degree to AMX (Graham et al., 2021). Therefore, AMX is considered the most reliable antibiotic therapy in almost all regimens (Kuo et al., 2021). Stomach acid however can decompose and destroy AMX, reducing its overall and local effectiveness. There are two approaches to overcome this limitation including intravenous administration for at least 7 days or the oral administration of high doses of AMX (Shah et al., 2021). The use of nanopolymers such as chitosan to encapsulate acid-sensitive drugs could protect AMX from degradation by gastric acid, prolong their retention/residence time, and improve its controlled release (Spósito et al., 2021). Chitosan is a cationic mucoadhesive biopolymer, and based on molecular weight (MW), can be divided into high, medium, and low MW, each having different biological properties. High MW chitosan containing high degrees of deacetylation is superior to low MW chitosan for the treatment of *H. pylori*. Moreover, chitosan exhibited more potent antibacterial activity against Gram-negative bacteria than Gram-positive bacteria and this effect was attributed to the stronger negative charge on the cell walls of the Gram-negative bacteria (Takahashi et al., 2008; Li et al., 2016; Chang et al., 2020).

Fatty acids (FAs) that exhibit antibacterial activity against multidrug-resistant (MDR) bacteria could provide the next generation of antibacterial agents for the treatment and prevention of bacterial infections (Coraça-Huber et al., 2021). A combination of FAs and antibiotics was tested suggesting their potential application in the treatment of bacterial resistance. The combination of FAs with beta-lactam antibiotics, fluoroquinolones, and aminoglycosides showed a synergistic effect against Gram-positive and Gram-negative bacteria (Casillas-Vargas et al., 2021). Docosahexaenoic acid (DHA) is one of the omega-3 polyunsaturated fatty acids (PUFAs) with anti-inflammatory and anti-*H. pylori* properties. In the presence of DHA, *H. pylori* expand its periplasmic space, resulting in the loss of membrane integrity, cytoplasmic leakage, and cell death (Correia et al., 2012). To date, there is only one report addressing the anti-*H. pylori* activity of the encapsulated DHA when administered through nanostructured lipid carriers (Seabra et al., 2017). Chitosan-based nanoparticles (NPs) possess mucoadhesive properties rendering them interesting candidates to be tested as enhancers of the antibacterial effect of AMX and DHA. The present study aimed to develop a chitosan-based oral drug delivery system containing DHA and AMX against *H. pylori*, both *in vitro* and *in vivo*. Chitosan/alginate (CA) composite NPs were used to entrap AMX and DHA. The physicochemical characterizations of the NPs were assessed. The antibacterial activity was determined using an *in vitro* growth inhibition assay, followed by the evaluation of the mucoadhesive potential of the FITC-labeled NPs. In the *in vivo* experiments, an aspirin-induced gastric ulcer was induced in rats and the rats were infected with *H. pylori*. To determine the biocidal effects against *H. pylori* and the curing effect of the composite NPs on the induced ulcer, the *H. pylori* colonization, ulcer area, and histopathological changes were monitored.

Materials and methods

In the Supplementary material, more details are provided regarding the materials and methods used in this study. The materials are described in the Supplementary section 1.

Fabrication of composite NPs and formulation

A CA-based NP was prepared based on a previous study by Friedman et al. (2013). Composite NPs were prepared by emulsifying a chitosan solution in an oil phase (DHA) and an ionic gelation method. Chitosan and alginate solutions were prepared as polycationic and polyanionic solutions (Supplementary section 2).

CA-DHA NPs were prepared in several formulations including chitosan (0.1, 0.5, and 1.0% v/v), DHA (0.0, 0.5, 1.5, and 2.0% v/v), and AMX (40, 60, and 100 mg/ml). The *in vivo* study was conducted to test CA-DHA, CA-AMX, and CA-DHA-AMX NPs with the following concentrations of the components: CA (1.0% v/v), DHA (2.0% v/v), and AMX at two concentrations (10 and 20 mg/kg).

Physicochemical characteristics

The physicochemical properties of the composite NPs were evaluated using a scanning electron microscope (SEM), Fourier transforms infrared spectroscopy (FTIR), X-ray diffraction (XRD), atomic force microscopy (AFM), zeta potential, and swelling index (SI) analysis, and the methods are described in detail in Supplementary section 3.

Drug content

The content of DHA and AMX in the recovered solution was measured using a UV/Vis spectrophotometer (JENWAY/6105) at 205 and 272 nm, respectively. To compare the loading of AMX with the hydrophobic and hydrophilic compounds, it was tested in the emulsion and aqueous environments. A detailed explanation of the method used to determine the drug content can be found at Supplementary section 3.

Antibacterial activity

The growth inhibitory assay was used to determine the antibacterial activity against clinically isolated *H. pylori* (H.12.5) *in vitro*. Briefly, 10 µl of the bacterial suspension (10^9 CFU/ml) was added to Columbia broth medium (190 µl) and the mixture was incubated under microaerophilic conditions for 6, 12, and 24 h. The growth inhibition assay was performed *in vitro*. Growth inhibition was estimated from the

absorbance of the medium at a wavelength of 600 nm. Supplementary section 4 describes the patient's details, the method of bacterial isolation, the *in vitro* antibacterial assay, and the formula for growth inhibition. To evaluate antibacterial activity *in vivo*, plate colony counts (CFU/gr stomach) and the number of bacteria in the biopsy samples were used (Supplementary section 4).

Bacterial binding and mucoadhesive activity

Bacterial adhesion was measured using FITC-labeled composite NPs (Supplementary section 5). The adhesion was determined by flow cytometry and was subsequently analyzed using the FlowJo program (Tree Star). The bacterial binding and mucoadhesive activity were conducted on the four composite NPs including unloaded NPs, CA-DHA with three different DHA concentrations, CA-AMX, and CA-DHA-AMX. The adhesion rate of NPs to the bacterial cell surface was determined at 2 and 4 h intervals.

The mucoadhesive activity was evaluated using the count method according to the previous method of Arora et al. on rat stomachs (Arora et al., 2011). The mucoadhesive potential of NPs was calculated by fluorescence microscopy using the following formula:

$$\text{Mucoadhesive}\% = \frac{(\text{Cs} - \text{Cd})}{\text{Cd}} \times 100$$

The input and output counts of NPs are represented by "Cs" and "Cd," respectively.

The *in vivo* study was performed with NPs on the mucosa in two different nutritional states including the fasting and fed states. ImageJ v1.52 software (NIH, United States) was used to calculate the fluorescence intensity of the adherent FITC-labeled NPs.

Animals

One hundred forty-seven male Sprague Dawley rats were involved in this study. Six rats were lost during infection and ulcer induction. Eighteen stomachs from rats were used to evaluate the *in vitro* mucoadhesive study. *In vivo* mucoadhesive activity was performed for two main feeding conditions: fasting and fed. Each of the two groups consisted of four different sub-groups (CA, CA-DHA, CA-AMX, and CA-DHA-AMX). A total of 24 rats were used to determine the mucoadhesive potential *in vivo*.

In the infected groups, rats were fasted overnight before being treated with 250 mg/kg body weight (BW) acetylsalicylic acid (ASA) on day 0 to induce gastric ulcers. Bacterial infection was induced by oral administration of *H. pylori* (5×10^8–10 CFU/ml, 1 ml/rat) at 24, 48, and 72 h after ASA ulceration. Infection was confirmed after 2 weeks, and treatment was initiated. Three rats were used to confirm *H. pylori* colonization and three rats were used for the gastric ulcer confirmation. The *in vivo* antibacterial activity of different formulations was assessed in thirty rats divided into ten groups at day 7 post-infection (Supplementary Tables S1, S2).

The *in vivo* studies were performed to investigate the ulcer healing activity by macroscopic and microscopic analysis of gastric ulcers by ulcer thickness, ulcer area, ulcer index, and *H. pylori* eradication was also determined by the direct bacterial counting method. Collagen accumulation and concentrations of inflammatory cytokines, including IL-1β, IL-6, and IL-17A, were determined in the treated and untreated groups on day 14 post-infection. Forty-two rats were randomly divided into seven groups (six rats/group); group 1 (NS, normal saline), groups 2 and 3: AMX (powder 10 and 20 mg/kg WB), groups 4 and 5: CA-AMX (10 and 20 mg/kg WB), and groups 6 and 7: CA-DHA-AMX (10 and 20 mg/kg WB) to evaluate ulcer healing and *H. pylori* eradication on day 14. Eighteen rats were divided into six treated groups to evaluate the relapse of infection on day 21 post-infection (three rats/group). One uninfected group was defined as control ($n = 3$).

We performed a histopathological examination on gastric biopsies. The ulcer evaluation was done on the whole stomach on day 14 to assess the healing effect. Ulcer indexing was performed according to the previous study by Bhattacharya et al. (2006). To measure the ulcer area, the length and thickness of the ulcer in mm^2 were measured at a magnification of 40× and the information was processed using IimageJ software. The area of the gastric ulcer in each section (5 sections/sample) was determined. Gastric histology was evaluated by 1 pathologist who was blinded to the other assays and results.

All animal experiments were performed according to accordance with the U.K. Animals (Scientific Procedures) Act, and protocol approved by the Ethics Committee of Ilam Medical University (approval number: R.MEDILAM. REC.1400.133).

Enzyme-linked immunosorbent assay

A whole blood sample was taken from the rats. The presence of IL-1β, IL-6, and IL-17A in serum was measured using ELISA kits according to the manufacturer's instructions. The intensity was determined at 450 nm using a microplate reader. To ensure consistency of the assay, all plates contained positive control (FBS) and negative control (PBS) samples.

Masson's trichrome staining and immunohistochemistry

Masson's trichrome staining, which stains collagen fibers blue and faint green, was used to assess collagen accumulation. Naturally, collagen fibers are usually accumulated in the gastric mucosa and submucosa. Immunohistochemistry was performed using antibodies against type I collagen. Sections were incubated with 0.3% hydrogen peroxide in PBS for 30 min and then with 10% normal donkey or goat serum in 0.05 M PBS for 30 min. They were then incubated with polyclonal antibodies labeling collagen I. Each sample was imaged using a Nikon TE 2000 fluorescence microscope (Nikon, Japan). The area of collagen in each section was measured using ImageJ software.

Statistical analysis

The obtained results were statistically analyzed using Mann–Whitney's *t*-test with a confidence level of 95% ($p < 0.05$). Statistical analysis was performed using the Wilcoxon Sum Rank test for the ulcer index. Differences between means were tested for more than two groups with a one-way analysis of variance (ANOVA) followed by a Bonferroni's *post-hoc* test. Differences between groups and time points were analyzed with a two-way analysis of variance (ANOVA) and subsequent multiple

comparisons using the Bonferroni correction. *$p < 0.05$; **$p < 0.001$; ***$p = 0.0002$; and ****$p < 0.0001$ indicated statistically significant results.

Results and discussion

Composite nanoparticle production

This study showed that the NPs were formed by the interactions between the positively charged amino groups of the polycationic agent (chitosan) and the negatively charged polyanionic agent (alginate). Based on the strong mucoadhesive properties of CA NPs (Chang et al., 2021), we developed a CA-based NP containing DHA and AMX to test their ulcer healing and *H. pylori* eradication properties. Based on the *in vitro* results, we tested the physicochemical properties of CA-DHA-AMX at the defined concentrations of 1% v/v, 2% v/v, and 60 mg/ml, respectively.

As demonstrated by SEM and FAM, the composite nanoparticles with DHA produced smaller NPs (350 ± 110 nm) with a smoother surface than the DHA-free NPs (600 ± 92 nm) in a concentration-dependent manner. Their spherical shape is due to a hydrophobic group (DHA) in their structure. NPs with smaller sizes were obtained during the oil-in-water micelle structure, resulting in a homogeneous dispersion of DHA (Figure 1A).

FTIR spectra of the composite NP CA-DHA-AMX and their components are shown in Figure 1B. The CA-DHA showed a significantly intensified peak at 1679 cm^{-1}, while the peaks of the amino group at 1596 cm^{-1} and carboxyl groups at 1619 cm^{-1} disappeared. An ionic interaction was confirmed between the carboxyl group of the alginates and the amino group of chitosan. The new major peak at 1750 cm^{-1} showed a significant increase in absorption confirming the presence of DHA in CA-based scaffolds. AMX major peaks were observed at 3,440 cm^{-1} (amide NH and phenol OH stretch), 3,020 cm^{-1} (benzene ring C-H stretch), 1,770 cm^{-1} (beta-lactam C-O stretch), 1,680 cm^{-1} (amide I C-O stretch), 1,500 cm^{-1} (benzene ring C-C stretch), and 1,480 cm^{-1} (N-H bend C-N stretch combination band). Characteristic peaks of AMX were also present in the FTIR spectrum of the composite beads with some broadening and reduction in intensity, indicating the absence of the chemical interactions between the drug, polymer, and counter ions after the formation of beads.

As shown in Figure 1C, the pattern of chitosan showed two wide typical diffraction peaks at 2θ = 13.5° and 25.5°, confirming the semicrystalline nature of this molecule, which are the hydrated and anhydrous polymorphs of chitosan, respectively. The XRD spectrum of alginate showed a typical wide crystalline peak at 2θ = 21.5°. No crystalline peak was observed for DHA. The peaks of chitosan and alginate disappeared, and two new peaks appeared at 2θ = 23.4° and 27.5° in the XRD spectrum of the CA-DHA scaffold, confirming the presence of DHA in the structure of the new scaffold. Strong interactions between the chitosan amino groups and the alginate cation groups were related to the changes in the membrane crystallinity. The ionic interaction between chitosan and alginate significantly decreased the crystallinity of the scaffold, indicating its amorphous state (Cui et al., 2008).

AFM analysis revealed that the synthesized NPs were almost monodisperse, without agglomeration (Figures 1D,E). Evidence suggested that particle aggregation decreased in the presence of hydrophobic agents (Dixon et al., 2012; Chang et al., 2021). In this study, the presence of DHA in CA-DHA formulations resulted in the reduction of particle aggregation. The particle size distribution was more homogeneous in the presence of 100 μM DHA than for the unloaded NPs. The variation of the zeta potential of the composite NPs was mainly due to the negative charge of the NP-loaded polymers. Compared with CA-DHA, the unloaded NPs exhibited a more positive charge, supporting the presence of the charged DHA in the NPs. The surface charges of the composite NPs were directly affected by the pH changes

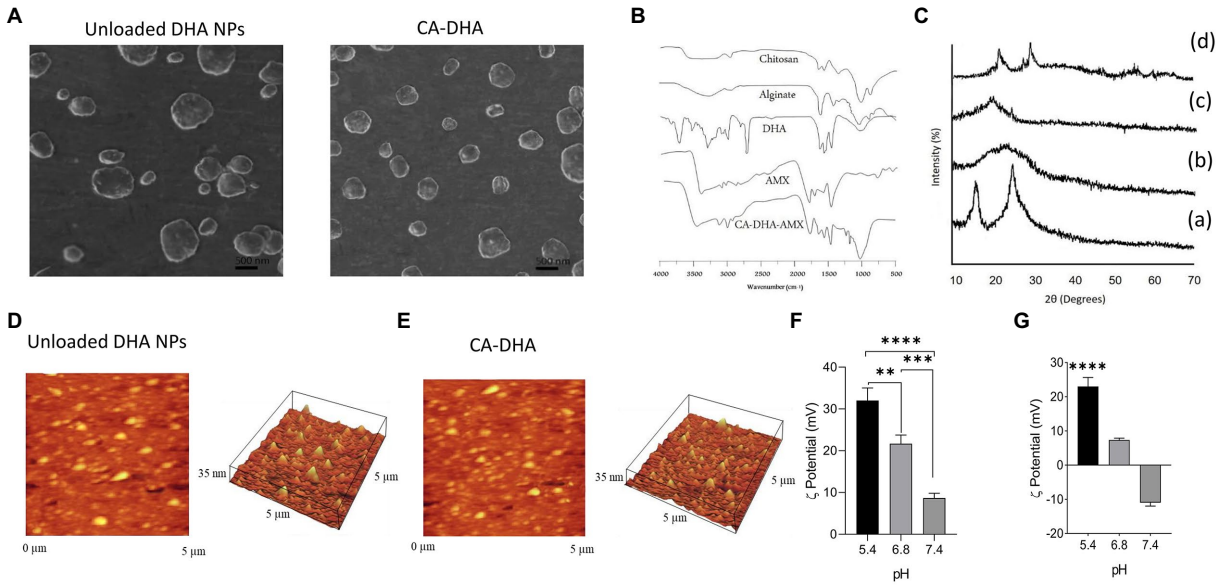

FIGURE 1
Physicochemical properties of CA-based NPs. **(A)** SEM micrograph of CA NPs and CA-DHA-AMX NPs (CA=1%, DHA=100μM, 2% v/v, and AMX=60mg/ml). **(B)** FTIR spectra of chitosan, alginate, DHA (100μM), AMX, and CA-DHA-AMX NP. **(C)** XRD patterns of chitosan (a), alginate (b), DHA (c), and CA-DHA (d). **(D,E)** AFM analysis of the surface topography of the unloaded and DHA-loaded NPs. **(F,G)** Zeta potentials of unloaded and DHA-loaded NPs (2% v/v) at various pH levels.

in the dispersion medium, and the highest value was observed at pH 5.4 (Figures 1F,G).

In a composite polymer, swelling occurs due to water absorption, causing the NPs to expand during water penetration, which leads to an increased crosslinking of the composite polymers (Pacheco et al., 2019). DHA concentration, the acidity of the medium, and time exhibit a direct effect on the rate of water uptake by NPs. The protonation of the carboxylic groups of the alginate increased at an acidic pH (pH < 4), resulting in shrinkage of the polymer due to the reduction of electrostatic repulsion between these hydrophobic groups (Rahaiee et al., 2017). This study showed a satisfactory correlation between the swelling indexes, is decreased by the addition of an extra hydrophobic group such as DHA (Supplementary Figure S1). A favorable agreement was observed in comparison with a previous study by Chang et al. who reported that the hydrophobicity of cobia liver oil (CBLO) decreased the swelling and aggregation of chitosan resulting in smaller particle size (Chang et al., 2021). At all pH, composite NPs were soluble after a 6 h adjustment (data not shown).

An influential factor that affects the effectiveness of drug encapsulation is the effectiveness of drug entrapment. The drug entrapment efficacy of DHA and AMX was also evaluated in the same way as shown in Table 1. The highest drug content was obtained at pH 5.4 in the chitosan solution, 65 ± 4% and 71 ± 1.9% for DHA and AMX, respectively. Also, when DHA was included in the CA-DHA-AMX formulation, the drug content increased.

Antibacterial activity

Previous reports indicated that DHA exhibited a potent antibacterial effect on *H. pylori* and inhibited its colonization in animal models (Correia et al., 2012; Ji et al., 2016; Henriques et al., 2020). In this study, the unloaded NPs with a chitosan concentration of 1.0% exhibited higher antibacterial activity than the NPs at other concentrations ($p < 0001$; Geisser–Greenhouse's epsilon = 0.510; Figure 2A). This result supported the findings of Luo et al. who reported that a high degree of deacetylation (95%) of chitosan exhibited stronger antibacterial activity than deacetylation of 88% (Luo et al., 2009). In our study, the antibacterial activity of DHA was the highest at 100 μM (Figure 2B). We formulated CA-DHA at a concentration of 1.0% v/v CA and three different concentrations of DHA, including 1, 1.5, and 2% v/v. The bacterial growth was strongly suppressed at 2% v/v DHA (Figure 2C).

Previous results showed that the encapsulation of DHA increased its antibacterial activity. To improve the antibacterial efficacy against *H. pylori*, previous research examined the nanoencapsulation of DHA alone (Seabra et al., 2017). In this study, DHA and AMX were incorporated into CA-based NPs to maximize drug delivery and reduce antibiotic concentration. The results showed that CA-DHA with 2% v/v DHA significantly increased the growth inhibition rates compared with the unloaded NPs ($p = 0.013$) (Figure 3A). According to previous studies, DHA-loaded NPs showed bactericidal activity against *H. pylori* but not against human gastric adenocarcinoma cells at bactericidal concentrations (Chang et al., 2020; Henriques et al., 2020). We also observed a significant difference between the two concentrations of DHA (1.5 and 2% v/v; $p < 0.0001$). Therefore, we examined the composite NPs with 2% v/v DHA. CA-DHA-AMX proved to be more effective against bacteria when the dose of AMX was increased (Figure 3A). Thus, we conducted further studies with the following formulation: CA (1% v/v)- DHA (2% v/v)-AMX (60 mg/ml). After 6 h of incubation, it was found that the composite NP exhibited a synergistic antibacterial effect when DHA and AMX were used together (Figure 3B). Despite the significantly higher antibacterial activity of CA-AMX NPs than CA-DHA NPs ($p = 0.0042$), the presence of DHA in the CA-DHA-AMX formulation significantly increased antibacterial activity ($p = 0.0009$) (Figure 3B).

After a diet, the pH of the stomach changes within 4–6 h. The acidity of the stomach is 2.5 during starvation, while it increases to 3.0–4.5 during feeding (Chen et al., 2008). Potent antibacterial activity was observed in CA-DHA-AMX at pH 4 (Figure 3C). Hu et al. reported that the antibacterial activity of chitosan decreased at pH > 5.8 (Hu et al., 2007). Among the tested groups, CA-DHA-AMX showed minimal growth activity, probably due to AMX and DHA. The low antibacterial activity in an acidic medium arises from the degradation of AMX, while at pH 7.0, only a small amount of the active ingredient is released from the NPs. Our study was conducted to determine how much of the active ingredient is released after 6 h at different pH values. The release of AMX and DHA at pH 4.0 was comparable to the release at pH 2.5, but the release at pH 7.0 was significantly less than the release at pH 4.0 (pH 4.0 vs. 7.0; $p = 0.029$ and > 0.001 for the release of AMX and DHA, respectively) (Figure 3D).

Compared with DHA, both CA-DHA and pure chitosan showed higher antibacterial activity *in vivo*. This suggested that the antibacterial properties of NPs may be derived from their chitosan coating ($p = 0.04$) (Figure 3E). The lower antibacterial activity of DHA can be attributed to its anionic charge and lipophobic content, while the bactericidal activity can be attributed to the electrostatic interactions between the cationic charges (NH_2; pH < 6) of chitosan and the polyanionic acid of the bacterial cell wall, leading to membrane disintegration, osmotic pressure disturbance, and eventually cell death (Chandrasekaran et al., 2020).

Significantly increased antibacterial activity was observed in the groups with AMX (Figure 3F). We investigated the effects of encapsulation of AMX and incorporating DHA on drug delivery and eradication of *H. pylori* by comparing the antibacterial activities of AMX, CA-AMX, and CA-DHA-AMX. In contrast to the free AMX, the encapsulated AMX showed a significant enhancement of antibacterial activity. Based on the results of this study, there was an additive effect of DHA in CA-DHA-AMX on the antibacterial activity of 10 mg/kg AMX (Figure 3G). Compared with CA-AMX, CA-DHA-AMX showed more potent antibacterial activity. Even when the AMX concentration decreased, the antibacterial activity increased more in the CA-DHA-AMX group than in the CA-AMX group (20 to 10 mg/kg) (Figure 3G). This increase might be related to the better localization and accessibility of the drug (Arora et al., 2011). Another possible explanation is that the treatment of DHA alters the composition of the membrane proteins and bacterial cell walls (Correia et al., 2013).

TABLE 1 The efficacy of NPs at entrapping DHA and AMX in different pH levels of the dispersion medium.

The pH of dispersion medium	Composite NPs			
	CA-DHA	CA-AMX	CA-DHA-AMX	
	DHA %	AMX %	DHA %	AMX %
5.4	65 ± 4	71 ± 1.9	63 ± 2.6	76 ± 5.7
6.8	62 ± 3.2	58 ± 1.9	64 ± 2.1	62 ± 3
7.4	51 ± 1.8	49 ± 5.3	47 ± 3.6	50 ± 6.2

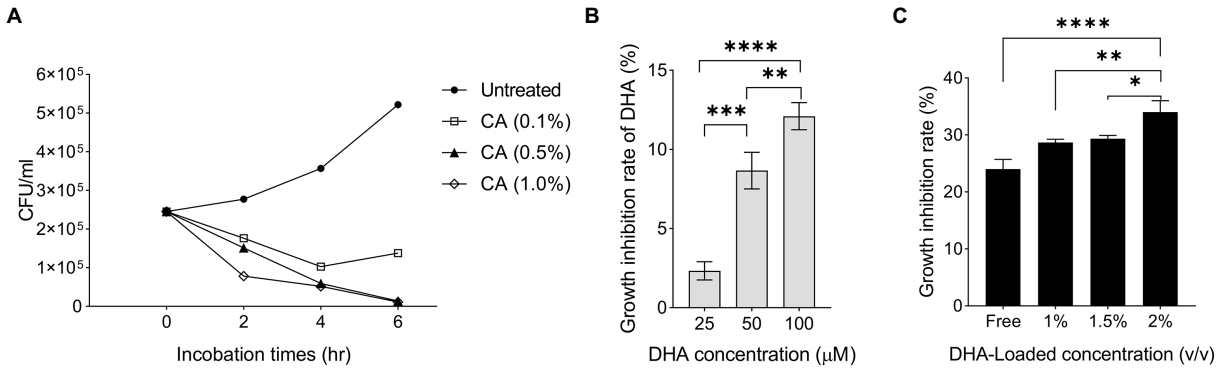

FIGURE 2
The antibacterial activity of DHA and chitosan alone and in combination. **(A)** The growth inhibition rate of CA NPs with different concentrations of chitosan (0.1, 0.5, and 1.0%). **(B)** The antibacterial activity of DHA with different concentrations (25, 50 and 100μM). **(C)** The antibacterial activity of DHA -loaded NPs at different loaded concentrations of DHA (CA 0.1%, DHA 1, 1.5 and 2%).

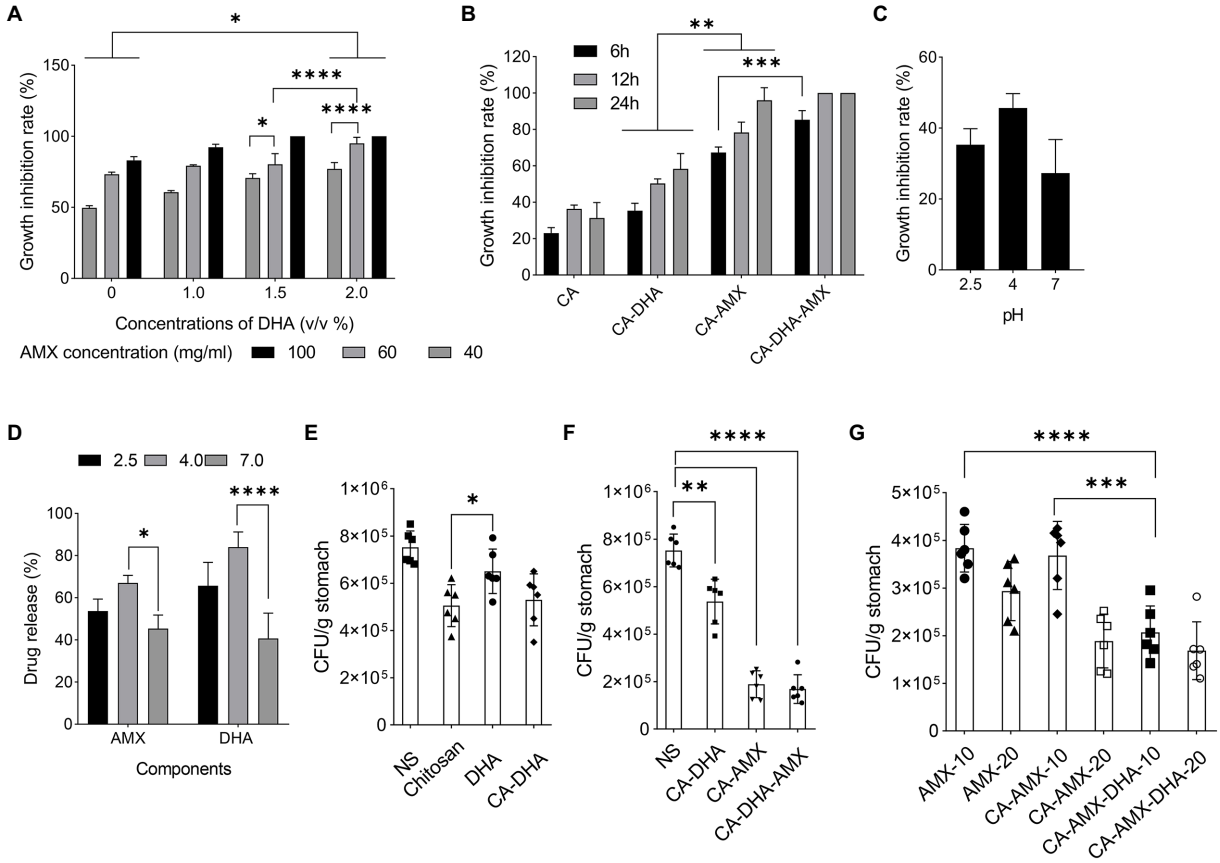

FIGURE 3
The growth inhibition activity of composite NPs. **(A)** The antibacterial activity of CA-NPs containing different concentrations of DHA and AMX. **(B)** The growth inhibition rate of CA-DHA (100μM)-AMX (60mg/ml) composite NPs at different time intervals 6, 12, and 24h. **(C,D)** CA-DHA (100μM)-AMX (60mg/ml) at different pH values after 6h incubation was investigated for their growth inhibition activity and release of drugs. **(E)** The *in vivo* antibacterial activity of chitosan, DHA and CA-DHA. **(F)** *In vivo* antibacterial activity of various formulations of composite NPs, including CA-DHA, CA-AMX, and CA-DHA-AMX compared with the untreated group. **(G)** Antibacterial activity was tested at a dose of 10 and 20mg/kg AMX in different formulations. Data are presented as mean±SEM.

The results showed that the most potent antibacterial activity in CA-DHA-AMX was at 20 mg/kg AMX (Figure 3G). Statistical analysis also showed that the nanoencapsulation and incorporation of DHA resulted in a decrease in the effective dose of the antibiotic. The CA-AMX-DHA group showed significantly higher antimicrobial activity at 10 mg/kg than CA-AMX formulations or free AMX in the same concentrations ($p = 0.007$ and 0.0002, respectively). The antibacterial activity of CA-DHA-AMX was almost the same at the

concentrations tested. These results are interesting, and it could be hypothesized that the incorporation of DHA in CA NPs could reduce the effective dose of AMX.

Bacterial binding and mucoadhesive properties of composite NPs

The CA-composite Bacterial binding was studied at different concentrations of DHA. Figure 4A shows that the unloaded NPs exhibited higher adhesion and DHA concentration is negatively correlated with bacterial adhesion. Due to the presence of anionic substances such as lipopolysaccharide groups on the surface of bacteria, this result was expected, as these substances tend to interact with the cationic parts of the chitosan molecules (Gafri et al., 2019). This results in strong interactions with the cationic NH_2 groups of the protonated chitosan under acidic conditions, which are reduced by DHA (Figures 1E,G). To further investigate this issue, we compared the values of each formulation. In contrast to DHA, AMX showed no effect on bacterial adhesion (Figure 4B). A previous study demonstrated that chitosan-based NPs possessed high mucoadhesive properties and the chitosan amino groups interacted with sialic acids in the mucosa in a pH-dependent manner (Mukhopadhyay et al., 2015).

Our results showed that DHA reduced mucoadhesive activity in a dose-dependent manner at all concentrations. We found that the mucoadhesive activity increased when DHA was removed from the formulation, especially at pH 4.5 ($p = 0.014$) (Figure 5A). The mucoadhesive activity was highest in acidic condition (2.5 and 4.5) than pH = 7.5 for different formulation (Figure 5A). The positive charge of chitosan under acidic conditions interacted strongly electrostatically with the negative charge of sialic acid on mucin. As a cationic polysaccharide, chitosan contains primary amino and hydroxyl groups in its repeating units. Primary amino groups carry a positive charge when protonated, which may facilitate electrostatic interactions with negatively charged epithelial cells. The electrostatic interactions are lost when these amino groups are deprotonated at a pH of >6.5. On the other hand, the net charge of mucin becomes more negative with increasing pH. At a pH of 2.5, H+ is abundant in the gastric niche, masking the negative charge of mucin, which creates a competitive effect against chitosan (Sogias et al., 2008; Ways et al., 2018). At pH = 7.5, mucin appears to have a greater net negative charge than at pH = 2.5, while chitosan appears to be more deprotonated and has fewer positive charges than at acidic pH. However, it was observed that the composite NPs interacted electrostatically with mucin molecules at optimal pH values (pH > 4.5).

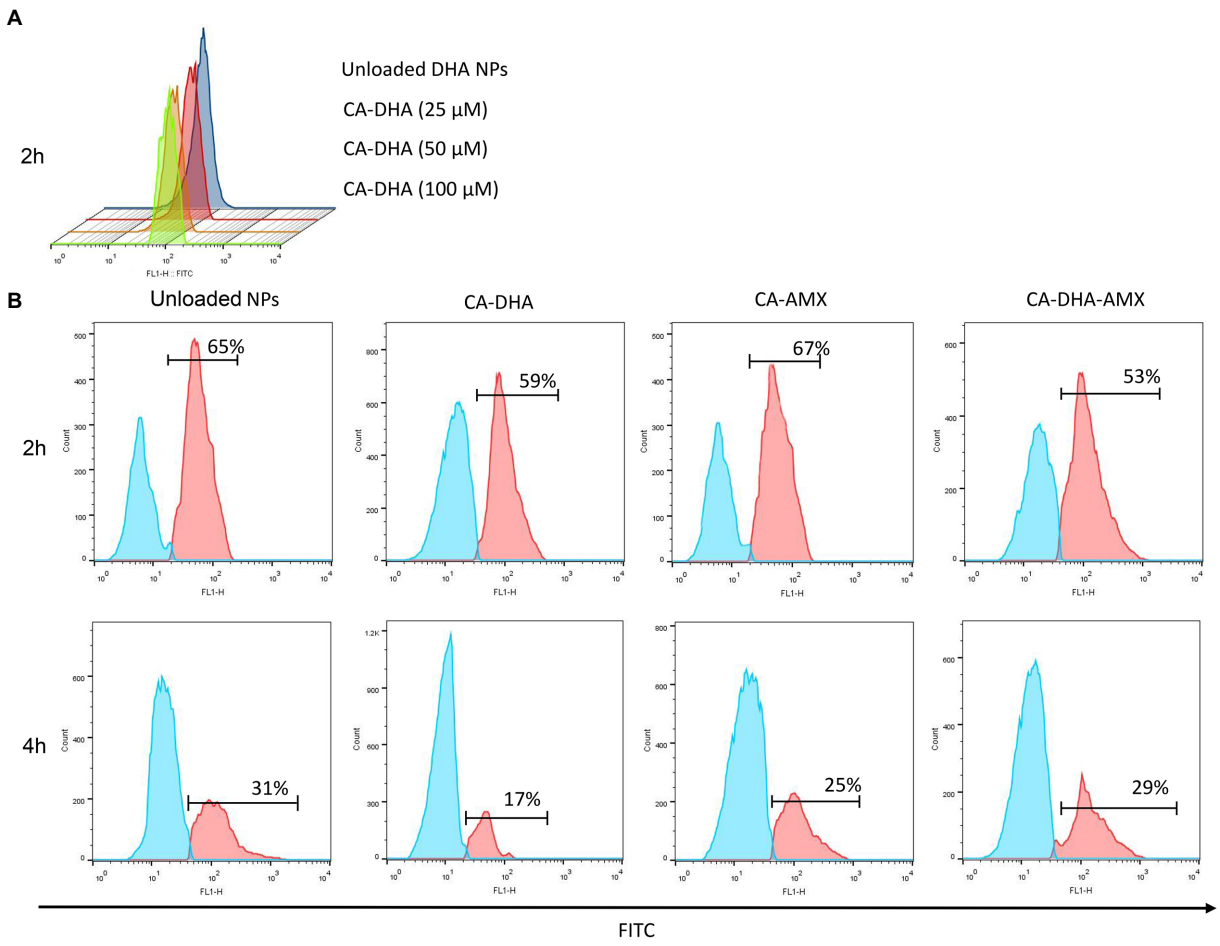

FIGURE 4
The bacterial binding capacity of composite NPs. **(A)** Bacterial adhesion of CA-DHA NPs and unloaded NPs at different concentrations of DHA. **(B)** The effect of different formulations of NPs on bacterial adhesion at two different time intervals; 2h and 4h.

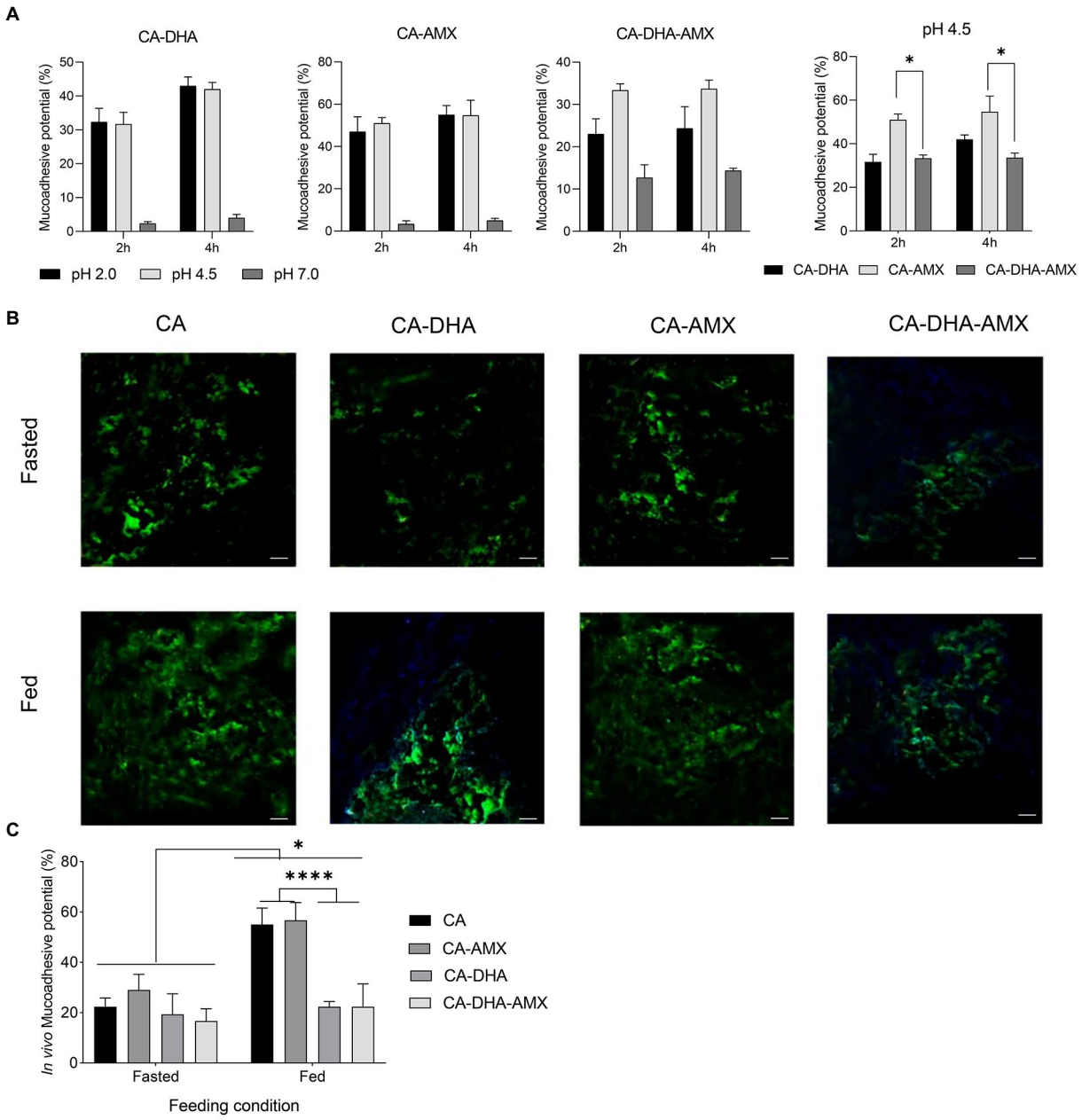

FIGURE 5
The mucoadhesion potential of composite NPs. **(A)** The *in vitro* assessment of mucoadhesive potential. Results of the unloaded NPs were similar to CA-AMX (data not shown). **(B)** *In vivo* mucoadhesive activity was evaluated by fluorescence microscopy under two distinct diet conditions; fasted (2h before feeding) and fed (2h after feeding, scale bar 500μM). **(C)** The *in vivo* mucoadhesive activity was performed under two feeding conditions, fasting and feeding. Data are presented as mean±SEM (n =3).

The mucoadhesive potential was significantly higher in fed than in fasting condition. The acidity of the stomach in the fasting condition (2 h before feeding) and the fed condition (2 h after feeding) is different: 2.5 and 3.0–4.5, respectively. The results showed that the mucoadhesive potential was significantly higher in the fed condition than in the fasting condition (Figure 5C). The mucoadhesive potential of the composite NPs was different at pH = 2.5 and pH = 4.5, although this difference was not significant, but the mucoadhesive potential was higher at pH 4.5 than the others. It was also found that the composite NPs containing DHA exhibited lower mucoadhesive capacity, especially under feeding conditions (p = 0.029) (Figures 5B,C). In contrast, a previous study showed that curcumin-loaded NPs with lipid components such as polyvinyl alcohol and polyethylene glycol were more mucoadhesive (Chanburee and Tiyaboonchai, 2017). Chitosan likely quenched DHA in our study.

Helicobacter pylori eradication and ulcer healing

In histopathological studies, NPs incorporated with AMX and DHA were more effective in eradicating *H. pylori*. On day 21, *H. pylori* were found to be completely eradicated with CA-DHA-AMX (10 and 20 mg/kg). We found that DHA significantly increased the efficacy of AMX in

the encapsulated formulations. AMX (10 mg/kg) in the encapsulated form significantly increased eradication rates compared with AMX powder 20 mg/kg ($p = 0.0184$) (Figure 6A). On the other hand, an equally high eradication rate was observed with CA-AMX (20 mg/kg) and CA-DHA-AMX (10 and 20 mg/kg). It is suggested that the membrane proteins changed and the permeability and accessibility of the antibiotic led to a significant decrease in the effective dose (Henostroza et al., 2022).

Figure 6B shows the phenotypic healing of ASA-induced ulcers. The ulcers were completely healed by day 14. The inflammation decreased during the administration of CA-DHA compared with AMX (20 mg/kg). CA-DHA-AMX at 10 mg/kg exhibited the same healing effect as 20 mg/kg and showed a higher healing effect than AMX powder (20 mg/kg) (Figure 6B). As shown in Figure 6C, CA-DHA-AMX demonstrated significantly higher ulcer healing activity than CA-AMX ($p = 0.009$). In this study, DHA was found to accelerate the healing of ulcers induced by ASA.

Histological examination of the gastric epithelium confirmed *H. pylori* infection (Figure 6D). Microscopically, we measured the length and thickness of the ulcer (40×, 5 sections/sample). Our results showed that in the CA-DHA-AMX groups with 10 mg/kg and 20 mg/kg AMX, the ulcer areas were significantly decreased compared with the other groups (Figure 6E). The presence of DHA in combination with 10 mg/kg AMX significantly reduced ulcer area compared with AMX powder (20 mg/kg) and the CA-AMX group at 10 mg/kg ($p = 0.003$ and < 0.0001, respectively) (Figure 6E). The encapsulation of AMX also significantly improved the ulcer healing effect, and the mucus thickness was similar between AMX

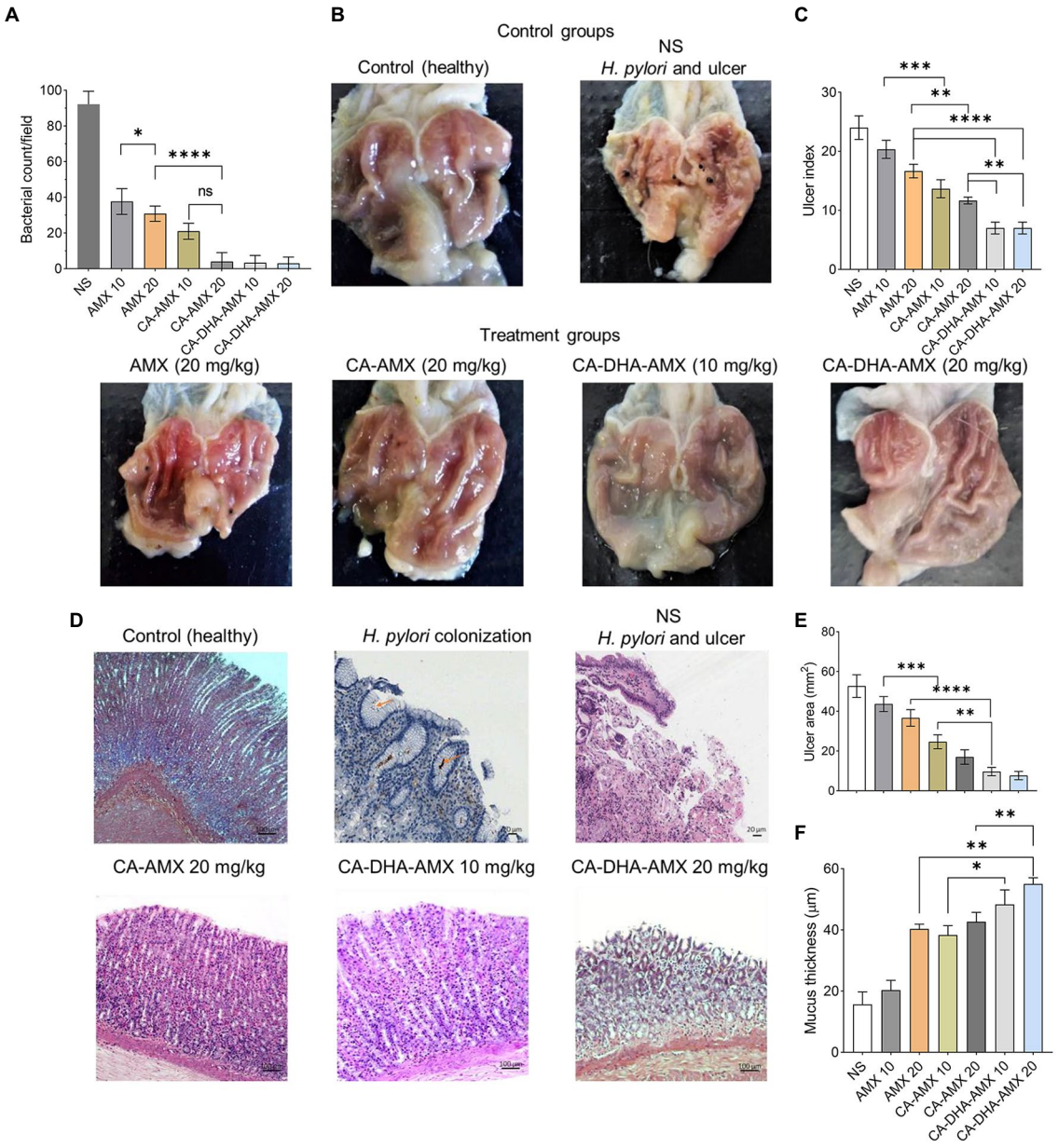

FIGURE 6
A histopathological evaluation of ASA-induced ulcers in rats infected with *H. pylori*. **(A)** The bacterial count of biopsies in treatment groups at day 14. **(B)** The phenotypic assessment of the rat stomach in different examined groups at day 14. **(C–F)** The analysis of ulcer index, histopathological features, ulcer area, and mucosa thickness of treated groups compared with control (untreated group). Data are presented as mean±SEM ($n = 3$).

powder (20 mg/kg) and CA-AMX (10 mg/kg) (Figure 6F). Accordingly, the incorporation of AMX with DHA-loaded NPs seemed to be beneficial. This result is consistent with the findings of Anandan et al. study suggesting that chitin and chitosan may be antiulcerogenic (Anandan et al., 2004). The pathological evaluation showed that CA-DHA-AMX reduced inflammatory and hemorrhagic conditions (Figure 6D). CA-DHA-AMX (20 mg/kg) significantly increased mucosal thickness compared with CA-AMX and AMX powder ($p = 0.0054$ and $= 0.0011$, respectively) (Figures 6D,F). The summary of physicochemical and biological activity of the different formulations is shown in ST. 2.

The macroscopic and microscopic evaluation of each group showed that inflammation decreased in the presence of DHA in different formulations (Figures 6B,D). The infiltration of immune cells was reduced after treatment with a formulation containing DHA (Figures 6D, 7A,B). Comparison of macrophages (MQ), neutrophils, and fibroblast cells at days 3 and 14 revealed that DHA in the formulation was associated with a significant decrease in innate immune response cells. The presence of DHA (CA-DHA-AMX groups) significantly decreased the number of MQ and neutrophils at day 14 compared with the absence of DHA (CA-AMX groups) (Figures 7A,B). As recently reported by Pineda-Pea et al., DHA has been shown to have anti-inflammatory and antioxidant properties that can alleviate indomethacin-induced gastric ulcers. Compared to the control group, they found that DHA significantly reduced neutrophil infiltration (Pineda-Peña et al., 2018).

Pro-inflammatory cytokines such as IL -6, IL -1β, and IL -17A were significantly lower in the formulations containing DHA than in those without. ELISA results showed that the presence of DHA decreased IL -1β in different formulations. In the CA-DHA-AMX (10 mg/kg) group, the concentration of IL -1β was significantly higher than in the formulations that did not contain it. The CA-DHA-AMX groups were compared with the AMX powder and CA-AMX groups, and the results indicated that DHA was responsible for the anti-inflammatory effect of the composite NPs (Figure 8A). The histopathological examination of the examined groups revealed that the collagen accumulation was different (Figure 8B). As demonstrated by immunohistochemical staining for collagen I, CA-AMX (20 mg/kg) accumulated more collagen I than CA-DHA-AMX (20 mg/kg) (Figures 8B,C). In a study by Motawee et al., it was found that chronic administration of DHA significantly reduced the expression of H+/K+-ATPase gene and the enzyme activity of COX −2 while improving the gastric ulcer index, percent ulcer protection, and significantly reducing the expression of gastric GSH, CCK, and e- NOS genes and significantly reducing the expression of gastric GSH, CCK, and e- NOS genes (Motawee et al., 2022). As reported in another study by Serini et al., resveratrol-based solid lipid nanoparticles containing DHA showed anti-inflammatory properties on keratinocytes with a decrease in the expression of IL -1β, IL -6, and MCP-1 (Serini et al., 2019). The results of our study show that chitosan nanoparticles are a reliable means of delivering drugs to the niches of the stomach. Although the addition of DHA reduces the mucoadhesive properties of CA-DHA-AMX NPs, it increases drug entrapment and shows high antibacterial activity and anti-inflammatory effects.

Conclusion

The development of drugs containing acid-sensitive antibiotics such as AMX is difficult with conventional gastric retention formulation techniques. The development of a therapeutically effective gastroprotective formulation of AMX, which has both excellent buoyancy and a suitable release pattern, could allow the targeting of drugs to specific sites in the stomach. Our developed system had none of the disadvantages of a single-dose formulation but offered the advantage of the ease of preparation and sustained release of the drug

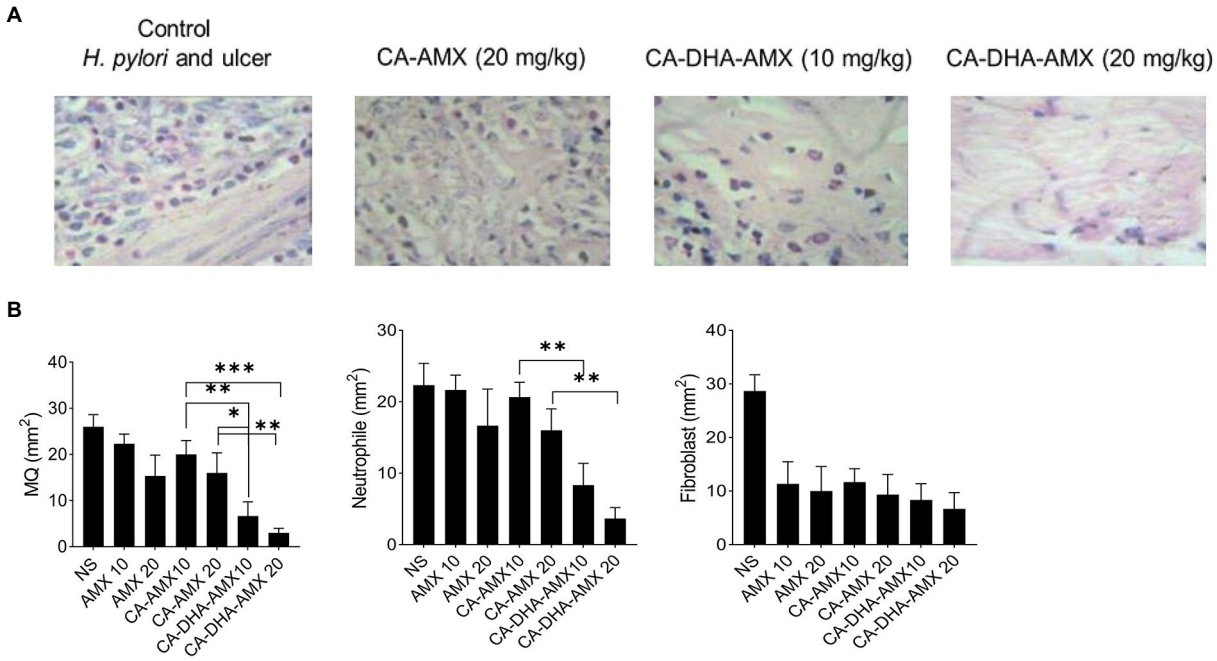

FIGURE 7
The distribution of macrophage (MQ), neutrophil and fibroblast cells. **(A)** The microscopic distribution of macrophage, neutrophil and fibroblast cells in four different group untreated group, CA-AMX (20mg/kg), CA-DHA-AMX (10mg/kg), and CA-DHA, AMX (20mg/kg) at 14. Hematoxylin and Eosin staining. **(B)** The comparison of macrophage, neutrophil and fibroblast cells at day 14 among all treated groups. Data are presented as mean±SEM ($n = 3$).

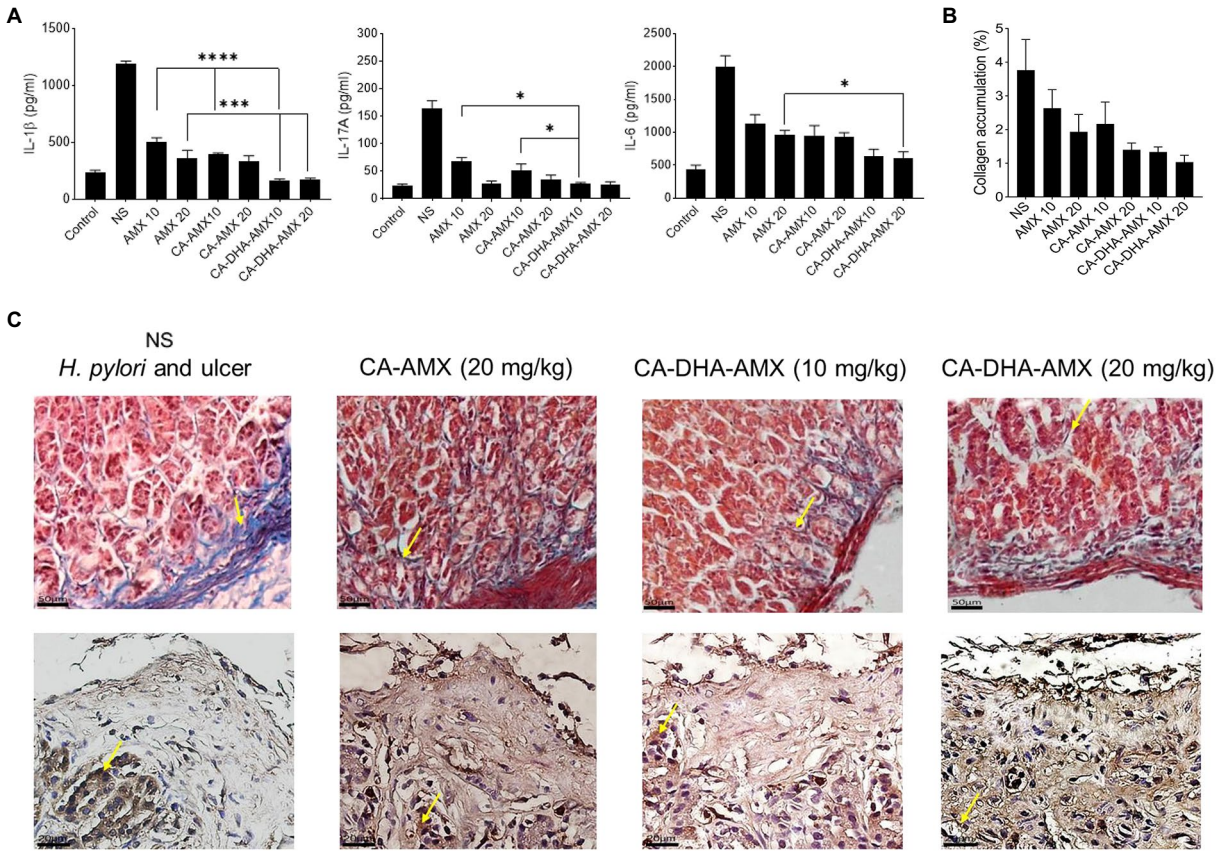

FIGURE 8
The histopathological evaluation and the pro-inflammatory cytokine production of gastric biopsies. **(A)** The levels of pro-inflammatory cytokines including IL-1β, IL-6, and IL-17A was conducted using ELISA method. **(B)** The collagen accumulation among different treated groups. **(C)** Masson's trichrome staining was used to evaluate the accumulation of collagen (yellow arrow), the blue and red are responsible for collagen and muscle fibers. Immunohistochemical staining for Collagen I (yellow arrow), high accumulation of collagen I in glands and endothelia observed in untreated group, while the accumulation was reduced in treated groups, the lowest accumulation was observed in CA-DHA-AMX (20mg/kg). Data are presented as mean±SEM (n =3).

over an extended period. A simple method of encapsulating AMX in DHA-loaded CA NPs can be used for biocidal effects against *H. pylori*, with a reduced effective dose of the antibiotic. As a mucoadhesive carrier, chitosan-based nanoparticles are an effective way to deliver acid-sensitive antibiotics such as AMX. The encapsulation of AMX significantly increased its antibacterial activity compared to single AMX, and incorporation of DHA decreased the effective dose. The DHA also decreased the effective dose of AMX in the encapsulated form by increasing its entrapment, which may be due to the modification of bacterial cell walls and its antibacterial activity. The incorporation of DHA into CA-AMX composite NPs enhanced the antibacterial activity *in vivo* and accelerated the healing of gastric ulcers, which could be attributed to the DHA -mediated dissolution of bacterial cell membrane, macrophage-dependent clearance, and anti-inflammatory effects of DHA. The *in vivo* anti-*H. pylori* effects of DHA may also be due to its immunomodulatory activities that elicit biocidal effects on *H. pylori*.

Data availability statement

The original contributions presented in the study are included in the article/Supplementary material, further inquiries can be directed to the corresponding author.

Ethics statement

The animal study was reviewed and approved by all animal experiments were performed according to a protocol approved by the Ethics Committee of Ilam Medical University (approval number: R.MEDILAM. REC.1400.133). Written informed consent was obtained from the owners for the participation of their animals in this study.

Author contributions

MH: conceptualization, visualization, and supervision. MH and MA: methodology and validation. SK and VK: investigation and data curation. SK, NS and MA: writing – original draft preparation. ME-S and BN: writing – reviewing and editing. All authors contributed to the article and approved the submitted version.

Acknowledgments

In recognition of their collaboration, we would like to thank the Clinical Microbiology Research Center of the Ilam University of Medical Sciences. We would like to extend our sincere gratitude to the Vice-Chancellor for Research Affairs at Ilam University of Medical Sciences, Ilam, Iran, for his assistance in managing and funding this project.

Conflict of interest

The authors declare that the research was conducted in the absence of any commercial or financial relationships that could be construed as a potential conflict of interest.

Publisher's note

All claims expressed in this article are solely those of the authors and do not necessarily represent those of their affiliated organizations, or those of the publisher, the editors and the reviewers. Any product that may be evaluated in this article, or claim that may be made by its manufacturer, is not guaranteed or endorsed by the publisher.

Supplementary material

The Supplementary material for this article can be found online at: https://www.frontiersin.org/articles/10.3389/fmicb.2023.1083330/full#supplementary-material

References

Anandan, R., Nair, P. G., and Mathew, S. (2004). Anti-ulcerogenic effect of chitin and chitosan on mucosal antioxidant defence system in HCl-ethanol-induced ulcer in rats. *J. Pharm. Pharmacol.* 56, 265–269. doi: 10.1211/0022357023079

Arora, S., Gupta, S., Narang, R. K., and Budhiraja, R. D. (2011). Amoxicillin loaded chitosan–alginate polyelectrolyte complex nanoparticles as mucopenetrating delivery system for *H. pylori*. *Sci. Pharm.* 79, 673–694. doi: 10.3797/scipharm.1011-05

Bhattacharya, A., Ghosal, S., and Bhattacharya, S. K. (2006). Effect of fish oil on offensive and defensive factors in gastric ulceration in rats. *Prostaglandins Leukot. Essent. Fatty Acids* 74, 109–116. doi: 10.1016/j.plefa.2005.11.001

Casillas-Vargas, G., Ocasio-Malave, C., Medina, S., Morales-Guzman, C., Del Valle, R. G., Carballeira, N. M., et al. (2021). Antibacterial fatty acids: an update of possible mechanisms of action and implications in the development of the next-generation of antibacterial agents. *Prog. Lipid Res.* 82:101093. doi: 10.1016/j.plipres.2021.101093

Chanburee, S., and Tiyaboonchai, W. (2017). Mucoadhesive nanostructured lipid carriers (NLCs) as potential carriers for improving oral delivery of curcumin. *Drug Dev. Ind. Pharm.* 43, 432–440. doi: 10.1080/03639045.2016.1257020

Chandrasekaran, M., Kim, K. D., and Chun, S. C. (2020). Antibacterial activity of chitosan nanoparticles: a review. *PRO* 8:1173. doi: 10.3390/pr8091173

Chang, S. H., Hsieh, P. L., and Tsai, G. J. (2020). Chitosan inhibits helicobacter pylori growth and urease production and prevents its infection of human gastric carcinoma cells. *Mar. Drugs* 18:542. doi: 10.3390/md18110542

Chang, P. K., Tsai, M. F., Huang, C. Y., Lee, C. L., Lin, C., Shieh, C. J., et al. (2021). Chitosan-based anti-oxidation delivery Nano-platform: applications in the encapsulation of DHA-enriched fish oil. *Mar. Drugs* 19:470. doi: 10.3390/md19080470

Chen, E. P., Mahar Doan, K. M., Portelli, S., Coatney, R., Vaden, V., and Shi, W. (2008). Gastric pH and gastric residence time in fasted and fed conscious cynomolgus monkeys using the bravo® pH system. *Pharm. Res.* 25, 123–134. doi: 10.1007/s11095-007-9358-5

Choi, I. J., Kim, C. G., Lee, J. Y., Kim, Y. I., Kook, M. C., Park, B., et al. (2020). Family history of gastric cancer and helicobacter pylori treatment. *N. Engl. J. Med.* 382, 427–436. doi: 10.1056/NEJMoa1909666

Coraça-Huber, D. C., Steixner, S., Wurm, A., and Nogler, M. (2021). Antibacterial and anti-biofilm activity of omega-3 polyunsaturated fatty acids against periprosthetic joint infections-isolated multi-drug resistant strains. *Biomedicine* 9:334. doi: 10.3390/biomedicines9040334

Correia, M., Michel, V., Matos, A. A., Carvalho, P., Oliveira, M. J., Ferreira, R. M., et al. (2012). Docosahexaenoic acid inhibits helicobacter pylori growth in vitro and mice gastric mucosa colonization. *PLoS One* 7:e35072. doi: 10.1371/journal.pone.0035072

Correia, M., Michel, V., Osório, H., El Ghachi, M., Bonis, M., Boneca, I. G., et al. (2013). Crosstalk between helicobacter pylori and gastric epithelial cells is impaired by docosahexaenoic acid. *PLoS One* 8:e60657. doi: 10.1371/journal.pone.0060657

Cui, Z., Xiang, Y., Si, J., Yang, M., Zhang, Q., and Zhang, T. (2008). Ionic interactions between sulfuric acid and chitosan membranes. *Carbohydr. Polym.* 73, 111–116. doi: 10.1016/j.carbpol.2007.11.009

Dixon, S. J., Lemberg, K. M., Lamprecht, M. R., Skouta, R., Zaitsev, E. M., Gleason, C. E., et al. (2012). Ferroptosis: an iron-dependent form of nonapoptotic cell death. *Cells* 149, 1060–1072. doi: 10.1016/j.cell.2012.03.042

Friedman, A. J., Phan, J., Schairer, D. O., Champer, J., Qin, M., Pirouz, A., et al. (2013). Antimicrobial and anti-inflammatory activity of chitosan–alginate nanoparticles: a targeted therapy for cutaneous pathogens. *J. Investig. Dermatol.* 133, 1231–1239. doi: 10.1038/jid.2012.399

Gafri, H. F. S., Zuki, F. M., Aroua, M. K., and Hashim, N. A. (2019). Mechanism of bacterial adhesion on ultrafiltration membrane modified by natural antimicrobial polymers (chitosan) and combination with activated carbon (PAC). *Rev. Chem. Eng.* 35, 421–443. doi: 10.1515/revce-2017-0006

Graham, D. Y., Lu, H., and Shiotani, A. (2021). Vonoprazan-containing helicobacter pylori triple therapies contribution to global antimicrobial resistance. *J. Gastroenterol. Hepatol.* 36, 1159–1163. doi: 10.1111/jgh.15252

Henostroza, M. A. B., Tavares, G. D., Yukuyama, M. N., De Souza, A., Barbosa, E. J., Avino, V. C., et al. (2022). Antibiotic-loaded lipid-based nanocarrier: a promising strategy to overcome bacterial infection. *Int. J. Pharm.* 621:121782. doi: 10.1016/j.ijpharm.2022.121782

Henriques, P. C., Costa, L. M., Seabra, C. L., Antunes, B., Silva-Carvalho, R., Junqueira-Neto, S., et al. (2020). Orally administrated chitosan microspheres bind helicobacter pylori and decrease gastric infection in mice. *Acta Biomater.* 114, 206–220. doi: 10.1016/j.actbio.2020.06.035

Hu, Y., Du, Y., Yang, J., Kennedy, J. F., Wang, X., and Wang, L. (2007). Synthesis, characterization and antibacterial activity of guanidinylated chitosan. *Carbohydr. Polym.* 67, 66–72. doi: 10.1016/j.carbpol.2006.04.015

Ji, H. G., Piao, J. Y., Kim, S. J., Kim, D. H., Lee, H. N., Na, H. K., et al. (2016). Docosahexaenoic acid inhibits helicobacter pylori-induced STAT3 phosphorylation through activation of PPARγ. *Mol. Nutr. Food Res.* 60, 1448–1457. doi: 10.1002/mnfr.201600009

Kim, J., and Wang, T. C. (2021). Helicobacter pylori and gastric cancer. *Gastrointest. Endosc. Clin.* 31, 451–465. doi: 10.1016/j.giec.2021.03.003

Krzyżek, P., Paluch, E., and Gościniak, G. (2020). Synergistic therapies as a promising option for the treatment of antibiotic-resistant helicobacter pylori. *Antibiotics* 9:658. doi: 10.3390/antibiotics9100658

Kuo, C. J., Lee, C. H., Chang, M. L., Lin, C. Y., Lin, W. R., Su, M. Y., et al. (2021). Multidrug resistance: the clinical dilemma of refractory helicobacter pylori infection. *J. Microbiol. Immunol. Infect.* 54, 1184–1187. doi: 10.1016/j.jmii.2021.03.006

Li, J., Wu, Y., and Zhao, L. (2016). Antibacterial activity and mechanism of chitosan with ultra high molecular weight. *Carbohydr. Polym.* 148, 200–205. doi: 10.1016/j.carbpol.2016.04.025

Luo, D., Guo, J., Wang, F., Sun, J., Li, G., Cheng, X., et al. (2009). Preparation and evaluation of anti-helicobacter pylori efficacy of chitosan nanoparticles in vitro and in vivo. *J. Biomater. Sci. Polym. Ed.* 20, 1587–1596. doi: 10.1163/092050609X12464345137685

Motawee, M. E., Hassan, F., Damanhory, A. M., Mohie, P. M., Khalifa, M. M., and Elbastawisy, Y. M. (2022). Possible protective effect of each of Omega-3 PUFA and leptin on indomethacin-induced gastric ulcer in rats with type II DM. *Bull. Egypt. Soc. Physiol. Sci.* 42, 329–343. doi: 10.21608/besps.2022.121674.1119

Mukhopadhyay, P., Chakraborty, S., Bhattacharya, S., Mishra, R., and Kundu, P. P. (2015). pH-sensitive chitosan/alginate core-shell nanoparticles for efficient and safe oral insulin delivery. *Int. J. Biol. Macromol.* 72, 640–648. doi: 10.1016/j.ijbiomac.2014.08.040

Pacheco, N., Naal-Ek, M. G., Ayora-Talavera, T., Shirai, K., Román-Guerrero, A., Fabela-Morón, M. F., et al. (2019). Effect of bio-chemical chitosan and gallic acid into rheology and physicochemical properties of ternary edible films. *Int. J. Biol. Macromol.* 125, 149–158. doi: 10.1016/j.ijbiomac.2018.12.060

Pineda-Peña, E. A., Martínez-Pérez, Y., Galicia-Moreno, M., Navarrete, A., Segovia, J., Muriel, P., et al. (2018). Participation of the anti-inflammatory and antioxidative activity of docosahexaenoic acid on indomethacin-induced gastric injury model. *Eur. J. Pharmacol.* 818, 585–592. doi: 10.1016/j.ejphar.2017.11.015

Qin, Y., Lao, Y.-H., Wang, H., Zhang, J., Yi, K., Chen, Z., et al. (2021). Combatting helicobacter pylori with oral nanomedicine. *J. Mater. Chem. B* 9, 9826–9838. doi: 10.1039/D1TB02038B

Rahaiee, S., Hashemi, M., Shojaosadati, S. A., Moini, S., and Razavi, S. H. (2017). Nanoparticles based on crocin loaded chitosan-alginate biopolymers: antioxidant activities, bioavailability and anticancer properties. *Int. J. Biol. Macromol.* 99, 401–408. doi: 10.1016/j.ijbiomac.2017.02.095

Seabra, C. L., Nunes, C., Gomez-Lazaro, M., Correia, M., Machado, J. C., Goncalves, I. C., et al. (2017). Docosahexaenoic acid loaded lipid nanoparticles with bactericidal activity against helicobacter pylori. *Int. J. Pharm.* 519, 128–137. doi: 10.1016/j.ijpharm.2017.01.014

Serini, S., Cassano, R., Facchinetti, E., Amendola, G., Trombino, S., and Calviello, G. (2019). Anti-irritant and anti-inflammatory effects of DHA encapsulated in resveratrol-based solid lipid nanoparticles in human keratinocytes. *Nutrients* 11:1400. doi: 10.3390/nu11061400

Shah, S. C., Iyer, P. G., and Moss, S. F. (2021). AGA clinical practice update on the Management of Refractory Helicobacter pylori infection: expert review. *Gastroenterology* 160, 1831–1841. doi: 10.1053/j.gastro.2020.11.059

Sogias, I. A., Williams, A. C., and Khutoryanskiy, V. V. (2008). Why is chitosan mucoadhesive? *Biomacromolecules* 9, 1837–1842. doi: 10.1021/bm800276d

Spósito, L., Fortunato, G. C., de Camargo, B. A. F., Ramos, M. A. D. S., Souza, M. P. C. D., Meneguin, A. B., et al. (2021). Exploiting drug delivery systems for oral route in the peptic ulcer disease treatment. *J. Drug Target.* 29, 1029–1047. doi: 10.1080/1061186X.2021.1904249

Suzuki, H., and Matsuzaki, J. (2018). Gastric cancer: evidence boosts helicobacter pylori eradication. *Nat. Rev. Gastroenterol. Hepatol.* 15, 458–460. doi: 10.1038/s41575-018-0023-8

Takahashi, T., Imai, M., Suzuki, I., and Sawai, J. (2008). Growth inhibitory effect on bacteria of chitosan membranes regulated with deacetylation degree. *Biochem. Eng. J.* 40, 485–491. doi: 10.1016/j.bej.2008.02.009

Ways, T. M. M., Lau, W. M., and Khutoryanskiy, V. V. (2018). Chitosan and its derivatives for application in mucoadhesive drug delivery systems. *Polymers* 10:267. doi: 10.3390/polym10030267

frontiers | Frontiers in Microbiology

TYPE Review
PUBLISHED 16 March 2023
DOI 10.3389/fmicb.2023.1081271

OPEN ACCESS

EDITED BY
Zhongming Ge,
Massachusetts Institute of Technology,
United States

REVIEWED BY
Norma Velazquez-Guadarrama,
Federico Gómez Children's Hospital,
Mexico
Hamed Hamouda,
Ocean University of China,
China

*CORRESPONDENCE
Yin Zhu
zhuyin27@sina.com

†These authors share first authorship

SPECIALTY SECTION
This article was submitted to Antimicrobials, Resistance and Chemotherapy, a section of the journal Frontiers in Microbiology

RECEIVED 27 October 2022
ACCEPTED 06 March 2023
PUBLISHED 16 March 2023

CITATION
Shu C, Xu Z, He C, Xu X, Zhou Y, Cai B and Zhu Y (2023) Application of biomaterials in the eradication of *Helicobacter pylori*: A bibliometric analysis and overview. *Front. Microbiol.* 14:1081271. doi: 10.3389/fmicb.2023.1081271

Application of biomaterials in the eradication of *Helicobacter pylori*: A bibliometric analysis and overview

Chunxi Shu[1†], Zhou Xu[2†], Cong He[1†], Xinbo Xu[1], Yanan Zhou[1], Baihui Cai[2] and Yin Zhu[1*]

[1]Department of Gastroenterology, Digestive Disease Hospital, The First Affiliated Hospital of Nanchang University, Nanchang, Jiangxi, China, [2]The Second Clinical Medical College of Nanchang University, Nanchang, Jiangxi, China

Helicobacter pylori is a prominent cause of gastritis, peptic ulcer, and gastric cancer. It is naturally colonized on the surface of the mucus layer and mucosal epithelial cells of the gastric sinus, surrounded not only by mucus layer with high viscosity that prevents the contact of drug molecules with bacteria but also by multitudinous gastric acid and pepsin, inactivating the antibacterial drug. With high-performance biocompatibility and biological specificity, biomaterials emerge as promising prospects closely associated with *H. pylori* eradication recently. Aiming to thoroughly summarize the progressing research in this field, we have screened 101 publications from the web of science database and then a bibliometric investigation was performed on the research trends of the application of biomaterials in eradicating *H. pylori* over the last decade utilizing VOSviewer and CiteSpace to establish the relationship between the publications, countries, institutions, authors, and most relevant topics. Keyword analysis illustrates biomaterials including nanoparticles (NPs), metallic materials, liposomes, and polymers are employed most frequently. Depending on their constituent materials and characterized structures, biomaterials exhibit diverse prospects in eradicating *H. pylori* regarding extending drug delivery time, avoiding drug inactivation, target response, and addressing drug resistance. Furthermore, we overviewed the challenges and forthcoming research perspective of high-performance biomaterials in *H. pylori* eradication based on recent studies.

KEYWORDS

***Helicobacter pylori*, biomaterials, eradication, nanoparticles, drug delivery, drug resistance**

1. Introduction

Helicobacter pylori is a pathogenic Gram-negative spiral-shaped bacteria that infects approximately 4.4 billion people worldwide, which is therefore considered to be one of the most prevalent infections worldwide (Rajinikanth et al., 2007; Hooi et al., 2017; Reshetnyak and Reshetnyak, 2017). Among those with the disease, *H. pylori* primarily generally cause chronic gastritis and lead to gastric ulcers and gastric atrophy, furthermore, induces intestinal metaplasia and, in severe cases, gastric cancer (Capurro et al., 2019). Such strong infectivity and pathogenicity make *H. pylori* recognized as Class 1 carcinogen and a major risk factor for the development of gastric cancer, which is highly thought of as the third leading cause of death worldwide (Mera et al., 2018). The pioneering *H. pylori* eradication regimen was the standard triple therapy consisting of

proton pump inhibitors (PPI), amoxicillin, and clarithromycin or metronidazole proposed by the European Maastricht V/Florence consensus report (Malfertheiner et al., 2007). However, the emergence of resistant strains of metronidazole and clarithromycin has led to a steady decline in the eradication rate of standard triple therapy. For this purpose, recently a new strategy has been implemented in various regions of the world, namely quadruple therapy containing bismuth agent (bismuth agent +PPI+ two antibiotics) is highly recommended when high resistance of clarithromycin and metronidazole occurs (Fallone et al., 2016; Malfertheiner et al., 2017). Nevertheless, eradication of established *H. pylori* infection *in vivo* is challenging due to several factors concerning the duration of drug administration, primary antibiotic resistance, and stability of gastric acid secretion therapy (Praditya et al., 2019). Conventional medicine necessitates frequent administration because of its short half-life in the gastric mucus, thus causing non-negligible side effects regarding the mucosal microbiome (Coker et al., 2018). Given these factors, a reasonable approach to promote therapeutic outcomes is to develop the ability to deliver anti-suitable drugs in the gastric niche, while considering the stability and compatibility of therapeutic agents in an acidic environment. Apparently, owing to their unique potential regarding beneficial biocompatibility and bioactivity, advanced biomaterials are rapidly becoming a promising research trend in the field (de Souza et al., 2021).

Biomaterials are currently defined as substances that have been designed to take a form that, alone or as part of a complex system, is designed to guide the process of any therapeutic or diagnostic process by controlling the interaction with the components of the living system (Zhang et al., 2020; Butkovich et al., 2021). Biomaterials are generally classified into three categories: organic, inorganic, and bio-based materials. Among them, bio-based materials are mainly derived from cells, bacteria, and viruses, such as protein-based nano systems and outer membrane vesicles. In addition, according to their sources, biomaterials can be divided into natural and synthetic materials (Han et al., 2022). Natural biomaterials have been utilized for a long time due to their superior biocompatibility, biodegradability, low toxicity, and hypoallergenic, and the degradation products yielded are less cytotoxic, thus metabolized more easily by host tissues (Zhu et al., 2021; Han et al., 2022). Nowadays, biomaterials have achieved encouraging prospects in various fields, as well as increasingly becoming a new hotspot in the treatment of *H. pylori* (de Souza et al., 2021). Combining drugs with advanced biomaterials systems not only enables specific response delivery to the *H. pylori* parasite site but also prolongs the release rate of drugs at the target site (Darroudi et al., 2021). The application of biomaterials for the eradication of high drug resistance of *H. pylori* has become a new research trend. Here, bibliometrics and visual analysis are primarily adopted in the "quantitative analysis" section to generally explore the characteristics of studies on eradicating *H. pylori* with biomaterials over the past decade. Additionally, the main research topics and emerging trends are reviewed in the "main text" section based on the bibliometric analysis, and the potential challenges and forthcoming prospects of *H. pylori* eradication by biomaterials are discussed insightfully.

Abbreviations: *H. pylori*, *Helicobacter pylori*; PPI, proton pump inhibitors; NPs, Nanoparticles; FRS, Floating raft system; Urel, urea transport channel protein; 3SL, 3′-sialoyl lactose; p3SLP, multiple 3′-sialoyl lactose (3SL)-coupled poly (l-lysine)-based photosensitizers; SabA, acid-binding adhesin; LPs, Liposomes; LLA, linolenic acid; NLC, nanostructured lipid carriers; PEI, polyethyleneimine.

2. Quantitative analysis

Focused on the research trends in biomaterials for *H. pylori* eradication, this study employs bibliometric analysis to achieve visualization of the related topic. The bibliometric analysis allows not only quantitative and qualitative evaluation of publications but also the prediction of trends in a research field. It makes it possible to present the most influential research results and provide a theoretical basis for further research quickly and accurately (Ouyang et al., 2021). Through a decade of relevant bibliometric analysis, we overviewed the research progress of treating *H. pylori* with biomaterials intensively. Based on the identified publication trends, biomaterials have been playing an irreplaceable role in not only drug delivery systems but also pharmaceutical ingredients for *H. pylori* therapy. Therefore, this section will summarize the current state of development and potential opportunities and challenges in this field, as well as evaluate the main research topics and emerging trends with a critical perspective.

2.1. Search methodology

The data used to perform bibliometric analysis in this paper were extracted from the Web of Science Collection Core of Nanchang University Library,[1] which is an important database platform for domestic and international scholars to retrieve and obtain information about relevant academic literature. We chose to obtain data from the core collection because it owns a stringent evaluation of publications, thus ensuring the high quality of the literature (Zhang et al., 2022). Additionally, the WoSCC database is constantly and dynamically updated and provides the most impactful, relevant, and reliable information (Palechor-Trochez et al., 2021). The search strategy was set as "(TS = (*Helicobacter pylori*)) AND TS = (biomaterials)." Listed as follows are the selection criteria: (Reshetnyak and Reshetnyak, 2017) timespan: ranging from 2012-01-01 to 2022-01-01; (Rajinikanth et al., 2007) type: article or review, language: English. Initially, a total of 219 articles were retrieved. Taking into account the deviations from daily updates to the database, all the data was collected at the same time on April 24, 2022. Two collaborators independently screened the title and abstract of each result excluding irrelevant literature. Ultimately, a total of 101 pieces of literature on the topic of biomaterial therapy for *H. pylori* were collected and downloaded as pure text with full citation and recorded in meta data named biomaterials eradicate *H. pylori*. Subsequently, VOSviewer (version 1.6.18.0), CiteSpace (version 6.1.R1), and R (version 4.2.1) were implemented for further data processing and visual analysis (Chen et al., 2020; Figure 1).

2.2. Annual publications and countries distribution

The annual distribution of the number of articles published in the past decade is presented in Figure 2A, indicating that the number of articles varies in an S-shape with the year. Although there was a transient declining volume in the intervening years, the trend remains

1 http://lib.ncu. http://edu.cn/

steady increment over the last 5 years. Noteworthily, the volume of publications in the last 3 years is confronted with the most rapid growth, dramatically accounting for more than half of the total. There are adequate reasons to believe that the heat of this field will keep rising sequentially for years to come. As illustrated in Figure 2B, among all countries, China (24 articles) possesses the largest number of published articles compared with other countries. Moreover, India (14 articles) and Portugal (13 articles) present an exceptional contribution in this field as well, respectively ranking second and third. Among all high-producing countries, China and Egypt, respectively, are more strongly engaged with other countries (Figures 2B,C). These discrepancies may be closely related to the local infection situation and the level of research. This division of relationships is beneficial to contribute to scientists exploring where they should establish some important data for those partnerships.

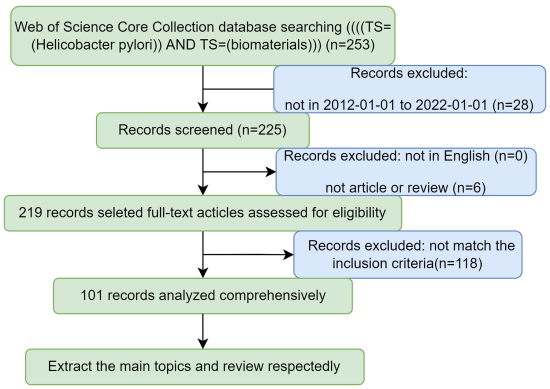

FIGURE 1
Flow charts of search strategies and filtering methods.

2.3. Journal distribution and co-citation analysis

Listed below are the journals that published the most papers in the last decade (Table 1). The "International journal of pharmaceutics" (8 articles) owns the highest outputs, followed by "Acta biomaterialia" (6 articles) and "International Journal of biological macromolecules" (6 articles). At the same time, the "International journal of pharmaceutics" is cited most among all the journals, totally reaching

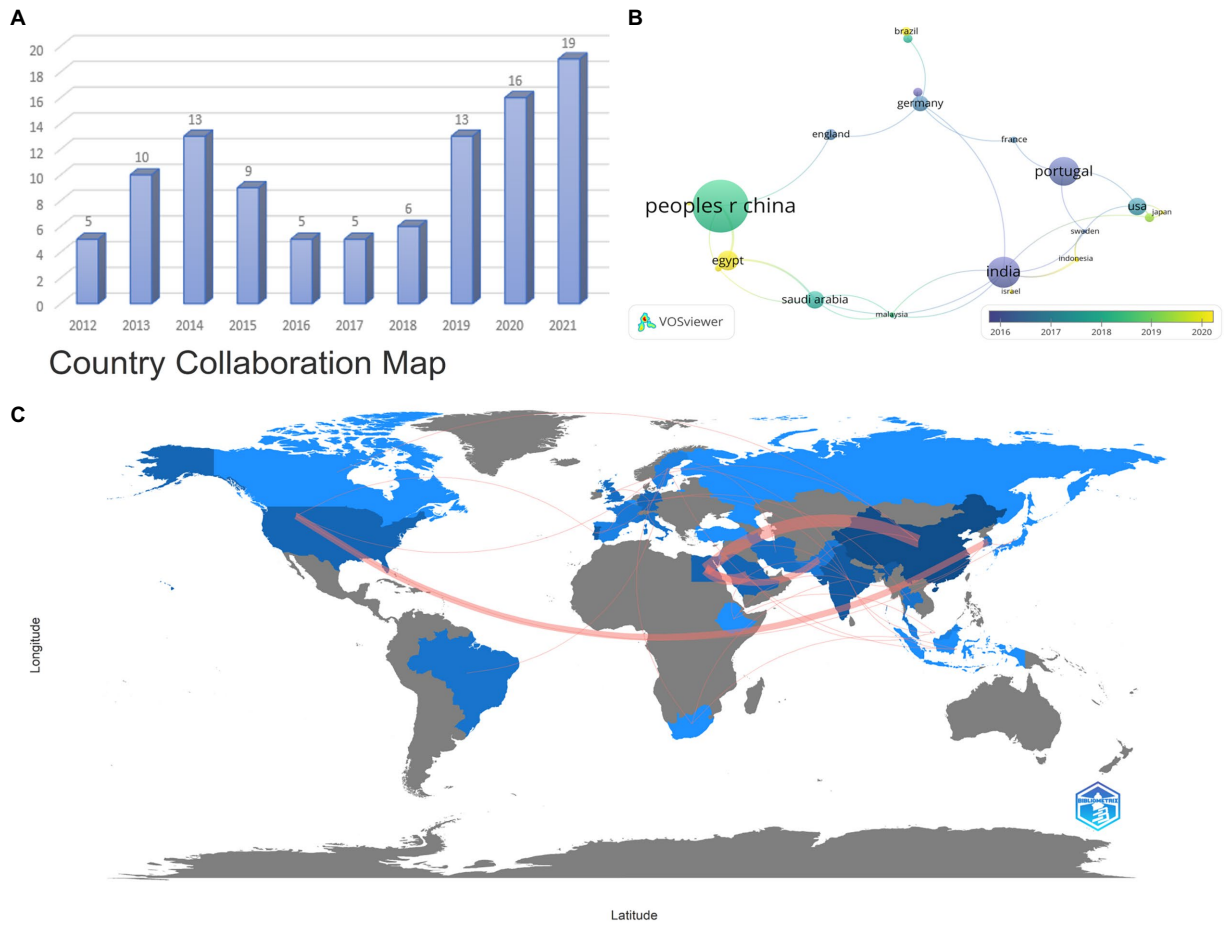

FIGURE 2
Annual publication status **(A)**, major productive countries distribution **(B)**, and Country Collaboration Map **(C)**. Each node represents a country, and the line between the two nodes indicates that they have a co-occurrence relationship. The larger the node means the greater the volume of national publications. The closer the distance, the stronger the relationship. Moreover, the more yellow the color tends to be, the more cutting-edge the research is **(A,B)**. The red path signifies the partnership between the countries, and the wider the red means the closer the cooperation **(C)**.

TABLE 1 Top 10 leading journals related to *H. pylori* and Biomaterials research from 2012 to 2021.

Journal title	Records	Citations	Average citation	IF (2022)
International journal of pharmaceutics	8	225	28.13	6.510
Acta biomaterialia	6	87	14.50	10.633
International journal of biological macromolecules	6	78	13.00	8.025
Scientific reports	4	66	16.50	4.996
European journal of pharmaceutics and biopharmaceutics	4	42	10.50	5.589
Molecular pharmaceutics	4	100	25.00	5.364
Expert review of anti-infective therapy	3	39	13.00	5.854
Journal of controlled release	3	142	47.33	11.467
Biomaterials	3	134	44.67	15.304
International journal of nanomedicine	3	54	18.00	7.033

225 times. However, the "Journal of controlled release" possesses the maximum average citations, which demonstrates it is relatively more widely recognized and authoritative. Overall, the top 10 journals with up to two-fifths of the total number of publications have an average impact factor (IF) of 8.0775, among which "Biomaterials" ranks highest (IF = 15.304). Additionally, the double overlay of journals reveals the distribution of relationships between journals. In Figure 3, the left side represents the distribution of the citing literature by journal, reflecting the dominant disciplines to which Science Mapping belongs; the right side is the distribution of the corresponding cited literature by journal, indicating which disciplines Science Mapping primarily cites. The orange and purple paths in the graph illustrate that articles published in the MOLECULAR/BIOLOGY/GENETICS and CHEMISTRY/MATERIALS/PHYSICS directions are frequently cited by articles in the MOLECULAR /BIOLOGY/ IMMUNOLOGY and. PHYSICS/ MATERIALS/ CHEMISTRY directions. Moreover, magazines in the same direction are clustered in the same color block to show the reference relationship between different fields.

2.4. The most productive institutions and authors

Figure 4 illustrates the cluster network of institutions and authors cited. A total of 168 institutions and 540 authors were analyzed, and we selected the top representative results for visualization. Subsequently, we analyzed the total number of publications, citations, and citations per article for the 10 most productive institutions and authors. As exhibited in Figure 4A, the University of Porto (13 articles) has the largest number of publications, more than twice as numerous as the second university. And it is most frequently cited by other institutions, reflecting the high credibility of this institution in the field of biomaterials treating *H. pylori*. Nevertheless, the output of the Ocean University of China has been cited more extensively in recent years, probably owing to its more cutting-edge research direction. Despite the lower volume of publications, the University of California San Diego holds the most citations and average citations, with an average of higher than 100 citations per article, which reveals the relatively advanced quality of this institution's publications (Table 2). In addition, the network map of each author's publications and citations over the last decade is depicted in Figure 4B. Among the top 10 authors, each contributing no less than 3 papers, Martins, M. Crastinal is the most prolific contributor to the field. Furthermore, he possesses a total of 253 citations, with the highest citation link strengths (Table 3). A three-Field Plot of authors, keywords, and institutions is exhibited in Figure 4C, which reveals the research orientation of each high-yield author and institution. Figure 4C highlights that the majority of scholars and research institutions have investigated biomaterials for the treatment of *H. pylori* focusing on the areas of chitosan, nanomaterials, drug delivery, and bacterial adhesion. The University of Porto has the broadest research area of any institution, while with a focus on chitosan materials.

2.5. The analysis of keywords and frontiers

As the core of scientific papers, keyword analysis is utilized to track the evolution of knowledge, hot spots, and future research directions. According to Figure 5A, both high occurrences and meaningful keywords of drug or biomaterials are revealed including nanoparticles (Wang et al., 2019), chitosan (Chen et al., 2020), drug-delivery (Darroudi et al., 2021), microspheres (Han et al., 2022), amoxicillin (Butkovich et al., 2021), Clarithromycin (Butkovich et al., 2021), eradication (Butkovich et al., 2021) and release (de Souza et al., 2021). Keywords with a frequency of at least five occurrences were extracted using VOSviewer to obtain a visual network for co-occurrence analysis, and the co-occurrence relationships between various types of keywords were analyzed, resulting in a total of four categories of hotspots for current research. As shown in Figure 5A, all keywords were clustered into four clusters displayed in different colors, and nodes with common attributes were partitioned into a color-coded cluster. Green clusters are mainly associated with *H. pylori* infection, including *Helicobacter pylori*, infection, *in-vitro*, chitosan, treatment, eradication, etc. Blue clusters are mostly relevant to nanoparticles, including nanoparticles, drug delivery, cytotoxicity, apoptosis, etc. Red clusters are largely involved with microparticles and carried drugs regarding amoxicillin, clarithromycin, microspheres and mucoadhesive, etc. Yellow clusters are chiefly concerned with the adhesion and resistance of biomaterials, including adhesion, biomaterials, resistance, etc. The keywords with the strongest bursts in this domain are highlighted in Figure 5B. The red line indicates the time of keyword bursts. Anchored in the burst keywords for discovery, the primary phase features mostly disease and drug keywords concerning gastric cancer, microsomes, and chitosan, suggesting that biomaterials may be applied largely in drug delivery to

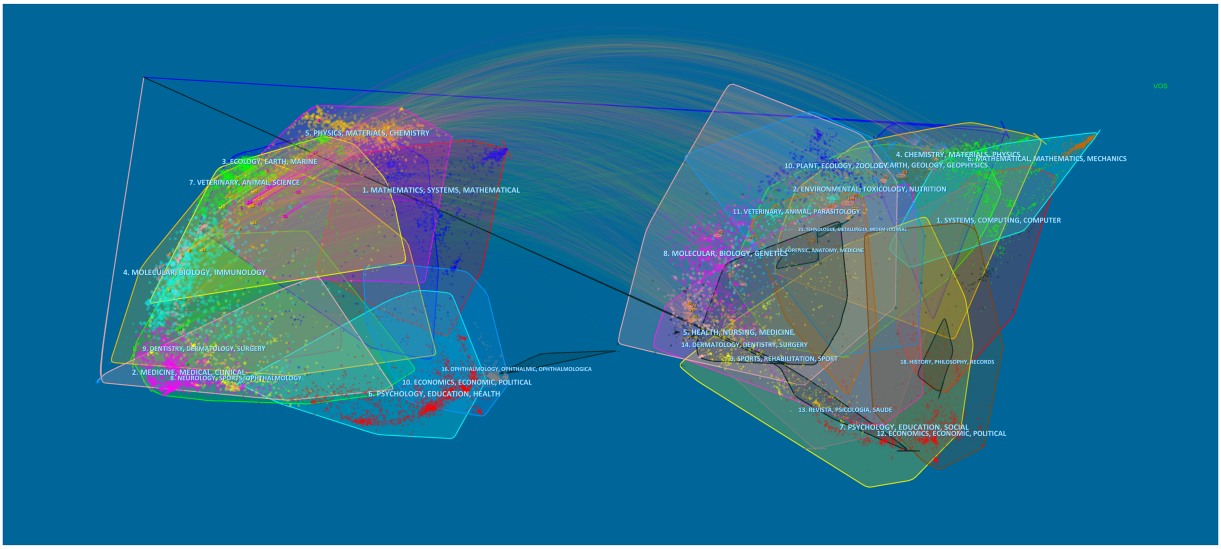

FIGURE 3
The dual-map overlay of journals on biomaterials eradicating *Helicobacter pylori*. The double map overlay of journals shows the relationship between the two and the distribution among journals, with the citing journals on the left and the cited journals on the right.

exert specific functions. In the middle of the period, the keywords "adhesion" and "adsorption" outbreak lasted for 2 years, which illustrates that biomaterials with adsorption and adhesion functions were comparatively promising at that time. Nonetheless, in recent years, with the emergence of drug resistance coming, the development of biomaterials applications has concentrated on antibacterial activity and antibiotic resistance solutions, which will remain a hot topic of research in the future.

2.6. Analysis of keyword evolution and continuity

The landscape generated using CiteSpace keyword clustering in Figure 6A shows 9 clusters, each labeled with the tag #. The 9 clusters are identified as follows: #0 *H. pylori*, #1 pectin, #2 inflammatory bowel disease, #3 bacterial infection, #4 glyceryl mono stearate, #5 bacterial adhesion, #6 nanoemulsion, #7gastric retention, and #8 antibacterial activity. The evolution of the various materials and methods over time is exhibited in each type of cluster. The close temporal connection between the main keywords is better visualized in Figure 6B, where one vertical bar represents one year. As is reflected that in the first 5 years, miscellaneous biomaterials are predominantly implemented in drug delivery, while the latter 5 years are focused on drug resistance applications. Additionally, emergent keywords are considered indicators of emerging trends. In the following section of "main text," this study will primarily overview the application of biomaterials in the eradication of *H. pylori*, and then further investigate the facing challenges and potential opportunities.

3. Main text

The difficulty of eradicating *H. pylori* is manifested in multiple aspects. As depicted in Figure 7, *H. pylori* are sheltered from gastric acid by the enzyme urease on the surface of its outer membrane, which breaks down the urea in the surroundings, thus creating a near-neutral microenvironment (Watanabe et al., 2009). Relying on the continuous movement of its flagellum, *H. pylori* penetrated and anchored on the epithelial cell surface of the gastric mucosa, not only effectively avoiding gastric acid erosion, but also significantly minimizing the effect of gastric emptying (Saha et al., 2010). Conversely, most antibacterial drugs are less active or even inactivated in the extremely acidic environment of the stomach (Khan et al., 2022). Even if not catabolized, regular gastric emptying diminishes the concentration of drug accumulation at the site of infection. Since *H. pylori* colonize deep in the mucus layer, the effective contact of antimicrobial drugs with the organism is blocked, making it impractical for the drugs to be efficacious (Vázquez and Villaverde, 2013). Additionally, *H. pylori* successfully evade the host immune response by modifying its outer membrane proteins to escape recognition by the organism, promoting apoptosis of macrophages, inhibiting the migration and uptake of immune cells, suppressing the T-cell immune response, etc. (Kao et al., 2010). Therefore, exploiting biomaterials that reinforce the body's immune response to *H. pylori* is essential for the eradication of *H. pylori* (Tshibangu-Kabamba and Yamaoka, 2021). Owing to the frequent interchange of DNA, *H. pylori* is susceptible to the development of highly variable strains in continuous infections (Suerbaum et al., 1998). Generally, *H. pylori* infections are persistent, and long-term infections tend to form biofilms, resulting in further resistance (Hathroubi et al., 2018).

The physicochemical properties of biomaterials and their intended routes of delivery have the potential to be systematically tailored to maximize therapeutic efficacy (Khan et al., 2022).

According to our bibliometric analysis, nanoparticles ranked second in the number of occurrences among the occurrence of keywords, trailing only *H. pylori*, indicating nanoparticles play a significant role in the eradication of *H. pylori*. Subsequently, the materials or drugs with a relatively high number of occurrences are "chitosan," "amoxicillin," "microspheres" and "clarithromycin"

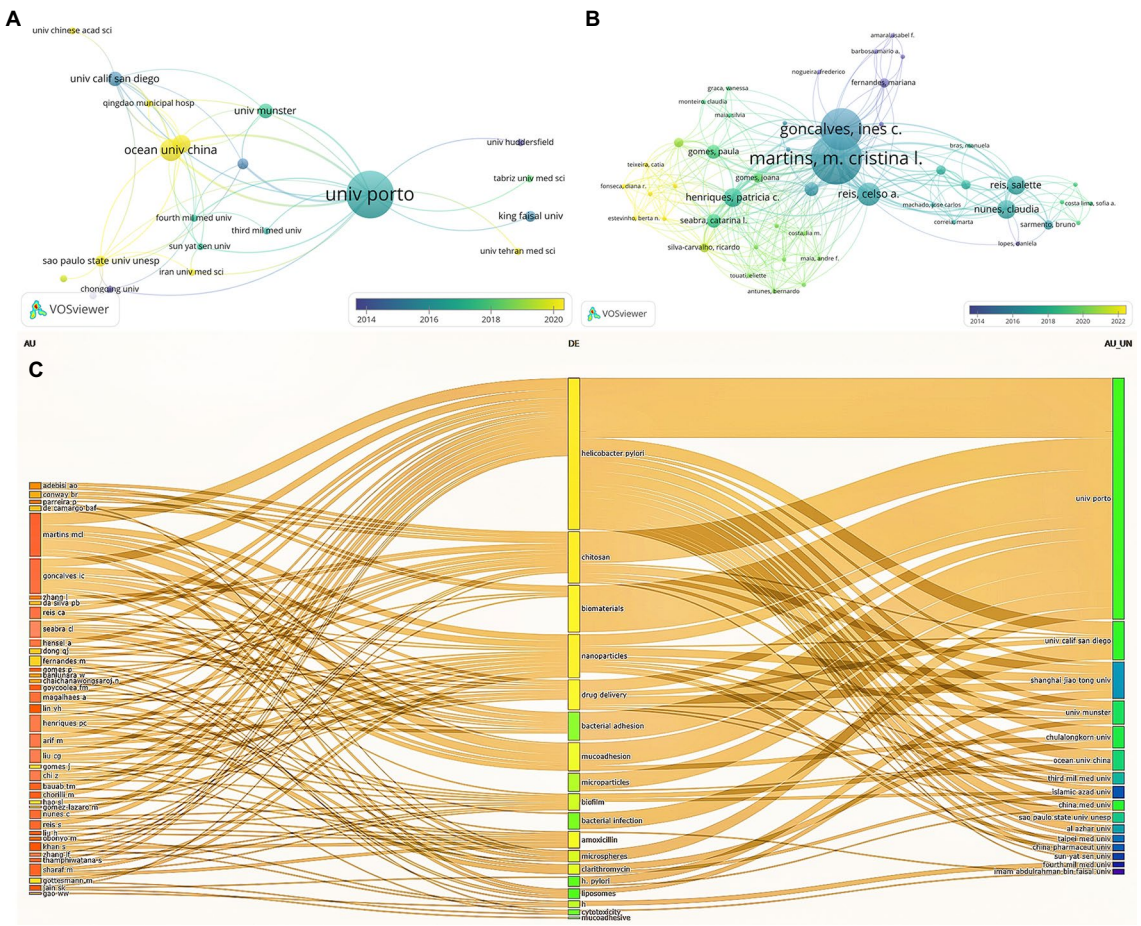

FIGURE 4
Cited institution **(A)**, author cooperation analysis **(B)**, and Three-Field Plot of author, keyword, and institution **(C)**. Each node represents an institution or an author, and the line between the two nodes indicates that they have a co-occurrence relationship. Moreover, the closer the distance, the stronger the relationship **(A,B)**. In **(C)**, the leftmost square represents the author, the middle is the keyword, and the rightmost is the institution and longer squares mean more research.

successively. Primarily this is because chitosan particles increase the stability of the nanoparticle structure and ameliorate the drug release rate to some extent. Amoxicillin and clarithromycin are frequently utilized to eradicate *H. pylori* as the primary optional antibacterial antibiotics in triple and quadruple therapies. Noteworthily, keywords including "drug delivery" and "release" are also listed as high-frequency terms, foreshadowing that biomaterials treat *H. pylori* majorly exert effects by improving the release of drug delivery systems. Biomaterials have improved the delivery and efficacy of a range of drug compounds (Langer, 1990). Most of these materials are designed to extend drug retention time and enable further targeted drug delivery, resulting in efficient eradication with reduced dosage and reduced toxicity to the patient.

Given the characteristics and therapeutic limitations of *H. pylori* eradication, the construction of appropriate drug delivery systems for the efficient delivery of existing antimicrobial drugs at the site of infection is a potential platform technology with relatively low risk and high return compared to novel antibacterial drugs (Hussain et al., 2018). On the basis of bibliometric analysis and literature review, we summarize four dominant directions of biomaterials in the field of *H. pylori* eradication from the historical perspective of biomaterials drug delivery research: (Reshetnyak and Reshetnyak, 2017) Release control biomaterials, (Rajinikanth et al., 2007) Targeted biomaterials, (Hooi et al., 2017) Bionic Biomaterials, and (Capurro et al., 2019) Overcoming *H. pylori* drug resistance. We highlight current challenges in the field of drug delivery, breakthroughs in biomaterials research to overcome these barriers, and future considerations and opportunities for biomaterials in clinical applications.

3.1. Release control biomaterials

Historically, innumerable clinical practices have demonstrated extremely challenging to eradicate *H. pylori* with single drug therapy (Graham, 2014; Boyanova et al., 2019; Tshibangu-Kabamba and Yamaoka, 2021). The contact time of the antibacterial agent with the organism needs to be sufficiently long. Early reports suggested that by increasing the *in vivo* contact time of the drug with *H. pylori*, the eradication efficiency would be significantly enhanced. Clinical experience has established that the necessity to evaluate the pharmacodynamics and pharmacokinetics of the agents to guarantee optimal bioavailability and concentration in the gastric mucosal fluid

TABLE 2 Analysis of the output and citations of the top 10 institutions.

Institute	Records	Citations	Average citations	Link strength
University of Porto	13	279	21.46	57
Ocean University of China	6	39	6.50	26
Al-Azhar University	5	13	2.60	24
University of California San Diego	4	431	107.75	21
University of Münster	4	129	32.25	10
China Medical University	3	151	50.33	14
King Faisal University	3	51	17.00	2
São Paulo State University	3	33	11.00	14
Chongqing University	2	43	21.50	0
China Pharmaceutical University	2	10	5.00	5

TABLE 3 Analysis of the output and co-authorship of the top 10 authors.

Author	Documents	Citations	Average citations	Link strength
Martins, m. Cristina l.	11	253	23.00	46
Goncalves, Ines c.	9	190	21.11	38
Reis, Celso a.	5	82	16.40	28
Arif, Muhammad	5	27	5.40	22
Henriques, Patricia c.	4	49	12.25	20
Sharaf, Mohamed	4	8	2.00	19
Chi, Zhe	4	26	6.50	18
Nunes, Claudia	4	112	28.00	17
Reis, Salette	4	112	28.00	17
Magalhaes, Ana	3	43	14.33	16

after administration is also an essential factor in the difficulty of *H. pylori* eradication (Graham and Dore, 2016). Variable forms of drug delivery systems by using materials with bioadhesive properties are able to maximize the drug residence time in the stomach (Sachin and Karn, 2021). Researchers have developed a variety of gastric retention and release control systems, ranging from bioadhesive systems, mucosal penetration systems, and floating raft systems to micro-motor systems et al., among which biomaterials have played an irreplaceable role in slowing the release rate and increasing drug concentration as novel delivery systems.

3.1.1. Biological adhesion materials

Biological adhesion materials are usually hydrophilic gel polymers containing a multitude of hydrogen bonding groups including carboxy and hydroxyl groups (Wang et al., 2019). The most prevalent polymeric materials utilized for biological adhesion of gastric mucus are chitosan and its derivatives, wheat soluble protein, Polyalkylcyanoacrylate, etc. (Qu et al., 2018). Among mucosal adhesion polymers, deacetylated chitosan is intriguing due to its biodegradability, biological adhesion, and ability to enhance the uptake of active macromolecules (Hejazi and Amiji, 2003). The -NH2 group of chitosan and its derivatives is protonated at the acidic pH of gastric juice and establishes electrostatic interactions with negatively charged gastric mucin and bacterial membranes, thereby exhibiting adhesion properties, and consequently has been developed recurrently for gastric applications (Chaves de Souza et al., 2020; Lang et al., 2020). The lipophilic amino acid residues of maltolysin are capable of interacting with biological tissues, while maltolysin nanoparticles are susceptible to aggregation by pH, temperature, and salt, thus achieving their adhesion properties (Arangoa et al., 2000).

In the recent decade, chitosan nanoparticles or biologically modified materials have been gradually found to be combined with loaded drugs to prolong drug delivery through bioadhesion (Gonçalves et al., 2014). The reacetylated chitosan microspheres developed and optimized by Portero et al. (2002) exhibited controlled water solubility and gelation at acidic pH, leading to prolonged release of encapsulated anti-*H. pylori* drugs. It was revealed that the time of reacetylation is a major factor affecting the drug release and the encapsulation efficiency and antimicrobial activity of the encapsulated compounds. These similar experiments provide a certain foundation for future design optimization of chitosan biomaterials. The *in vivo* and *in vitro* experiments of chitosan nanoparticles against *H. pylori* designed by Luo's team demonstrated that the anti-*H. pylori* effect of chitosan (CS) nanoparticles solution was negatively correlated with pH when pH was 4–6. Moreover, this work revealed that the anti-*H. pylori* effect of 88.5% deacetylated (DD88.5) CS NPs and 95% deacetylated (DD95) CS NPs was 55 and 75%, respectively. A more in-depth study was conducted by Chang et al. (2020) They observed that at pH 2.0, 4,000 g/ml DD95 suppressed the urease activity of *H. pylori* by 37.86 to 46.53%. In the presence of 50 g/mL of the antibiotics amoxicillin, tetracycline, or metronidazole at pH 6.0 and pH 2.0, *H. pylori* counts decreased by 1.51–3.19 and 1.47–2.82 Log

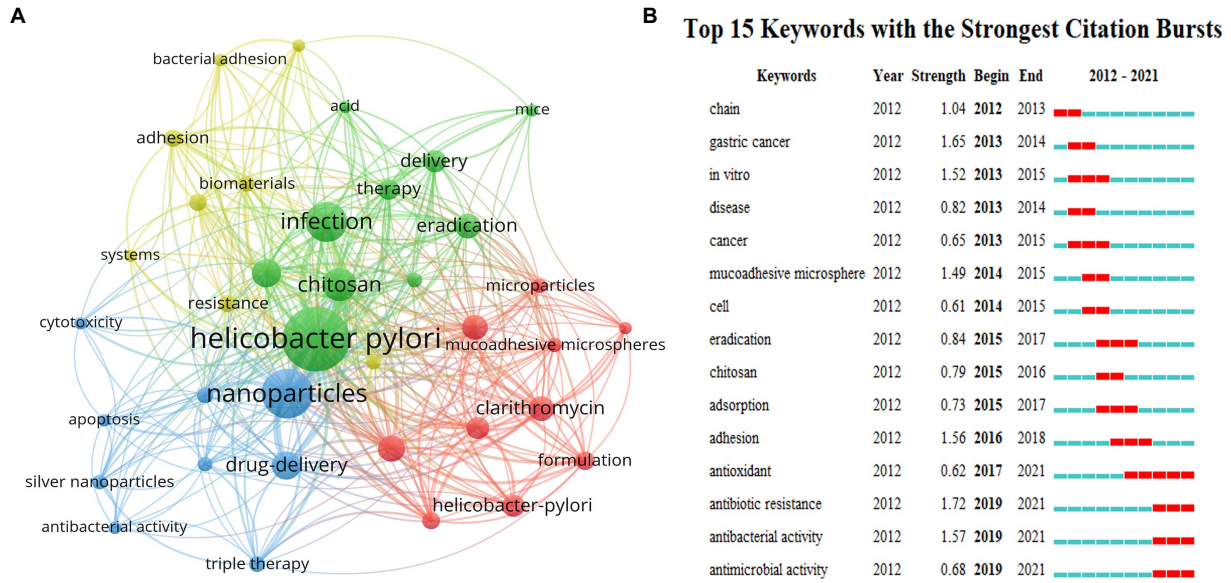

FIGURE 5
Co-occurrence network of keywords with a minimum of 5 occurrences **(A)**. The top 15 keywords with the strongest citation bursts **(B)**. All the keywords are divided into four clusters, each represented by a different color. Every node symbolizes a keyword, and the line between two keywords indicates that they have a co-occurrence relationship. Additionally, the closer the distance, the stronger the relationship **(A)**. Top 15 bursting keywords in articles related to eradication of *H. pylori* by biomaterials. The blue line represents the time line, and the interval at which bursts were found is indicated by the red portion of the blue timeline, representing the start year, end year, and outbreak duration **(B)**.

CFU/mL, respectively, while the addition of the same dose and concentration of DD95 under the same conditions strongly depressed the total *H. pylori* counts by 3.67–7.61 and 6.61–6.70 Log CFU/mL. With the loading of antibiotics such as tetracycline and metronidazole, the delivery system suppressed the adhesion of *H. pylori* to cells, thereby promoting the eradication rate of *H. pylori*. Therefore, biological adhesion materials are promising carriers for the controlled delivery of antimicrobial agents to the gastric cavity and therefore for the eradication of *H. pylori*, a pathogen closely associated with gastric ulcers and possibly gastric cancer.

3.1.2. Mucus-penetrating system

Given that *H. pylori* are colonized under the mucus layer, mucus-penetrating agents facilitate drug delivery to the site of infection and thus enhance eradication rates (Chmiela and Kupcinskas, 2019). Depending on the properties of mucin, a major component of mucus, it is assumed that nanoparticles with hydrophilic, negatively charged surfaces and small particle sizes are capable of effectively penetrating the mucus layer (Nogueira et al., 2013). Previous research has established that positively charged chitosan nanoparticles facilitate mucosal penetration. However, Zhang et al. (2018) designed a biomaterial in which nanoparticles were electrostatically self-assembled with antigen and cell-penetrating peptide (CPP) and then coated with a "mucus-inert" PEG derivative that gradually dissociated from the nanoparticles in the mucus, exposing the CPP-rich core and thus enabling penetration. The experiment results demonstrated that the nanoparticles overcome the mucus barrier for active drug delivery after oral administration. Compared with the positively charged chitosan nanoparticles, the PEG-modified nanoparticles weakened the interaction with mucin and could effectively penetrate the mucus layer to reach the infection site, which further strengthened the elimination rate of *H. pylori*. Consequently, the whole material reduces the contact with gastric mucin and also achieves the effect of drug delivery by osmosis.

In addition to the construction of nanoparticles with a hydrophilic surface, negative charge, and small particle size, the applied magnetic field is capable of facilitating the effective penetration of the drug delivery system into the gastric mucus layer and reaching the site of *H. pylori* infection (Silva et al., 2009). For instance, Chitosan/polyacrylic acid particles co-loaded with superparamagnetic iron oxide nanoparticles and amoxicillin prepared by Yang et al. (2020) were employed as drug nanocarriers for *H. pylori* eradication therapy. The nanocarriers noticeably enhanced the penetration into the gastric mucus layer and improved the eradication of *H. pylori* when exposed to an applied magnetic field. The results showed that all the nanoparticles accumulated at the bottom of the mucus layer after 10 min of the applied magnetic field, indicating that the mucus penetration efficiency of the prepared magnetic nanoparticles could be controlled by the applied magnetic field. Similarly, Walker et al. (2015) prepared a magnetic microhelix system with immobilized urease on the surface by simulating the movement of *H. pylori* through the gastric mucus layer. The results exhibited that the applied magnetic field allowed the system to advance efficiently in the gastric mucus layer, while the surface-immobilized urease significantly promoted the mobility of the microparticles. Therefore, these nanocarriers prolong the residence time of the drug in the stomach, reducing the drug dose and treatment time required for *H. pylori* eradication therapy.

3.1.3. Floating raft system (FRS)

Among the dwelling drug delivery systems, the floating raft system achieves drug gastric retention by floating on the gastric contents for prolonged drug delivery as a result of its low density and

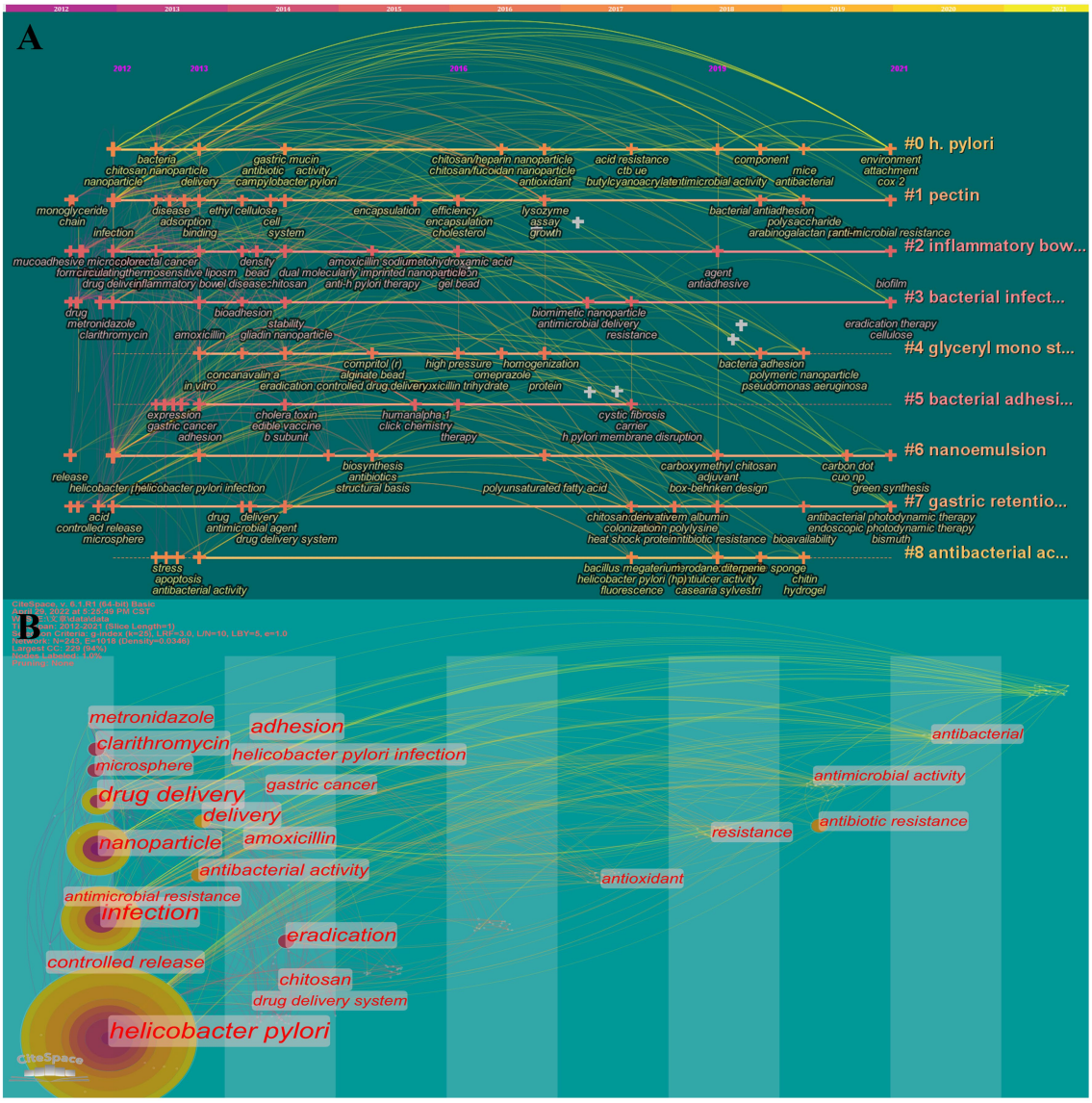

FIGURE 6
Timeline **(A)** and timezone **(B)** of keywords. 11 clusters are shown in A, and each is labeled with the tag #. The smaller the number, the more keywords are included in the cluster. Each node represents a keyword, and the time when the node appears indicates the time when the keyword emerged. The line between nodes indicates the relationship between keywords and the continuity in time.

has been evaluated for maintaining drug delivery and targeting (Thombre and Gide, 2016). Conway's group (Adebisi et al., 2015) developed calcium alginate microspheres by ionic gelation and modified them with chitosan and oil to optimize float ability, adhesion, and drug release. The experimental results revealed that the floating beads remained for at least 24 h. More than 75% of the beads were adherent to the gastric mucosa for more than 8 h and guaranteed drug release, indicating the fresh dosage form ensures better retention time in the stomach than the convention. Additionally, Rajinikanth et al. (2007) demonstrated the feasibility of prolonging the gastric residence time and release rate of metronidazole utilizing an FRS prepared from ion-sensitive *in situ* gels. FRS consists of sodium alginate and gellan gum, sodium citrate and calcium carbonate, and lipids. Release kinetic studies of the selected formulation revealed that FRS had a short-term gelation lag time (3 s) and a duration of up to 24 h, with a reliable slow release of the drug. The refined properties of the selected FRS make it an excellent candidate for gastric-targeted eradication of *H. pylori*.

3.1.4. Nanomotor system

The protracted administration of PPI is prone to side effects involving osteoporosis, vitamin C deficiency, etc. (Pouwels et al., 2011; Heidelbaugh, 2013). Nevertheless, bio-inspired design principles and advances in nanomaterials have generated significant advances in the field of intra-gastrointestinal drug delivery, especially in nano/micro motors, which are essentially chemically neutralized to modulate the harsh acidic environment to neutral and avoid reducing the efficacy of the drug. Micromotors commonly refer to chemically driven nanomotors, which are small devices facilitated by catalytic reactions in liquids (Sánchez et al., 2015). Artificial micromotors enable self-propulsion in the stomach, enhanced retention of intestinal fluid in

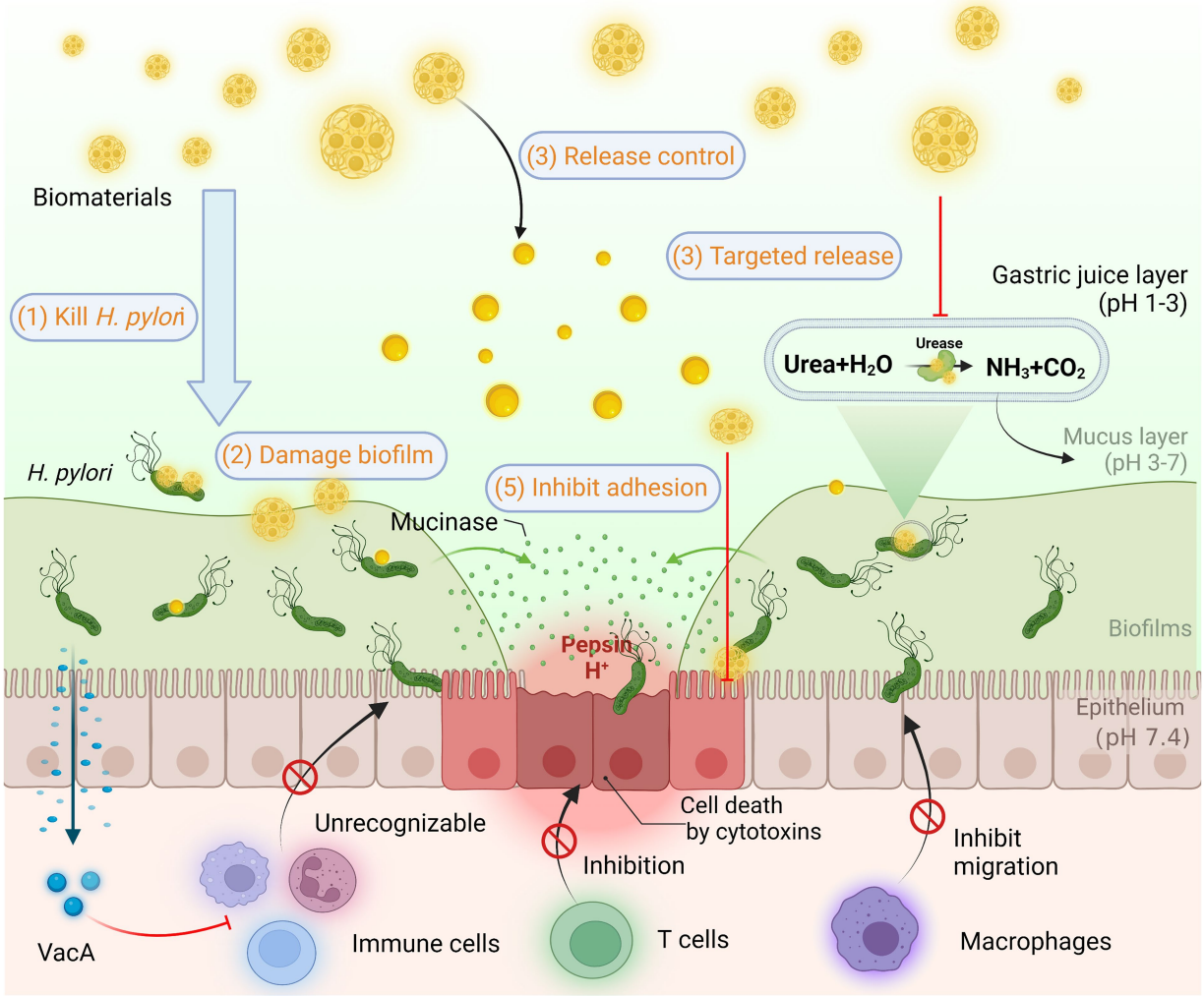

FIGURE 7
Helicobacter pylori infection and common methods of biomaterials in Anti-*H. pylori*. *H. pylori* colonizes and survives for a long time in the body through resistance to acidic environment, biofilm formation, and immune escape. Biomaterials are designed for *H. pylori* eradication by killing *H. pylori*, destroying biofilms, releasing controlled drugs, targeting drug delivery, inhibiting adhesion, and enhancing immunity based on superior biocompatibility.

the gastric mucosal layer, and targeted delivery in the gastrointestinal tract. Walker et al. (2015) demonstrated the ability of magnetic micro propellers to move through gastric mucus gel by simulating the mucus permeation strategy of *H. pylori*.

In regard to eradicating *H. pylori*, Wu et al. (2021) report a nanomotor that allows small molecules of clarithromycin, calcium peroxide nanoparticles (CaO_2) and platinum nanoparticles to be loaded into the motor *via* ultrasound. The nanomotor can rapidly consume gastric acid and temporarily neutralize gastric acid by the chemical reaction of CaO_2. The reaction of CaO2 with gastric juice has been demonstrated by *in vivo* experiments to result in rapid consumption of protons, thereby temporarily neutralizing acid without affecting normal gastric function. In particular, the acid-driven nanomotors can be effectively loaded with antimicrobial drugs and exhibit prominent bactericidal activity. Similarly, Wang et al. (de Ávila et al. 2017) experimented with the efficient propulsion of magnesium-based micromotors in an acidic gastric environment. Upon temporary depletion of gastric acid, they were actively and persistently retained in the gastric mucosa. The experimental results illustrate that acid-driven magnesium-based micromotors efficiently load clinical doses of drugs and exert significant *H. pylori* eradication capabilities. These conclusions implicate the nanomotor as a promising alternative to PPI in *H. pylori* eradication.

3.1.5. Magnetic release control biomaterials

Magnetic drug delivery particle carriers are a tremendously effective modality for delivering drugs to localized disease sites in the gastrointestinal tract. The speed of passage through the GI tract can be slowed down at specific locations by external magnets, thus altering the time and extent of drug absorption in the stomach or intestines (Häfeli, 2004). Furthermore, Thamphiwatana et al. (2013) attached chitosan-modified gold nanoparticles to the outer surface of doxycycline-loaded anionic liposomes. Under a gastric acidic

environment, the gold nanoparticles spontaneously bound to the surface of the anionic liposomes by the mutual attraction of heterogeneous charges, which effectively delayed the drug release. Once the neutral pH environment was reached, the surface charge of gold nanoparticles was reduced to detach from the liposomes, exposing the drug-loaded liposomes, which released the drug by fusing with *H. pylori* cell membranes. Compared with free doxycycline, the gold nanoparticle-encapsulated liposomes displayed a stronger antibacterial effect against *H. pylori*.

With multidisciplinary cross-fertilization, Yang et al. (2014) Chitosan/polyacrylic acid particles physically co-loaded with superparamagnetic iron oxide nanoparticles and amoxicillin (SPIO/AMO@PAA/CHI) were used as drug nanocarriers for *H. pylori* eradication therapy. *In vitro* and *in vivo* results showed that the designed SPIO/AMO@PAA/CHI nanoparticles were biocompatible and could retain the biofilm inhibitory and bactericidal effects of amoxicillin against *H. pylori*. In addition, the mucosal adhesion properties of chitosan allow SPIO/AMO/PAA/CHI nanoparticles to adhere to the gastric mucus layer and to rapidly cross the mucus layer after exposure to a magnetic field. Consequently, the application of this nanocarrier allows for prolonged drug residence time in the stomach, reduced drug doses, and treatment cycles for *H. pylori* eradication therapy (Yun et al., 2015).

3.2. Targeted biomaterials

To date, polymers that respond to numerous different triggers have been developed and explored for biomaterial applications (Chen et al., 2019). The aims of each of these systems are to promote drug accuracy, as well as to augment the quality of life of patients. Recently, stimulus-responsive "smart" biomaterials have been designed to initiate drug release in response to a range of environmental stimuli (e.g., pH, urel, photo response). In this section, we highlight specifically targeted drug delivery biomaterials for the treatment of *H. pylori* from multiple perspectives.

3.2.1. PH-response biomaterials

pH-sensitive specific materials hold promising prospects for a widespread application in anti-*H. pylori* drug delivery systems. Su et al. (2016) synthesized a poly (glutamic acid-arginine) complex peptide, which exhibited different morphologies in different pH environments to control drug release. At pH 2.5, the nanoparticles formed by peptide self-assembly were dense and intact spheres with little release of amoxicillin. The peptide nanoparticles exhibited a diffuse state when pH 7.0, therefore contributing to the steady release of amoxicillin. Furthermore, Jing et al. (2016) designed and synthesized a pH-response drug delivery system against *H. pylori* using UCCs/TPP nanoparticles encapsulated with amoxicillin. The results showed that the amoxicillin- UCCs /TPP nanoparticles had superior PH-sensitivity and could delay the release of amoxicillin in gastric acid, enabling the effective delivery and targeting of the drug to the survival region of *H. pylori*. The protective effect of these bio-nanoparticles on amoxicillin and the controlled release resulted in the inhibition of *H. pylori* growth about 5.1 times higher than that of single amoxicillin.

In a further breakthrough, low molecular weight rockrose gums/CS-N-Arg NPs have been developed (Lin et al., 2017). The NPs were further cross-linked with genipin to obtain pH-responsive nanogels. Ultimately, they were found to exert inhibitory effects on *H. pylori* adherence and preventive effects on pathogen-induced gastric epithelial cytotoxicity. Recently, Yan et al. (2021) report a pH-responsive persistent luminescence enzyme for *in vivo* imaging and inactivation of *H. pylori*. The persistent luminescence enzyme, composed of mesoporous silica-coated sustained luminescence nanoparticles, Au nanoparticles, and chitosan-benzoic acid, exhibits good resistance to gastric acid corrosion and exhibiting pH-activated dual-nano activity, thereby catalyzing the performance of bactericidal reactive oxygen species.

3.2.2. Urel targeted materials

The urea transport channel protein (Urel) is one of the most essential factors for the survival of *H. pylori* in the stomach, as it modulates the opening and closing state according to the pH value of the stomach (Cui et al., 2019). UreI is utilized as a target for delivering drugs to block the transport of urea and disrupt the survival environment of *H. pylori* so as to make it fail to colonize the gastric mucosa, thereby achieving the eradication of *H. pylori*. Building on the UreI-mediated targeted drug delivery system, scientists have invented biological nanomaterials for the specific eradication of *H. pylori*. Luo et al. (2018) reported that ureido-conjugated chitosan showed the ability to target UreI specifically expressed by *H. pylori*. The ability of the drug delivery system constructed on the basis to eliminate *H. pylori* was significantly enhanced. Analogously, Cong et al. (2019) coupled carboxymethyl chitosan modified with stearic acid to urea and presented exceptional *H. pylori* targeting and anti-*H. pylori* efficacy as well.

3.2.3. Photo responsive biomaterials

Photo-responsive therapy, a therapeutic technique in which a photosensitizer oxidizes biomolecules and causes irreversible damage by generating reactive oxygen species under laser irradiation, has attracted increasing attention as a promising strategy for eliminating bacteria (Huang et al., 2012; Jeong et al., 2014). To develop a photo-responsive *H. pylori*-based therapeutic regimen, Na et al. (Im et al., 2021) proposed a photo-responsive system targeting *H. pylori* consisting of multiple 3′-sialoyl lactose (3SL)-coupled poly (l-lysine)-based photosensitizers (p3SLP). P3SLP achieves specific delivery of *H. pylori*-based drugs through the specificity between 3SL and sialic acid-binding adhesin (SabA) on the membrane of *H. pylori* interaction to achieve specific *H. pylori*-based drug delivery (Garcez et al., 2010). This is principally attributed to the fact that one of the outer membrane proteins of *H. pylori* is sialic acid-binding adhesin (SabA), while the 3SL receptor is not expressed in mammalian cells thus avoiding undesirable phototoxicity to normal cells (Ling et al., 2012). The authors' gastrointestinal assays in *H. pylori*-infected mice exhibited that the photo-responsive system had a pronounced *H. pylori*-specific antibacterial effect with no side effects on normal tissues. Additionally, an anti-inflammatory response was observed at the site of infection following p3SLP treatment. Although the clinical application of photo-responsive treatment of *H. pylori* is still an underdeveloped field, this approach does not contribute to adverse drug resistance compared to conventional antibiotic-based treatment (Demidova and Hamblin, 2004; Dai et al., 2009). However, the specific wavelength of laser light required for a

particular type of photosensitizer varies from one to another. Therefore, we can continuously explore more photosensitizers to improve the potential of photosensitization therapy for *H. pylori* eradication (Park et al., 2016).

3.3. Bionic biomaterials

Cell membranes have attracted extensive attention in the field of biomedicine in recent years due to their properties concerning prolonged circulation time *in vivo* and homologous targeting. For example, natural cell membranes are encapsulated with nanoparticles in their cores as a shell, allowing the nanoparticles to possess the biological properties of natural cells.

3.3.1. Liposomes

Liposomes (LPs) LPs are defined as lipid vesicles composed of one or more phospholipid bilayers, with spherical shapes and sizes between 25 and 1,000 nm. They can encapsulate lipophilic and hydrophilic drugs in lipid membranes and aqueous cores, respectively. LPs show many advantages, such as the flexibility to change their chemical composition and, moreover, allow for surface functionalization or targeted delivery. Considering the cell membrane-like structure of LPs, they exhibit good biocompatibility, low toxicity, etc. Thamphiwatana et al. (2013) evaluated the activity of LPs containing integrated linolenic acid (LLA), naming the system LipoLLA, against *H. pylori*. Several free fatty acids, including LLA, have been investigated as new drugs because of their antibacterial activity against various bacteria. In this study, fusion with bacteria was confirmed by a lipophilic fluorophore label, illustrating that LipoLLA was able to cause some damage to the bacterial membrane.

Recently, Martins' team employed precrol®ATO5 and Miglyol®812 as lipids and Tween®60 as a surfactant to prepare nanostructured lipid carriers (NLC). Seabra et al. (2018) demonstrated that NLC, even without any drug loading, is capable of destroying *H. pylori* at low concentrations. NLC is designed to rapidly bind and destroy the *H. pylori* bacterial film without affecting other bacteria, resulting in bacterial death. This study reveals that NLC is a bright avenue to explore in the quest for innovative antibiotic-free treatments against *H. pylori* infection.

3.3.2. Membrane biomaterials

The application of natural cell membranes in the field of biomimetic nanomedicine has attracted much attention in recent years on account of their prolonged circulation time *in vivo* and outstanding biocompatibility. For instance, natural cell membranes are encapsulated with nanoparticles in their cores as a shell, thus giving the nanoparticles the biological properties of natural cells. Angsantikul et al. (2018) coated gastric epithelial cell membranes with clarithromycin-loaded polymers, and the nanoparticles preferentially adhered to the surface of *H. pylori* and presented better therapeutic effects in an *in vitro* test. In addition to host cell membrane mimicry, pathogenic cell membrane mimicry nanoparticles could interfere with the interaction between pathogenic bacteria and the host. The NPs compete with *H. pylori* for the binding sites on the host cells and detach the adherent *H. pylori*, exerting a noteworthy anti-adhesive effect (Zhang et al., 2019). These explorations are proved to be a pioneering choice as a coating material to boost the biocompatibility of drugs, exhibiting properties concerning immune escape, high circulation time, moderating elimination of the reticuloendothelial system, mimics cellular glycocalyx to prevent serum protein adsorption and counteract complement response.

3.3.3. Phage biomaterials

Specially modified phages are available to bind to specific pathogenic bacteria. Aiming to strengthen the antibacterial ability of phages, genetic engineering and chemotherapeutic drug coupling technologies have been established for the modification of phages and drug delivery. Cao et al. (2000) constructed a modified phage M13 to express a shell protein that fused with *H. pylori* cell membrane surface-specific antigen. The results indicated that the recombinant phage M13 exhibited bactericidal effects and specifically inhibited the growth of six *H. pylori* strains. Moreover, oral pretreatment with M13 significantly attenuated the colonization of *H. pylori* in the stomach of mice. Sequentially, Ardekani et al. (2013) successfully exploited an M13 phage-based nanovirus. Through sodium dodecyl sulfate-polyacrylamide gel electrophoresis and Western blotting analysis, the nanovirus was confirmed to inhibit urease activity, further disrupting the survival environment of *H. pylori*. There are few studies on phages against *H. pylori*, and no studies have been conducted on their application as drug carriers in the field of anti-*H. pylori*. As the mechanism of phage bactericidal activity is completely different from that of antibacterial drugs, phage therapy is expected to be an attractive approach to addressing the multidrug resistance of *H. pylori*. However several human gut microbiota research studies have demonstrated that phages perform a function in intestinal homeostasis (Ferreira et al., 2022). Currently, phages are thought to precisely affect the intestinal microbiota and exert beneficial effects on numerous gastrointestinal disorders (Muñoz et al., 2020). However, whether the M13 phages discussed above have a specific impact on the intestinal microbiota still deserves a lot of investigation.

3.4. Overcoming *Helicobacter pylori* drug resistance

Some researchers have recognized *H. pylori* gene mutations, for instance, infB and rpl22 (Binh et al., 2014), as the root cause of drug resistance (Gong and Yuan, 2018). Currently, the majority of clinical *H. pylori* therapies are antibiotic therapies. Each antibiotic is associated with a specific target, and when the corresponding target is structurally altered, the antibiotic is prevented from exerting its original efficacy (Gong and Yuan, 2018). The integration of a multi-target antibacterial mechanism into the drug delivery system is expected to reduce the drug resistance of *H. pylori*. As portrayed in Figure 8, multiple target eradication modalities for *H. pylori* have been developed in recent years. Metallic materials in disrupting *H. pylori* biofilm and urease activity (de Reuse et al., 2013), and probiotic materials in relieving inflammation, mitigating *H. pylori* adhesion, and enhancing immune response (Zhang et al., 2022) have all been demonstrated to be promising alternative therapeutic modalities to overcome antibiotic resistance.

3.4.1. Metallic biomaterials

Metal nanoparticles exert antibacterial effects through metal ion release, oxidative stress, and non-oxidative stress (Zaidi et al., 2017).

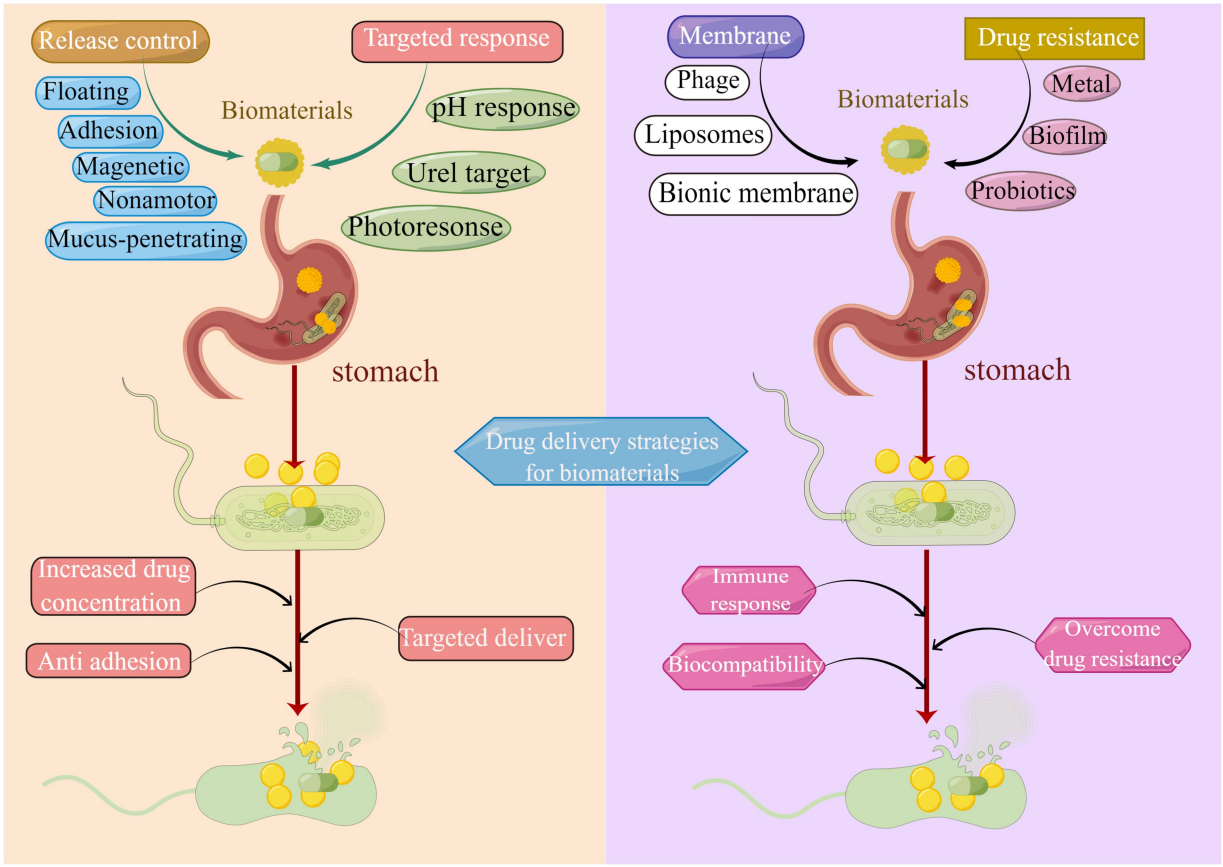

FIGURE 8
Drug delivery strategies of biomaterials in *H. pylori* eradication. Common strategies utilized for drug release control include bioadhesion, mucosal penetration, floating raft, nanomotor, and magnetic materials. Methods applied for targeted drug delivery are pH response, Urel targeting, and photo response. Biomimetic biological membrane materials are liposomes, cell membranes, and phages. Strategies to overcome drug resistance include metal materials, probiotic materials, and the elimination of biofilm.

As a result of various antibacterial mechanisms, metal nanoparticles are efficient at low concentrations and not easily induced to develop drug resistance. It was demonstrated that the antibacterial activity of silver nanoparticles not only inhibited the respiratory system and biofilm formation of *H. pylori* but also directly interfered with the nickel in the urease of *H. pylori* to inactivate the urease, exerting the antibacterial efficacy (Amin et al., 2012). Sreelakshmi et al. (2011) synthesized silver nanoparticles using Glycyrrhiza glabra root extract, which has known therapeutic activity in the treatment of gastric ulcers. In the agar diffusion test, the nanoparticles showed activity against *H. pylori* and can be considered a new method to eradicate this bacterium in the treatment of gastric ulcers.

Besides silver, other metals have also been used in the biosynthesis of nanoparticles as an alternative treatment for *H. pylori* infection. It is worth mentioning that ZnO NPs have been approved and generally recognized as safe for normal cells. Chakraborti et al. (2013) employed polyethyleneimine (PEI) functionalized ZnONPs (ZnO-PEI NPs), which greatly reduced the surface energy of ZnO NPs. The ZnO-PEI NPs were effective against *H. pylori* metronidazole-resistant strains, and their mechanism of action included promoting the production of intracellular reactive oxygen species and causing cell membrane and RNA damage. Wu et al. (2019) designed bifunctional magnetic nanoparticles placed in a moderate AC magnetic field to locally deposit heat and effectively inhibit the growth and virulence of *H. pylori in vitro*. The survival rate of *H. pylori* was reduced to 1/7 and 1/5 after treatment with amoxicillin-loaded metal nanoparticles compared with that of amoxicillin alone or blank metal nanoparticles, respectively. The mechanism may be the damage of the cell membrane and increased penetration of amoxicillin into *H. pylori*, and thus elevated the deracinating efficiency of drug-resistant strains. In clinical applications and against intestinal microbial infections, pH-sensitive cis-aconitate anhydride-modified anti-*H. pylori* conjugated gold nanostars synthesized by Zhi et al. (2019). The near-infrared laser photothermal treatment enhanced the bactericidal effect, reduced the emergence of *H. pylori* drug resistance, and even eradicated drug-resistant strains of *H. pylori* isolated from clinical patients. Additionally, most patients were eliminated from the body within 7 days after the completion of treatment. Therefore biomaterials do hold a promising clinical translation in the eradication of *H. pylori*. However, the side effects of metal nanomaterials and their dosages on normal tissues are not well investigated. Kim et al. (2010) evaluated the toxic effects of 30 mg/kg, 125 mg/kg, and 500 mg/kg of silver nanoparticles injected into rats. As a result, rats injected with more than 125 mg/kg of silver nanoparticles exhibited toxic reactions and weight loss in the liver. The team revealed that the minimum dose at which harmful effects were observed and the minimum dose at which

adverse effects were observed were determined to be 125 mg/kg and 30 mg/kg, respectively. Accordingly, the tendency of most metal nanoparticles to accumulate in organs such as the kidney (Garcia et al., 2016), liver, lung, and spleen, as well as the under-studied toxicity of metal nanoparticles to gastric cell lines, have limited the use of metal nanoparticles in the treatment of *H. pylori*.

3.4.2. Elimination of biofilm

Bacterial biofilm formation is an overwhelming mechanism of bacterial drug resistance (Chen et al., 2018). Since the discovery of *H. pylori* biofilm in clinical patients, the problem of drug resistance caused by *H. pylori* biofilm has become a hot topic of interest. It has been exhibited that natural products containing N-acetylcysteine, polysaccharide sulfate, and curcumin hold the ability to inhibit the formation of *H. pylori* biofilm, while alginate lyase can eliminate *H. pylori* biofilm by disrupting the biofilm structure (Bugli et al., 2016). On this foundation, Gurunathan et al. (2015) confirmed that the silver nanoparticles stabilized with N-acylhomoserine lactase significantly inhibited the formation of *H. pylori* biofilm, which may be related to the inhibition of biofilm population sensing (Gopalakrishnan et al., 2020).

3.4.3. Hydrogen therapy

Interestingly, hydrogen therapy has previously been applied to eradicate *H. pylori*. Wang's group has presented a pH-responsive metal–organic backbone hydrogen nanoparticle (Pd(H) @ZIF-8). The nanoparticle was wrapped in ascorbyl palmitate hydrogel to target and adhere to the site of inflammation by electrostatic interactions, and thereafter hydrolyzed at the site of inflammation by an enriched matrix metalloproteinase. The released Pd(H) @ZIF-8 nanoparticles are further broken down by gastric acid to produce zinc ions (Zn^{2+}) and hydrogen gas, thus effectively disintegrating *H. pylori* and alleviating inflammation while repairing the damaged gastric mucosa. Unexpectedly, animal experiments have demonstrated that this biomaterial also can avoid intestinal flora dysbiosis, thus providing a more precise, effective, and healthy strategy for the treatment of *H. pylori* infection (Zhang et al., 2022).

3.4.4. Probiotic biomaterials

Probiotics are defined as live microorganisms that, when given in sufficient amounts, provide benefits to the host (Chen et al., 2019). Recent investigations have indicated that probiotics are capable of increasing antibiotic activity and may block some resistance mechanisms. For instance, in a meta-analysis, the addition of probiotics to triple therapy was observed to enhance the eradication rate of *H. pylori* by >12% (Lau et al., 2016). Furthermore, probiotics dramatically minimize the adverse effects of treatment regimens ranging from maintaining intestinal flora homeostasis, moderating inflammation, and diminishing *H. pylori* adhesion, to elevating the immune response (Lionetti et al., 2010). The antimicrobial, immunomodulatory, and antioxidant properties of lactoferrin increased when it was attached to the surface of bionic nanocrystals (Nocerino et al., 2014). Fulgione et al. (2016) designed a combination material consisting of bionic hydroxyapatite nanoparticles and *Lactobacillus paracasei* probiotic supernatant based on this efficacy as an alternative therapy for *H. pylori* infection. The experimental results demonstrated that the supernatant group of lactoferrin (200–600 μg/mL) plus *Lactobacillus paracasei* had higher antibacterial activity than the conventional antibiotic combination (amoxicillin 200–600 μg/mL, clarithromycin 200–600 μg/mL), even lower levels of pro-inflammatory cytokines such as IFN-γ and higher concentrations of IgG antibodies in the body. This further reveals that probiotics may ameliorate *H. pylori*-induced gastrointestinal inflammation and improve immunity, thus increasing eradication rates (Lin et al., 2020). Consequently, the combination of probiotics and biomaterials is anticipated to be an attractive approach to drug resistance or adjuvant therapy for *H. pylori* infection (Chen et al., 2018).

4. Conclusion

In a nutshell, this paper primarily investigates the application of biomaterials in the eradication of *H. pylori* in the last decade using bibliometric analysis from multiple perspectives, ranging from the number of annual publications to hot keywords of research. Subsequently, we explored the research hotspots in each period and conducted a comprehensive literature review with reference to the evolution of the keywords. Moreover, this study analyzed the characteristics of *H. pylori* infection and the underlying reasons for its difficult eradication and focused on drug delivery strategies and novel therapeutic approaches to maximize *H. pylori* eradication rates while mitigating drug resistance.

With the evolution of biomaterials for drug delivery in the last decades, there has been a dramatic expansion in the development of biomaterials for controlled release, using adhesion, floating raft, nanomotor, and magnetic-based mechanisms to control the release rate of the incorporated drug. In these biomaterials, chitosan exerts a constructive role. However, the anti-*H. pylori* activity of chitosan and its derivatives are influenced by various parameters, with significant discrepancies in the degree of deacetylation, modification groups, and molecular weight required for different flora. Therefore, their safety and stability in clinical applications require further refinement and validation. In recent years, targeted "smart" biomaterials have been designed to initiate target responses to *H. pylori* based on a range of environmental stimuli regarding pH, urel, and photo response. Besides, novel biomaterials in other fields have been developed that can be remotely triggered by stimuli including ultrasound, electric current, and magnetic fields for on-demand drug delivery. Hence there is considerable potential for targeted drug delivery against *H. pylori*. In terms of cell membranes, liposomes and biofilm materials have been engineered as novel bionic drug delivery systems owing to their extended *in vivo* circulation time and homologous targeting properties. Furthermore, Phage therapies are emerging in the field of anti-*H. pylori* and their specificity, low resistance, and extensive sources make them a promising alternative for the prevention and control of *H. pylori* infection. Of necessity, phage therapy presents problems in terms of dose and duration of treatment as well as potential toxicity and needs to be researched extensively as a novel drug delivery system. Materials such as metallic biomaterials that perform the function of disrupting the biofilm formed by *H. pylori* have an irreplaceable role in alleviating drug resistance. Generally, probiotic composites are employed to assist in the eradication of *H. pylori* as well, while the key to boosting its clinical value lays clarifying the timing, dosage, and duration of probiotic addition. In conclusion, despite the achievements of anti-*H. pylori* drug delivery strategies, there are still

numerous challenges for anti-*H. pylori* drug delivery strategies given the high complexity of *H. pylori* infection. In the context of the global bacterial drug resistance problem, biomaterials will certainly create more possibilities for the development and practical application of innovative antimicrobial drug delivery systems in the next few years as they are continuously tried and optimized in clinical trials.

Author contributions

YiZ: conceptualization, methodology, and funding acquisition. CS and ZX: writing–original draft preparation. CH performed the statistical analysis. XX: screening literature. YaZ and BC: validation and software. YiZ and CH: reviewing and editing. All authors contributed to the article and approved the submitted version.

Funding

This work was supported by the National Natural Science Foundation of China (Grant No. 82170580) and Double-Thousand Plan of Jiangxi Province (Grant No. jxsq2019201028).

Acknowledgments

The figures were created with www.biorender.com and www.figdraw.com.

Conflict of interest

The authors declare that the research was conducted in the absence of any commercial or financial relationships that could be construed as a potential conflict of interest.

The handling editor ZG declared a past co-authorship with the author CH.

Publisher's note

References

Adebisi, A. O., Laity, P. R., and Conway, B. R. (2015). Formulation and evaluation of floating mucoadhesive alginate beads for targeting *Helicobacter pylori*. *J. Pharm. Pharmacol.* 67, 511–524. doi: 10.1111/jphp.12345

Amin, M., Anwar, F., Janjua, M. R., Iqbal, M. A., and Rashid, U. (2012). Green synthesis of silver nanoparticles through reduction with *Solanum xanthocarpum* L. berry extract: characterization, antimicrobial and urease inhibitory activities against *Helicobacter pylori*. *Int. J. Mol. Sci.* 13, 9923–9941. doi: 10.3390/ijms13089923

Angsantikul, P., Thamphiwatana, S., Zhang, Q., Spiekermann, K., Zhuang, J., Fang, R. H., et al. (2018). Coating nanoparticles with gastric epithelial cell membrane for targeted antibiotic delivery against *Helicobacter pylori* infection. *Adv. Therap.* 1:16. doi: 10.1002/adtp.201800016

Arangoa, M., Ponchel, G., Orecchioni, A., Renedo, M., Duchene, D., and Irache, J. (2000). Bioadhesive potential of gliadin nanoparticulate systems. *Eur. J. Pharm. Sci.* 11, 333–341. doi: 10.1016/S0928-0987(00)00121-4

Ardekani, L. S., Gargari, S. L., Rasooli, I., Bazl, M. R., Mohammadi, M., Ebrahimizadeh, W., et al. (2013). A novel nanobody against urease activity of *Helicobacter pylori*. *Int. J. Infect. Dis.* 17, e723–e728. doi: 10.1016/j.ijid.2013.02.015

Binh, T. T., Shiota, S., Suzuki, R., Matsuda, M., Trang, T. T., Kwon, D. H., et al. (2014). Discovery of novel mutations for clarithromycin resistance in *Helicobacter pylori* by using next-generation sequencing. *J. Antimicrob. Chemother.* 69, 1796–1803. doi: 10.1093/jac/dku050

Boyanova, L., Hadzhiyski, P., Kandilarov, N., Markovska, R., and Mitov, I. (2019). Multidrug resistance in *Helicobacter pylori*: current state and future directions. *Expert. Rev. Clin. Pharmacol.* 12, 909–915. doi: 10.1080/17512433.2019.1654858

Bugli, F., Palmieri, V., Torelli, R., Papi, M., De Spirito, M., Cacaci, M., et al. (2016). In vitro effect of clarithromycin and alginate lyase against *Helicobacter pylori* biofilm. *Biotechnol. Prog.* 32, 1584–1591. doi: 10.1002/btpr.2339

Butkovich, N., Li, E., Ramirez, A., Burkhardt, A. M., and Wang, S. W. (2021). Advancements in protein nanoparticle vaccine platforms to combat infectious disease. *Wiley Interdiscip. Rev. Nanomed. Nanobiotechnol.* 13:e1681. doi: 10.1002/wnan.1681

Cao, J., Sun, Y., Berglindh, T., Mellgård, B., Li, Z., Mårdh, B., et al. (2000). *Helicobacter pylori*-antigen-binding fragments expressed on the filamentous M13 phage prevent bacterial growth. *Biochim. Biophys. Acta* 1474, 107–113. doi: 10.1016/S0304-4165(00)00005-2

Capurro, M. I., Greenfield, L. K., Prashar, A., Xia, S., Abdullah, M., Wong, H., et al. (2019). VacA generates a protective intracellular reservoir for *Helicobacter pylori* that is eliminated by activation of the lysosomal calcium channel TRPML1. *Nat. Microbiol.* 4, 1411–1423. doi: 10.1038/s41564-019-0441-6

Chakraborti, S., Bhattacharya, S., Chowdhury, R., and Chakrabarti, P. (2013). The molecular basis of inactivation of metronidazole-resistant *Helicobacter pylori* using polyethyleneimine functionalized zinc oxide nanoparticles. *PLoS One* 8:e70776. doi: 10.1371/journal.pone.0070776

Chang, S. H., Hsieh, P. L., and Tsai, G. J. (2020). Chitosan inhibits *Helicobacter pylori* growth and urease production and prevents its infection of human gastric carcinoma cells. *Mar. Drugs* 18:542. doi: 10.3390/md18110542

Chaves de Souza, M. P., de Mattos, N. H., Pedreiro, L. N., Boni, F. I., dos Santos Ramos, M. A., Bauab, T. M., et al. (2020). Design of Mucoadhesive Nanostructured Polyelectrolyte Complexes Based on chitosan and Hypromellose phthalate for metronidazole delivery intended to the treatment of *Helicobacter pylori* infections. *Pharmaceutics* 12:1211. doi: 10.3390/pharmaceutics12121211

Chen, Y., Li, Y., Guo, L., Hong, J., Zhao, W., Hu, X., et al. (2020). Bibliometric analysis of the Inflammasome and Pyroptosis in brain. *Front. Pharmacol.* 11:626502. doi: 10.3389/fphar.2020.626502

Chen, X., Li, P., Shen, Y., Zou, Y., Yuan, G., and Hu, H. (2019). Rhamnolipid-involved antibiotics combinations improve the eradication of *Helicobacter pylori* biofilm in vitro: a comparison with conventional triple therapy. *Microb. Pathog.* 131, 112–119. doi: 10.1016/j.micpath.2019.04.001

Chen, X.-n., Shen, Y.-n., Li, P.-y., Zou, Y.-q., and Hu, H.-y. (2018). Bacterial biofilms: characteristics and combat strategies. *Acta Pharm. Sin.* 12, 2040–2049. doi: 10.16438/J.05134870.2018-0892

Chen, Q., Wang, C., Zhang, X., Chen, G., Hu, Q., Li, H., et al. (2019). *In situ* sprayed bioresponsive immunotherapeutic gel for post-surgical cancer treatment. *Nat. Nanotechnol.* 14, 89–97. doi: 10.1038/s41565-018-0319-4

Chen, L., Xu, W., Lee, A., He, J., Huang, B., Zheng, W., et al. (2018). The impact of *Helicobacter pylori* infection, eradication therapy and probiotic supplementation on gut microenvironment homeostasis: an open-label, randomized clinical trial. *EBioMedicine* 35, 87–96. doi: 10.1016/j.ebiom.2018.08.028

Chmiela, M., and Kupcinskas, J. (2019). Review: pathogenesis of *Helicobacter pylori* infection. *Helicobacter* 24:e12638. doi: 10.1111/hel.12638

Coker, O. O., Dai, Z., Nie, Y., Zhao, G., Cao, L., Nakatsu, G., et al. (2018). Mucosal microbiome dysbiosis in gastric carcinogenesis. *Gut* 67, 1024–1032. doi: 10.1136/gutjnl-2017-314281

Cong, Y., Geng, J., Wang, H., Su, J., Arif, M., Dong, Q., et al. (2019). Ureido-modified carboxymethyl chitosan-graft-stearic acid polymeric nano-micelles as a targeted delivering carrier of clarithromycin for *Helicobacter pylori*: preparation and in vitro evaluation. *Int. J. Biol. Macromol.* 129, 686–692. doi: 10.1016/j.ijbiomac.2019.01.227

Cui, Y., Zhou, K., Strugatsky, D., Wen, Y., Sachs, G., Zhou, Z. H., et al. (2019). pH-dependent gating mechanism of the *Helicobacter pylori* urea channel revealed by cryo-EM. *Sci. Adv.* 5:8423. doi: 10.1126/sciadv.aav8423

Dai, T., Huang, Y. Y., and Hamblin, M. R. (2009). Photodynamic therapy for localized infections—state of the art. *Photodiagn. Photodyn. Ther.* 6, 170–188. doi: 10.1016/j.pdpdt.2009.10.008

Darroudi, M., Gholami, M., Rezayi, M., and Khazaei, M. (2021). An overview and bibliometric analysis on the colorectal cancer therapy by magnetic functionalized

nanoparticles for the responsive and targeted drug delivery. *J. Nanobiotechnol.* 19:399. doi: 10.1186/s12951-021-01150-6

de Ávila, B. E., Angsantikul, P., Li, J., Angel Lopez-Ramirez, M., Ramírez-Herrera, D. E., Thamphiwatana, S., et al. (2017). Micromotor-enabled active drug delivery for in vivo treatment of stomach infection. *Nat. Commun.* 8:272. doi: 10.1038/s41467-017-00309-w

de Reuse, H., Vinella, D., and Cavazza, C. (2013). Common themes and unique proteins for the uptake and trafficking of nickel, a metal essential for the virulence of *Helicobacter pylori*. *Front. Cell. Infect. Microbiol.* 3:94. doi: 10.3389/fcimb.2013.00094

de Souza, M. P. C., de Camargo, B. A. F., Spósito, L., Fortunato, G. C., Carvalho, G. C., Marena, G. D., et al. (2021). Highlighting the use of micro and nanoparticles based-drug delivery systems for the treatment of *Helicobacter pylori* infections. *Crit. Rev. Microbiol.* 47, 435–460. doi: 10.1080/1040841X.2021.1895721

Demidova, T. N., and Hamblin, M. R. (2004). Photodynamic therapy targeted to pathogens. *Int. J. Immunopathol. Pharmacol.* 17, 245–254. doi: 10.1177/039463200401700304

Fallone, C. A., Chiba, N., van Zanten, S. V., Fischbach, L., Gisbert, J. P., Hunt, R. H., et al. (2016). The Toronto consensus for the treatment of *Helicobacter pylori* infection in adults. *Gastroenterology* 151, 51–69.e14. doi: 10.1053/j.gastro.2016.04.006

Ferreira, R., Sousa, C., Gonçalves, R. F. S., Pinheiro, A. C., Oleastro, M., Wagemans, J., et al. (2022). Characterization and genomic analysis of a new phage infecting *Helicobacter pylori*. *Int. J. Mol. Sci.* 23:885. doi: 10.3390/ijms23147885

Fulgione, A., Nocerino, N., Iannaccone, M., Roperto, S., Capuano, F., Roveri, N., et al. (2016). Lactoferrin adsorbed onto biomimetic hydroxyapatite Nanocrystals controlling–*in vivo*–the *Helicobacter pylori* infection. *PLoS One* 11:e0158646. doi: 10.1371/journal.pone.0158646

Garcez, A. S., Nuñez, S. C., Hamblim, M. R., Suzuki, H., and Ribeiro, M. S. (2010). Photodynamic therapy associated with conventional endodontic treatment in patients with antibiotic-resistant microflora: a preliminary report. *J. Endod.* 36, 1463–1466. doi: 10.1016/j.joen.2010.06.001

Garcia, T., Lafuente, D., Blanco, J., Sánchez, D. J., Sirvent, J. J., Domingo, J. L., et al. (2016). Oral subchronic exposure to silver nanoparticles in rats. *Food Chem. Toxicol.* 92, 177–187. doi: 10.1016/j.fct.2016.04.010

Gonçalves, I. C., Henriques, P. C., Seabra, C. L., and Martins, M. C. (2014). The potential utility of chitosan micro/nanoparticles in the treatment of gastric infection. *Expert Rev. Anti-Infect. Ther.* 12, 981–992. doi: 10.1586/14787210.2014.930663

Gong, Y., and Yuan, Y. (2018). Resistance mechanisms of *Helicobacter pylori* and its dual target precise therapy. *Crit. Rev. Microbiol.* 44, 371–392. doi: 10.1080/1040841X.2017.1418285

Gopalakrishnan, V., Masanam, E., Ramkumar, V. S., Baskaraligam, V., and Selvaraj, G. (2020). Influence of N-acylhomoserine lactonase silver nanoparticles on the quorum sensing system of *Helicobacter pylori*: a potential strategy to combat biofilm formation. *J. Basic Microbiol.* 60, 207–215. doi: 10.1002/jobm.201900537

Graham, D. Y. (2014). History of *Helicobacter pylori*, duodenal ulcer, gastric ulcer and gastric cancer. *World J. Gastroenterol.* 20, 5191–5204. doi: 10.3748/wjg.v20.i18.5191

Graham, D. Y., and Dore, M. P. (2016). *Helicobacter pylori* therapy: a paradigm shift. *Expert Rev. Anti-Infect. Ther.* 14, 577–585. doi: 10.1080/14787210.2016.1178065

Gurunathan, S., Jeong, J. K., Han, J. W., Zhang, X. F., Park, J. H., and Kim, J. H. (2015). Multidimensional effects of biologically synthesized silver nanoparticles in *Helicobacter pylori*, *Helicobacter felis*, and human lung (L132) and lung carcinoma A549 cells. *Nanoscale Res. Lett.* 10:35. doi: 10.1186/s11671-015-0747-0

Häfeli, U. O. (2004). Magnetically modulated therapeutic systems. *Int. J. Pharm.* 277, 19–24. doi: 10.1016/j.ijpharm.2003.03.002

Han, X., Alu, A., Liu, H., Shi, Y., Wei, X., Cai, L., et al. (2022). Biomaterial-assisted biotherapy: a brief review of biomaterials used in drug delivery, vaccine development, gene therapy, and stem cell therapy. *Bioact. Mat.* 17, 29–48. doi: 10.1016/j.bioactmat.2022.01.011

Hathroubi, S., Servetas, S. L., Windham, I., Merrell, D. S., and Ottemann, K. M. (2018). *Helicobacter pylori* biofilm formation and its potential role in pathogenesis. *Microbiol. Mol. Biol. Rev.* 82:18. doi: 10.1128/MMBR.00001-18

Heidelbaugh, J. J. (2013). Proton pump inhibitors and risk of vitamin and mineral deficiency: evidence and clinical implications. *Therap. Adv. Drug Safety* 4, 125–133. doi: 10.1177/2042098613482484

Hejazi, R., and Amiji, M. (2003). Chitosan-based gastrointestinal delivery systems. *J. Control. Release* 89, 151–165. doi: 10.1016/S0168-3659(03)00126-3

Hooi, J. K. Y., Lai, W. Y., Ng, W. K., Suen, M. M. Y., Underwood, F. E., Tanyingoh, D., et al. (2017). Global prevalence of *Helicobacter pylori* infection: systematic review and meta-analysis. *Gastroenterology* 153, 420–429. doi: 10.1053/j.gastro.2017.04.022

Huang, L., Xuan, Y., Koide, Y., Zhiyentayev, T., Tanaka, M., and Hamblin, M. R. (2012). Type I and type II mechanisms of antimicrobial photodynamic therapy: an in vitro study on gram-negative and gram-positive bacteria. *Lasers Surg. Med.* 44, 490–499. doi: 10.1002/lsm.22045

Hussain, Z., Arooj, M., Malik, A., Hussain, F., Safdar, H., Khan, S., et al. (2018). Nanomedicines as emerging platform for simultaneous delivery of cancer therapeutics: new developments in overcoming drug resistance and optimizing anticancer efficacy. *Artif. Cells Nanomed. Biotechnol.* 46, 1015–1024. doi: 10.1080/21691401.2018.1478420

Im, B. N., Shin, H., Lim, B., Lee, J., Kim, K. S., Park, J. M., et al. (2021). *Helicobacter pylori*-targeting multiligand photosensitizer for effective antibacterial endoscopic photodynamic therapy. *Biomaterials* 271:120745. doi: 10.1016/j.biomaterials.2021.120745

Jeong, S., Park, W., Lee, C. S., and Na, K. (2014). A cancer-recognizing polymeric photosensitizer based on the tumor extracellular pH response of conjugated polymers for targeted cancer photodynamic therapy. *Macromol. Biosci.* 14, 1688–1695. doi: 10.1002/mabi.201400361

Jing, Z. W., Jia, Y. Y., Wan, N., Luo, M., Huan, M. L., Kang, T. B., et al. (2016). Design and evaluation of novel pH-sensitive ureido-conjugated chitosan/TPP nanoparticles targeted to *Helicobacter pylori*. *Biomaterials* 84, 276–285. doi: 10.1016/j.biomaterials.2016.01.045

Kao, J. Y., Zhang, M., Miller, M. J., Mills, J. C., Wang, B., Liu, M., et al. (2010). *Helicobacter pylori* immune escape is mediated by dendritic cell-induced Treg skewing and Th17 suppression in mice. *Gastroenterology* 138, 1046–1054. doi: 10.1053/j.gastro.2009.11.043

Khan, S., Sharaf, M., Ahmed, I., Khan, T. U., Shabana, S., Arif, M., et al. (2022). Potential utility of nano-based treatment approaches to address the risk of *Helicobacter pylori*. *Expert Rev. Anti-Infect. Ther.* 20, 407–424. doi: 10.1080/14787210.2022.1990041

Kim, Y. S., Song, M. Y., Park, J. D., Song, K. S., Ryu, H. R., Chung, Y. H., et al. (2010). Subchronic oral toxicity of silver nanoparticles. *Part. Fibre Toxicol.* 7:20. doi: 10.1186/1743-8977-7-20

Lang, X., Wang, T., Sun, M., Chen, X., and Liu, Y. (2020). Advances and applications of chitosan-based nanomaterials as oral delivery carriers: a review. *Int. J. Biol. Macromol.* 154, 433–445. doi: 10.1016/j.ijbiomac.2020.03.148

Langer, R. (1990). New methods of drug delivery. *Science* 249, 1527–1533. doi: 10.1126/science.2218494

Lau, C. S., Ward, A., and Chamberlain, R. S. (2016). Probiotics improve the efficacy of standard triple therapy in the eradication of *Helicobacter pylori*: a meta-analysis. *Infect. Drug Resist.* 9, 275–289. doi: 10.2147/IDR.S117886

Lin, C. C., Huang, W. C., Su, C. H., Lin, W. D., Wu, W. T., Yu, B., et al. (2020). Effects of multi-strain probiotics on immune responses and metabolic balance in *Helicobacter pylori*-infected mice. *Nutrients* 12:2476. doi: 10.3390/nu12082476

Lin, Y. H., Lu, K. Y., Tseng, C. L., Wu, J. Y., Chen, C. H., and Mi, F. L. (2017). Development of genipin-crosslinked fucoidan/chitosan-N-arginine nanogels for preventing helicobacter infection. *Nanomedicine* 12, 1491–1510. doi: 10.2217/nnm-2017-0055

Ling, D., Bae, B. C., Park, W., and Na, K. (2012). Photodynamic efficacy of photosensitizers under an attenuated light dose via lipid nano-carrier-mediated nuclear targeting. *Biomaterials* 33, 5478–5486. doi: 10.1016/j.biomaterials.2012.04.023

Lionetti, E., Indrio, F., Pavone, L., Borrelli, G., Cavallo, L., and Francavilla, R. (2010). Role of probiotics in pediatric patients with *Helicobacter pylori* infection: a comprehensive review of the literature. *Helicobacter* 15, 79–87. doi: 10.1111/j.1523-5378.2009.00743.x

Luo, M., Jia, Y. Y., Jing, Z. W., Li, C., Zhou, S. Y., Mei, Q. B., et al. (2018). Construction and optimization of pH-sensitive nanoparticle delivery system containing PLGA and UCCs-2 for targeted treatment of *Helicobacter pylori*. *Colloids Surf. B Biointerfaces* 164, 11–19. doi: 10.1016/j.colsurfb.2018.01.008

Malfertheiner, P., Megraud, F., O'Morain, C., Bazzoli, F., el-Omar, E., Graham, D., et al. (2007). Current concepts in the management of *Helicobacter pylori* infection: the Maastricht III consensus report. *Gut* 56, 772–781. doi: 10.1136/gut.2006.101634

Malfertheiner, P., Megraud, F., O'Morain, C. A., Gisbert, J. P., Kuipers, E. J., Axon, A. T., et al. (2017). Management of *Helicobacter pylori* infection-the Maastricht V/Florence consensus report. *Gut* 66, 6–30. doi: 10.1136/gutjnl-2016-312288

Mera, R. M., Bravo, L. E., Camargo, M. C., Bravo, J. C., Delgado, A. G., Romero-Gallo, J., et al. (2018). Dynamics of *Helicobacter pylori* infection as a determinant of progression of gastric precancerous lesions: 16-year follow-up of an eradication trial. *Gut* 67, 1239–1246. doi: 10.1136/gutjnl-2016-311685

Muñoz, A. B., Stepanian, J., Trespalacios, A. A., and Vale, F. F. (2020). Bacteriophages of *Helicobacter pylori*. *Front. Microbiol.* 11:549084. doi: 10.3389/fmicb.2020.549084

Nocerino, N., Fulgione, A., Iannaccone, M., Tomasetta, L., Ianniello, F., Martora, F., et al. (2014). Biological activity of lactoferrin-functionalized biomimetic hydroxyapatite nanocrystals. *Int. J. Nanomedicine* 9, 1175–1184. doi: 10.2147/IJN.S55060

Nogueira, F., Gonçalves, I. C., and Martins, M. C. (2013). Effect of gastric environment on *Helicobacter pylori* adhesion to a mucoadhesive polymer. *Acta Biomater.* 9, 5208–5215. doi: 10.1016/j.actbio.2012.09.011

Ouyang, Y., Zhu, Z., Huang, L., Zeng, C., Zhang, L., Wu, W. K., et al. (2021). Research trends on clinical *Helicobacter pylori* eradication: a Bibliometric analysis from 1983 to 2020. *Helicobacter* 26:e12835. doi: 10.1111/hel.12835

Palechor-Trochez, J. J., Ramírez-Gonzales, G., Villada-Castillo, H. S., and Solanilla-Duque, J. F. (2021). A review of trends in the development of bionanocomposites from lignocellulosic and polyacids biomolecules as packing material making alternative: a bibliometric analysis. *Int. J. Biol. Macromol.* 192, 832–868. doi: 10.1016/j.ijbiomac.2021.10.003

Park, H., Lee, J., Jeong, S., Im, B. N., Kim, M. K., Yang, S. G., et al. (2016). Lipase-sensitive Transfersomes based on photosensitizer/Polymerizable lipid conjugate for selective antimicrobial photodynamic therapy of acne. *Adv. Healthc. Mater.* 5, 3139–3147. doi: 10.1002/adhm.201600815

Portero, A., Remuñán-López, C., Criado, M. T., and Alonso, M. J. (2002). Reacetylated chitosan microspheres for controlled delivery of anti-microbial agents to the gastric mucosa. *J. Microencapsul.* 19, 797–809. doi: 10.1080/0265204021000022761

Pouwels, S., Lalmohamed, A., Souverein, P., Cooper, C., Veldt, B. J., Leufkens, H. G., et al. (2011). Use of proton pump inhibitors and risk of hip/femur fracture: a population-based case-control study. *Osteoporosis Int.* 22, 903–910. doi: 10.1007/s00198-010-1337-8

Praditya, D., Kirchhoff, L., Brüning, J., Rachmawati, H., Steinmann, J., and Steinmann, E. (2019). Anti-infective properties of the Golden spice Curcumin. *Front. Microbiol.* 10:912. doi: 10.3389/fmicb.2019.00912

Qu, J., Zhao, X., Liang, Y., Zhang, T., Ma, P. X., and Guo, B. (2018). Antibacterial adhesive injectable hydrogels with rapid self-healing, extensibility and compressibility as wound dressing for joints skin wound healing. *Biomaterials* 183, 185–199. doi: 10.1016/j.biomaterials.2018.08.044

Rajinikanth, P. S., Balasubramaniam, J., and Mishra, B. (2007). Development and evaluation of a novel floating in situ gelling system of amoxicillin for eradication of *Helicobacter pylori*. *Int. J. Pharm.* 335, 114–122. doi: 10.1016/j.ijpharm.2006.11.008

Reshetnyak, V. I., and Reshetnyak, T. M. (2017). Significance of dormant forms of *Helicobacter pylori* in ulcerogenesis. *World J. Gastroenterol.* 23, 4867–4878. doi: 10.3748/wjg.v23.i27.4867

Sachin, K., and Karn, S. K. (2021). Microbial fabricated Nanosystems: applications in drug delivery and targeting. *Front. Chem.* 9:617353. doi: 10.3389/fchem.2021.617353

Saha, A., Hammond, C. E., Beeson, C., Peek, R. M. Jr., and Smolka, A. J. (2010). *Helicobacter pylori* represses proton pump expression and inhibits acid secretion in human gastric mucosa. *Gut* 59, 874–881. doi: 10.1136/gut.2009.194795

Sánchez, S., Soler, L., and Katuri, J. (2015). Chemically powered micro- and nanomotors. *Angew. Chem. Int. Ed. Engl.* 54, 1414–1444. doi: 10.1002/anie.201406096

Seabra, C. L., Nunes, C., Brás, M., Gomez-Lazaro, M., Reis, C. A., Gonçalves, I. C., et al. (2018). Lipid nanoparticles to counteract gastric infection without affecting gut microbiota. *Eur. J. Pharm. Biopharm.* 127, 378–386. doi: 10.1016/j.ejpb.2018.02.030

Silva, É. L., Carvalho, J. F., Pontes, T. R., Oliveira, E. E., Francelino, B. L., Medeiros, A. C., et al. (2009). Development of a magnetic system for the treatment of *Helicobacter pylori* infections. *J. Magn. Magn. Mater.* 321, 1566–1570. doi: 10.1016/j.jmmm.2009.02.087

Sreelakshmi, C., Datta, K. K., Yadav, J. S., and Reddy, B. V. (2011). Honey derivatized au and ag nanoparticles and evaluation of its antimicrobial activity. *J. Nanosci. Nanotechnol.* 11, 6995–7000. doi: 10.1166/jnn.2011.4240

Su, Y.-R., Yu, S.-H., Chao, A.-C., Wu, J.-Y., Lin, Y.-F., Lu, K.-Y., et al. (2016). Preparation and properties of pH-responsive, self-assembled colloidal nanoparticles from guanidine-containing polypeptide and chitosan for antibiotic delivery. *Colloids Surf. A Physicochem. Eng. Asp.* 494, 9–20. doi: 10.1016/j.colsurfa.2016.01.017

Suerbaum, S., Smith, J. M., Bapumia, K., Morelli, G., Smith, N. H., Kunstmann, E., et al. (1998). Free recombination within *Helicobacter pylori*. *Proc. Natl. Acad. Sci. U. S. A.* 95, 12619–12624. doi: 10.1073/pnas.95.21.12619

Thamphiwatana, S., Fu, V., Zhu, J., Lu, D., Gao, W., and Zhang, L. (2013). Nanoparticle-stabilized liposomes for pH-responsive gastric drug delivery. *Langmuir* 29, 12228–12233. doi: 10.1021/la402695c

Thombre, N. A., and Gide, P. S. (2016). Floating-bioadhesive gastroretentive Caesalpinia pulcherrima-based beads of amoxicillin trihydrate for *Helicobacter pylori* eradication. *Drug Deliv.* 23, 405–419. doi: 10.3109/10717544.2014.916766

Tshibangu-Kabamba, E., and Yamaoka, Y. (2021). *Helicobacter pylori* infection and antibiotic resistance–from biology to clinical implications. *Nat. Rev. Gastroenterol. Hepatol.* 18, 613–629. doi: 10.1038/s41575-021-00449-x

Vázquez, E., and Villaverde, A. (2013). Microbial biofabrication for nanomedicine: biomaterials, nanoparticles and beyond. *Nanomedicine* 8, 1895–1898. doi: 10.2217/nnm.13.164

Walker, D., Käsdorf, B. T., Jeong, H. H., Lieleg, O., and Fischer, P. (2015). Enzymatically active biomimetic micropropellers for the penetration of mucin gels. *Sci. Adv.* 1:e1500501. doi: 10.1126/sciadv.1500501

Wang, M., Wang, C., Chen, M., Xi, Y., Cheng, W., Mao, C., et al. (2019). Efficient angiogenesis-based diabetic wound healing/skin reconstruction through bioactive antibacterial adhesive ultraviolet shielding Nanodressing with exosome release. *ACS Nano* 13, 10279–10293. doi: 10.1021/acsnano.9b03656

Watanabe, Y., Kim, H. S., Castoro, R. J., Chung, W., Estecio, M. R., Kondo, K., et al. (2009). Sensitive and specific detection of early gastric cancer with DNA methylation analysis of gastric washes. *Gastroenterology* 136, 2149–2158. doi: 10.1053/j.gastro.2009.02.085

Wu, Y., Song, Z., Deng, G., Jiang, K., Wang, H., Zhang, X., et al. (2021). Gastric acid powered Nanomotors release antibiotics for in vivo treatment of *Helicobacter pylori* infection. *Small* 17:e2006877. doi: 10.1002/smll.202006877

Wu, T., Wang, L., Gong, M., Lin, Y., Xu, Y., Ye, L., et al. (2019). Synergistic effects of nanoparticle heating and amoxicillin on *H. pylori* inhibition. *J. Magn. Magn. Mater.* 485, 95–104. doi: 10.1016/j.jmmm.2019.04.076

Yan, L. X., Wang, B. B., Zhao, X., Chen, L. J., and Yan, X. P. (2021). A pH-responsive persistent luminescence Nanozyme for selective imaging and killing of *Helicobacter pylori* and common resistant bacteria. *ACS Appl. Mater. Interfaces* 13, 60955–60965. doi: 10.1021/acsami.1c21318

Yang, S. J., Huang, C. H., Yang, J. C., Wang, C. H., and Shieh, M. J. (2020). Residence time-extended nanoparticles by magnetic field improve the eradication efficiency of *Helicobacter pylori*. *ACS Appl. Mater. Interfaces* 12, 54316–54327. doi: 10.1021/acsami.0c13101

Yang, J. C., Lu, C. W., and Lin, C. J. (2014). Treatment of *Helicobacter pylori* infection: current status and future concepts. *World J. Gastroenterol.* 20, 5283–5293. doi: 10.3748/wjg.v20.i18.5283

Yun, Y. H., Lee, B. K., and Park, K. (2015). Controlled drug delivery: historical perspective for the next generation. *J. Control. Release* 219, 2–7. doi: 10.1016/j.jconrel.2015.10.005

Zaidi, S., Misba, L., and Khan, A. U. (2017). Nano-therapeutics: a revolution in infection control in post antibiotic era. *Nanomedicine* 13, 2281–2301. doi: 10.1016/j.nano.2017.06.015

Zhang, Y., Chen, Y., Lo, C., Zhuang, J., Angsantikul, P., Zhang, Q., et al. (2019). Inhibition of pathogen adhesion by bacterial outer membrane-coated nanoparticles. *Angew. Chem. Int. Ed. Engl.* 58, 11404–11408. doi: 10.1002/anie.201906280

Zhang, Y., Li, H., Wang, Q., Hao, X., Li, H., Sun, H., et al. (2018). Rationally designed self-assembling nanoparticles to overcome mucus and epithelium transport barriers for oral vaccines against *Helicobacter pylori*. *Adv. Funct. Mater.* 28:1802675. doi: 10.1002/adfm.201802675

Zhang, N., Mei, K., Guan, P., Hu, X., and Zhao, Y. (2020). Protein-based artificial Nanosystems in cancer therapy. *Small* 16:e1907256. doi: 10.1002/smll.201907256

Zhang, T., Zhang, B., Tian, W., Ma, X., Wang, F., Wang, P., et al. (2022). A Bibliometric analysis of atrophic gastritis from 2011 to 2021. *Front. Med.* 9:843395. doi: 10.3389/fmed.2022.843395

Zhang, W., Zhou, Y., Fan, Y., Cao, R., Xu, Y., Weng, Z., et al. (2022). Metal-organic-framework-based hydrogen-release platform for multieffective *Helicobacter pylori* targeting therapy and intestinal Flora protective capabilities. *Adv. Mater.* 34:e2105738. doi: 10.1002/adma.202105738

Zhi, X., Liu, Y., Lin, L., Yang, M., Zhang, L., Zhang, L., et al. (2019). Oral pH sensitive GNS@ab nanoprobes for targeted therapy of *Helicobacter pylori* without disturbance gut microbiome. *Nanomedicine* 20:102019. doi: 10.1016/j.nano.2019.102019

Zhu, S., Liu, Y., Gu, Z., and Zhao, Y. (2021). A Bibliometric analysis of advanced healthcare materials: research trends of biomaterials in healthcare application. *Adv. Healthc. Mater.* 10:e2002222. doi: 10.1002/adhm.202002222

frontiers | Frontiers in Microbiology

TYPE Review
PUBLISHED 27 April 2023
DOI 10.3389/fmicb.2023.1130001

OPEN ACCESS

EDITED BY
Paula Roszczenko-Jasinska,
University of Warsaw, Poland

REVIEWED BY
Dong Yang,
Tianjin Institute of Environmental and Operational Medicine, China
Kathryn Haley,
Grand Valley State University, United States

*CORRESPONDENCE
Wenxian Guan
✉ medguanwx@163.com
Chao Ding
✉ dingchao19910521@126.com
Hao Wang
✉ wanghao0349@sina.com

†These authors have contributed equally to this work

RECEIVED 22 December 2022
ACCEPTED 04 April 2023
PUBLISHED 27 April 2023

CITATION
Zhou S, Li C, Liu L, Yuan Q, Miao J, Wang H, Ding C and Guan W (2023) Gastric microbiota: an emerging player in gastric cancer. *Front. Microbiol.* 14:1130001. doi: 10.3389/fmicb.2023.1130001

Gastric microbiota: an emerging player in gastric cancer

Shizhen Zhou[1†], Chenxi Li[2†], Lixiang Liu[3], Qinggang Yuan[4], Ji Miao[1], Hao Wang[1*], Chao Ding[1*] and Wenxian Guan[1*]

[1]Department of General Surgery, Nanjing Drum Tower Hospital, The Affiliated Hospital of Nanjing University Medical School, Nanjing, Jiangsu, China, [2]Laboratory Medicine Center, The Second Affiliated Hospital of Nanjing Medical University, Nanjing, Jiangsu, China, [3]Department of General Surgery, Nanjing Drum Tower Hospital Clinical College of Nanjing Medical University, Nanjing, Jiangsu, China, [4]Department of General Surgery, Nanjing Drum Tower Hospital Clinical College of Xuzhou Medical University, Nanjing, Jiangsu, China

Gastric cancer (GC) is a common cancer worldwide with a high mortality rate. Many microbial factors influence GC, of which the most widely accepted one is *Helicobacter pylori* (*H. pylori*) infection. *H. pylori* causes inflammation, immune reactions and activation of multiple signaling pathways, leading to acid deficiency, epithelial atrophy, dysplasia and ultimately GC. It has been proved that complex microbial populations exist in the human stomach. *H. pylori* can affect the abundance and diversity of other bacteria. The interactions among gastric microbiota are collectively implicated in the onset of GC. Certain intervention strategies may regulate gastric homeostasis and mitigate gastric disorders. Probiotics, dietary fiber, and microbiota transplantation can potentially restore healthy microbiota. In this review, we elucidate the specific role of the gastric microbiota in GC and hope these data can facilitate the development of effective prevention and therapeutic approaches for GC.

KEYWORDS

gastric cancer, *H. pylori*, gastric microbiota, non-*H. pylori*, microbiome diversity

Introduction

Gastric cancer (GC) ranks fifth most common and third most deadly cancer globally (Rawla and Barsouk, 2019). Factors that induce gastric carcinogenesis include gastric microbiota, alcohol, smoking, and unhealthy dietary (Dong and Thrift, 2017; Zhao et al., 2017). Among many risk factors for GC, gastric microbiota act as an emerging one. Human gastric microbiota are subject-specific species and include a variety of bacteria. *H. pylori* is classified as a Class I risk factor for GC by the World Health Organization (WHO), and *H. pylori* infection is widely regarded as the strongest threat to GC (Wroblewski et al., 2010). *H. pylori* has a high infection rate and frequently colonized more than half of the world's population. The infection of *H. pylori* usually occurs during childhood and will last for a lifetime (Malaty et al., 2002). *H. pylori* can disturb the human immune system and promote inflammation responses, leading to acid deficiency, epithelial atrophy, and dysplasia (Doorakkers et al., 2016). Diverse species more common than *H. pylori* have been found in gastric samples, such as *Streptococcus*, *Prevotella*, *Veronella*, *Clostridium*, *Haemophilus*, and *Neisseria* (Rajilic-Stojanovic et al., 2020). These gastrointestinal microbiota exhibit different biological functions, for instance, preventing the invasion of pathogens, digesting complex carbohydrates, regulating immune response, or regulating the central nervous system (Alarcón et al., 2017).

The process for analyzing the diversity of the gastric microbiota has undergone a change from culture-based methods to molecular assays. Early studies relied on culture-based analysis

(Wang et al., 2020a). And the emergence of next-generation sequencing (NGS) enabled researchers to analyze the composition and function of microbiota in a diverse environment with higher throughput and resolution, mainly including targeted amplicon sequencing by 16S ribosomal RNA (rRNA) genes and shotgun metagenomics (Boers et al., 2019), providing fascinating insights into the human gastric microbiota. In this review, we mainly analyzed the basic composition of microbiota in the human stomach, illustrated the changes and interactions of gastric microbiota in GC, and discussed promising strategies to regulate gastric microbiota.

Composition of the gastric microbiota

In earlier times, Monstein et al. used temperature gradient gel electrophoresis of 16S rRNA amplicons to classify the gastric microbiota into three main phyla (*Proteobacteria*, *Firmicutes*, and *Actinobacteria*; Monstein et al., 2000). As high-throughput sequencing developed, more bacteria were found in the human stomach. G2 PhyloChip (16S rRNA chip) data revealed 44 bacterial phyla in the human stomach, of which 4 phyla dominate: *Actinobacteria*, *Firmicutes*, *Bacteroidetes*, and *Proteobacteria* (Maldonado-Contreras et al., 2011). Based on barcoded 16S pyrosequencing data indicated that the human stomach contains of five phyla: *Actinobacteria*, *Firmicutes*, *Bacteroidetes*, *Proteobacteria*, and *Fusobacteria* (Andersson et al., 2008; Figure 1). In addition,researchers found that it contained the most common genera for each phylum, such as *Streptococcus* (*phylum Firmicutes*), *Neisseria* and *Haemophilus* (*Proteobacteria*), as well as *Prevotella* and *Porphyromonas* (*Bacteroidetes*; Li et al., 2009).

H. pylori, a spiral-shaped flagellated bacterium belonging to the Proteobacteria phylum, is considered a constituent of the normal human gastric microbiome (Falush et al., 2003; Linz et al., 2007; Bruno et al., 2018). The remarkable survival capacity of *H. pylori* in the harsh gastric environment can be attributed to its motility and chemotaxis, which facilitate penetration of the mucus layer and colonization of epithelial cells (Amieva and Peek, 2016). *H. pylori* can hydrolyze urea and produce urease to increase the pH of its surrounding environment (Schulz et al., 2018).

Apart from *H. pylori*, many members other than *H. pylori* have been found in the stomach, including *Streptococcus* spp., *Lactobacillus* spp., *Neisseria* spp., *Klebsiella* spp., *Escherichia coli*, *Rothia* sp., *Burkholderia pseudomallei*., *Bacillus* sp., *Morganella morganii*, *Acinetobacter* sp., *Haemophilus* sp., *Veillonella* sp., *Clostridium* sp., *Corynebacterium* sp., *Bacteroides* sp., and *Peptococcus* sp. (Zilberstein et al., 2007; Khosravi et al., 2014; Schulz et al., 2018). Interestingly, some uncultured bacteria correlated with the extremophile *Deinococcus* and members of the enigmatic uncultured bacteria-TM7 group were detected in the stomachs of normal individuals (He et al., 2015; Ye et al., 2016), and another uncultured bacteria-SR1 phylum was also found in the normal stomach (Li et al., 2009).

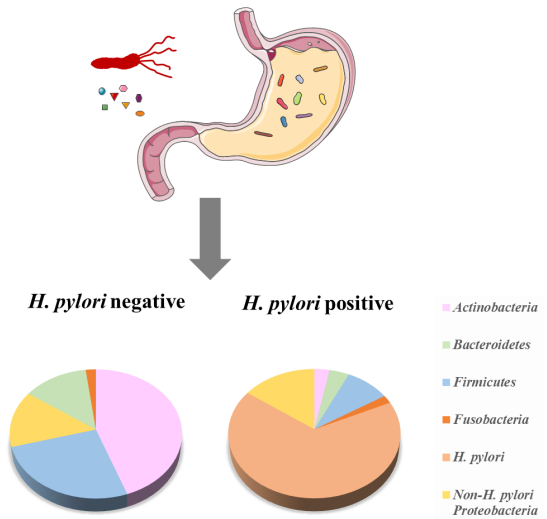

FIGURE 1
The composition of the human stomach microbiota and the effect of *H. pylori* on the microbiota. The microbiota of *H. pylori* (–) cases has higher diversity, with a higher relative abundance of *Firmicutes* and *Actinobacteria*. *H. pylori* (+) cases have a lower prevalence of *Actinobacteria*, *Bacteroidetes*, and *Firmicutes*, while increase *Proteobacteria* (adopted from Andersson et al., 2008 and Maldonado-Contreras et al., 2011).

Factors affecting gastric microbiota

Various factors are affecting the survival and function of gastric microbiota. The harsh environment in the stomach, which contains antibacterial enzymes, defensins, immunoglobulin, and high gastric acid, was a challenge for gastric microbiota (Zhang et al., 2017). These substances could effectively protect the host's gastric mucosa from the attack of the microbiota. Low pH in the stomach cavity hinders the growth of the gastric microbiota. The hydrochloric acid secreted by parietal cells can convert pepsinogen into pepsin, an effective enzyme that denatures proteins and inhibits the survival of microbiota (Zhang et al., 2017). Immunoglobulin A (IgA) could prevent bacteria from penetrating the epithelial barrier and potentially maintain the diversity of normal gastrointestinal microbiota (Suzuki et al., 2004). Stomach commercial bacteria, especially S24-7, which belonged to *Bacteroides*, effectively induce the secretion of ILC2-dependent IgA. The secreted IgA is coated with other pathogenic bacteria (such as *H. pylori*) to prevent it from invading the epithelial mucosa, so as to maintain the gastric bacterial homeostasis (Satoh-Takayama et al., 2020). Children's ILC2 is immature, unable to activate plasma cells to release enough IgA, resulting in *H. pylori* susceptibility (Ohno and Satoh-Takayama, 2020; Satoh-Takayama et al., 2020).Other antimicrobial compounds in gastric epithelial cells produced by the host, such as cathelicidins and C-type lectins, also had selective killing effects on microbiota (Walter and Ley, 2011).

Some external factors also influence the human gastric microbiota, including diet (Cires et al., 2016), antibiotics, proton pump inhibitor (PPI; Nardone and Compare, 2015; Tsuda et al., 2015), geography (Yang et al., 2016), and surgical intervention (Tseng et al., 2016). For instance, in the stomach of healthy cases, the most enriching family was *Prevotellaceae*, followed by *Streptococcaceae*, *Paraprevotellaceae*, and *Fusobacteriaceae*. While among patients who received PPI treatment, *Streptococcaceae* were the prevalent family, followed by *Prevotellaceae*, *Campylobacteraceae*, and *Leptotrichiaceae* (Parsons et al., 2017). Long-term application of PPI increases the intra-gastric pH, which allows the bacteria to reach the growth phase, resulting in increased bacterial load and increased bacterial translocation

(Scarpignato et al., 2016), leading to a new bacterial balance, in which oral bacteria are significantly increased, such as *Pepto-streptococcus stomatis*, *Parvimonas micra*, *Slackia exigua*, *Streptococcus anginosus*, and *Dialist pneumonitis* (Bruno et al., 2019). Besides, the diversity of gastric microbiota increased significantly after subtotal gastrectomy. *Helicobacter* and *Ralstonia* were the two most abundant genera in stomachs before surgery, while *Prevotella* and *Streptococcus* were the two most prevalent bacteria after surgery (Tseng et al., 2016). The parietal cells that secrete gastric acid are mainly located in the stomach body and gastric antrum, so the gastric acid secretion is significantly reduced after distal gastrectomy, as well as highly selective vagotomy and bile reflux after surgery, all of which increase the pH value in the stomach and change the composition of bacteria.

Changes of gastric microbiota in gastric cancer

The dysbiosis of gastric microbiota may be responsible for gastric malignancies. The microbiota changes aggravated gastric environmental disorders and promoted the development of GC (Lofgren et al., 2011; Lertpiriyapong et al., 2014; Guo et al., 2022). The detailed changes in the bacterial community in GC patients were listed as follows (Table 1).

GC patients were more likely to suffer from acid deficiency, which may affect the colonization of microorganisms. In the early stages of GC, the relative abundance of *H. pylori*, *Propionibacterium acnes*, and *Prevotella copri* in the stomach was higher than that of non-cancer-bearing people (Gunathilake et al., 2019). However, Wang LL et al. found that unlike advanced gastric cancer, no significant biodiversity alteration was found in the early stage of gastric cancer (Wang L. et al., 2020). As cancer develops, the prevalence of *H. pylori* in the stomach may gradually decrease, and the overall microbial population in the stomach may also change. Dicksved et al. found a decreased abundance of *H. pylori* in the stomach of GC patients and a predominance of different species of the gastric microbial population, which include the genera *Lactobacillus*, *Streptococcus, Prevotella*, and *Veillonella* (Dicksved et al., 2009). Coker et al. found five taxa (*Dialister pneumosintes*, *Parvimonas micra*, *Peptostreptococcus stomatis*, *Slackia exigua*, and *Streptococcus anginosus*) as the core of the GC microbiota network (Coker et al., 2018). These studies revealed the difference in gastric microbiota profiles between GC patients and non-cancer-bearing people.

The gastric microbiota also showed different changes in patients with different histological stages from gastritis to GC. Ferreira et al. confirmed that the dysbiosis of gastric microbiota with potential genotoxicity existed in the GC patients, which differed from that of patients with chronic gastritis (CG; Ferreira et al., 2018). From non-atrophic gastritis and intestinal metaplasia (IM) to GC, the abundance of *Neisseria*, *Porphyromonas*, *Streptococcus sinensis*, and TM7 group showed a decreasing trend. In contrast the abundance of *Lachnospiraceae* and *Lactobacillus coleohominis* displayed an increasing trend (Aviles-Jimenez et al., 2014). In another study, compared with CG and IM groups, the abundance of *Streptococcaceae* and *Bacilli* increased at the class level, and the abundance of *Helicobacter* decreased at the family level in the stomach of the GC patients (Eun et al., 2014). In *H. pylori*-negative patients from atrophic gastritis (AG) to dysplasia (Dys) precancerous stage, the abundance of *Burkholderiaceae* continued to increase, while the abundance of *Streptococcaceae* and *Prevotellaceae* continued to decrease (Sun et al., 2022). Interestingly, some oral bacteria, genera *Aggregatibacter*, *Alloprevotella*, and *Neisseria* were abundant in GC patients compared with the superficial gastritis (SG) group. The relative abundance of these bacteria was completely separated between the two groups. This discovery suggested we can distinguish GC from SG patients based on any of the three genera detected in GC (Hu et al., 2018).

Previous studies have primarily focused on the abundance and diversity of the gastric microbiota in diverse patient cohorts. However, uncertain host factors may exert significant influence on research outcomes, thereby confounding interpretation of the results. To minimize the impact of these confounding factors, some investigators have adopted a paired design approach, wherein the profiles of the gastric microbiota in paired tumor tissues and non-malignant tissues from the same GC patient are comparatively analyzed in greater detail. Seo et al. detected 350 bacterial species from paired cancer and non-cancer biopsies among 16 GC patients by 16S rRNA gene sequencing. Compared with non-cancer tissue, the populations of *Prevotella* spp. and *Clostridium* spp. were increased, while *H. pylori*, *Propionibacterium* spp., *Staphylococcus* spp., and *Corynebacterium* spp. were decreased in cancer biopsies (Seo et al., 2014; Dai et al., 2021). In a study of carcinoma and adjacent tissues from 276 GC patients, genera *Halomonas*, *Shewanella*, and *Helicobacter* were enriched in the tumor-adjacent tissues, while *Corynebacterium*, *Fusobacterium*, *Selenomonas*, *Propionibacterium*, and *Streptococcus* were enriched in the carcinoma tissues. Similar to the previous reports, the community of *H. pylori* was also *significantly* reduced in the tumoral sites (Liu X. et al., 2019). The significant reduction of *H. pylori* may be due to the changes in the gastric environment of GC patients.

There are significant differences in the composition of gastric microbiota in GC patients based on race and region. A Portuguese cohort study showed an increased abundance of *Achromobacter* in GC patients compared to gastritis patients, while *Achromobacter* was completely absent in the validation cohort of Chinese GC subjects (Ferreira et al., 2018). Yu et al. analyzed bacterial abundance and diversity in GC tissues from 80 Chinese and 80 Mexican patients. Similar to the gastric microbiota profiles in non-cancer tissues, microbiota in cancer tissues of Mexican and Chinese patients were also composed mainly of *Proteobacteria*, followed by *Firmicutes* in Mexican cancer tissues or *Bacteroides* in Chinese cancer tissues. Mexican samples showed an increased relative abundance of *Clostridium* in cancer tissues but no difference in the alpha diversity, while cancer samples from Chinese patients presented substantial differences in alpha diversity and the abundance of several genera has increased, such as *Treponema*, *Helicobacter*, *Selenomonas*, *Fusobacterium*, *Streptococcus*, *Pseudomonas* (Yu et al., 2017a). These studies indicated that geographical and ethnic factors could influence the composition of stomach microbes.

Notably, a robust correlation existed between stomach microbes and the epidemiology of GC. Compared with cases without a family history of upper gastrointestinal cancer, cases with a family history of upper gastrointestinal cancer have lower alpha diversity and a higher abundance of *H. pylori* (Yu et al., 2017b). Among populations with similar *H. pylori* prevalence, the gastric microbiota composition significantly differed in populations from two towns with different GC risks in Colombia. *Leptotrichia wadei* and *Veillonella* sp. were

10.3389/fmicb.2023.1130001

TABLE 1 Changes of gastric microbiota in GC.

Reference	Study participants	Samples	Methods	Significant outcomes
Aviles-Jimenez et al. (2014)	NAG (5), IM (5), GC (5)	Gastric biopsy samples from antrum and corpus	G3 PhyloChip (16S rRNA microarray)	From NAG to IM to GC, decreased bacterial diversity, increased *Lachnospiraceae* and *Lactobacillus coleohominis*, decreased *Porphyromonas, Neisseria* and TM7.
Castaño-Rodríguez et al. (2017)	GC (12), FD (20)	Gastric biopsy samples from antrum, whole blood samples	16S rRNA sequencing V4	Increased richness and phylogenetic diversity but not Shannon's diversity in GC, enriched *Veilonella*, *Lactococcus*, and *Fusobacteriaceae* (*Leptotrichia* and *Fusobacterium*); enriched short chain fatty acid production pathways in GC.
Chen et al. (2019)	GC (62)	Pairs of matched GC tissues and adjacent non-cancerous tissues	16S rRNA sequencing V4-V5	Increased oral bacteria (*Fusobacterium, Streptococcus* and *Peptostreptococcus*) in tumor tissues, increased lactic acid-producing bacteria (*Lactobacillus brevis* and *Lactococcus lactis*) in adjacent non-tumor tissues.
Png et al. (2022)	EC (4), IM (22), SG (17)	Gastric biopsy samples from antrum	16S rRNA sequencing V3-V4	Increased the abundances of Proteobacteria (in particular Proteus genus) in EC. Decreased the abundances of Bacteroidetes (in particular S24-7 family)
Coker et al. (2018)	GC (20), IM (17), AG (23), SG (21) Validate: C (19), AG (51), SG (56)	Gastric biopsy samples from antrum, body and fundus	16S rRNA sequencing V4	Enriched *Dialister pneumosintes, Parvimonas micra, Peptostreptococcus stomatis, Slackia exigua* and *Streptococcus anginosus* in GC.
Dai et al. (2021)	GC (37)	Pairs of matched GC tissues and adjacent non-cancerous tissues	16S rRNA sequencing V3-V4	Increased the abundances of Lactobacillus, Prevotella, Streptococcus, Acinetobacter, Sphingomonas, Bacteroides, Comamonas, Fusobacterium, Empedobacter, and Faecalibacterium in the tumor tissues.
Dicksved et al. (2009)	GC (10), FD (5)	Gastric biopsy samples from antrum and corpus	T-RFLP,16S rRNA sequencing V3	Increased *Streptococcus, Lactobacillus, Veillonella* and *Prevotella*, decreased *H. pylori* in GC.
Eun et al. (2014)	GC (11), IM (10), CG (10)	Gastric biopsy samples	16S rRNA sequencing V5	Increased the diversity of gastric microbiota, increased *Streptococcaceae* and *Bacilli* at the class level, decreased *Helicobacter* at the familiy level in GC.
Ferreira et al. (2018)	CG (81), GC (54)	Gastric biopsy samples	16S rRNA sequencing V5-V6	Decreased microbial diversity, decreased *Helicobacter* abundance and increased other bacterial genera (include intestinal commensals) in GC.
Hsieh et al. (2018)	CG (9), IM (7), GC (11)	Gastric biopsy samples	16S rRNA sequencing V3-V4	Similar abundance of *Burkholderia, Enterobacter,* and *Leclercia* in cancer and non-cancer groups. Increased the abundance of *Fusobacterium*, *Lactobacillus* and *Clostridium*; decreased the abundance of *H. pylori* in GC.
Hu et al. (2018)	SG (5), GC (6)	Gastric wash samples	shotgun metagenomic sequencing	Decreased species richness in GC group, especially *Sphingobium yanoikuyae*, increased 13 bacterial taxa and decreased 31 taxa in GC; genera *Aggregatibacter, Alloprevotella and Neisseria* in GC were different from SG. Enriched L-arginine and lipopolysaccharide production pathways in GC.
Jo et al. (2016)	*H. pylori* (−) control (13), *H. pylori* (+) control (16), *H. pylori* (−) GC (19), *H. pylori* (+) GC (15)	Gastric biopsy samples from antrum and corpus, blood samples	16S rRNA sequencing V1-V3	Increased the proportion of *Actinobacteria* in GC groups. *Stenotrophomonas* genus (*Stenotrophomonas maltophilia*) was the most abundant in *H. pylori* (−) GC group, while *Helicobacter* genus was the most abundant in *H. pylori* (+) GC group.
Li et al. (2017)	CG (9), IM (9), GC (7), *H. pylori* (−) control (8)	Gastric biopsy samples from antrum and corpus	16S rRNA sequencing V3-V4	Decreased microbial diversity, enriched the abundance of 13 high OTUs (e.g.*Flavobacterium, Klebsiella, Serratia marcescens*, *Stenotrophomnonas*, *Achromobacter* and *Pseudomonas*) in GC group.
Ling et al. (2019)	GC (64)	Normal, peritumoral and tumoral tissues	16S rRNA sequencing V3-V4	Composition, diversity and function of gastric microbiota changed more obvious in tumoral tissues than in normal and peritumoral tissues.

(Continued)

TABLE 1 (Continued)

Reference	Study participants	Samples	Methods	Significant outcomes
Liu X. et al. (2019)	GC (276)	Normal, peritumoral and tumoral tissues	16S rRNA sequencing V3-V4	Decreased bacterial richness in tumoral and peritumoral tissues, decreased the abundance of *H. pylori*, *Bacteroides uniformis* and *Prevotella copri*, increased the abundance of *Propionibacterium acnes, Streptococcus anginosus* and *Prevotella melaninogenica* in tumoral tissues.
Gunathilake et al. (2019)	GC (268), non-cancer-bearing controls (288)	Gastric biopsy samples	16S rRNA sequencing V3-V4	Increased the abundances of *H. pylori* and *Prevotella copri*, *Propionibacterium acnes*, decreased the abundances of *Lactococcus lactis* in GC.
Park et al. (2019)	GC (55), IM (19), CG (62)	Gastric biopsy samples from antrum	16S rRNA sequencing V3-V4	Increased the abundances of *Moraxellaceae, Pseudomonadaceae, Streptococcaceae* and *Xanthomonadaceae* in *H. pylori* (−) GC compared to *H. pylori* (−) CG and *H. pylori* (−) IM groups. Decreased the abundances of *Cyanobacteria* and *Rhizobiales* in *H. pylori* (−) GC.
Seo et al. (2014)	GC (16)	Tumor and non-tumor biopsy samples	16S rRNA sequencing	Increased *Prevotella spp.* and *Clostridium* spp. in tumor tissue, decreased *Corynebacterium* spp., *Propionibacterium* spp. and *Staphylococcus* spp. at the genus level, and decreased *H. pylori* at the species level in tumor tissue.
Shao et al. (2019)	GC (36)	Gastric tumor tissues, non-malignant tissues	16S rRNA sequencing V4	Increased the abundances of *Haemophilus, Neisseria, Prevotella*, *Streptococcus* and *Veillonella*, decreased the abundance of *Helicobacter* genus in tumor tissues. Increased the abundance of *Helicobacter* in non-tumor tissues.
Sohn et al. (2017)	*H. pylori* (−) control (2), *H. pylori* (+) control (3), *H. pylori* (−) GC (2), *H. pylori* (+) GC (5)	Gastric biopsy samples from antrum and body	16S rRNA sequencing V1-V3	Increased the number of non- *H. pylori* urease-producing bacteria and non- *H. pylori* nitrosating or nitroreducing bacteria (e.g., *S. pseudopneumoniae, S. parasanguinis*, and *S. oralis*) in *H. pylori* (−) GC groups.
Sun et al. (2022)	*H. pylori* (−) SG (56), *H. pylori* (−) AG (9), *H. pylori* (−) IM (27), *H. pylori* (−) Dys (29), *H. pylori* (−) GC (13).	Gastric mucosal biopsy samples, and Gastric juice	16S rRNA sequencing V3-V4	Increased the abundances of Burkholderiaceae, decreased the abundance of Streptococcaceae and Prevotellaceae
Tseng et al. (2016)	GC (6)	Gastric cancerous tissues, adjacent normal tissues	16S rRNA sequencing V1-V3	Increased *Ralstonia* and *Helicobacter* in cancerous tissues before surgery; increased *Streptococcus* and *Prevotella* in cancerous tissues after surgery, increased the diversity of gastric microbiota after surgery.
Wang et al. (2016)	GC (103), CG (212)	Gastric biopsy samples	16S rRNA sequencing V1-V3	Increased the quantity and diversity of bacteria, enriched bacteria with potential cancer-promoting activities in GC.
Wang L. et al. (2020)	EC (30),AC (30),CG (60)	Gastric mucosal biopsy, adjacent normal tissues	16S rRNA sequencing V3-V4	Increased the levels of *Ochrobactrum*,*Lactobacillus*,*Propionibac*,*serratiaterium* et al.*in EC.*
Wang et al. (2020b)	CG (21), IM (27), IN (25), GC (29), non-cancer-bearing controls (30)	Gastric mucosal biopsy	16S rRNA sequencing V4	Decreased the diversity and abundances of phyla *Nitrospirae*, *Chloroflexi*, *Armatimonadetes*, *Elusimicrobia*, *Verrucomicrobia*, *Planctomycetes* and WS3 from CG, IM, IN to GC. Enriched *Bacteriodes, Actinobacteria, Fusobacteria, Firmicutes,* TM7, and SR1 in the IN and GC group.
Wu et al. (2020)	GC (18), SG (32)	Paired tumor and paracancerous mucosa samples	16S rRNA sequencing	Increased the levels of *Lactobacillus spp. Dialister spp., Rhodococcus spp., Helicobacter spp., Sediminibacterium* spp. and *Rudaea* spp. in GC, decreased species *Fusobacterium spp., Actinomyces spp., Brevundimonas spp., Leptotrichia spp., Haemophilus spp., Alloprevotella spp., Campylobacter spp., Arthrobacter spp., Neisseria spp., Bradyrhizobium spp., Phyllobacterium spp., Prevotella spp., Porphyromonas spp., Veillonella* spp. and *Rothia* spp., etc. in GC.
Yu et al. (2017b)	GC (77)	Gastric tumor tissues, paired non-malignant tissues	16S rRNA sequencing	Decreased *H. pylori* and increased *Bacteroidetes* abundance in lower tumor grade. Increased *H. pylori* abundance and decreased alpha diversity in advanced tumor grade. Class *Epsilonproteobacteria,* order *Campylobacterales*, family *Helicobacteraceae*, and genus *Helicobacter*, were also related to tumor grade.

(Continued)

TABLE 1 (Continued)

Reference	Study participants	Samples	Methods	Significant outcomes
Yu et al. (2017a)	GC (160)	Gastric tumor tissues, paired non-malignant tissues	16S rRNA sequencing V3-V4	Dominated *Proteobacteria*, followed by *Bacteroidetes* in Chinese tumor samples or *Firmicutes* in Mexican tumor samples. Dominated *H. pylori* in both Chinese and Mexican tumor tissues, but *H. pylori* abundance is lower than that of matched non-malignant tissues.

GC, gastric cancer; AC, advanced gastric cancer; EC, early gastric cancer; IM, intestinal metaplasia; AG, atrophic gastritis; SG, superfcial gastritis; NAG, non-atrophic gastritis; CG, chronic gastritis; FD, functional dyspepsia; AH, atypical hyperplasia; IN, intraepithelial neoplasia; Dys, dysplasia.

considerably abundant in populations from Túquerres, a town with high GC risk, while *Staphylococcus* sp. were strikingly abundant in populations from Tumaco, a town with low GC risk (Yang et al., 2016). These findings demonstrated that the characteristics of the gastric microbiota in GC patients were associated with both familial history of gastrointestinal tumors and diverse environmental conditions.

Helicobacter pylori and gastric cancer

The first animal experiment on the pathogenicity of *H. pylori* was performed by the Mongolian gerbil model. It revealed that *H. pylori* induced a continuous development from superficial gastritis to pre-malignant lesions (Hirayama et al., 1996). Compared with age-matched uninfected mice, mice infected with *H. pylori* had more severe inflammation, acid atrophy, hyperplasia, epithelial defects, and dysplasia (Lee et al., 2008). Likewise, compared with the control gerbils, low differentiated adenocarcinoma and carcinoid were discovered in the gerbils inoculated with *H. pylori* (Hirayama et al., 1999).

H. pylori infection is one of the main causes of gastric cancer and can increase the risk of gastric cancer by 2.2–21 times (Uemura et al., 2001; Suerbaum and Michetti, 2002). *H. pylori* infection could induce chronic inflammation in the stomach, which was accompanied by genetic alterations and DNA damage in gastric epithelial cells. *H. pylori* infection has been found to trigger ubiquitination and proteasomal degradation of p53, a critical regulator of genome stability, thereby impairing the repair of genome damage. *H. pylori* infection reduces the expression of the transcription factor USF1, which can stabilize the function of P53, and thereby increasing viability of gastric epithelial cells with persistent DNA damage and promoting gastric carcinogenesis (Costa et al., 2020). *H. pylori* could also downregulate the expression of genes associated with tumor suppression by inducing abnormal DNA methylation (Servetas et al., 2016; Choi et al., 2020). Abnormal DNA methylation in the gene promoter region leads to the inactivation of tumor suppressor and other cancer-related genes in cancer cells, which is the most clear epigenetic marker in gastric cancer (Qu et al., 2013). Chan AO et al. observed that *H. pylori* infection caused E-cadherin methylation to be more frequent in the gastric mucosa compared to cases without *H. pylori* infection (Chan et al., 2003). Maekita et al. found that *H. pylori* infection can effectively induce CpG islands methylation to varying degrees (Maekita et al., 2006). *H. pylori* infection also delays gastric epithelial cell apoptosis (Sáenz and Mills, 2020; Imai et al., 2021). *H. pylori* infection induced an increase in cellular spermine oxidase (SMOX), and phosphorylated EGFR (pEGFR), resulting in the generation of a subpopulation of gastric epithelial cells with high levels of DNA damage and resistance to apoptosis (Chaturvedi et al., 2011, 2014).

Among possible explanations of GC caused by *H. pylori*, the two most widely accepted virulence factors were Cytotoxin-associated gene A (*CagA*) and Vacuolating cytotoxin A (*VacA*; Amieva and Peek, 2016), which have been linked to the carcinogenic potential of this bacterium. The *CagA* gene is the most important pathogenic factor of *H. pylori*. Compared with the strains without *CagA*, strains containing *CagA* increase the risk of gastric cancer by 1.64-fold overall (Censini et al., 1996; Huang et al., 2003). *Cag* (+) *H. pylori* induced TP53 gene mutation and aberrant expression of activation-induced cytidine deaminase, which may be responsible for the accumulation of mutation in gastric carcinogenesis (Matsumoto et al., 2007; Yong et al., 2015). *CagA* (+) *H. pylori* infection caused the activation of multiple oncogenic pathways, including ERK/MAPK, PI3K/AKT, NF-kB, Wnt/β-catenin, Ras, Hippo, and STAT3 (Udhayakumar et al., 2007; Salama et al., 2013; Yong et al., 2015; Imai et al., 2021). *CagA* also disturbed the host'sepithelial cells, precursor cells and stem cells (Bessède et al., 2014; Wroblewski et al., 2015). Another virulence factor, *VacA*, was involved in regulating immune responses and autophagy. *VacA* regulated host cell metabolism by inhibiting mTORC1 and promoted gastric epithelial cell apoptosis by interfering with the function of mitochondria (Kim et al., 2018). In addition, *VacA* promotes Treg differentiation by inducing dendritic cell expression and releasing some anti-inflammatory cytokines, such as IL-18 and IL-10, thus suppressing anti-tumor immunity (Kao et al., 2010; Oertli et al., 2012). Prolonged exposure to *VacA* can interrupt autophagy, which is manifested by the accumulation of P62. Autophagy is an important protective mechanism of the stomach against *H. pylori* infection. The interruption of this mechanism will cause cell death, inflammation and genetic instability, forming a microenvironment prone to cancer (Raju et al., 2012).

Other pathogenic mechanisms of *H. pylori* have also been widely reported. Some adhesins, such as sialic acid-binding adhesin (SabA), blood-antigen binding protein A (BabA) and neutrophil-activating protein (NAP), attached to host cell receptors and increased risk of peptic ulcer and GC (Kao et al., 2016). Targosz et al. proved that *H. pylori* up-regulated the expression of cyclooxygenase-2 (COX-2) mRNA in gastric epithelial cells, which was known to be a carcinogenesis-related rate-limiting enzyme (Targosz et al., 2012; Shao et al., 2014). The accumulation of activated β-catenin in the nucleus of gastric epithelial cells induced by *H. pylori* was closely connected with tumor invasion (Cheng et al., 2004), indicating the aberrant activation of β-catenin may be a key member in regulating pre-malignant epithelial responses to *H. pylori*. In addition, *H. pylori*

infection induced the expression of hepatoma-derived growth factor (HDGF), which stimulated the differentiation of human mesenchymal stem cells into myofibroblast-like cells and further promoted the survival and invasion of human GC cells (Liu et al., 2018).

Other gastric microbiota and gastric cancer

Under conditions of absent acidity (such as AG and IM), some non-*H. pylori* bacteria produce active oxygen or nitrogen to regulate inflammatory reactions, and the gastric micro-ecosystem became more complex (Sheh and Fox, 2013). The abundance of some genera showed a consistent increase in GC patients, including *Staphylococcus* (Jo et al., 2016; Castaño-Rodríguez et al., 2017; Shen et al., 2022), *Lactobacillus* (Castaño-Rodríguez et al., 2017; Coker et al., 2018; Ferreira et al., 2018), *Clostridium* (Castaño-Rodríguez et al., 2017; Ferreira et al., 2018), *Fusobacterium* (Castaño-Rodríguez et al., 2017; Coker et al., 2018), *Streptococcus* (Dicksved et al., 2009; Castaño-Rodríguez et al., 2017; Coker et al., 2018), *Bifidobacterium*, and *Lactococcus* (Castaño-Rodríguez et al., 2017). These bacteria had different effects on stomach pathogenesis. A prospective study concluded that the characteristics of gastric microbiota in non-tumor patients could accurately classify patients who may develop EC. They identified a constellation of six bacterial taxonomic markers, including the *Moryella genus*, *Vibro genus*, *Comamonadaceae*, *Paludibacter*, *Agrobacterium*, and *Clostridiales* (Png et al., 2022).

Some non-*H. pylori* bacteria promote the inflammatory response to accelerate the progression of GC, such as *Lactobacillus murinus*, *Clostridium,* and *Streptococcus salivarius* (Lertpiriyapong et al., 2014). It has been proved that the overgrowth of *Propionibacterium acnes* may contribute to lymphocytic gastritis through *in vitro* cell experiments. Lymphocytic gastritis caused by *Propionibacterium acnes* produces pro-inflammatory cytokine IL-15, which is a potential trigger for GC (Montalban-Arques et al., 2016). *Prevotella* had the classification ability to distinguish GC patients from non-cancer-bearing people with an area under the curve of 0.76 (Wu et al., 2018). The pathogenicity of *Prevotella copri* has been proven to produce redox proteins in the human body (Hofer, 2014; Wu et al., 2018). Besides, the Insulin-Gastrin (INS-GAS) transgenic mice colonized *Lactobacillus murinus*, *Clostridium* and *Bacteroides* developed gastrointestinal intraepithelial neoplasia, which strongly related to the upregulation of pro-inflammatory and oncogenic genes (Lertpiriyapong et al., 2014). The microflora of non-*H. pylori* in the stomach also influenced the severity of *H. pylori*-induced gastric cancer. Shen et al. found that *Streptococcus salivarius* coinfection with *H. pylori* induced significantly higher gastric pathology than in *H. pylori*-monoinfected mice. In contrast, *Staphylococcus* epidermidis coinfection caused significantly lower *H. pylori*-induced pro-inflammatory cytokine responses than in *H. pylori*-monoinfected mice (Shen et al., 2022).

Some non-*H. pylori* bacteria could disturb the function of immune cells in the tumor microenvironment to promote GC. Previous studies found a positive correlation between *Stenotrophomonas* in GC tissues and plasmacytoid dendritic cells that have the function of suppressing immune effector cells (Huang et al., 2014; Ling et al., 2019). Similarly, in GC microhabitats, *Selenomonas* was positively associated with regulatory T cells with immunosuppressive effects (Ahmetlić et al., 2019; Ling et al., 2019). These studies suggest *Selenomonas* and *Stenotrophomonas* may promote cancer cells to evade surveillance by the immune system. Besides, it was reported that *Fusobacterium nucleatum* disturbed the phenotypes and functions of immune cells such as neutrophils, T cells, NK cells, dendritic cells and macrophages, forming an immunosuppressive microenvironment conducive to cancer growth (Wu et al., 2019). The increase of *Fusobacterium* in *H. pylori* (−) GC patients may be related to this mechanism (Hsieh et al., 2018). Li Q et al. found that excess *Propionibacterium acnes* promotes gastric cancer progression by promoting M2 polarization of macrophages through TLR4/PI3K/Akt signaling (Li et al., 2021).

Non-*H. pylori* bacteria produced metabolites that may promote the occurrence of GC. Higher levels of non-*H. pylori* nitrosated or nitrate-reducing bacteria (NB) and non-*H. pylori* urease-producing bacteria (UB) were found in *H. pylori* (−) GC patients (Jo et al., 2016; Sohn et al., 2017). It is well known that N-nitroso compounds (NOCs) are potent carcinogens (Hernández-Ramírez et al., 2009; Jo et al., 2016). NOCs formed from nitrite and secondary amines and were observed in some nitrate-reducing gastric bacteria, including *Clostridium*, *Veillonella*, *Haemophilus*, *Staphylococcus*, *Streptococcus*, and *Neisseria* (Ayanaba and Alexander, 1973; Hu et al., 2012; Jo et al., 2016). Similarly, urease is the main trigger of innate immune response produced by various non-*H. pylori* such as *Lactococcus*, *Clostridium*, *Haemophilus*, and *Actinomyces* (Sohn et al., 2017). These nitrate-reducing and urease-producing bacteria may be involved in the pathological mechanism of stomach disorders. However, the detailed pathogenic mechanism remains to be further confirmed.

Not all microbes in the stomach are harmful, and some studies have found the presence of bacteria in the stomach that can inhibit the progression of gastric cancer. For example, Kim SY et al. found that *Lactococcus lactis ssp. lactis* can affect the expression of p53 and p21 to induce cell cycle arrest and apoptosis to inhibit the proliferation of gastric cancer cells (Kim et al., 2004, 2009). In addition, Hwang CH et al. studied that Heat-Killed *Lactobacillus* can induce the expression of pro-apoptotic genes and inhibit the proliferation of gastric cancer cell line AGS *in vitro*. However it still needs to be verified by *in vivo* experiments (Hwang et al., 2022).

Interaction between *Helicobacter pylori* and other gastric microbiota

H. pylori infection altered the composition of the human stomach microbiome (Figure 1). Compared with the gastric microbiota of healthy cases, *H. pylori*-infection individuals have a lower diversity, with a lower abundance of *Actinobacteria*, *Firmicutes* and *Bacteroidetes*, while increased *Proteobacteria* (Andersson et al., 2008; Maldonado-Contreras et al., 2011).In *H. pylori* (+) GC patients, the proportion of the *Streptococcus mitis* group (such as *S. oralis*, *S. infantis*, *S. mitis*, *S. tigurinus,* and *S. pseudopneumoniae*) was significantly lower than that of the *H. pylori* (−) GC group (Sohn et al., 2017). These reduced bacteria may be related to the unfavorable conditions caused by *H. pylori* infection. The tendency of co-occurrence/co-competition among gastric microbiota has been further investigated. Das et al. found

that in *H. pylori* (+) patients, *H. pylori* showed a negative association (inhibit other bacteria) with some gastric members, such as *Acidovorax*, *Aeromonas*, *Bacillus*, *Bradyrhizobium*, *Halomonas*, *Cloacibacterium*, *Meiothermus*, *Methylobacterium*, and *Ralstonia*, while the interactions of these non-*H. pylori* members were positively correlated (das et al., 2017).

The possible influence of *H. pylori* on the structure and function of the gastric microbes has been demonstrated by animal experiments. The addition of restricted microbiota (*Clostridium* ASF356, *Bacteroides* ASF519, *Lactobacillus* ASF361) in the stomach of INS-GAS mice was sufficient to promote gastric mucosal lesions such as moderate inflammation, gland atrophy, epithelial defects, dysplasia, but no gastrointestinal intraepithelial neoplasia. However, mice co-infected with these restricted bacteria and *H. pylori* developed higher-grade glandular abnormalities, and 69% of mice with dysplasia were identified as gastrointestinal intraepithelial neoplasia compared with mice infected only with restricted bacteria (Lertpiriyapong et al., 2014). It indicated that *H. pylori* synergistically accelerated the onset and progression of gastrointestinal intraepithelial neoplasia in mice infected with restricted bacteria. One year after inoculation with *H. pylori*, the numbers of *Atopobium* cluster increased and *Bifidobacterium* spp., *C. coccoides* group, and *C. leptum* subgroup decreased in *H. pylori* (−) gerbils compared to the uninfected gerbils. Besides, *Prevotella spp.* and *Eubacterium cylindroides* group were absent in *H. pylori* (+) gerbils (Osaki et al., 2012). These results suggested that infection with *H. pylori* for a long time may disturb the composition of the gastric microbiota in mice (Osaki et al., 2012). Similarly, the localization and levels of *Bifidobacterium spp.*, *Bacteroides spp.*, *Enterococcus spp.*, *Staphylococcus aureus* and aerobes were modified and caused more severe gastritis in Mongolian gerbils after *H. pylori* infection. Prolonged colonization of *H. pylori* made the stomach environment unsuitable for the reproduction of lactobacilli, while *Bacteroides*, *Bifidobacteria*, *S. aureus* and *Enterococci* could better adapt to the stomach environment (Yin et al., 2011).

H. pylori eradication studies have also demonstrated the relationship between the growth of non-*H. pylori* and *H. pylori*. An inverse correlation was observed between the bacterial diversity and relative abundance of *H. pylori* in GC patients. Compared with non-GC patients with similar levels of *H. pylori*, GC patients showed lower bacterial diversity. After the eradication of *H. pylori*, the diversity of the gastric microbes was increased, and the microbiota abundance was restored to be similar to that of cases without *H. pylori* infection (Li et al., 2017). Likewise, *H. pylori* in the stomach inhibited the colonization of *Enterobacteria*, *Clostridium leptum* and *Lactobacillus*. After eradicaing of *H. pylori*, the bacteria in the patient's stomach increased significantly (Li et al., 2016). In another study, in the *H. pylori* (+) patients, the total number of non- *H. pylori*- NB decreased in the eradicated gastric biopsies and increased in the non-eradicated or failed to eradicate samples (Jo et al., 2016). These studies indirectly confirmed the role of *H. pylori* infection in disturbing gastric microbiota composition.

To sum up, the mechanism of gastric microbiota causing GC is a multi-factor and multi-step process. *H. pylori* is the main trigger of histopathological changes in GC, and its interactions with non-*H. pylori* are jointly involved in the development of GC. *H. pylori* may be more important in the early stages of GC. But the state of achlorhydric induced by *H. pylori* can disturb gastric microbiota, which may play a key role in the later stages of GC (Dias-Jácome et al., 2016).

Regulation of gastric microbiota

Medication

Among the drug interventions to reduce the risk of GC, one of the most studied approaches is *H. pylori* eradication therapy. All patients who test positive for *H. pylori* should be offered eradication therapy. The internationally recommended treatment is the combination of PPI, 2–3 antibiotics, and bismuth, and it should be taken in strictly accordance with the course of treatment. Antibiotic abuse and irregular medication during the treatment of *H. pylori* have made *H. pylori* resistant to clarithromycin, levofloxacin, metronidazole and other drugs. The combination of drugs and the course of treatment vary according to different populations. The main recommended first-line treatment options were Bismuth quadruple therapy, Concomitant therapy, Sequential therapy, Levofloxacin triple therapy and so on (Chey et al., 2017). After 8 weeks of eradication treatment for CG or IM patients, *H. pylori* was significantly reduced, and the diversity of the microbiota increased (increased 31 operational taxonomic units; Li et al., 2017). It indicated that eradication treatment restored the diversity of gastric microbiota. Some studies have shown that eradicating *H. pylori* effectively alleviated stomach pathology (Bae et al., 2018; Sakitani et al., 2018). Eradication treatment also reduced the incidence of GC in healthy cases and patients with gastric neoplasia, reducing GC-related mortality (Choi et al., 2018; Doorakkers et al., 2020; Ford et al., 2020). However, there is evidence that *H. pylori*-eradicated patients were associated with an increased risk of GC (Cheung et al., 2019). Therefore, the effect of *H. pylori* eradication on the incidence of GC still needs to be clarified.

Probiotics and dietary

Probiotics and dietary fiber regulate the gastrointestinal microbiota and immune response; supplementing them was considered a preventive intervention (Zhang et al., 2013; Hill et al., 2014). It was reported that probiotics increased the eradication rate of *H. pylori* and reduced the incidence of side effects of antibacterial treatment (especially diarrhea; de Bortoli et al., 2007; Ojetti et al., 2012; Wang et al., 2013; Keikha and Karbalaei, 2021). It is worth noting that probiotics are not effective *per se* and can only be used as adjunctive therapy for clinical improvement (Wang et al., 2013). Probiotics also improve anticancer properties by producing lactic acid and other organic acids to inhibit the growth of microorganisms that produce mutagens and carcinogens (Dugas et al., 1999). *Lactobacillus* spp. is one of the best-known probiotics and their anti-*H. pylori* properties have been proven (Bahmanyar and Ye, 2006).Apart from probiotics, prebiotics and dietary fiber also synergistically affected *H. pylori* eradication therapy and were strongly associated with a lower risk of GC (Zhang et al., 2013; Shafaghi et al., 2016). Wheat bran acted as a nitrite scavenger, potentially offsetting the carcinogenic

effects of NOCs produced by nitrate-reducing bacteria (Møller et al., 1988). The inhibitory effect of garlic on the growth of *H. pylori* was observed (Jonkers et al., 1999). The antibacterial properties of garlic may be attributed to allicin. Allicin has been confirmed to have a direct antibacterial effect on the growth of *H. pylori in vitro* (Cañizares et al., 2004).

Studies have reported synergistic relationships between multiple dietary components, such as vegetables, fruits, pickles, and soy products, in the development of GC (Bahmanyar and Ye, 2006).Fresh vegetables contain a various of antioxidants that acted as protectants, potentially ameliorating the effects of microbial dysbiosis (Epplein et al., 2008). Broccoli sprouts were rich in sulforaphane, the sulforaphane which had a strong bactericidal effect on *H. pylori* (Yanaka et al., 2009). Dietary patterns of high vegetables and seafood were associated with lower gastric dysbiosis index and lower the risk of GC in males. Sheu et al. pointed out that yogurt containing *lactobacilli* and *bifidobacteria* can improve the cure rate of *H. pylori* infection (Sheu et al., 2002).And the high-dairy dietary pattern was associated with a lower gastric dysbiosis index to reduce GC risk in females (Gunathilake et al., 2021). The intake of red meat and processed meat is related to the increased risk of gastric cancer, especially in H. pylori (+) subjects (González et al., 2006; Huang et al., 2021). Salt induces gastritis by directly damaging the gastric mucosa and increasing the rate of mitosis, and excess salt intake enhances *H. pylori* colonization. Therefore, long-term excessive salt intake will increase the risk of gastric cancer (Yamaguchi and Kakizoe, 2001; Peleteiro et al., 2011; D'Elia et al., 2012; Smyth et al., 2020). Therefore, the change of dietary structure, including reducing the intake of salt and red meat, and increasing the intake of vegetables and fruits, is a possible strategy to prevent gastric cancer.

Transplantation of rumen microbes

In recent years, fecal bacteria transplantation has been a focus to restore the healthy microbiota of the recipient. This effective strategy has been demonstrated in the treatment of various diseases, such as recurrent *Clostridium difficile* infection (Garza-González et al., 2019), inflammatory bowel disease (Colman and Rubin, 2014) and cancers (McQuade et al., 2020; Baruch et al., 2021). Liu et al. investigated the beneficial effects of rumen fluid transplantation on rumen morphology and function in a sheep model of rumen acidosis. Rumen fluid transplantation accelerated the rapid reconstruction of bacterial homeostasis in the rumen from an obvious acidosis state to a healthy level (similar to that of the donor). Furthermore, it reduced the damage of rumen epithelial cells caused by acute rumen acidosis (Liu J. et al., 2019). The results indicated that rumen microbiota transplantation is a promising strategy for reconstructing bacterial homeostasis. However, rumen transplantation is only an early attempt at the animal level, and it needs to be further verified in cancer models and clinical trials.

Conclusion

A healthy stomach environment is a basis for disease prevention, while the imbalance of gastric microbiota is a potential trigger of stomach carcinogenesis. Although *H. pylori* is considered the main cause of GC, studies have shown that other gastric microbiota are also involved in the development of cancer. Therefore, we analyzed the specific interactions between *H. pylori* and non-*H. pylori* in the progression of GC and discussed effective measures to reestablish a balance stomach environment. Probiotics and dietary fiber are considered to be a preventive intervention and adjuvant treatment, while gastric microbiota transplantation may fundamentally rebuild a normal microbiota in the stomach.

In summary, the gastric microbiota is an extremely complex group. The specific mechanism that causes the occurrence and development of GC is still unclear. Gastric tumorigenesis studies should take into account the virulence diversity of *H. pylori* strains, host genetic features, entire microbiota community and diverse environmental conditions.

Author contributions

SZ and CL conceived and designed the study, collected, and drafted the manuscript. LL, QY, and JM revised it critically for important intellectual content. WG, CD, and HW revised the manuscript. All authors contributed to the article and approved the submitted version.

Funding

This research was funded the Fundamental Research Funds for the Central Universities (0214-14380502).

Conflict of interest

The authors declare that the research was conducted in the absence of any commercial or financial relationships that could be construed as a potential conflict of interest.

Publisher's note

References

Ahmetlić, F., Riedel, T., Hömberg, N., Bauer, V., Trautwein, N., Geishauser, A., et al. (2019). Regulatory T cells in an endogenous mouse lymphoma recognize specific antigen peptides and contribute to immune escape. *Cancer Immunol. Res.* 7, 600–608. doi: 10.1158/2326-6066.CIR-18-0419

Alarcón, T., Llorca, L., and Perez-Perez, G. (2017). Impact of the microbiota and gastric disease development by *Helicobacter pylori*. *Curr. Top. Microbiol. Immunol.* 400, 253–275. doi: 10.1007/978-3-319-50520-6_11

Amieva, M., and Peek, R. M. Jr. (2016). Pathobiology of *Helicobacter pylori*-induced gastric cancer. *Gastroenterology* 150, 64–78. doi: 10.1053/j.gastro.2015.09.004

Andersson, A. F., Lindberg, M., Jakobsson, H., Bäckhed, F., Nyrén, P., and Engstrand, L. (2008). Comparative analysis of human gut microbiota by barcoded pyrosequencing. *PLoS One* 3:e2836. doi: 10.1371/journal.pone.0002836

Aviles-Jimenez, F., Vazquez-Jimenez, F., Medrano-Guzman, R., Mantilla, A., and Torres, J. (2014). Stomach microbiota composition varies between patients with non-atrophic gastritis and patients with intestinal type of gastric cancer. *Sci. Rep.* 4:4202. doi: 10.1038/srep04202

Ayanaba, A., and Alexander, M. (1973). Microbial formation of nitrosamines in vitro. *Appl. Microbiol.* 25, 862–868. doi: 10.1128/am.25.6.862-868.1973

Bae, S. E., Choi, K. D., Choe, J., Kim, S. O., Na, H. K., Choi, J. Y., et al. (2018). The effect of eradication of *Helicobacter pylori* on gastric cancer prevention in healthy asymptomatic populations. *Helicobacter* 23:e12464. doi: 10.1111/hel.12464

Bahmanyar, S., and Ye, W. (2006). Dietary patterns and risk of squamous-cell carcinoma and adenocarcinoma of the esophagus and adenocarcinoma of the gastric cardia: a population-based case-control study in Sweden. *Nutr. Cancer* 54, 171–178. doi: 10.1207/s15327914nc5402_3

Baruch, E. N., Youngster, I., Ben-Betzalel, G., Ortenberg, R., Lahat, A., Katz, L., et al. (2021). Fecal microbiota transplant promotes response in immunotherapy-refractory melanoma patients. *Science* 371, 602–609. doi: 10.1126/science.abb5920

Bessède, E., Staedel, C., Acuña Amador, L. A., Nguyen, P. H., Chambonnier, L., Hatakeyama, M., et al. (2014). *Helicobacter pylori* generates cells with cancer stem cell properties via epithelial-mesenchymal transition-like changes. *Oncogene* 33, 4123–4131. doi: 10.1038/onc.2013.380

Boers, S. A., Jansen, R., and Hays, J. P. (2019). Understanding and overcoming the pitfalls and biases of next-generation sequencing (NGS) methods for use in the routine clinical microbiological diagnostic laboratory. *Eur. J. Clin. Microbiol. Infect. Dis.* 38, 1059–1070. doi: 10.1007/s10096-019-03520-3

Bruno, G., Rocco, G., Zaccari, P., Porowska, B., Mascellino, M. T., and Severi, C. (2018). *Helicobacter pylori* infection and gastric Dysbiosis: can probiotics administration be useful to treat this condition? *Can. J. Infect. Dis. Med. Microbiol.* 2018:6237239. doi: 10.1155/2018/6237239

Bruno, G., Zaccari, P., Rocco, G., Scalese, G., Panetta, C., Porowska, B., et al. (2019). Proton pump inhibitors and dysbiosis: current knowledge and aspects to be clarified. *World J. Gastroenterol.* 25, 2706–2719. doi: 10.3748/wjg.v25.i22.2706

Cañizares, P., Gracia, I., Gómez, L. A., García, A., Martín de Argila, C., Boixeda, D., et al. (2004). Thermal degradation of allicin in garlic extracts and its implication on the inhibition of the in-vitro growth of *Helicobacter pylori*. *Biotechnol. Prog.* 20, 32–37. doi: 10.1021/bp034135v

Castaño-Rodríguez, N., Goh, K. L., Fock, K. M., Mitchell, H. M., and Kaakoush, N. O. (2017). Dysbiosis of the microbiome in gastric carcinogenesis. *Sci. Rep.* 7:15957. doi: 10.1038/s41598-017-16289-2

Censini, S., Lange, C., Xiang, Z., Crabtree, J. E., Ghiara, P., Borodovsky, M., et al. (1996). Cag, a pathogenicity island of *Helicobacter pylori*, encodes type I-specific and disease-associated virulence factors. *Proc. Natl. Acad. Sci. U. S. A.* 93, 14648–14653. doi: 10.1073/pnas.93.25.14648

Chan, A. O., Lam, S. K., Wong, B. C., Wong, W. M., Yuen, M. F., Yeung, Y. H., et al. (2003). Promoter methylation of E-cadherin gene in gastric mucosa associated with *Helicobacter pylori* infection and in gastric cancer. *Gut* 52, 502–506. doi: 10.1136/gut.52.4.502

Chaturvedi, R., Asim, M., Piazuelo, M. B., Yan, F., Barry, D. P., Sierra, J. C., et al. (2014). Activation of EGFR and ERBB2 by *Helicobacter pylori* results in survival of gastric epithelial cells with DNA damage. *Gastroenterology* 146, 1739–51.e14. doi: 10.1053/j.gastro.2014.02.005

Chaturvedi, R., Asim, M., Romero–Gallo, J., Barry, D. P., Hoge, S., de Sablet, T., et al. (2011). Spermine oxidase mediates the gastric cancer risk associated with *Helicobacter pylori* CagA. *Gastroenterology* 141, 1696–1708.e2. doi: 10.1053/j.gastro.2011.07.045

Chen, X. H., Wang, A., Chu, A. N., Gong, Y. H., and Yuan, Y. (2019). Mucosa-associated microbiota in gastric cancer tissues compared with non-cancer tissues. *Front. Microbiol.* 10:1261. doi: 10.3389/fmicb.2019.01261

Cheng, X. X., Sun, Y., Chen, X. Y., Zhang, K. L., Kong, Q. Y., Liu, J., et al. (2004). Frequent translocalization of beta-catenin in gastric cancers and its relevance to tumor progression. *Oncol. Rep.* 11, 1201–1207. doi: 10.3892/or.11.6.1201

Cheung, K. S., Chan, E. W., Chen, L., Seto, W. K., Wong, I. C. K., and Leung, W. K. (2019). Diabetes increases risk of gastric cancer after *Helicobacter pylori* eradication: a territory-wide study with propensity score analysis. *Diabetes Care* 42, 1769–1775. doi: 10.2337/dc19-0437

Chey, W. D., Leontiadis, G. I., Howden, C. W., and Moss, S. F. (2017). ACG clinical guideline: treatment of *Helicobacter pylori* infection. *Am. J. Gastroenterol.* 112, 212–239. doi: 10.1038/ajg.2016.563

Choi, J. M., Kim, S. G., Yang, H. J., Lim, J. H., Cho, N. Y., Kim, W. H., et al. (2020). *Helicobacter pylori* eradication can reverse the methylation-associated regulation of miR-200a/b in gastric carcinogenesis. *Gut Liver* 14, 571–580. doi: 10.5009/gnl19299

Choi, I. J., Kook, M. C., Kim, Y. I., Cho, S. J., Lee, J. Y., Kim, C. G., et al. (2018). *Helicobacter pylori* therapy for the prevention of Metachronous gastric cancer. *N. Engl. J. Med.* 378, 1085–1095. doi: 10.1056/NEJMoa1708423

Cires, M. J., Wong, X., Carrasco-Pozo, C., and Gotteland, M. (2016). The gastrointestinal tract as a Key target organ for the health-promoting effects of dietary Proanthocyanidins. *Front. Nutr.* 3:57. doi: 10.3389/fnut.2016.00057

Coker, O. O., Dai, Z., Nie, Y., Zhao, G., Cao, L., Nakatsu, G., et al. (2018). Mucosal microbiome dysbiosis in gastric carcinogenesis. *Gut* 67, 1024–1032. doi: 10.1136/gutjnl-2017-314281

Colman, R. J., and Rubin, D. T. (2014). Fecal microbiota transplantation as therapy for inflammatory bowel disease: a systematic review and meta-analysis. *J. Crohns Colitis* 8, 1569–1581. doi: 10.1016/j.crohns.2014.08.006

Costa, L., Corre, S., Michel, V., le Luel, K., Fernandes, J., Ziveri, J., et al. (2020). USF1 defect drives p53 degradation during *Helicobacter pylori* infection and accelerates gastric carcinogenesis. *Gut* 69, 1582–1591. doi: 10.1136/gutjnl-2019-318640

D'Elia, L., Rossi, G., Ippolito, R., Cappuccio, F. P., and Strazzullo, P. (2012). Habitual salt intake and risk of gastric cancer: a meta-analysis of prospective studies. *Clin. Nutr.* 31, 489–498. doi: 10.1016/j.clnu.2012.01.003

Dai, D., Yang, Y., Yu, J., Dang, T., Qin, W., Teng, L., et al. (2021). Interactions between gastric microbiota and metabolites in gastric cancer. *Cell Death Dis.* 12:1104. doi: 10.1038/s41419-021-04396-y

das, A., Pereira, V., Saxena, S., Ghosh, T. S., Anbumani, D., Bag, S., et al. (2017). Gastric microbiome of Indian patients with *Helicobacter pylori* infection, and their interaction networks. *Sci. Rep.* 7:15438. doi: 10.1038/s41598-017-15510-6

de Bortoli, N., Leonardi, G., Ciancia, E., Merlo, A., Bellini, M., Costa, F., et al. (2007). *Helicobacter pylori* eradication: a randomized prospective study of triple therapy versus triple therapy plus lactoferrin and probiotics. *Am. J. Gastroenterol.* 102, 951–956. doi: 10.1111/j.1572-0241.2007.01085.x

Dias-Jácome, E., Libânio, D., Borges-Canha, M., Galaghar, A., and Pimentel-Nunes, P. (2016). Gastric microbiota and carcinogenesis: the role of non-*Helicobacter pylori* bacteria - a systematic review. *Rev. Esp. Enferm. Dig.* 108, 530–540. doi: 10.17235/reed.2016.4261/2016

Dicksved, J., Lindberg, M., Rosenquist, M., Enroth, H., Jansson, J. K., and Engstrand, L. (2009). Molecular characterization of the stomach microbiota in patients with gastric cancer and in controls. *J. Med. Microbiol.* 58, 509–516. doi: 10.1099/jmm.0.007302-0

Dong, J., and Thrift, A. P. (2017). Alcohol, smoking and risk of oesophago-gastric cancer. *Best Pract. Res. Clin. Gastroenterol.* 31, 509–517. doi: 10.1016/j.bpg.2017.09.002

Doorakkers, E., Lagergren, J., Engstrand, L., and Brusselaers, N. (2016). Eradication of *Helicobacter pylori* and gastric cancer: a systematic review and meta-analysis of cohort studies. *J. Natl. Cancer Inst.* 108:djw132. doi: 10.1093/jnci/djw132

Doorakkers, E., Lagergren, J., Engstrand, L., and Brusselaers, N. (2020). Reply to: *Helicobacter pylori* eradication treatment and the risk of gastric adenocarcinoma in a western population. *Gut* 69, 1149–1150. doi: 10.1136/gutjnl-2019-319000

Dugas, B., Mercenier, A., Lenoir-Wijnkoop, I., Arnaud, C., Dugas, N., and Postaire, E. (1999). Immunity and probiotics. *Immunol. Today* 20, 387–390. doi: 10.1016/S0167-5699(99)01448-6

Epplein, M., Nomura, A. M. Y., Hankin, J. H., Blaser, M. J., Perez-Perez, G., Stemmermann, G. N., et al. (2008). Association of *Helicobacter pylori* infection and diet on the risk of gastric cancer: a case-control study in Hawaii. *Cancer Causes Control* 19, 869–877. doi: 10.1007/s10552-008-9149-2

Eun, C. S., Kim, B. K., Han, D. S., Kim, S. Y., Kim, K. M., Choi, B. Y., et al. (2014). Differences in gastric mucosal microbiota profiling in patients with chronic gastritis, intestinal metaplasia, and gastric cancer using pyrosequencing methods. *Helicobacter* 19, 407–416. doi: 10.1111/hel.12145

Falush, D., Wirth, T., Linz, B., Pritchard, J. K., Stephens, M., Kidd, M., et al. (2003). Traces of human migrations in *Helicobacter pylori* populations. *Science* 299, 1582–1585. doi: 10.1126/science.1080857

Ferreira, R. M., Pereira-Marques, J., Pinto-Ribeiro, I., Costa, J. L., Carneiro, F., Machado, J. C., et al. (2018). Gastric microbial community profiling reveals a dysbiotic cancer-associated microbiota. *Gut* 67, 226–236. doi: 10.1136/gutjnl-2017-314205

Ford, A. C., Yuan, Y., and Moayyedi, P. (2020). *Helicobacter pylori* eradication therapy to prevent gastric cancer: systematic review and meta-analysis. *Gut* 69, 2113–2121. doi: 10.1136/gutjnl-2020-320839

Garza-González, E., Mendoza-Olazarán, S., Morfin-Otero, R., Ramírez-Fontes, A., Rodríguez-Zulueta, P., Flores-Treviño, S., et al. (2019). Intestinal microbiome changes in fecal microbiota transplant (FMT) vs. FMT enriched with lactobacillus in the treatment of recurrent Clostridioides difficile infection. *Can. J. Gastroenterol. Hepatol.* 2019:4549298. doi: 10.1155/2019/4549298

González, C. A., Jakszyn, P., Pera, G., Agudo, A., Bingham, S., Palli, D., et al. (2006). Meat intake and risk of stomach and esophageal adenocarcinoma within the European prospective investigation into cancer and nutrition (EPIC). *J. Natl. Cancer Inst.* 98, 345–354. doi: 10.1093/jnci/djj071

Gunathilake, M. N., Lee, J., Choi, I. J., Kim, Y. I., Ahn, Y., Park, C., et al. (2019). Association between the relative abundance of gastric microbiota and the risk of gastric cancer: a case-control study. *Sci. Rep.* 9:13589. doi: 10.1038/s41598-019-50054-x

Gunathilake, M., Lee, J. H., Choi, I. J., Kim, Y. I., and Kim, J. S. (2021). Effect of the Interaction between Dietary Patterns and the Gastric Microbiome on the Risk of Gastric Cancer. *Nutrients* 13:2692. doi: 10.3390/nu13082692

Guo, Y., Cao, X. S., Zhou, M. G., and Yu, B. (2022). Gastric microbiota in gastric cancer: different roles of *Helicobacter pylori* and other microbes. *Front. Cell. Infect. Microbiol.* 12:1105811. doi: 10.3389/fcimb.2022.1105811

He, X., McLean, J. S., Edlund, A., Yooseph, S., Hall, A. P., Liu, S. Y., et al. (2015). Cultivation of a human-associated TM7 phylotype reveals a reduced genome and epibiotic parasitic lifestyle. *Proc. Natl. Acad. Sci. U. S. A.* 112, 244–249. doi: 10.1073/pnas.1419038112

Hernández-Ramírez, R. U., Galván-Portillo, M. V., Ward, M. H., Agudo, A., González, C. A., Oñate-Ocaña, L. F., et al. (2009). Dietary intake of polyphenols, nitrate and nitrite and gastric cancer risk in Mexico City. *Int. J. Cancer* 125, 1424–1430. doi: 10.1002/ijc.24454

Hill, C., Guarner, F., Reid, G., Gibson, G. R., Merenstein, D. J., Pot, B., et al. (2014). Expert consensus document. The international scientific Association for Probiotics and Prebiotics consensus statement on the scope and appropriate use of the term probiotic. *Nat. Rev. Gastroenterol. Hepatol.* 11, 506–514. doi: 10.1038/nrgastro.2014.66

Hirayama, F., Takagi, S., Iwao, E., Yokoyama, Y., Haga, K., and Hanada, S. (1999). Development of poorly differentiated adenocarcinoma and carcinoid due to long-term *Helicobacter pylori* colonization in Mongolian gerbils. *J. Gastroenterol.* 34, 450–454. doi: 10.1007/s005350050295

Hirayama, F., Takagi, S., Kusuhara, H., Iwao, E., Yokoyama, Y., and Ikeda, Y. (1996). Induction of gastric ulcer and intestinal metaplasia in mongolian gerbils infected with *Helicobacter pylori*. *J. Gastroenterol.* 31, 755–757. doi: 10.1007/BF02347631

Hofer, U. (2014). Microbiome: pro-inflammatory Prevotella? *Nat. Rev. Microbiol.* 12:5. doi: 10.1038/nrmicro3180

Hsieh, Y. Y., Tung, S. Y., Pan, H. Y., Yen, C. W., Xu, H. W., Lin, Y. J., et al. (2018). Increased abundance of clostridium and Fusobacterium in gastric microbiota of patients with gastric cancer in Taiwan. *Sci. Rep.* 8:158. doi: 10.1038/s41598-017-18596-0

Hu, Y., He, L. H., Xiao, D., Liu, G. D., Gu, Y. X., Tao, X. X., et al. (2012). Bacterial flora concurrent with *Helicobacter pylori* in the stomach of patients with upper gastrointestinal diseases. *World J. Gastroenterol.* 18, 1257–1261. doi: 10.3748/wjg.v18.i11.1257

Hu, Y. L., Pang, W., Huang, Y., Zhang, Y., and Zhang, C. J. (2018). The gastric microbiome is perturbed in advanced gastric adenocarcinoma identified through shotgun Metagenomics. *Front. Cell. Infect. Microbiol.* 8:433. doi: 10.3389/fcimb.2018.00433

Huang, Y., Cao, D., Chen, Z., Chen, B., Li, J., Guo, J., et al. (2021). Red and processed meat consumption and cancer outcomes: umbrella review. *Food Chem.* 356:129697. doi: 10.1016/j.foodchem.2021.129697

Huang, X. M., Liu, X. S., Lin, X. K., Yu, H., Sun, J. Y., Liu, X. K., et al. (2014). Role of plasmacytoid dendritic cells and inducible costimulator-positive regulatory T cells in the immunosuppression microenvironment of gastric cancer. *Cancer Sci.* 105, 150–158. doi: 10.1111/cas.12327

Huang, J. Q., Zheng, G. F., Sumanac, K., Irvine, E. J., and Hunt, R. H. (2003). Meta-analysis of the relationship between cagA seropositivity and gastric cancer. *Gastroenterology* 125, 1636–1644. doi: 10.1053/j.gastro.2003.08.033

Hwang, C. H., Lee, N. K., and Paik, H. D. (2022). The anti-cancer potential of heat-killed lactobacillus brevis KU15176 upon AGS cell lines through intrinsic apoptosis pathway. *Int. J. Mol. Sci.* 23:4073. doi: 10.3390/ijms23084073

Imai, S., Ooki, T., Murata-Kamiya, N., Komura, D., Tahmina, K., Wu, W., et al. (2021). *Helicobacter pylori* CagA elicits BRCAness to induce genome instability that may underlie bacterial gastric carcinogenesis. *Cell Host Microbe* 29, 941–58.e10. doi: 10.1016/j.chom.2021.04.006

Jo, H. J., Kim, J., Kim, N., Park, J. H., Nam, R. H., Seok, Y. J., et al. (2016). Analysis of gastric microbiota by pyrosequencing: minor role of bacteria other than *Helicobacter pylori* in the gastric carcinogenesis. *Helicobacter* 21, 364–374. doi: 10.1111/hel.12293

Jonkers, D., van den Broek, E., van Dooren, I., Thijs, C., Dorant, E., Hageman, G., et al. (1999). Antibacterial effect of garlic and omeprazole on *Helicobacter pylori*. *J. Antimicrob. Chemother.* 43, 837–839. doi: 10.1093/jac/43.6.837

Kao, C. Y., Sheu, B. S., and Wu, J. J. (2016). *Helicobacter pylori* infection: an overview of bacterial virulence factors and pathogenesis. *Biom. J.* 39, 14–23. doi: 10.1016/j.bj.2015.06.002

Kao, J. Y., Zhang, M., Miller, M. J., Mills, J. C., Wang, B., Liu, M., et al. (2010). *Helicobacter pylori* immune escape is mediated by dendritic cell-induced Treg skewing and Th17 suppression in mice. *Gastroenterology* 138, 1046–1054. doi: 10.1053/j.gastro.2009.11.043

Keikha, M., and Karbalaei, M. (2021). Probiotics as the live microscopic fighters against *Helicobacter pylori* gastric infections. *BMC Gastroenterol.* 21:388. doi: 10.1186/s12876-021-01977-1

Khosravi, Y., Dieye, Y., Poh, B. H., Ng, C. G., Loke, M. F., Goh, K. L., et al. (2014). Culturable bacterial microbiota of the stomach of *Helicobacter pylori* positive and negative gastric disease patients. *ScientificWorldJournal* 2014:610421. doi: 10.1155/2014/610421

Kim, S. Y., Kim, J. E., Lee, K. W., and Lee, H. J. (2009). Lactococcus lactis ssp. lactis inhibits the proliferation of SNU-1 human stomach cancer cells through induction of G0/G1 cell cycle arrest and apoptosis via p53 and p21 expression. *Ann. N. Y. Acad. Sci.* 1171, 270–275. doi: 10.1111/j.1749-6632.2009.04721.x

Kim, S. Y., Lee, K. W., Kim, J. Y., and Lee, H. J. (2004). Cytoplasmic fraction of Lactococcus lactis ssp. lactis induces apoptosis in SNU-1 stomach adenocarcinoma cells. *Biofactors* 22, 119–122. doi: 10.1002/biof.5520220123

Kim, I. J., Lee, J., Oh, S. J., Yoon, M. S., Jang, S. S., Holland, R. L., et al. (2018). *Helicobacter pylori* infection modulates host cell metabolism through VacA-dependent inhibition of mTORC1. *Cell Host Microbe* 23, 583–93.e8. doi: 10.1016/j.chom.2018.04.006

Lee, C. W., Rickman, B., Rogers, A. B., Ge, Z., Wang, T. C., and Fox, J. G. (2008). *Helicobacter pylori* eradication prevents progression of gastric cancer in hypergastrinemic INS-GAS mice. *Cancer Res.* 68, 3540–3548. doi: 10.1158/0008-5472.CAN-07-6786

Lertpiriyapong, K., Whary, M. T., Muthupalani, S., Lofgren, J. L., Gamazon, E. R., Feng, Y., et al. (2014). Gastric colonisation with a restricted commensal microbiota replicates the promotion of neoplastic lesions by diverse intestinal microbiota in the *Helicobacter pylori* INS-GAS mouse model of gastric carcinogenesis. *Gut* 63, 54–63. doi: 10.1136/gutjnl-2013-305178

Li, T. H., Qin, Y., Sham, P. C., Lau, K. S., Chu, K. M., and Leung, W. K. (2017). Alterations in gastric microbiota after H. pylori eradication and in different histological stages of gastric carcinogenesis. *Sci. Rep.* 7:44935. doi: 10.1038/srep44935

Li, X. X., Wong, G. L. H., To, K. F., Wong, V. W. S., Lai, L. H., Chow, D. K. L., et al. (2009). Bacterial microbiota profiling in gastritis without *Helicobacter pylori* infection or non-steroidal anti-inflammatory drug use. *PLoS One* 4:e7985. doi: 10.1371/journal.pone.0007985

Li, Q., Wu, W., Gong, D., Shang, R., Wang, J., and Yu, H. (2021). Propionibacterium acnes overabundance in gastric cancer promote M2 polarization of macrophages via a TLR4/PI3K/Akt signaling. *Gastric Cancer* 24, 1242–1253. doi: 10.1007/s10120-021-01202-8

Li, L., Zhou, X., Xiao, S., Ye, F., and Zhang, G. (2016). The effect of *Helicobacter pylori* eradication on the gastrointestinal microbiota in patients with duodenal ulcer. *J. Gastrointestin. Liver Dis.* 25, 139–146. doi: 10.15403/jgld.2014.1121.252.hpe

Ling, Z., Shao, L., Liu, X., Cheng, Y., Yan, C., Mei, Y., et al. (2019). Regulatory T cells and Plasmacytoid dendritic cells within the tumor microenvironment in gastric cancer are correlated with gastric microbiota Dysbiosis: a preliminary study. *Front. Immunol.* 10:533. doi: 10.3389/fimmu.2019.00533

Linz, B., Balloux, F., Moodley, Y., Manica, A., Liu, H., Roumagnac, P., et al. (2007). An African origin for the intimate association between humans and *Helicobacter pylori*. *Nature* 445, 915–918. doi: 10.1038/nature05562

Liu, J., Li, H., Zhu, W., and Mao, S. (2019). Dynamic changes in rumen fermentation and bacterial community following rumen fluid transplantation in a sheep model of rumen acidosis: implications for rumen health in ruminants. *FASEB J.* 33, 8453–8467. doi: 10.1096/fj.201802456R

Liu, X., Shao, L., Liu, X., Ji, F., Mei, Y., Cheng, Y., et al. (2019). Alterations of gastric mucosal microbiota across different stomach microhabitats in a cohort of 276 patients with gastric cancer. *EBioMedicine* 40, 336–348. doi: 10.1016/j.ebiom.2018.12.034

Liu, C. J., Wang, Y. K., Kuo, F. C., Hsu, W. H., Yu, F. J., Hsieh, S., et al. (2018). *Helicobacter pylori* infection-induced Hepatoma-derived growth factor regulates the differentiation of human Mesenchymal stem cells to Myofibroblast-like cells. *Cancers* 10:479. doi: 10.3390/cancers10120479

Lofgren, J. L., Whary, M. T., Ge, Z., Muthupalani, S., Taylor, N. S., Mobley, M., et al. (2011). Lack of commensal flora in *Helicobacter pylori*-infected INS-GAS mice reduces gastritis and delays intraepithelial neoplasia. *Gastroenterology* 140, 210–220.e4. doi: 10.1053/j.gastro.2010.09.048

Maekita, T., Nakazawa, K., Mihara, M., Nakajima, T., Yanaoka, K., Iguchi, M., et al. (2006). High levels of aberrant DNA methylation in *Helicobacter pylori* - infected gastric mucosae and its possible association with gastric cancer risk. *Clin. Cancer Res.* 12, 989–995. doi: 10.1158/1078-0432.CCR-05-2096

Malaty, H. M., el-Kasabany, A., Graham, D. Y., Miller, C. C., Reddy, S. G., Srinivasan, S. R., et al. (2002). Age at acquisition of *Helicobacter pylori* infection: a follow-up study from infancy to adulthood. *Lancet* 359, 931–935. doi: 10.1016/S0140-6736(02)08025-X

Maldonado-Contreras, A., Goldfarb, K. C., Godoy-Vitorino, F., Karaoz, U., Contreras, M., Blaser, M. J., et al. (2011). Structure of the human gastric bacterial community in relation to *Helicobacter pylori* status. *ISME J.* 5, 574–579. doi: 10.1038/ismej.2010.149

Matsumoto, Y., Marusawa, H., Kinoshita, K., Endo, Y., Kou, T., Morisawa, T., et al. (2007). *Helicobacter pylori* infection triggers aberrant expression of activation-induced cytidine deaminase in gastric epithelium. *Nat. Med.* 13, 470–476. doi: 10.1038/nm1566

McQuade, J. L., Ologun, G. O., Arora, R., and Wargo, J. A. (2020). Gut microbiome modulation via fecal microbiota transplant to augment immunotherapy in patients with melanoma or other cancers. *Curr. Oncol. Rep.* 22:74. doi: 10.1007/s11912-020-00913-y

Møller, M. E., Dahl, R., and Bøckman, O. C. (1988). A possible role of the dietary fibre product, wheat bran, as a nitrite scavenger. *Food Chem. Toxicol.* 26, 841–845. doi: 10.1016/0278-6915(88)90024-5

Monstein, H. J., Tiveljung, A., Kraft, C. H., Borch, K., and Jonasson, J. (2000). Profiling of bacterial flora in gastric biopsies from patients with *Helicobacter pylori*-associated gastritis and histologically normal control individuals by temperature gradient gel electrophoresis and 16S rDNA sequence analysis. *J. Med. Microbiol.* 49, 817–822. doi: 10.1099/0022-1317-49-9-817

Montalban-Arques, A., Wurm, P., Trajanoski, S., Schauer, S., Kienesberger, S., Halwachs, B., et al. (2016). Propionibacterium acnes overabundance and natural killer group 2 member D system activation in corpus-dominant lymphocytic gastritis. *J. Pathol.* 240, 425–436. doi: 10.1002/path.4782

Nardone, G., and Compare, D. (2015). The human gastric microbiota: is it time to rethink the pathogenesis of stomach diseases? *United European Gastroenterol J* 3, 255–260. doi: 10.1177/2050640614566846

Oertli, M., Sundquist, M., Hitzler, I., Engler, D. B., Arnold, I. C., Reuter, S., et al. (2012). DC-derived IL-18 drives Treg differentiation, murine *Helicobacter pylori*-specific immune tolerance, and asthma protection. *J. Clin. Invest.* 122, 1082–1096. doi: 10.1172/JCI61029

Ohno, H., and Satoh-Takayama, N. (2020). Stomach microbiota, *Helicobacter pylori*, and group 2 innate lymphoid cells. *Exp. Mol. Med.* 52, 1377–1382. doi: 10.1038/s12276-020-00485-8

Ojetti, V., Bruno, G., Ainora, M. E., Gigante, G., Rizzo, G., Roccarina, D., et al. (2012). Impact of lactobacillus reuteri supplementation on anti-*Helicobacter pylori* levofloxacin-based second-line therapy. *Gastroenterol. Res. Pract.* 2012:740381. doi: 10.1155/2012/740381

Osaki, T., Matsuki, T., Asahara, T., Zaman, C., Hanawa, T., Yonezawa, H., et al. (2012). Comparative analysis of gastric bacterial microbiota in Mongolian gerbils after long-term infection with *Helicobacter pylori*. *Microb. Pathog.* 53, 12–18. doi: 10.1016/j.micpath.2012.03.008

Park, C. H., Lee, A. R., Lee, Y. R., Eun, C. S., Lee, S. K., and Han, D. S. (2019). Evaluation of gastric microbiome and metagenomic function in patients with intestinal metaplasia using 16S rRNA gene sequencing. *Helicobacter* 24:e12547. doi: 10.1111/hel.12547

Parsons, B. N., Ijaz, U. Z., D'Amore, R., Burkitt, M. D., Eccles, R., Lenzi, L., et al. (2017). Comparison of the human gastric microbiota in hypochlorhydric states arising as a result of *Helicobacter pylori*-induced atrophic gastritis, autoimmune atrophic gastritis and proton pump inhibitor use. *PLoS Pathog.* 13:e1006653. doi: 10.1371/journal.ppat.1006653

Peleteiro, B., Lopes, C., Figueiredo, C., and Lunet, N. (2011). Salt intake and gastric cancer risk according to *Helicobacter pylori* infection, smoking, tumour site and histological type. *Br. J. Cancer* 104, 198–207. doi: 10.1038/sj.bjc.6605993

Png, C. W., Lee, W. J. J., Chua, S. J., Zhu, F., Gastric Consortium5Yeoh, K. G., et al. (2022). Mucosal microbiome associates with progression to gastric cancer. *Theranostics* 12, 48–58. doi: 10.7150/thno.65302

Qu, Y., Dang, S., and Hou, P. (2013). Gene methylation in gastric cancer. *Clin. Chim. Acta* 424, 53–65. doi: 10.1016/j.cca.2013.05.002

Rajilic-Stojanovic, M., Figueiredo, C., Smet, A., Hansen, R., Kupcinskas, J., Rokkas, T., et al. (2020). Systematic review: gastric microbiota in health and disease. *Aliment. Pharmacol. Ther.* 51, 582–602. doi: 10.1111/apt.15650

Raju, D., Hussey, S., Ang, M., Terebiznik, M. R., Sibony, M., Galindo–Mata, E., et al. (2012). Vacuolating cytotoxin and variants in Atg16L1 that disrupt autophagy promote *Helicobacter pylori* infection in humans. *Gastroenterology* 142, 1160–1171. doi: 10.1053/j.gastro.2012.01.043

Rawla, P., and Barsouk, A. (2019). Epidemiology of gastric cancer: global trends, risk factors and prevention. *Prz. Gastroenterol.* 14, 26–38. doi: 10.5114/pg.2018.80001

Sáenz, J. B., and Mills, J. C. (2020). *Helicobacter pylori*: preying on SIVA for survival in the stomach. *J. Clin. Invest.* 130, 2183–2185. doi: 10.1172/JCI135508

Sakitani, K., Nishizawa, T., Arita, M., Yoshida, S., Kataoka, Y., Ohki, D., et al. (2018). Early detection of gastric cancer after *Helicobacter pylori* eradication due to endoscopic surveillance. *Helicobacter* 23:e12503. doi: 10.1111/hel.12503

Salama, N. R., Hartung, M. L., and Müller, A. (2013). Life in the human stomach: persistence strategies of the bacterial pathogen *Helicobacter pylori*. *Nat. Rev. Microbiol.* 11, 385–399. doi: 10.1038/nrmicro3016

Satoh-Takayama, N., Kato, T., Motomura, Y., Kageyama, T., Taguchi-Atarashi, N., Kinoshita-Daitoku, R., et al. (2020). Bacteria-induced group 2 innate lymphoid cells in the stomach provide immune protection through induction of IgA. *Immunity* 52, 635–49.e4. doi: 10.1016/j.immuni.2020.03.002

Scarpignato, C., Gatta, L., Zullo, A., and Blandizzi, C.for the SIF-AIGO-FIMMG Groupon behalf of the Italian Society of Pharmacology, the Italian Association of Hospital Gastroenterologists, and the Italian Federation of General Practitioners (2016). Effective and safe proton pump inhibitor therapy in acid-related diseases - a position paper addressing benefits and potential harms of acid suppression. *BMC Med.* 14:179. doi: 10.1186/s12916-016-0718-z

Schulz, C., Schütte, K., Koch, N., Vilchez-Vargas, R., Wos-Oxley, M. L., Oxley, A. P. A., et al. (2018). The active bacterial assemblages of the upper GI tract in individuals with and without helicobacter infection. *Gut* 67, 216–225. doi: 10.1136/gutjnl-2016-312904

Seo, I., Jha, B. K., Suh, S. I., Suh, M. H., and Baek, W. K. (2014). Microbial profile of the stomach: comparison between Normal mucosa and cancer tissue in the same patient. *J. Bus. Ventur.* 44, 162–169. doi: 10.4167/jbv.2014.44.2.162

Servetas, S. L., Bridge, D. R., and Merrell, D. S. (2016). Molecular mechanisms of gastric cancer initiation and progression by *Helicobacter pylori*. *Curr. Opin. Infect. Dis.* 29, 304–310. doi: 10.1097/QCO.0000000000000248

Shafaghi, A., Pourkazemi, A., Khosravani, M., Fakhrie Asl, S., Amir Maafi, A., Atrkar Roshan, Z., et al. (2016). The effect of probiotic plus prebiotic supplementation on the tolerance and efficacy of *Helicobacter pylori* eradication quadruple therapy: a randomized prospective double blind controlled trial. *Middle East J. Dig. Dis.* 8, 179–188. doi: 10.15171/mejdd.2016.30

Shao, Y., Sun, K., Xu, W., Li, X. L., Shen, H., and Sun, W. H. (2014). *Helicobacter pylori* infection, gastrin and cyclooxygenase-2 in gastric carcinogenesis. *World J. Gastroenterol.* 20, 12860–12873. doi: 10.3748/wjg.v20.i36.12860

Shao, D., Vogtmann, E., Liu, A., Qin, J., Chen, W., Abnet, C. C., et al. (2019). Microbial characterization of esophageal squamous cell carcinoma and gastric cardia adenocarcinoma from a high-risk region of China. *Cancer* 125, 3993–4002. doi: 10.1002/cncr.32403

Sheh, A., and Fox, J. G. (2013). The role of the gastrointestinal microbiome in *Helicobacter pylori* pathogenesis. *Gut Microbes* 4, 505–531. doi: 10.4161/gmic.26205

Shen, Z., Dzink-Fox, J. A., Feng, Y., Muthupalani, S., Mannion, A. J., Sheh, A., et al. (2022). Gastric non-*Helicobacter pylori* urease-positive Staphylococcus epidermidis and streptococcus salivarius isolated from humans have contrasting effects on H. pylori-associated gastric pathology and host immune responses in a murine model of gastric cancer. *mSphere* 7:e0077221. doi: 10.1128/msphere.00772-21

Sheu, B. S., Wu, J. J., Lo, C. Y., Wu, H. W., Chen, J. H., Lin, Y. S., et al. (2002). Impact of supplement with lactobacillus- and Bifidobacterium-containing yogurt on triple therapy for *Helicobacter pylori* eradication. *Aliment. Pharmacol. Ther.* 16, 1669–1675. doi: 10.1046/j.1365-2036.2002.01335.x

Smyth, E. C., Nilsson, M., Grabsch, H. I., van Grieken, N. C. T., and Lordick, F. (2020). Gastric cancer. *Lancet* 396, 635–648. doi: 10.1016/S0140-6736(20)31288-5

Sohn, S. H., Kim, N., Jo, H. J., Kim, J., Park, J. H., Nam, R. H., et al. (2017). Analysis of gastric body microbiota by pyrosequencing: possible role of bacteria other than *Helicobacter pylori* in the gastric carcinogenesis. *J. Cancer Prev.* 22, 115–125. doi: 10.15430/JCP.2017.22.2.115

Suerbaum, S., and Michetti, P. (2002). Medical progress: *Helicobacter pylori* infection. *N. Engl. J. Med.* 347, 1175–1186. doi: 10.1056/NEJMra020542

Sun, Q. H., Zhang, J., Shi, Y. Y., Zhang, J., Fu, W. W., and Ding, S. G. (2022). Microbiome changes in the gastric mucosa and gastric juice in different histological stages of *Helicobacter pylori*-negative gastric cancers. *World J. Gastroenterol.* 28, 365–380. doi: 10.3748/wjg.v28.i3.365

Suzuki, K., Meek, B., Doi, Y., Muramatsu, M., Chiba, T., Honjo, T., et al. (2004). Aberrant expansion of segmented filamentous bacteria in IgA-deficient gut. *Proc. Natl. Acad. Sci. U. S. A.* 101, 1981–1986. doi: 10.1073/pnas.0307317101

Targosz, A., Brzozowski, T., Pierzchalski, P., Szczyrk, U., Ptak-Belowska, A., Konturek, S. J., et al. (2012). *Helicobacter pylori* promotes apoptosis, activates cyclooxygenase (COX)-2 and inhibits heat shock protein HSP70 in gastric cancer epithelial cells. *Inflamm. Res.* 61, 955–966. doi: 10.1007/s00011-012-0487-x

Tseng, C. H., Lin, J. T., Ho, H. J., Lai, Z. L., Wang, C. B., Tang, S. L., et al. (2016). Gastric microbiota and predicted gene functions are altered after subtotal gastrectomy in patients with gastric cancer. *Sci. Rep.* 6:20701. doi: 10.1038/srep20701

Tsuda, A., Suda, W., Morita, H., Takanashi, K., Takagi, A., Koga, Y., et al. (2015). Influence of proton-pump inhibitors on the luminal microbiota in the gastrointestinal tract. *Clin. Transl. Gastroenterol.* 6:e89. doi: 10.1038/ctg.2015.20

Udhayakumar, G., Jayanthi, V., Devaraj, N., and Devaraj, H. (2007). Interaction of MUC1 with beta-catenin modulates the Wnt target gene cyclinD1 in H. pylori-induced gastric cancer. *Mol. Carcinog.* 46, 807–817. doi: 10.1002/mc.20311

Uemura, N., Okamoto, S., Yamamoto, S., Matsumura, N., Yamaguchi, S., Yamakido, M., et al. (2001). *Helicobacter pylori* infection and the development of gastric cancer. *N. Engl. J. Med.* 345, 784–789. doi: 10.1056/NEJMoa001999

Walter, J., and Ley, R. (2011). The human gut microbiome: ecology and recent evolutionary changes. *Annu. Rev. Microbiol.* 65, 411–429. doi: 10.1146/annurev-micro-090110-102830

Wang, Z. H., Gao, Q. Y., and Fang, J. Y. (2013). Meta-analysis of the efficacy and safety of lactobacillus-containing and Bifidobacterium-containing probiotic compound preparation in *Helicobacter pylori* eradication therapy. *J. Clin. Gastroenterol.* 47, 25–32. doi: 10.1097/MCG.0b013e318266f6cf

Wang, Z., Ren, R., and Yang, Y. (2020a). Mucosa microbiome of gastric lesions: fungi and bacteria interactions. *Prog. Mol. Biol. Transl. Sci.* 171, 195–213. doi: 10.1016/bs.pmbts.2020.03.004

Wang, L., Xin, Y., Zhou, J., Tian, Z., Liu, C., Yu, X., et al. (2020). Gastric mucosa-associated microbial signatures of early gastric cancer. *Front. Microbiol.* 11:1548. doi: 10.3389/fmicb.2020.01548

Wang, L., Zhou, J., Xin, Y., Geng, C., Tian, Z., Yu, X., et al. (2016). Bacterial overgrowth and diversification of microbiota in gastric cancer. *Eur. J. Gastroenterol. Hepatol.* 28, 261–266. doi: 10.1097/MEG.0000000000000542

Wang, Z., Gao, X., Zeng, R., Wu, Q., Sun, H., Wu, W., et al. (2020b). Changes of the gastric mucosal microbiome associated with histological stages of gastric carcinogenesis. *Front. Microbiol.* 11:997. doi: 10.3389/fmicb.2020.00997

Wroblewski, L. E., Peek, R. M. Jr., and Wilson, K. T. (2010). *Helicobacter pylori* and gastric cancer: factors that modulate disease risk. *Clin. Microbiol. Rev.* 23, 713–739. doi: 10.1128/CMR.00011-10

Wroblewski, L. E., Piazuelo, M. B., Chaturvedi, R., Schumacher, M., Aihara, E., Feng, R., et al. (2015). *Helicobacter pylori* targets cancer-associated apical-junctional constituents in gastroids and gastric epithelial cells. *Gut* 64, 720–730. doi: 10.1136/gutjnl-2014-307650

Wu, J., Li, Q., and Fu, X. (2019). Fusobacterium nucleatum contributes to the carcinogenesis of colorectal cancer by inducing inflammation and suppressing host immunity. *Transl. Oncol.* 12, 846–851. doi: 10.1016/j.tranon.2019.03.003

Wu, J., Xu, S., Xiang, C., Cao, Q., Li, Q., Huang, J., et al. (2018). Tongue coating microbiota community and risk effect on gastric cancer. *J. Cancer* 9, 4039–4048. doi: 10.7150/jca.25280

Wu, Z. F., Zou, K., Wu, G.-N., Jin, Z.-J., Xiang, C.-J., Xu, S., et al. (2020). A comparison of tumor-associated and non-tumor-associated gastric microbiota in gastric cancer patients. *Dig. Dis. Sci.* 66, 1673–1682. doi: 10.1007/s10620-020-06415-y

Yamaguchi, N., and Kakizoe, T. (2001). Synergistic interaction between *Helicobacter pylori* gastritis and diet in gastric cancer. *Lancet Oncol.* 2, 88–94. doi: 10.1016/S1470-2045(00)00225-4

Yanaka, A., Fahey, J. W., Fukumoto, A., Nakayama, M., Inoue, S., Zhang, S., et al. (2009). Dietary sulforaphane-rich broccoli sprouts reduce colonization and attenuate gastritis in *Helicobacter pylori*-infected mice and humans. *Cancer Prev. Res. (Phila.)* 2, 353–360. doi: 10.1158/1940-6207.CAPR-08-0192

Yang, I., Woltemate, S., Piazuelo, M. B., Bravo, L. E., Yepez, M. C., Romero-Gallo, J., et al. (2016). Different gastric microbiota compositions in two human populations with high and low gastric cancer risk in Colombia. *Sci. Rep.* 6:18594. doi: 10.1038/srep18594

Ye, F., Shen, H., Li, Z., Meng, F., Li, L., Yang, J., et al. (2016). Influence of the biliary system on biliary bacteria revealed by bacterial communities of the human biliary and upper digestive tracts. *PLoS One* 11:e0150519. doi: 10.1371/journal.pone.0150519

Yin, Y. N., Wang, C. L., Liu, X. W., Cui, Y., Xie, N., Yu, Q. F., et al. (2011). Gastric and duodenum microflora analysis after long-term *Helicobacter pylori* infection in Mongolian gerbils. *Helicobacter* 16, 389–397. doi: 10.1111/j.1523-5378.2011.00862.x

Yong, X., Tang, B., Li, B. S., Xie, R., Hu, C. J., Luo, G., et al. (2015). *Helicobacter pylori* virulence factor CagA promotes tumorigenesis of gastric cancer via multiple signaling pathways. *Cell Commun. Signal* 13:30. doi: 10.1186/s12964-015-0111-0

Yu, G., Hu, N., Wang, L., Wang, C., Han, X. Y., Humphry, M., et al. (2017b). Gastric microbiota features associated with cancer risk factors and clinical outcomes: a pilot study in gastric cardia cancer patients from Shanxi, China. *Int. J. Cancer* 141, 45–51. doi: 10.1002/ijc.30700

Yu, G., Torres, J., Hu, N., Medrano-Guzman, R., Herrera-Goepfert, R., Humphrys, M. S., et al. (2017a). Molecular characterization of the human stomach microbiota in gastric cancer patients. *Front. Cell. Infect. Microbiol.* 7:302. doi: 10.3389/fcimb.2017.00302

Zhang, C., Powell, S. E., Betel, D., and Shah, M. A. (2017). The gastric microbiome and its influence on gastric carcinogenesis: current knowledge and ongoing research. *Hematol. Oncol. Clin. North Am.* 31, 389–408. doi: 10.1016/j.hoc.2017.01.002

Zhang, Z., Xu, G., Ma, M., Yang, J., and Liu, X. (2013). Dietary fiber intake reduces risk for gastric cancer: a meta-analysis. *Gastroenterology* 145, 113–20.e3. doi: 10.1053/j.gastro.2013.04.001

Zhao, Z., Yin, Z., and Zhao, Q. (2017). Red and processed meat consumption and gastric cancer risk: a systematic review and meta-analysis. *Oncotarget* 8, 30563–30575. doi: 10.18632/oncotarget.15699

Zilberstein, B., Quintanilha, A. G., Santos, M. A. A., Pajecki, D., Moura, E. G., Alves, P. R. A., et al. (2007). Digestive tract microbiota in healthy volunteers. *Clinics* 62, 47–56. doi: 10.1590/S1807-59322007000100008

frontiers | Frontiers in Microbiology

TYPE Original Research
PUBLISHED 19 May 2023
DOI 10.3389/fmicb.2023.1071603

OPEN ACCESS

EDITED BY
Rao Narasimha Desirazu,
Indian Institute of Science (IISc), India

REVIEWED BY
Kathryn Haley,
Grand Valley State University, United States
Maria Teresa Mascellino,
Sapienza University of Rome, Italy

*CORRESPONDENCE
Lu-yao Wang
✉ 00864@ymun.edu.cn
Gan-rong Huang
✉ 88193724@qq.com
Yan-Qiang Huang
✉ hyq77615@163.com

†These authors have contributed equally to this work

RECEIVED 16 October 2022
ACCEPTED 04 May 2023
PUBLISHED 19 May 2023

CITATION
Li R-j, Xu J-y, Wang X, Liao L-j, Wei X, Xie P, Xu W-y, Xu Z-y, Xie S-h, Jiang Y-y, Huang L, Wang L-y, Huang G-r and Huang Y-q (2023) Therapeutic effect of demethylated hydroxylated phillygenin derivative on *Helicobacter pylori* infection. *Front. Microbiol.* 14:1071603. doi: 10.3389/fmicb.2023.1071603

Therapeutic effect of demethylated hydroxylated phillygenin derivative on *Helicobacter pylori* infection

Ru-Jia Li[1,2], Jia-yin Xu[1], Xue Wang[1], Li-juan Liao[1], Xian Wei[1], Ping Xie[1], Wen-yan Xu[1], Zhen-yi Xu[1], Shuo-hua Xie[1], Yu-ying Jiang[1], Liang Huang[1], Lu-yao Wang[1*†], Gan-rong Huang[1*†] and Yan-Qiang Huang[1*†]

[1]Key Laboratory of the Prevention and Treatment of Drug Resistant Microbial Infecting (Youjiang Medical University for Nationalities), Education Department of Guangxi Zhuang Autonomous Region, Baise, China, [2]Clinical Laboratory of 980 Hospital of PLA Joint Logistics Support Force (Bethune International Peace Hospital), Shijiazhuang, Hebei, China

Modifying and transforming natural antibacterial products is a novel idea for developing new efficacious compounds. Phillygenin has an inhibitory effect on *H. pylori*. The aim of the present study was to prepare a phillygenin derivative (PHI-Der) through demethylation and hydroxylation. The minimum inhibitory concentration of 18 strains of *H. pylori* from different sources was 8–32μg/mL *in vitro*, and the activity increased 2–8 times than that of phillygenin. PHI-Der could significantly inhibit the colonization of *H. pylori in vivo*, reduce the inflammatory response, and promote the repair of inflammatory damage. Further, we used SwissTargetPrediction to predict that its main targets are *ALOX5*, *MCL1*, and *SLC6A4*, and find that it can inhibit bacterial biofilm formation and reduce bacterial infection of cells. It can enhance the intracellular oxidative capacity of *H. pylori* to inhibit *H. pylori* growth. Further, it could prevent the oxidation of *H. pylori*-infected cells and reduce the inflammatory response, which plays a role in protection. In conclusion, compared to phillygenin, PHI-Der had better antibacterial activity and was more effective in treating *H. pylori* infection. It has characteristics of high safety, specificity, resistance to drug resistance and better antibacterial activity than phillygenin, it's a good antioxidant for host cells.

KEYWORDS

***Helicobacter pylori*, phillygenin, demethyl hydroxylation, derivatives, therapeutic effect**

1. Introduction

Helicobacter pylori is a spiral-shaped, micro-anaerobic, Gram-negative bacteria that requires harsh growth conditions (Martin Nuñez Gracia et al., 2021). Currently, antibiotics are mainly used for treatment. However, with the widespread use and abuse of antibiotics, the resistance rate of *H. pylori* has gradually increased (Morilla et al., 2019). Therefore, the World Health Organization in 2017 listed *H. pylori*, which is resistant to clarithromycin, as one of the 12 pathogens that urgently require the development of new antibiotics (Branswell, 2017). An effective way to prepare new antibacterial drugs is to find active ingredients from natural products (natural plants, microbial secondary metabolites, marine organisms) and then modify and transform them to form derivatives (Adjissi et al.,

10.3389/fmicb.2023.1071603

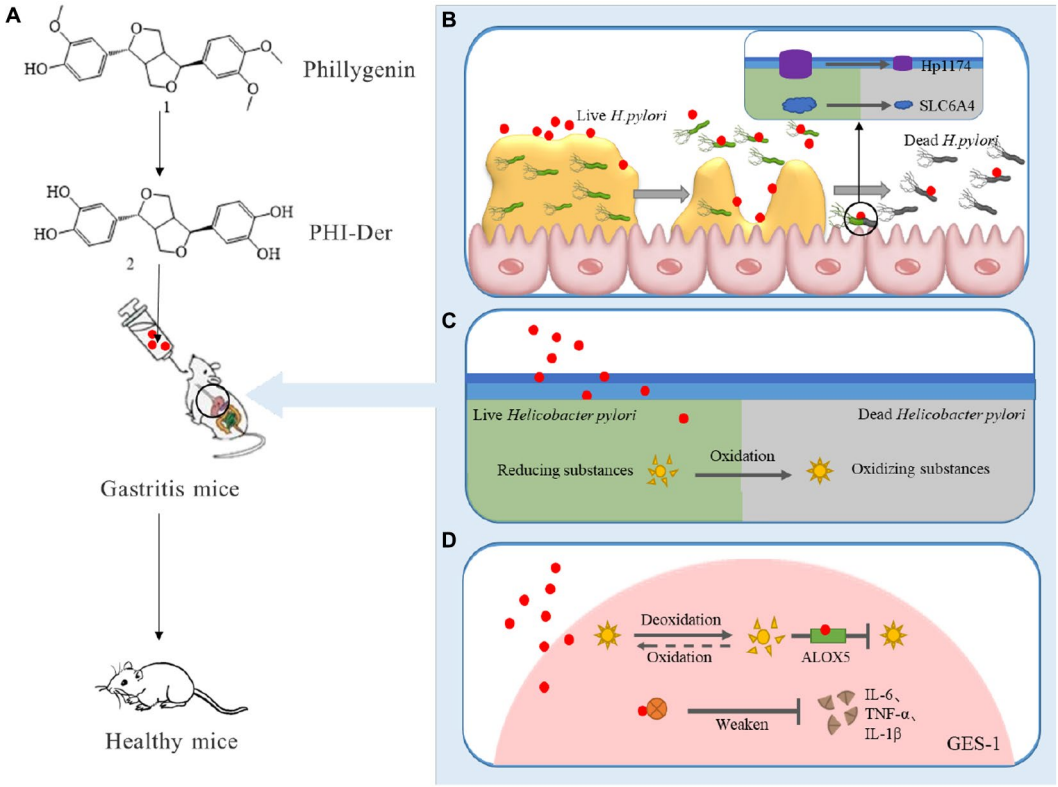

GRAPHICAL ABSTRACT
The figure shows the hypothesis of the mechanism of phillygenin derivatives (PHI-Der). A is PHI-Der in the treatment of gastritis mice; B is the inhibitory effect of PHI-Der on *H. pylori* biofilm; C is PHI-Der that enhance the oxidation of *H. pylori*; D is PHI-Der reduce the oxidative effect and the expression of inflammatory factors in *H. pylori*-infected cells.

2022). Phillygenin belongs to the class of diepoxylignans, in which two molecular phenylpropanoid side chains are connected to each other to form two epoxy structures. Phillygenin has various functions, including anti-inflammatory, anti-tumor, and antibacterial (Siqi et al., 2021; Yufeng and Peng, 2021; Wang J. et al., 2022). Preliminary research in our laboratory showed that phillygenin had a good inhibitory effect on *H. pylori*, although not comparable to the level of antibiotics. Therefore, the aim of this study was to modify and transform phillygenin to improve its antibacterial activity and explore its mechanism of action to provide an experimental basis for better utilization of phillygenin and its derivatives.

2. Materials and methods

2.1. Recovery and culture of strains

We extracted *H. pylori* strains containing the preservation solution at −80°C. Standard strains 26,695, NSH57, MSD132, and G27 were donated by Bi Hongkai from the Nanjing Medical University, and clinical strains HPBS001–HPBS016 were isolated at our laboratory. *H. pylori* strains were cultured on the Columbia blood agar plate (OXOID, UK) or in the brain-heart infusion (BHI, OXOID, UK) broth medium containing 10% serum (Pingrui, China) and placed under microaerophilic (85% nitrogen, 5% oxygen, 10% carbon dioxide; model CB160; Binder, Germany) conditions at 37°C for 3 days. Bacterial species other than *H. pylori* were cultured on nutrient agar or Luria–Bertani plates at 37°C for 1–2 days. Supplementary Table S1 shows the information of *Staphylococcus aureus* and other information.

2.2. Synthesis, identification and prediction of physicochemical properties of PHI-Der

First, we dissolved phillygenin (7 mg) in dry dichloromethane (5 mL). Second, we slowly added boron tribromide in dichloromethane dropwise into phillygenin at −50°C (5.0 eq, 125 mg in 5 mL dichloromethane) and placed it under ice bath for 1 h. Third, we quenched the reaction with 1 mL methanol and concentrated the reaction solution. Fourth, we performed high-performance liquid chromatography for purification (acetonitrile in water, 5–95%; flow rate, 2 mL/min, trifluoroacetic acid, 0.1%; room temperature 25°C ± 5°C) to obtain PHI-Der at a yield of 45%. After Fourier-transform infrared analysis, mass spectrometry and

Abbreviations: LEV, levofloxacin; CLA, clarithromycin; MET, metronidazole; AMO, amoxicillin.

hydrogen and carbon nuclear magnetic resonance (NMR), the structure of PHI-Der was determined. The 3D structure of PHI-Der was visualized using ChemDraw3D. The SMILES structure was uploaded to PaddleHelix[1] to predict the physical and chemical properties (Fang et al., 2022).

2.3. Microdilution to detect the minimum inhibitory concentration (MIC)

In the first well of the 96-well plate, we add 173.6 μL of the culture medium and 6.4 μL of PHI-Der (4 mg/mL) and diluted them sequentially. Negative (sterile, only medium and drug) and positive (no drug, only medium and bacteria) wells were used as controls. Bacteria growing in the logarithmic phase on the solid plate were used to create a bacterial suspension with the corresponding medium. Optical density at 600 nm (OD_{600}) of *H. pylori* was adjusted to 1.0×10^7 colony forming unit (CFU)/mL. OD_{600} of the remaining bacteria and the fungus were adjusted to 1×10^6 and 5×10^3 CFU/mL, respectively, and 10 μL was added to each well. Cultivation was performed for 24–72 h before further analyses (Wang Y. et al., 2022).

2.4. Detection of the minimum bactericidal concentration (MBC) using microdilution and the spread plate method

We added 173.6 μL of the culture medium and 6.4 μL of PHI-Der (4 mg/mL) to the first well of the 96-well plate. The wells were sequentially folded and diluted. The wells of phosphate-buffered saline (PBS; Sangon Biotech, China) were used as positive controls. *H. pylori* G27 grown in the logarithmic phase on the solid plate was used to create a bacterial suspension in the BHI medium, and OD_{600} of the bacterial solution was adjusted to 1×10^7 CFU/mL. We added 10 μL of the bacterial solution to each well and performed culture in a three-gas incubator. After PHI-Der had been used for a certain time period (such as 2 h), we diluted (100 times, 1,000 times, and so on) the bacterial liquid, spread it on Columbia agar plates, and performed culture in a three-gas incubator for 4–5 days. We calculated the number of bacteria growing on the agar plate. The drug concentration at which the number of bacteria was inhibited by 99.9% was considered to be MBC.

2.5. Detection of drug resistance of PHI-Der

Long-term contact of bacteria with low doses of drugs causes changes in the medicinal chemical processes of the cells themselves, so that bacteria gradually tolerate drugs. The drug resistance of PHI-Der was detected with the *H. pylori* G27 strain. MICs of metronidazole and PHI-Der were 2 and 16 μg/mL, respectively. We used one-fourth of MIC to induce the strain, which was detected every 3 days over 24 days of induction. The induction concentration was adjusted with changes in MIC. For example, when MIC of metronidazole changed to 16 μg/mL, the induction concentration was adjusted to 4 μg/mL.

2.6. Cytotoxicity detection of PHI-Der

GES-1 and BGC823 (KeyGen Biotech, Nanjing, China) cell suspensions were adjusted to 1×10^5. We inoculated 100 μL/well into 96-well plates and replicated three same samples. Incubation was performed at 37°C for 24 h. The final concentrations of PHI-Der were 200, 150, 100, 50, and 0 μg/mL. Subsequently, incubation was performed at 37°C for 24 h. We added 10 μL of Cell Counting Kit-8 (CCK-8; Beyotime, China) to each well, tapped to mix, and incubated for 4 h. Finally, we measured the absorbance at 450 nm.

2.7. Animal toxicity of PHI-Der

We purchased 6–8-week-old specific-pathogen-free (SPF) C57BL/6 mice from Changsha Tianqin Biotechnology Co., Ltd. (license number: SYXK Gui2017-0004; animal experiment ethics committee approval number: NO.2019112501). Twenty animals were randomly divided into administration and negative control groups, with ten animals in each group (Not infected with Hp), and raised in SPF environment. The administration group was administered with 10 times the therapeutic dose daily for 3 consecutive days, while the negative control group was administered with PBS solution. The mice were weighed consecutively for 7 days, starting 1 day before administration. Three days after drug withdrawal, the mice in each group were weighed, and the average body weight was calculated. Blood was collected from the eyeball, and the mice were sacrificed through dislocation and neck dislocation. Stomach, kidney, liver, and spleen tissues were obtained for pathological sectioning and hematoxylin and eosin (H&E) staining.

2.8. Construction of an animal model of acute gastritis to detect the inhibitory effect of PHI-Der on *Helicobacter pylori*

PHI-Der, omeprazole (Sigma-Aldrich, Germany), amoxicillin (Sigma–Aldrich, Germany), and clarithromycin (Sigma-Aldrich, Germany) were dissolved and diluted to 10 mg/mL. We successfully modeled (HPBS001) 6–8-week-old SPF C57BL/6 mice and divided them into four groups: the omeprazole + amoxicillin + clarithromycin group (omeprazole, 138.2 mg/kg; amoxicillin, 28.5 mg/kg; clarithromycin, 14.3 mg/kg), the omeprazole + PHI-Der (28 mg/kg) group, the omeprazole + PHI-Der (7 mg/kg) group, and the PBS/negative control group. Each group comprised of ten mice. The negative control group comprised of ten mice not infected with *H. pylori*. Drugs were administered daily for 3 consecutive days. Two days after drug withdrawal, blood was collected from the eyes of the mice in the infected group, and the mice were sacrificed through cervical dislocation. Gastric tissues were collected and crushed. A portion of gastric tissues was paraffin-sectioned and stained with H&E. Terminal deoxynucleotidyl transferase biotin-dUTP nick end labeling immunohistochemistry and immunofluorescence

1 https://paddlehelix.baidu.com/

histochemistry were performed, and ImageJ was used to quantify the fluorescent signal of the immunohistochemical staining done on the tissue samples.

2.9. Target prediction

PHI-Der targets were obtained from the SwissTargetPrediction database.[2] The targets duplicated with "*Helicobacter pylori* infection" were screened from the GeneCards database as potential targets of PHI-Der against *H. pylori* infection. The target interaction relationship was obtained from the STRING database.[3] Potential targets were imported. The species selected for the study was "*Homo sapiens*."

2.10. Molecular docking

The three-dimensional structure of PHI-Der was imported into Discovery Studio. We used the module for preparing ligands in molecules to process small molecules. The module mainly minimizes the energy of small molecules and yields CHARMM force fields. The crystal structure of the target protein corresponding to the core target was downloaded from the Protein Data Bank website.[4] The protein was preprocessed using Discovery Studio to remove water molecules, hydrogenation, and charges, and the crystal structure was extracted. PyMOL was used to visualize the processed protein. AutoDock Vina performed molecular docking. PyMOL was used to combine the docking results to form a complex, and Discovery Studio was finally used for the interaction analysis and visualization of docking.

2.11. Inhibition experiment of PHI-Der in biofilms

The OD of the *H. pylori* G27 bacterial suspension was adjusted to 0.1, and the biofilm formed under microaerophilic conditions for 3 days. PHI-Der was added at concentrations of 128, 64, 32, and 16 μg/mL for 24 h. Its anti-biofilm activity was evaluated using crystal violet (Macklin, China) and Alamar blue (Solarbio, China) staining. The biofilm protein content was determined using the bicinchoninic protein concentration assay kit (Beyotime, China).

2.12. Oxidation effect of PHI-Der on *Helicobacter pylori*

Helicobacter pylori G27 was cultured to the logarithmic phase. The bacterial suspension was adjusted to 1×10^7 CFU/mL. We added 10 μM of 2′,7′-dichlorofluorescein diacetate (DCFH-DA, Biyuntian, S0033S) to the bacterial suspension, and cultivate in a three-gas incubator for 1 h. The cocultured bacterial solution was washed twice with PBS buffer, in order to remove excess DCFH-DA. Phillygenin and PHI-Der were added at concentrations of 32 μg/mL each. PBS and Rosup were used as negative and positive controls, respectively. After 2 h of action, 15 μL of the solution was added dropwise onto the slides and observed under a fluorescence microscope.

2.13. Detection of the antioxidative activity of PHI-Der in GES-1 cell lines

Bacterial adhesion cell experiment GES-1(Rhodamine staining) cells were cultured in RPMI1640 medium containing 10% FBS without antibiotics, the *H. pylori* suspension was collected and labeled with SYTO9 for 15 min, and then treated with different drug concentrations and co-cultured with the cells for 2 h. The plate is placed under a fluorescence microscope for observation.

GES-1 cells were seeded (5×10^4 cells/well) and grown in 96-well plates until 70% confluence. PHI-Der was incubated with cells for 2 h at 37°C. The cells were washed with PBS, incubated with 20 μM of DCFH-DA for 30 min at 37°C, and washed twice with PBS to remove the unabsorbed probe. Suspensions in the serum and antibiotic free medium were infected with *H. pylori* (1×10^8 CFU/mL). Reactive oxygen species (ROS) levels were measured for 180 min using a fluorescence microplate Synergy HT reader with λex of 485 nm and λem of 530 nm.

2.14. Reverse transcription quantitative polymerase chain reaction (RT-qPCR)

Helicobacter pylori G27 was cultured to the logarithmic phase, and the bacterial suspension was adjusted to 1×10^8 CFU/mL, then add PHI-Der. The cells were plated to a 70% fit and divided into the cell group, drug action group, *H. pylori* infection group, and drug action following *H. pylori* infection group. Pellets were collected using centrifugation. RNA was extracted using the TRIzol reagent (Takara, China) and reverse-transcribed into complementary DNA using a reverse transcription kit (MONPURE, China). RT-qPCR was performed using LightCycler according to the kit (MONPURE, China), with pre-denaturation at 95°C for 30 s, denaturation at 95°C for 10 s, and annealing and extension at 60°C for 30 s for 40 cycles. Supplementary Table S2 shows the primers (Sangon Biotech, Shanghai). Changes in transcript levels were determined by applying a relative quantification ($2^{-\Delta\Delta CT}$ method) approach, with 16S ribosomal RNA amplicons used as an internal control for data normalization.

2.15. Statistical analysis

Data are expressed as mean ± standard deviation. Statistical analyses were performed using SPSS 25.0. One-way analysis of variance was performed, and $p < 0.05$ was considered statistically significant.

3. Results

3.1. Preparation of PHI-Der

Through the preparation route (Figure 1A), PHI-Der was successfully prepared with a yield of 45%. The molecular formula of

2 http://www.Swisstargetprediction.ch/
3 https://STRING-db.org/
4 http://www.rcsb.org/

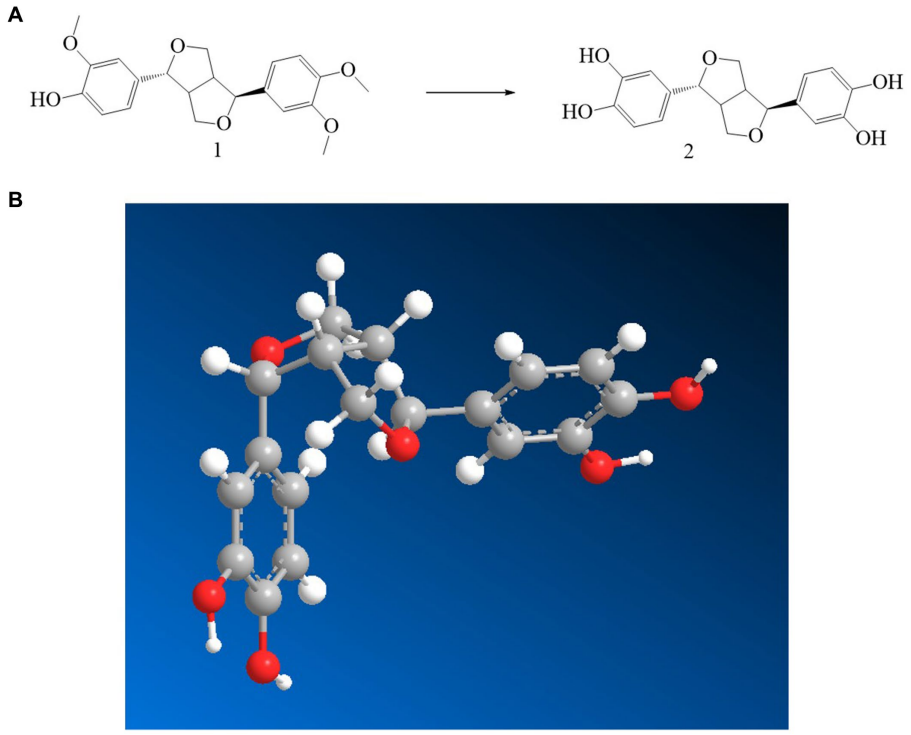

FIGURE 1
Synthesis and structure diagram of PHI-Der. **(A)** Preparation circuit of PHI-Der. **(B)** Three-dimensional structure of PHI-Der.

PHI-Der is $C_{18}H_{18}O_6$, and the structural formula of PHI-Der SMILES is OC1 = CC=C(C=C1O)[C@H]1OCC2C1CO[C@H]2C1 = CC=C(O)C(O) = C1. Figure 1B shows the 3D structure of PHI-Der. Figure 2A shows the identification of PHI-Der using mass spectrometry. $C_{18}H_{18}O_6$ ideal characteristic peak was $[M]^+ = 330.33$. However, the evident characteristic peak was $[M-17]^+ = 313.32$. One hydroxyl group had been removed because of the unstable connection. Figure 2B shows the NMR identification (hydrogen spectrum) of PHI-Der: ^{1}H NMR (400 MHz, $CDCl_3$–MeOD) δ 6.64 (s, 2H), 6.54 (d, J = 6.6 Hz, 2H), 6.36 (d, J = 6.6 Hz, 2H), 4.03.97 (m, 4H), 3.77 (d, J = 12.4 Hz, 2H), and 2.65–2.50 (m, 2H) and deuterium with chloroform–deuterium with the methanol solvent. Table 1 shows the physicochemical properties of PHI-Der, in which the lipid–water partition coefficient (logarithm) is 2.58 log(mol/mol), which is less than 3 log(mol/mol), indicating that PHI-Der has good water solubility. Supplementary Figure S1 shows the Fourier transform infrared analysis image of PHI-Der. Supplementary Figure S2 shows the NMR identification (carbon spectrum) of PHI-Der.

3.2. *In vitro* antibacterial activity of PHI-Der against *Helicobacter pylori*

PHI-Der MIC was 8–32 μg/mL in 18 *H. pylori* strains (Table 2). PHI-Der exerted better inhibitory effects on sensitive and resistant strains compared to phillygenin. The MBC of PHI-Der against *H. pylori* was 16 times the PHI-Der MIC, reaching 99.9 and 99.999% after 6 and 8 h, respectively. The antibacterial rate was 8 times the PHI-Der MIC, reaching 90, 99, and 99.9% after 4, 6, and 8 h, respectively. The bactericidal effect was related to the concentration and time (Figure 3).

3.3. Antibacterial activity of PHI-Der against *Helicobacter pylori in vivo*

The efficacy of PHI-Der against *H. pylori in vivo* was assessed using the C57BL/6 mouse model infected with *H. pylori* (HPBS001; Supplementary Figure S3). Based on the counted number of colonies, the bacteriostatic effect of PHI-Der was better than that of the triple therapy. Further, the bacteriostatic effect at high PHI-Der concentrations was better than that at low PHI-Der concentrations (Figure 4A). According to the H&E staining and immunohistochemical images of the PHI-Der group, apoptotic cells and inflammatory factors in the gastric mucosa reduced significantly (Figure 4B). As for the expression of inflammatory factors in tissue samples, expression levels of interleukin-6, tumor necrosis factor-α, and interleukin-1β were the lowest in the PHI-Der group (Figures 4B,C), use ImageJ for quantification. PHI-Der exerted good bacteriostatic effects *in vivo*.

3.4. Biosafety of PHI-Der

The toxicity test of PHI-Der showed that PHI-Der at 100 μg/mL exerted no cytotoxic effect on GES-1 gastric epithelial or BGC823 gastric cancer cells, and the survival rates were above 90% (Figures 5A,B). After the intragastric administration of 10 times the therapeutic dose of PHI-Der, the body weight showed no significant

10.3389/fmicb.2023.1071603

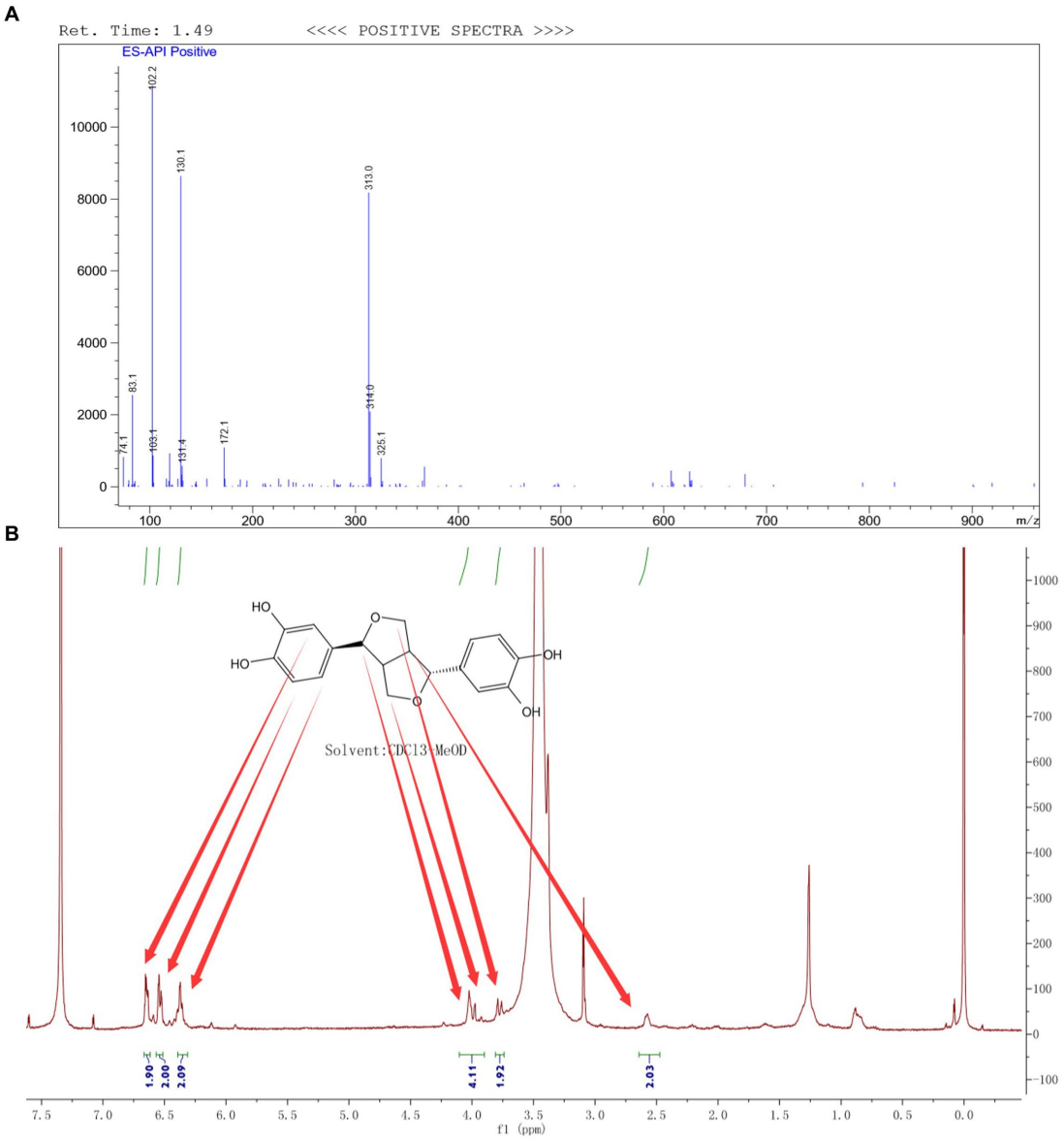

FIGURE 2
Identification of PHI-Der. **(A)** Identification of PHI-Der using mass spectrometry. **(B)** Identification of PHI-Der using NMR (hydrogen spectrum).

change within 7 days (Figure 5C). The stomach, liver, spleen, or kidney showed no pathological damage (Figure 5D). Pathology scores were in Supplementary Table S3. PHI-Der had low toxicity *in vitro* and *in vivo* and high safety and could be used as first-line drugs to treat *H. pylori*.

3.5. Antimicrobial spectrum and drug resistance of PHI-Der

A total of 20 non-*H. pylori* strains were detected, and MICs were above 128 μg/mL. PHI-Der could act on *H. pylori* alone (Table 3) as a narrow-spectrum antibacterial, with specific effects on other bacteria.

In the 24-day drug resistance induction detection of PHI-Der against *H. pylori* G27 strains, the MIC of PHI-Der had changed only two folds on day 6 and occurred on day 12. However, the MIC of metronidazole increased by 64 times (Figure 6). Resistance to PHI-Der was difficult.

3.6. Prediction of targets of PHI-Der

A total of 12 genes were screened using SwissTargetPrediction to predict the targets of PHI-Der (Supplementary Table S4). The target interaction relationship was obtained from the STRING database. Supplementary Figure S4 shows that the interaction relationship between the targets was not close, and targets and pathways were multiple. Targets related to "*H. pylori* infection" were screened using the GeneCards database, and disease targets were collected, including four targets that were repeated with PHI-Der (Table 4).

3.7. Inhibitory effect of PHI-Der on *Helicobacter pylori* biofilm

Staining with Alma blue staining solution, pink represents the number of living cells and blue represents the number of dead cells, result showed that PHI-Der at 50–100 μg/mL could effectively inhibit biofilm formation, with a better inhibitory effect than that of PHI(100–150 μg/mL) (Figure 7A). Crystal violet staining showed that 16 times the PHI-Der MIC could inhibit 50% of biofilm formation, which was better than the effect of clarithromycin (Figure 7B). The main component of the extracellular matrix in *H. pylori* biofilms is protein (Pinho et al., 2022), a protein content of biofilm 8–16 times the PHI-Der MIC could inhibit 50% of the biofilm formation, consistent with the results of crystal violet and Alma blue staining (Figure 7C).

The expression of biofilm-related genes (Cai et al., 2020; Spiegel et al., 2021; Pinho et al., 2022) was detected (Figure 7D). *SpoT* is a bifunctional enzyme with the properties of guanosine tetraphosphate (p-ppGpp) synthase and hydrolase (Hathroubi et al., 2017), *Hp1174* is a gene of the major facilitator superfamily (MFS) efflux pump family (Xiaoran et al., 2018), PHI-Der could downregulate *SpoT* and *Hp1174*, indicating that it could inhibit *H. pylori* biofilms through these genes. The serotonin transporter (*SLC6A4*) indirectly regulated the formation of extracellular polymeric substances (EPSs) that induce functional gastrointestinal diseases (Arisawa et al., 2012). The *SLC6A4* expression was upregulated after PHI-Der acted on infected cells (Figure 7E). PHI-Der was docked with SLC6A4 molecules (Figure 7F). The binding energy of docking was −6.6 kcal/mol, which is less than −5 kcal/mol, indicating that PHI-Der can stably bind to the cavity of the SLC6A4 protein. It can separate from amino acids, such as TYR175, LEU179, and ARG176, in the protein. The formation of hydrogen bonds, van der Waals forces, and Pi-Alkyl/Alkyl bond interactions enable PHI-Der to bind to the main active site of the SLC6A4 protein.

TABLE 1 Physicochemical properties of PHI-Der.

Name	Numerical value
Molecular weight	330.34 g/mol
Heavy atoms	24
Aromatic heavy atoms	12
Fraction Csp3	0.33
Rotatable bonds	2
H-bond acceptors	6
H-bond donors	4
Ring count	4
Aromatic ring count	2
Molar refractivity	83.91 m^3/mol
Topological polar surface area (TPSA)	99.38 $Å^2$
Lipid-water partition coefficient (log)	2.58 log(mol/mol)
Acid dissociation constant (pKa)	8.32 log(mol/mol)
Water solubility (log)	−3.75 log(mol/L)

TABLE 2 MICs of PHI-Der against *H. pylori* (μg/mL).

Strain	Drug resistance	PHI-Der	Phillygenin
26695	Sensitive	16	32
HPBS001	Sensitive	16	16
G27	Sensitive	16	16
HPBS002	Sensitive	16	32
HPBS003	Resistant to LEV, CLA, and MET	16	16
HPBS004	Resistant to MET	16	16
HPBS005	Resistant to CLA	16	16
HPBS006	Resistant to LEV	16	32
HPBS007	Resistant to LEV and LEV	8	64
HPBS010	Resistant to CLA and MET	16	16
HPBS011	Resistant to CLA	16	32
HPBS012	Resistant to MET, CLA, and LEV	8	16
HPBS013	Resistant to MET and CLA	16	16
HPBS014	Sensitive	32	64
HPBS015	Resistant to MET, CLA, and LEV	16	16
HPBS016	Resistant to MET, CLA, AMO, and LEV	16	16
MSD132	Sensitive	8	16
NSH57	Sensitive	16	16

3.8. Effects of PHI-Der on *Helicobacter pylori* oxidation (ROS production)

After the drug penetrates into *H. pylori*, it may undergo redox reactions with proteins, nucleic acids, lipids, etc., and produce some peroxides, such as hydrogen peroxide, which can decompose DCFH-DA into dichlorofluorescein yellow and generate fluorescence.

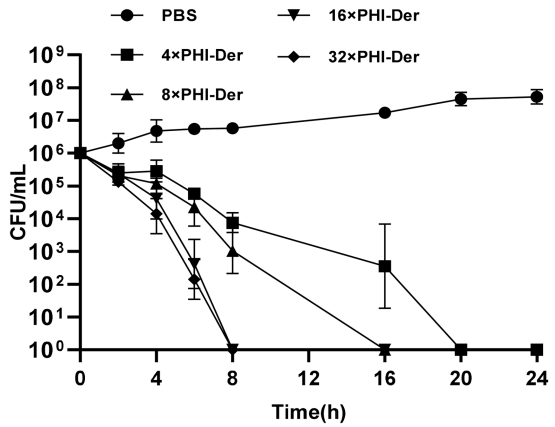

FIGURE 3
MBC of PHI-Der on *H. pylori*. 4×, 8×, 16×, 32× means the concentration tested in terms of MIC.

10.3389/fmicb.2023.1071603

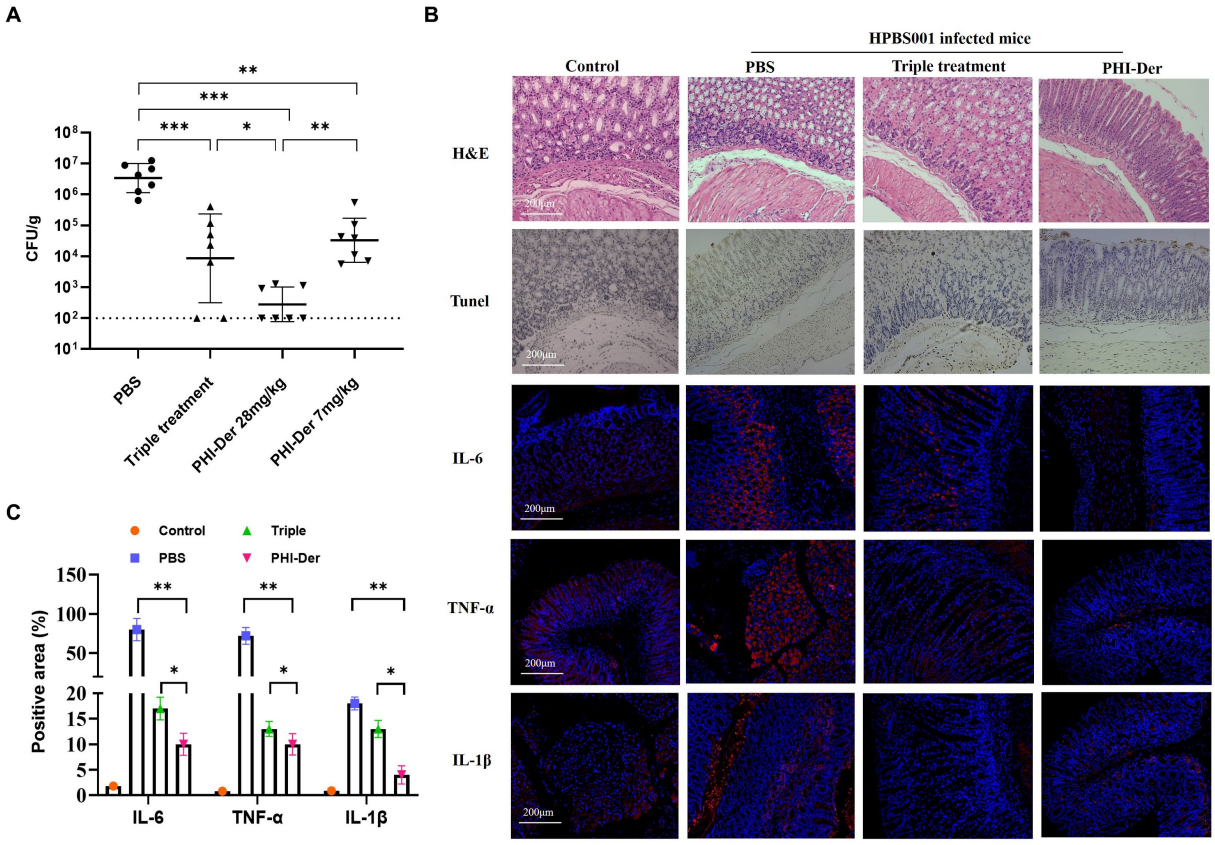

FIGURE 4
Antibacterial effect of PHI-Der in mice. **(A)** HPBS001 colonization amount in mice with acute gastritis. **(B)** Gastric mucosal tissue repair and inflammatory response in mice with acute gastritis (100 times). **(C)** Quantification of inflammatory factors. *p<0.05, **p<0.01, ***p<0.001.

At a concentration of 32 μg/mL, the oxidation reaction effect of PHI-Der was better than that of phillygenin (Figures 8A,B).

3.9. Antioxidative effect of PHI-Der on infected GES-1

Helicobacter pylori adherence to the cell surface is the first step in infection, which is also a critical step in biofilm formation, with the addition of PHI-Der, the number of *H. pylori* in infecting cells decrease, PHI-Der prevented bacteria from infecting cells (Figure 9A). The activation of inflammatory cells could increase ROS production at the site of inflammation. Without antioxidants, cell function is hindered, and tissue damage occurs, eventually leading to oxidative DNA damage and activation of signaling pathways related to the pathogenesis of gastric cancer (Komatsu et al., 2015). After PHI-Der acted on infected GES-1, the antioxidant effect was not obvious at 2 times the MIC but significantly increased at 4 times the MIC, showing a dose-dependent effect (Figure 9B). PHI-Der could exert an antioxidant effect on GES-1 infected with *H. pylori*. Arachidonic acid lipoxygenase 5 (ALOX5), a key enzyme that mediates lipid peroxidation by producing lipid peroxides, plays a central regulatory role in inflammation (Tang et al., 2021). The *ALOX5* expression was downregulated after PHI-Der acted on infected cells (Figure 9C). PHI-Der was docked with ALOX5 molecules (Figure 9D). The binding energy of docking was −9.9 kcal/mol, indicating that PHI-Der could stably bind to the compound in the cavity of the ALOX5 protein and interact with it. Amino acids, such as THR497, VAL501, and TYR95, formed hydrogen bonds, van der Waals forces, and Pi-Alkyl/Alkyl bond interactions, which enabled PHI-Der to bind to the main active site of the ALOX5 protein.

4. Discussion

The drug resistance of *H. pylori* has been increasing yearly. An effective way to prepare novel antibacterial drugs is to find active ingredients from natural products (natural plants, microbial secondary metabolites, marine organisms) and modify and transform them into derivatives (Shen et al., 2020). In traditional Chinese medicine, the active ingredient phillygenin was screened from *Forsythia*, which belongs to the category of diepoxy lignans. As a type of natural aromatic polymer, lignans contain phenolic hydroxyl, alcohol hydroxyl, and carbonyl groups (Westwood et al., 2016). Demethylation modification enhances its molecular reactivity (Huan et al., 2021). PHI-Der had been prepared by removing the methyl group of the ortho-methoxy group from the phenolic hydroxyl group, but this method only removed one methyl group (Liu et al., 2022). In

10.3389/fmicb.2023.1071603

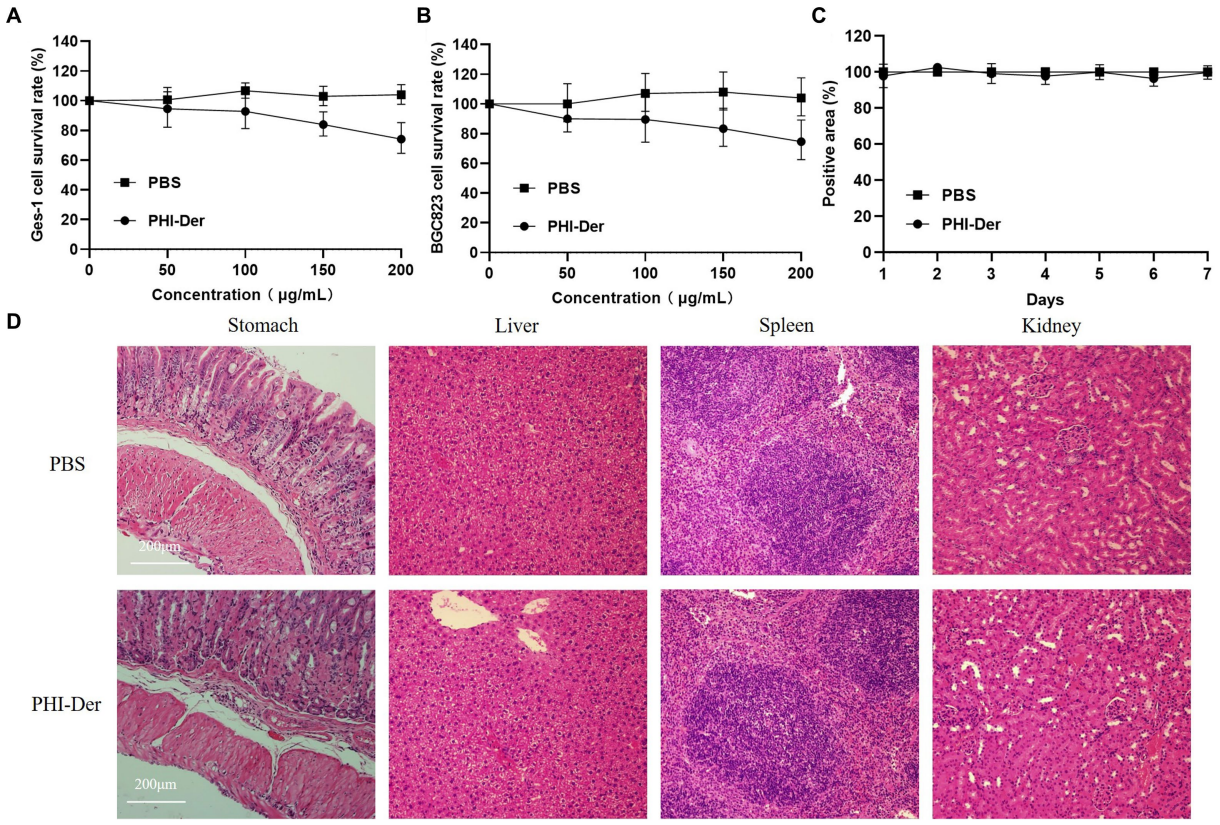

FIGURE 5
PHI-Der toxicity assay. **(A)** PHI-Der on GES-1 cytotoxicity. **(B)** PHI-Der on BGC823 cytotoxicity. **(C)** PHI-Der effect on the body weight of mice. **(D)** Damage detection of PHI-Der in the stomach, liver, spleen, and kidney of mice (100 times).

TABLE 3 MICs (μg/mL) of PHI-Der against non-*H. pylori*.

Strain	Drug resistance	PHI-Der
Proteus mirabilis	Sensitive	>128
Cryptococcus neoformans	Resistance	>128
Candida tropicalis	Sensitive	>128
Campylobacter	Sensitive	>128
Bacillus subtilis	Sensitive	>128
Morganella morganii	Sensitive	>128
Staphylococcus haemolyticus	Sensitive	>128
Stenotrophomonas maltophilia	Sensitive	>128
Acetobacter pasteurianus	Sensitive	>128
Escherichia coli	Sensitive	>128
Lactobacillus curvatus	Sensitive	>128
Saccharomyces cerevisiae Hansen	Sensitive	>128
B. fragilis	Sensitive	>128
Bifidobacterium longum	Sensitive	>128
Enterobacter hormaechei	Sensitive	>128
Staphylococcus aureus	Methicillin-resistant	>128
Candida Albicans	Sensitive	>128
Klebsiella pneumoniae	Sensitive	>128
Pseudomonas aeruginosa	Sensitive	>128
Acinetobacter baumannii	Sensitive	>128

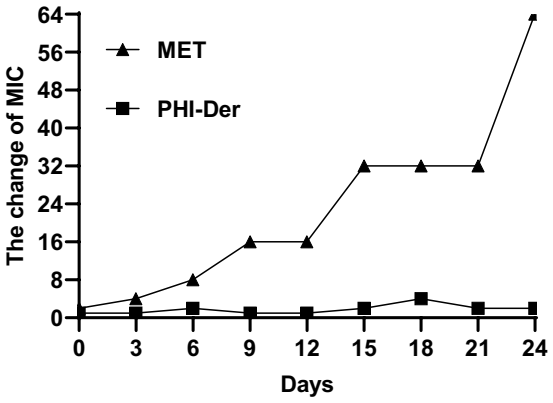

FIGURE 6
Resistance detection of PHI-Der.

a previous study, the ideal molecular weight of PHI-Der was 330.33; however, mass spectrometry showed a characteristic peak at 313.32, which may be because of the unstable connection of the hydroxyl group (Hannah et al., 2022). Therefore, one hydroxyl group was removed, and the molecular weight of the hydroxyl group was optimally 17, consistent with our speculation.

Due to the complexity of strains of infectious diseases, multiple subtypes of pathogenic bacteria might cause the same disease (Xunlei et al., 2019). To evaluate the antibacterial activity of PHI-Der against

10.3389/fmicb.2023.1071603

different *H. pylori* strains, we randomly selected 18 *H. pylori* strains with different sources and sensitivities. After testing, the MIC of PHI-Der was 8–32 μg/mL. It had the same effect on sensitive and resistant *H. pylori* strains, with an antibacterial effect 2–8 times better than that of phillygenin. Antibacterial rates were 90, 99, and 99.9% under the action of 8 times the MIC for 4, 6, and 8 h, respectively. Thus, sterilization was related to concentration and time. The efficacy was evaluated *in vitro*, and the MIC of PHI-Der against 20 non-*H. pylori* strains was detected. It had the characteristics of specific inhibition of *H. pylori*. The CCK-8 cytotoxicity test showed that the survival rates of GES-1 and BGC823 cells were above 90% when the PHI-Der concentration was 100 μg/mL. In addition, the mice were administered with 10 times the therapeutic dose *via* gavage, and no organ damage was found. Thus, both *in vivo* and *in vitro* experiments proved that PHI-Der was relatively safe. In the *in vivo* evaluation of drug efficacy, the effect of PHI-Der was better than that of the triple therapy. After treatment with PHI-Der, apoptotic cells were reduced, and inflammation was alleviated. PHI-Der was effective against drug-resistant strains *in vivo*, with a better therapeutic effect. A certain PHI-Der concentration had a good

TABLE 4 PHI-Der act on *H. pylori* infection targets.

Target	Common name	Uniprot ID	ChEMBL ID	Target class
Arachidonate 5-lipoxygenase	ALOX5	P09917	CHEMBL215	Oxidoreductase
Induced myeloid leukemia cell differentiation protein Mcl-1	MCL1	Q07820	CHEMBL4361	Other cytosolic protein
PI3-kinase p110-alpha subunit	PIK3CA	P42336	CHEMBL4005	Enzyme
Serotonin transporter	SLC6A4	P31645	CHEMBL228	Electrochemical transporte

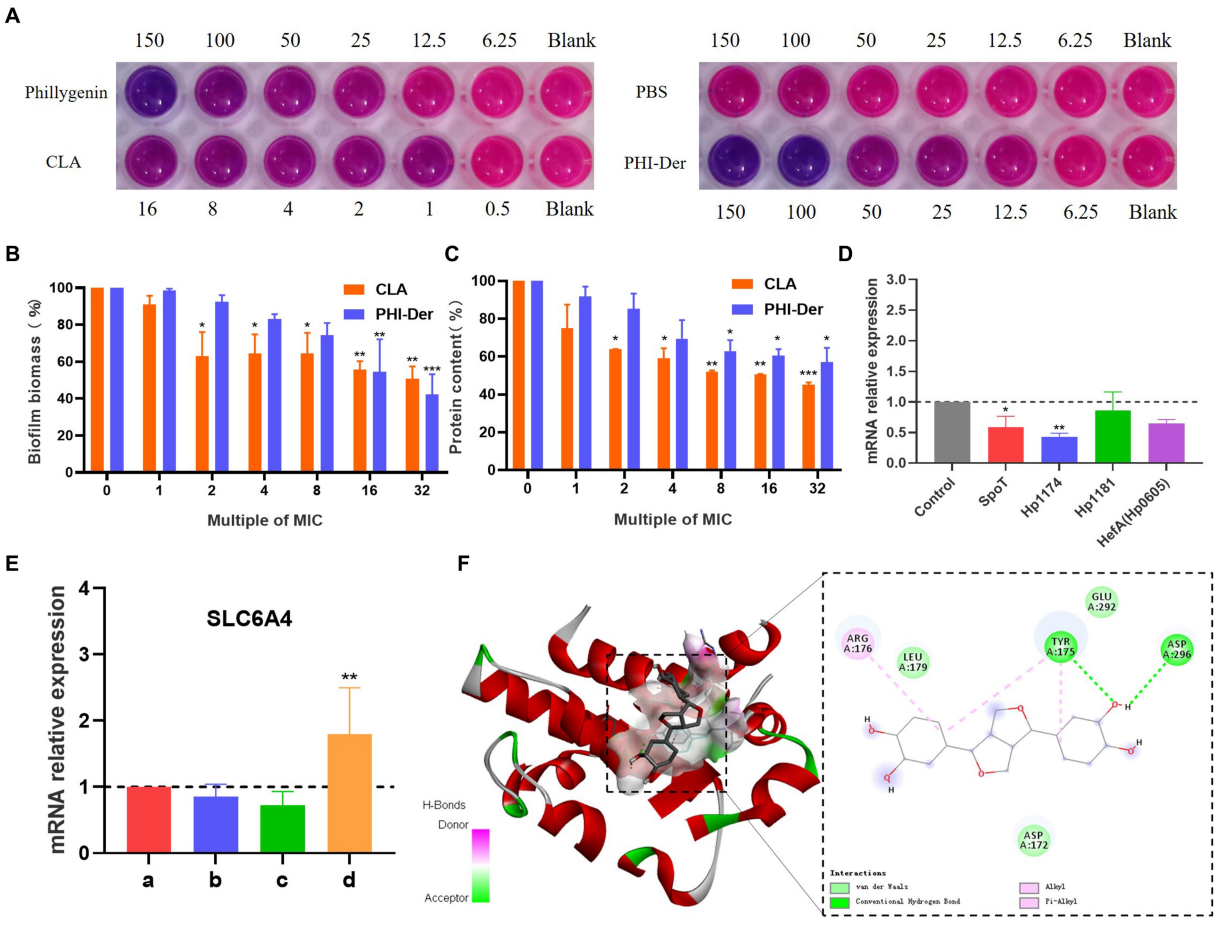

FIGURE 7
Inhibitory effect of PHI-Der on biofilms. **(A)** Alpha blue showing biofilm inhibition. **(B)** Crystal violet showing biofilm expression. **(C)** Biofilm protein expression. **(D)** Changes in the relative messenger RNA (mRNA) expression of biofilm-related genes after the administration of PHI-Der. **(E)** Changes in the relative expression of *SLC6A4* mRNA after the administration of PHI-Der (a: cell group; b: cells+PHI-Der group; c: infected cell group; d: infected cell+PHI-Der group). **(F)** PHI-Der and *SLC6A4* molecule docking. *p<0.05, **p<0.01, ***p<0.001.

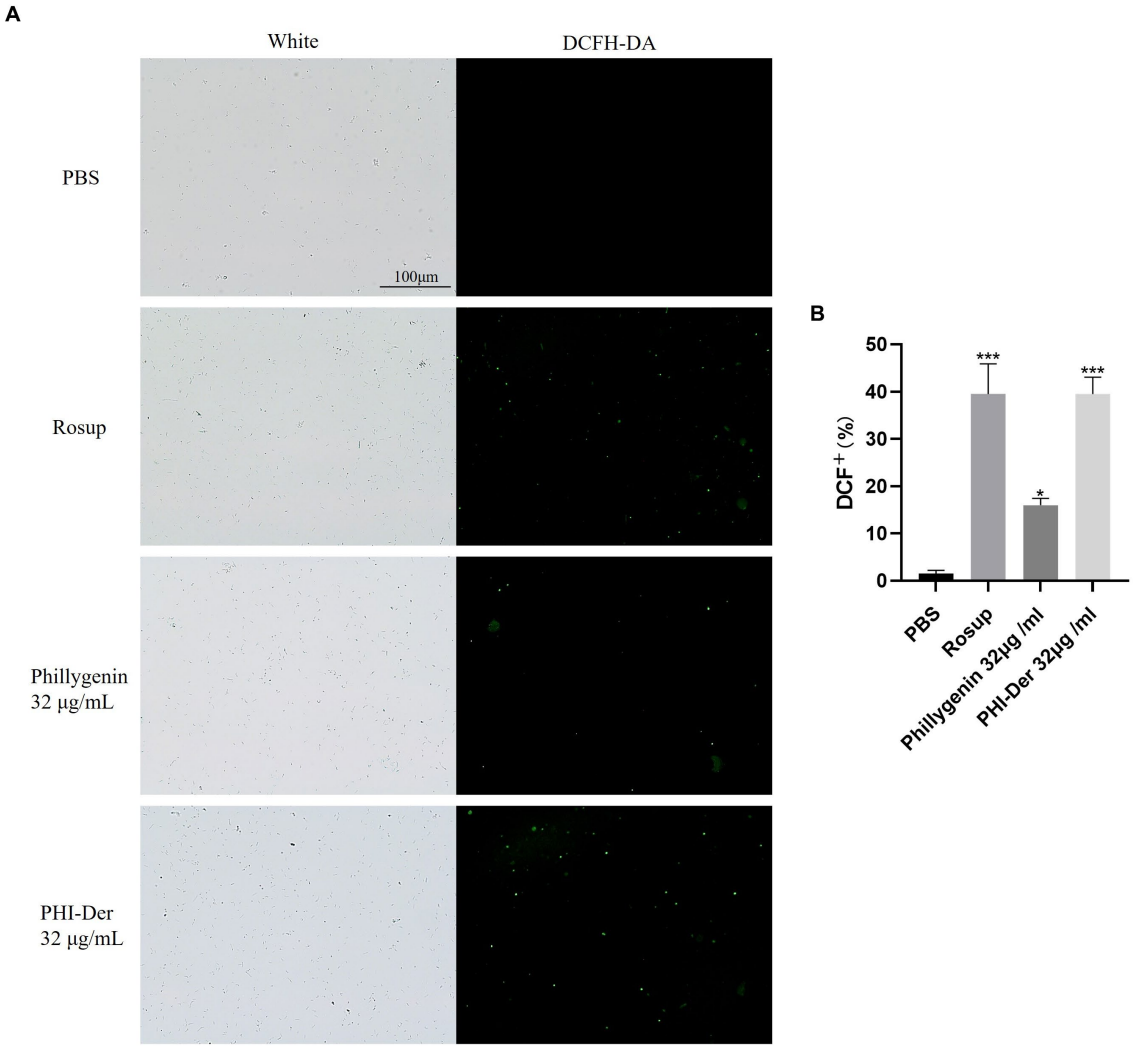

FIGURE 8
(A) Effect of PHI-Der on the oxidation (ROS production) of *H. pylori*. **(B)** Quantitative diagram of the oxidative (ROS production) effect. *$p < 0.05$, **$p < 0.01$, ***$p < 0.001$.

therapeutic effect on refractory gastritis caused by clinical drug-resistant *H. pylori* infection. PHI-Der could become a leading drug or candidate drug against *H. pylori*.

Bacterial biofilms are bacterial communities located in self-assembled matrices called EPS, which are mainly composed of proteins (Hou et al., 2022). After formation, biofilms serve as a sanctuary for bacteria to resist antibiotic treatment and immune defense, thereby causing drug resistance (Krzyżek et al., 2022). *Hp1174*, a gene of the major facilitator superfamily efflux pump family, is involved in biofilm formation. In this study, PHI-Der could effectively inhibit biofilm formation, with a better effectiveness than that of phillygenin. Its mechanism is related to downregulation of *Hp1174* expression. The serotonin transporter (*SLC6A4*) is associated with functional dyspepsia in *H. pylori* infection (Hwang et al., 2014). miR-325 regulates and induces the formation of functional gastrointestinal disease EPS and is present in *SLC6A4*. At a strong binding site, miR-325 expression is attenuated upon binding (Arisawa et al., 2012). In this study, *SLC6A4* was significantly upregulated after the effect of PHI-Der, which indicated that EPS formation was weakened and that biofilm formation was inhibited. In target prediction, PHI-Der could regulate *SLC6A4*, consistent with the phenotype of inhibiting biofilm formation. The inhibitory effect of demethylated hydroxylated PHI-Der on biofilm is better than that of phillygenin (Li et al., 2022), which may be because of the fact that the hydroxyl group attached to anthraquinone can target and regulate *SLC6A4* and *Hp1174*, attenuating miR-325 expression, thereby inhibiting EPS formation more effectively (Song et al., 2021).

Helicobacter pylori promotes persistent inflammation, thereby maintaining a microenvironment rich in cytokines/chemokines, reactive nitrogen species, and ROS, which destabilize normal cellular homeostasis (Maciej et al., 2021). PHI-Der can prevent bacteria from infecting cells and cells from oxidizing and exert a protective effect on *H. pylori*-induced GES-1 cells. *ALOX5* can regulate cell death in two ways: inflammation and lipid peroxidation. Excessive lipid peroxidation easily occurs in phospholipids, the main component of plasma membrane, leading to membrane rupture and cell death (Sun et al.,

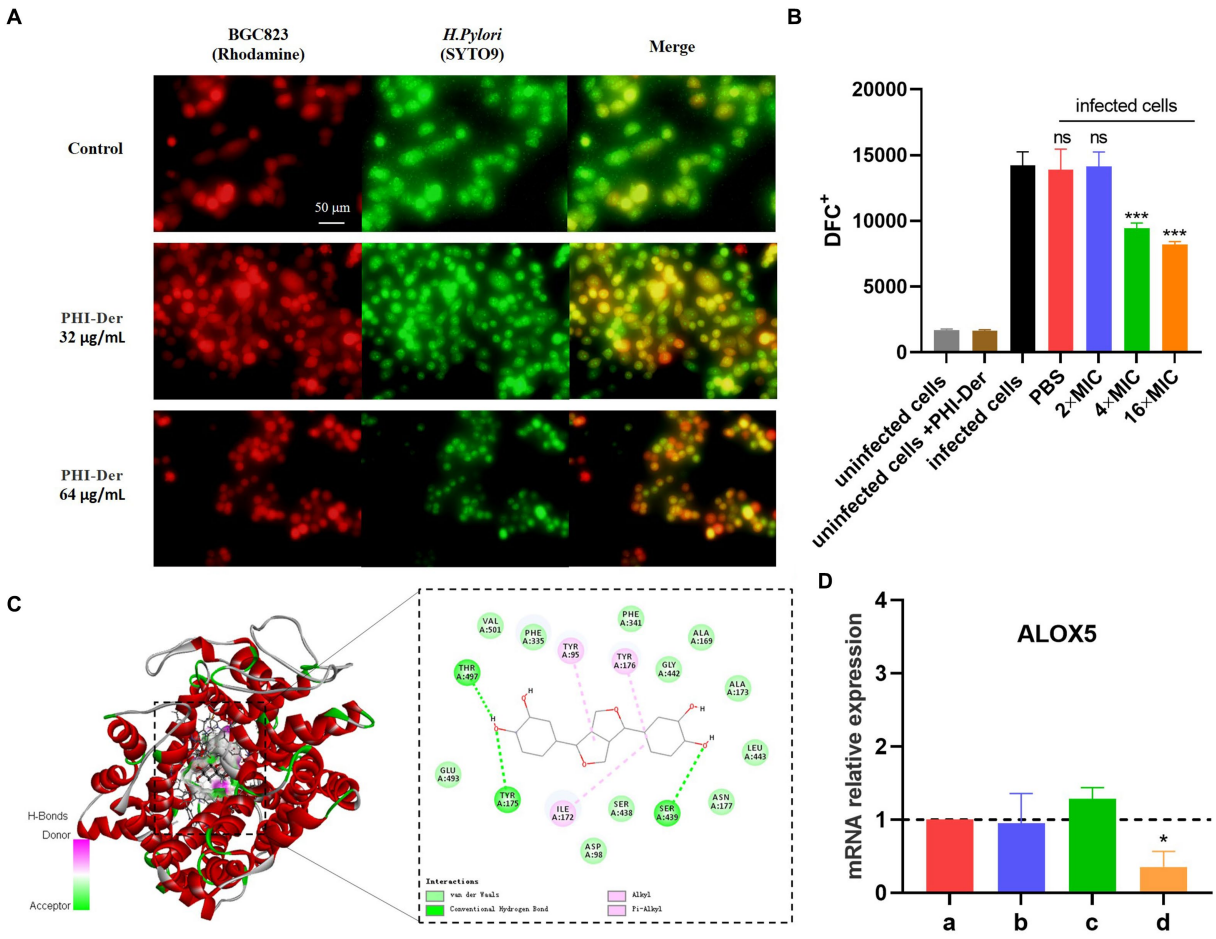

FIGURE 9
Antioxidative effect of PHI-Der on infected GES-1. **(A)** PHI-Der preventing bacteria from infecting cells. **(B)** Antioxidative effects of PHI-Der on infected GES-1 cells. **(C)** Changes in the relative expression of *ALOX5* mRNA after the action of PHI-Der (a: cell group; b: cell+PHI-Der action group; c: infected cell group; d: infected cell+PHI-Der group). **(D)** PHI-Der was docked with ALOX5 molecules. *p<0.05, ***p<0.001.

2019). *ALOX5* expression is upregulated after *H. pylori* infection and downregulated after the action of PHI-Der. PHI-Der can regulate inflammation and lipid peroxidation by mediating *ALOX5*, thereby reducing the inflammatory response of infected cells. Thus, cells receive a certain protective effect.

The oxidation of PHI-Der because of *H. pylori* was significantly enhanced, but the mechanism of its action remains unknown. Further, the reason behind enhanced oxidation of *H. pylori* and weakened oxidation of infected cells is unknown. Owing to the increase in hydroxyl groups, oxidative properties of drugs increase (Gao et al., 2020); however, substances that are oxidized differ significantly between prokaryotic and eukaryotic cells. In *H. pylori*, *ALOX5* was not found. In contrast, no *H. pylori*-associated oxidized proteins may be present in eukaryotic cells. This issue needs to be further explored.

In addition, PHI-Der could also regulate ATP leakage of *H. pylori* (Arya et al., 2019) and downregulate virulence factors (Xia et al., 2022) (see Supplementary materials for details). Some pathogens that have evolved virulence factors highly resistant to oxidative stress can adhere and form biofilms on cell surfaces. Therefore, PHI-Der can reduce the oxidative damage of infected cells by inhibiting biofilm formation and the expression of virulence factors, enhancing the oxidation reaction in *H. pylori*, thereby achieving better killing and protection of *H. pylori* and protecting the gastric mucosa.

5. Conclusion and outlook

This study showed that demethylated hydroxylated PHI-Der was more effective than phillygenin in treating *H. pylori* infection, with advantages of low toxicity, less likelihood of drug resistance, and specific action on *H. pylori* with better medicinal properties, it's a good antioxidant for host cells. Chemical modification of demethyl hydroxylation enhanced oxidation and inhibited biofilm formation, which could help modify compounds for improved activity, it provide a new approach for improving the activity of the compound.

Data availability statement

The original contributions presented in the study are included in the article/Supplementary material, further inquiries can be directed to the corresponding authors.

Ethics statement

The animal study was reviewed and approved by SYXK Gui 2017-0004.

Author contributions

R-JL was responsible for the experimental research, performed to consult literature and write the first draft. J-yX, XUW, L-jL, XIW, PX, W-yX, Z-yX, S-hX, Y-yJ, and LH writing—review and editing. L-yW, G-rH, and Y-QH designed, checked and modified finalize the manuscript. All authors contributed to the article and approved the submitted version.

Funding

This study was supported by National Natural Science Foundation of China, Nos. 81760739 and 32060018 and through special fund projects for Guide Local Science and Technology Development by the China Government (GUIKEZY20198004).

Acknowledgments

The authors would like to thank all the reviewers who participated in the review, as well as MJEditor (www.mjeditor.com) for providing English editing services during the preparation of this manuscript.

Conflict of interest

The authors declare that the research was conducted in the absence of any commercial or financial relationships that could be construed as a potential conflict of interest.

Publisher's note

All claims expressed in this article are solely those of the authors and do not necessarily represent those of their affiliated organizations, or those of the publisher, the editors and the reviewers. Any product that may be evaluated in this article, or claim that may be made by its manufacturer, is not guaranteed or endorsed by the publisher.

Supplementary material

The Supplementary material for this article can be found online at: https://www.frontiersin.org/articles/10.3389/fmicb.2023.1071603/full#supplementary-material

References

Adjissi, L., Chafai, N., Benbouguerra, K., Kirouani, I., Hellal, A., Layaida, H., et al. (2022, 2022). Synthesis, characterization, DFT, antioxidant, antibacterial, pharmacokinetics and inhibition of SARS-CoV-2 main protease of some heterocyclic hydrazones. *J. Mol. Struct.* 1270, 1270:134005. doi: 10.1016/j.molstruc.2022.134005

Arisawa, T., Tahara, T., Fukuyama, T., Hayashi, R., Matsunaga, K., Hayashi, N., et al. (2012). Genetic polymorphism of pri-microRNA 325, targeting SLC6A4 3'-UTR, is closely associated with the risk of functional dyspepsia in Japan. *J. Gastroenterol.* 47, 1091–1098. doi: 10.1007/s00535-012-0576-1

Arya, T., Oudouhou, F., Casu, B., Bessette, B., Sygusch, J., and Baron, C. (2019). Fragment-based screening identifies inhibitors of ATPase activity and of hexamer formation of Cagα from the *Helicobacter pylori* type IV secretion system. *Sci. Rep.* 9, 628–638. doi: 10.1038/s41598-019-42876-6

Branswell, Helen. WHO releases list of world's most dangerous superbugs. World Health Organization website [EB/OL]. (2017)

Cai, Y., Wang, C., Chen, Z., Xu, Z., Li, H., Li, W., et al. (2020). Transporters HP0939, HP0497, and HP0471 participate in intrinsic multidrug resistance and biofilm formation in *Helicobacter pylori* by enhancing drug efflux. *Helicobacter* 25. doi: 10.1111/hel.12715

Fang, X., Liu, L., Lei, J., He, D., Zhang, S., Zhou, J., et al. (2022). Geometry-enhanced molecular representation learning for property prediction. *Nat. Mach. Intell.* 4, 127–134. doi: 10.1038/s42256-021-00438-4

Gao, S., Zhou, J., and Chen, J. Identification of flavonoids 3-hydroxylase from [*Silybum marianum* (L.) Gaertn] and its application in enhanced production of taxifolin. *Sheng Wu Gong Cheng Xue Bao*, (2020);*36*:2838–2849. Chinese. doi: 10.13345/j.cjb.200178

Hannah, J., Ines, B. G., Franck, B., Philippe, C., and Myriam, S. (2022). The reductive Dehydroxylation catalyzed by IspH, a source of inspiration for the development of novel anti-Infectives. *Molecules* 27:708. doi: 10.3390/MOLECULES27030708

Hathroubi, S., Mekni, M. A., Domenico, P., Nguyen, D., and Jacques, M. (2017). Biofilms: microbial shelters against antibiotics. *Microb. Drug Resist.* 23, 147–156. doi: 10.1089/mdr.2016.0087

Hou, C., Yin, F., Wang, S., Zhao, A., Li, Y., and Liu, Y. (2022). *Helicobacter pylori* biofilm-related drug resistance and new developments in its anti-biofilm agents. *Infect. Drug Resist.* 15, 1561–1571. doi: 10.2147/IDR9.S357473

Huan, C., Zongtao, W., Shiqing, C., and Dongbin, F. (2021). Study on lignin Epoxidized graft and its preparation of soy protein adhesive. *Mater. Rev.* 35, 20190–20194. doi: 10.1039/C9RA05931H

Hwang, S. W., Kim, N., Jung, H. K., Park, J. H., Choi, Y. J., Kim, H., et al. (2014). Association of SLC6A4 5-HTTLPR and TRPV1 945G>C with functional dyspepsia in Korea. *J. Gastroenterol. Hepatol.* 29, 1770–1777. doi: 10.1111/jgh.12596

Komatsu, S., Ichikawa, D., Takemoto, K.-I., Kosuga, T., Okamoto, K., Konishi, H., et al. (2015). Therapeutic value of lymphadenectomy and prediction of station no.5 or 6 lymph node metastasis in the upper-third gastric cancer. *J. Am. Coll. Surg.* 221, e134–e135. doi: 10.1016/j.jamcollsurg.2015.08.260

Krzyżek, P., Migdał, P., Grande, R., and Gościniak, G. (2022). Biofilm formation of *Helicobacter pylori* in both static and microfluidic conditions is associated with resistance to clarithromycin. *Front. Cell. Infect. Microbiol.* 12:868905. doi: 10.3389/fcimb.2022.868905

Li, R. J., Qin, C., Huang, G. R., Liao, L. J., Mo, X. Q., and Huang, Y. Q. (2022). Phillygenin inhibits *Helicobacter pylori* by preventing biofilm formation and inducing ATP leakage. *Front. Microbiol.* 13:863624. doi: 10.3389/fmicb.2022.863624

Liu, L., Sun, Y., Wen, C., Jiang, T., Tian, W., Xie, X., et al. (2022). Metabolome analysis of genus Forsythia related constituents in *Forsythia suspensa* leaves and fruits using UPLC-ESI-QQQ-MS/MS technique. *PLoS One* 17:e0269915. doi: 10.1371/journal.pone.0269915

Maciej, S., Paweł, K., Ewa, D., Ryszard, A., and Zbigniew, S. (2021). *In silico* screening and in vitro assessment of natural products with anti-virulence activity against *Helicobacter pylori*. *Molecules* 27:20. doi: 10.3390/MOLECULES27010020

Martin Nuñez Gracia, M., Isabel, C. P., Mercedes, C. P., and Tinahones, F. J. (2021). Gut microbiota: the missing link between *Helicobacter pylori* infection and metabolic disorders? *Front. Endocrinol.* 12:639856. doi: 10.3389/FENDO.2021.639856

Morilla, A. M., Álvarez-Argüelles, M. E., Duque, J. M., Armesto, E., Villar, H., and Melón, S. (2019). Primary antimicrobial resistance rates and prevalence of *Helicobacter pylori* infection in the north of Spain. A 13-year retrospective study. *Gastroenterol. Hepatol.* 42, 476–485. doi: 10.1016/j.gastrohep.2019.05.002

Pinho, A. S., Seabra, C. L., Nunes, C., Reis, S., Martins, M. C., and Parreira, P. (2022). *Helicobacter pylori* biofilms are disrupted by nanostructured lipid carriers: a path to eradication? *J. Control. Release* 348, 489–498. doi: 10.1016/j.jconrel.2022.05.050

Shen, Y., Zou, Y., Chen, X., Li, P., Rao, Y., Yang, X., et al. (2020). Antibacterial self-assembled nanodrugs composed of berberine derivatives and rhamnolipids against *Helicobacter pylori*. *J. Control. Release* 328, 575–586. doi: 10.1016/j.jconrel.2020.09.025.

Siqi, Z., Haiyan, W., Xiaotao, H., and Haohuan, L. (2021). Phillygenin protects against osteoarthritis by repressing inflammation via PI3K/Akt/NF-κB signaling: *in vitro* and *in vivo* studies. *J. Funct. Foods* 80:104456. doi: 10.1016/J.JFF.2021.104456

Song, Z. M., Zhang, J. L., Zhou, K., Yue, L. M., Zhang, Y., Wang, C. Y., et al. (2021). Anthraquinones as potential Antibiofilm agents against methicillin-resistant *Staphylococcus aureus*. *Front. Microbiol.* 12:709826. doi: 10.3389/fmicb.2021.709826

Spiegel, M., Krzyżek, P., Dworniczek, E., Adamski, R., and Sroka, Z. (2021). *In silico* screening and in vitro assessment of natural products with anti-virulence activity against *Helicobacter pylori*. *Molecules* 27:20. doi: 10.3390/molecules27010020, 35011255

Sun, Q. Y., Zhou, H. H, and Mao, X. Y. (2019). Emerging roles of 5-Lipoxygenase phosphorylation in inflammation and cell death. *Oxidative Med. Cell. Longev.* 2019:1–9. doi: 10.1155/2019/2749173

Tang, J., Zhang, C., Lin, J., Duan, P., Long, J., and Zhu, H. (2021, 2021). ALOX5-5-HETE promotes gastric cancer growth and alleviates chemotherapy toxicity via MEK/ERK activation. *Cancer Med.* 10, 5246–5255. doi: 10.1002/cam4.4066

Wang, J., Luo, L., Zhao, X., Xue, X., Liao, L., Deng, Y., et al. (2022). Forsythiae Fructuse extracts alleviates LPS-induced acute lung injury in mice by regulating PPAR-γ/RXR-α in lungs and colons. *J. Ethnopharmacol.* 293:115322. doi: 10.1016/j.jep.2022.115322

Wang, Y., Wu, S., Wang, L., Wang, Y., Liu, D., Fu, Y., et al. (2022). The activity of liposomal Linolenic acid against *Helicobacter pylori* in vitro and its impact on human fecal Bacteria. *Front. Cell. Infect. Microbiol.* 12:865320. doi: 10.3389/fcimb.2022.865320.

Westwood, N. J., Panovic, I., and Lancefield, C. S. (2016). "Chemical modification of lignin for renewable polymers or chemicals" in *Production of biofuels and chemicals from lignin. Biofuels and biorefineries*. eds. Z. Fang and SmithR. Jr. (Singapore: Springer)

Xia, X., Zhang, L., Wu, H., Chen, F., Liu, X., Xu, H., et al. (2022). CagA+*Helicobacter pylori*, not CagA-*Helicobacter pylori*, infection impairs endothelial function through Exosomes-mediated ROS formation. *Front. Cardiovasc. Med.* 9:881372. doi: 10.3389/fcvm.2022.881372

Xiaoran, G., Cai, Y., Chen, Z., Gao, S., Geng, X., Li, Y., et al. (2018). Bifunctional enzyme SpoT is involved in biofilm formation of *Helicobacter pylori* with multidrug resistance by Upregulating efflux pump Hp1174 (gluP). *Antimicrob. Agents Chemother.* 62:e00957-18. doi: 10.1128/AAC.00957-18

Xunlei, P., Yanhong, W., Li, L., Zuan, Z., Yanchao, Z., Bei, M., et al. (2019). The distribution of colorectal polyps and colorectal cancer and its relationship with different subtypes of *Helicobacter pylori* infection. *Xuzhou Med. Univ. Chin. J.* 10, 734–736. doi: 10.4251/wjgo.v12.i5.582

Yufeng, L., and Peng, Y. (2021). Phillygenin inhibits the inflammation and apoptosis of pulmonary epithelial cells by activating PPARγ signaling via downregulation of MMP8. *Mol. Med.* 24:775. doi: 10.3892/MMR.2021.12415

Frontiers in Microbiology

Explores the habitable world and the potential of microbial life

The largest and most cited microbiology journal which advances our understanding of the role microbes play in addressing global challenges such as healthcare, food security, and climate change.

Discover the latest Research Topics

See more →

Frontiers

Avenue du Tribunal-Fédéral 34
1005 Lausanne, Switzerland
frontiersin.org

Contact us

+41 (0)21 510 17 00
frontiersin.org/about/contact